Acta Universitatis Agriculturae Sueciae

Doctoral Thesis No. 2025:42
Faculty of Natural Resources and Agricultural Sciences

Syntrophic propionate oxidation in high ammonia systems

Cooperation, metabolism, and stress adaption

Nils Weng

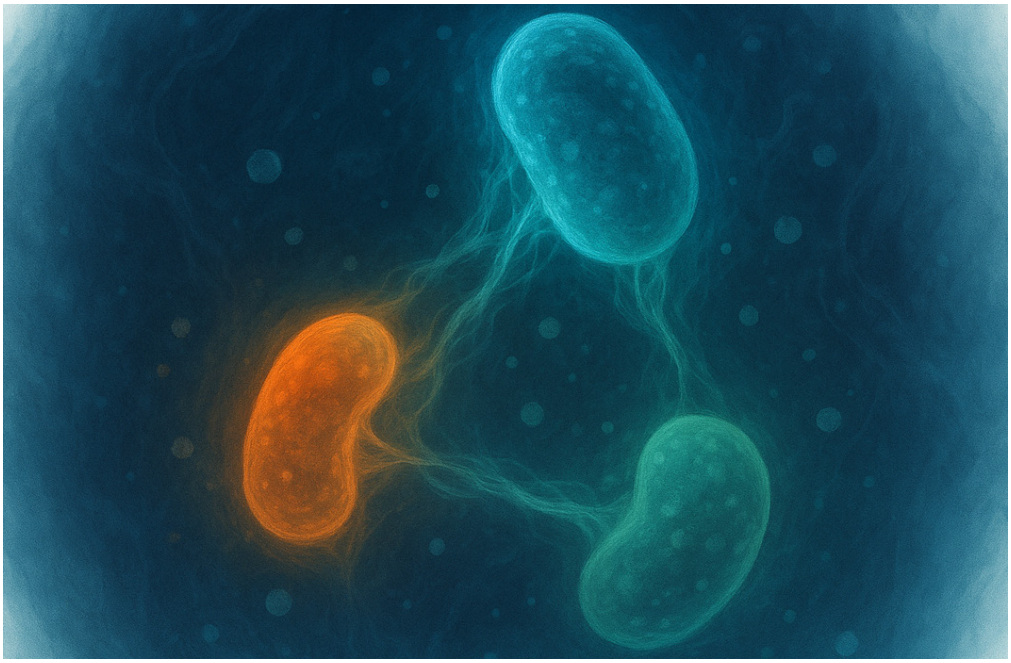

Syntrophic propionate oxidation in high ammonia systems

Cooperation, metabolism, and stress adaption

Nils Weng
Faculty of Natural Resources and Agricultural Sciences
Department of Molecular Sciences
Uppsala

SLU
SWEDISH UNIVERSITY OF AGRICULTURAL SCIENCES

DOCTORAL THESIS
Uppsala 2025

Acta Universitatis Agriculturae Sueciae
2025:42

Cover: Artistic representation of syntrophic microbial interactions. Image generated using OpenAI's DALL·E, April 2025

ISSN 1652-6880
ISBN (print version) 978-91-8046-527-4
ISBN (electronic version) 978-91-8046-527-4
https://doi.org/10.54612/a.5npuc4rg9r
© 2025 Nils Weng, https://orcid.org/0009-0009-9291-6641
Swedish University of Agricultural Sciences, Department of Molecular Sciences, Uppsala, Sweden

Print: SLU Grafisk service, Uppsala 2025

Syntrophic propionate oxidation in high ammonia systems
Cooperation, metabolism, and stress adaption

Abstract

Anaerobic digestion (AD) is a microbial process for converting organic matter into methane-rich biogas, serving as both a renewable energy source and a waste treatment strategy. High ammonia concentrations, often stemming from the degradation of protein-rich feedstocks, can destabilise AD systems by inhibiting microbial activity, particularly among acetate-utilising methanogens and certain propionate degraders. Under these conditions, ammonia tolerant syntrophic propionate-oxidising bacteria (SPOB) and syntrophic acetate-oxidising bacteria (SAOB) become vital for volatile fatty acid (VFA) conversion. These bacteria depend on hydrogenotrophic methanogens to consume metabolic products like hydrogen and formate, rendering the acid oxidation thermodynamically favourable. However, these ammonia-tolerant syntrophic communities are often present at low abundance in AD systems, limiting propionate and acetate degradation rates. Current knowledge about these communities is constrained by challenges in studying them in complex AD systems. This thesis aimed to deepen the understanding of syntrophic propionate-oxidising bacteria under high-ammonia mesophilic conditions and their interactions with SAOB and hydrogenotrophic methanogenic archaea. The research utilised a highly enriched syntrophic communities from a high-ammonia digester, employing molecular and cultivation-based methods, complemented by thermodynamic calculations and novel visualisation tools. This research identified the metabolic pathway and cooperating strategies used by syntrophic microbial partners crucial for propionate and acetate oxidation under high ammonia. Furthermore, a novel methanogen was identified, demonstrating electron transfer via both hydrogen and formate. Findings revealed that disrupting microbial aggregation significantly impeded propionate degradation. Moreover, it was demonstrated that the community adapted to high salt and ammonia stress by inducing aggregation and employed specific tolerance strategies like ion transport and compatible solutes. Overall, this thesis deepened the understanding of the factors that disrupt the intricate interplay between syntrophs and highlighted their unique stress-resilience features. In the long term, these insights may support the development of strategies to mitigate VFA accumulation in high-ammonia biogas digesters.

Keywords: syntrophic propionate oxidation, syntrophic acetate oxidation, hydrogenotrophic methanogenesis, anaerobic digestion, ammonia inhibition, syntrophy, biogas, flocculation, interspecies electron transfer

Syntrof propionatoxidation i system med hög ammoniakhalt

Samarbete, metabolism och stressanpassning

Sammanfattning

Anaerob nedbrytning (rötning) är en mikrobiell process som omvandlar organiskt material till metanrik biogas, och är således en källa till förnybar energi och en strategi för avfallshantering. Höga ammoniaknivåer från nedbrytningen av proteinrika substrat kan destabilisera processen genom att hämma mikrobiell aktivitet, särskilt hos acetatnyttjande metanogener och vissa propionatnedbrytare. Under sådana förhållanden blir ammoniaktoleranta syntrofa propionat- och acetatoxiderande bakterier (SPOB och SAOB) avgörande för fortsatt nedbrytning av propionat och acetat. Dessa bakterier får ett överflöd av elektroner vid syranedbrytningen och måste samarbeta med en hydrogenotrof metanogen som kan använda dessa för att möjliggöra termodynamiskt gångbar nedbrytning. Dessa syntrofa mikroorganismer förekommer ofta i låg förekomst i rötningsprocessen, vilket begränsar nedbrytningshastigheten och gör dem svåra att studera. Denna avhandling syftade till att fördjupa förståelsen kring SPOB under mesofila och ammoniakrika förhållanden, samt deras interaktion med SAOB och metanogener. En syntrof kultur anrikad från en högammoniakreaktor analyserades med molekylära och odlingsbaserade metoder, i kombination med termodynamiska beräkningar och nya visualiseringsverktyg. Studien kartlade de metaboliska vägarna och samarbetsstrategierna som används av mesofila och ammoniak-toleranta SPOB, SAOB och metanogen, samt identifierade en ny metanogen som utnyttjar både väte och format för elektronöverföring. Mikroorganismerna anpassade sig till salt- och ammoniakstress genom aggregering och genom strategier som jontransport och användning av kompatibla lösta ämnen. Studierna visade även att störd aggregering via omrörning hämmade propionatnedbrytningen. Sammantaget så fördjupade denna avhandling förståelsen för faktorerna som stör det komplexa samspelet mellan syntrofa mikroorganismer och belyste deras unika egenskaper för stresstålighet. På lång sikt kan dessa insikter användas för att förbättra processstrategier för att motverka ackumulering av flyktiga fettsyror i biogasreaktorer med höga ammoniakhalter.

Keywords: syntrof propionat oxidation, syntrof acetate oxidation, hydrogenotrof metanogenes, rötning, ammoniak inhibering, syntrofi, biogas, flockulering, elektronöverföring mellan arter

Contents

List of publications

This thesis is based on the work contained in the following Papers, referred to by Roman numerals in the text:

I. Weng N, Singh A, Ohlsson JA, Dolfing J, Westerholm M (2024). Catabolism and interactions of syntrophic propionate- and acetate oxidising microorganisms under mesophilic, high-ammonia conditions. Frontiers in Microbiology, 15 (1389257), https://doi.org/10.3389/fmicb.2024.1389257

II. Weng N, Nadali Najafabadi M, Westerholm M. (2025) Disruption-induced changes in syntrophic propionate and acetate oxidation: flocculation, cell proximity, and microbial activity. Biotechnology for Biofuels and Bioproducts,18, 45, https://doi.org/10.1186/s13068-025-02644-3

III. Weng N, Jonas Ohlsson, Pinela E, Westerholm M. Microbial strategies for ammonia tolerance by syntrophic propionate and acetate oxidising microbial communities originating from biogas processes. (Manuscript)

IV. Weng N, Ohlsson JA, Westerholm M. Development of time-lapse imaging systems and 3D-printed bioreactors for studying cellular aggregation in strictly anaerobic microorganism (Manuscript)

The contribution of Nils Weng to the Papers included in this thesis was as follows:

I. Participated in the laboratory work and performed data compilation and analysis, bioinformatic work and analysis of sequencing data. Main writer of the manuscript.

II. Co-creator of study design, performed all laboratory work and bioinformatical analysis. Main writer of the manuscript

III. Co-creator of study design, performed RNA extraction and bioinformatical analysis of sequencing data. Main writer of the manuscript

IV. Developed and constructed the 3D-printed bioreactors, the macroscale imaging system, and the software for automated microscopic image acquisition. Main writer of the manuscript.

List of figures

Abbreviations

AD	Anaerobic digestion
ANI	Average nucleotide identity
CSTR	Continuous stirred-tank reactor
DDH	DNA–DNA hybridization
dDDH	Digital DNA–DNA hybridisation
DIET	Direct interspecies electron transfer
DE	Differentially expressed
EPS	Extracellular polymeric substances
FDH	Formate dehydrogenase
GSRP	Glycine synthase reductase pathway
GTDB	Genome Taxonomy Database
HRT	Hydraulic retention time
IET	Interspecies electron transfer
MAG	Metagenome-assembled genome
MIET	Mediated interspecies electron transfer
MMC	Methylmalonyl-CoA pathway
OLR	Organic loading rate
PCR	Polymerase chain reaction
q-PCR	Quantitative PCR
SAO	Syntrophic acetate oxidation
SAOB	Syntrophic acetate-oxidising bacteria
SPO	Syntrophic propionate oxidation
SPOB	Syntrophic propionate-oxidising bacteria
TAN	Total ammonia nitrogen
VFA / VFAs	Volatile fatty acid(s)
WLP	Wood–Ljungdahl pathway

1. Introduction

Anaerobic digestion (AD) is a microbial process that converts organic material into methane-rich gas (biogas) under oxygen-free conditions. This methane is a renewable energy source that can substitute fossil fuels in heating, electricity and as a vehicle fuel. Additionally, AD is an effective waste treatment solution, utilising feedstocks like food waste, agricultural residues, industrial by-products, and manure (Kougias and Angelidaki, 2018). Conducting AD in controlled environments also mitigates the release of this potent greenhouse gas into the atmosphere from landfills and animal manure storage. Furthermore, AD generates a nutrient-rich residue (digestate) that when used as a biofertiliser can enhance soil health and contribute to more sustainable agriculture (Ehmann et al., 2018; Tampio et al., 2024). Furthermore, using digestate as biofertiliser reduces reliance on mineral fertilisers, which are both produced via energy-intensive methods (i.e., ammonium synthesis) (Smith et al., 2020), or mined from finite natural resources (phosphorous, potassium) (Cordell et al., 2011; Al Rawashdeh, 2020). The AD sector has significant growth potential (World Biogas Association, 2019), and in Sweden, the greatest potential lies in utilising manure, a largely untapped resource for biogas production (Regeringskansliet, 2019).

During AD, the feedstock composition is an important parameter impacting the microbial community that emerges within the anaerobic (oxygen-free) reactors. Anaerobic digestion is catalysed by a diverse consortium of cooperating microorganisms in a series of consecutive steps, ultimately forming methane and CO_2. A major challenge to the stability of AD systems is the presence of high ammonia concentrations, which arise from the degradation of protein-rich substrates such as slaughterhouse waste and chicken manure (Yenigün and Demirel, 2013). While these substrates provide high biogas yields and produce ammonium-rich digestates, excessive ammonia levels can inhibit microbial activity at all stages of the degradation process (Fischer et al., 2019). Among the more sensitive groups are acetate-utilising (acetoclastic) methanogens and certain propionate-degrading microorganisms (De Vrieze et al., 2015; Fischer et al., 2019; Wang et al., 2022; Westerholm et al., 2022). This inhibition leads to an accumulation of volatile fatty acids (VFAs), such as propionate and acetate, which further diminishes process performance and, if not mitigated, can lead to complete process failure.

The microbial community in AD is far from static, continuously adapting and restructuring in response to environmental conditions. In high-ammonia AD processes, ammonia tolerant syntrophic propionate-oxidising (SPOB) and acetate-oxidising bacteria (SAOB) frequently emerge as central microorganisms in the conversion of VFAs in the absence of acetoclastic methanogens (Westerholm et al., 2016; Ruiz-Sánchez et al., 2018; Buhlmann et al., 2019; Singh et al., 2023). In syntrophic acetate oxidation (SAO), acetate is converted to CO_2 and H_2 and for syntrophic propionate oxidation (SPO) propionate is converted to CO_2, H_2 and acetate. The resulting acetate can then be utilised either by acetoclastic methanogens in low-ammonia conditions (Rajagopal et al., 2013; Westerholm et al., 2020) or by SAOB in high-ammonia conditions (Singh et al., 2021). SPO occurs in both low- and high-ammonia environments, although the bacterial species involved differ (Singh et al., 2021, 2023). Both types of acid oxidisers rely on syntrophy, a form of mutualistic metabolic cooperation which depends on a hydrogenotrophic methanogen to overcome the otherwise energetically unfavorable oxidation of the acids. These oxidation processes generate a surplus of reducing equivalents, such as H_2 or formate. By using these reducing equivalents to reduce CO_2 to methane, hydrogenotrophic methanogens maintain the low H_2 or formate concentrations necessary for the acid oxidation to occur. However, the abundance and activity of the syntrophic community in the AD process is often low, especially under high-ammonia conditions which restrict the degradation rates of propionate and acetate (Westerholm et al., 2016; Campanaro et al., 2020). Improved understanding of these syntrophic interactions could inform the development of strategies to enhance the resilience and efficiency of AD systems. Furthermore, fundamental insights into archaeal–bacterial interactions may provide valuable knowledge applicable to other biotechnological processes, such as H_2-amended biogas upgrading in power-to-gas systems (De Bernardini et al., 2022), syngas-to-biofuel conversion (Sancho Navarro et al., 2016), microbial electrochemical technologies (Hari et al., 2016), and the production of value-added products from syngas (Robazza et al., 2024).

Aims

Given the critical role of syntrophic acid oxidation in preventing VFA accumulation in the AD process, the primary aim of this thesis was to advance the understanding of syntrophic propionate-oxidising bacteria under high-ammonia mesophilic conditions and their interactions with syntrophic acetate-oxidising bacteria and hydrogenotrophic methanogenic archaea. To address this aim, highly enriched syntrophic propionate- and acetate-oxidising communities derived from a high-ammonia digester were studied to explore their metabolic pathways, modes of cooperation, the role of flocculation, the effects of mixing on syntrophic interactions and their strategies for coping with ammonia stress. This research combined molecular and cultivation-based approaches with thermodynamic calculations. The specific objectives are presented and explored in **Papers I–IV**:

1) To investigate the metabolic pathways and cooperative mechanisms of syntrophic propionate- and acetate-oxidising bacteria in partnership with an hydrogenotrophic methanogen and assess their degradation dynamics and thermodynamic constraints (**Paper I**).
2) To assess the impact of physical disturbance on acid degradation, metabolic pathways and floc formation in syntrophic acid-oxidising communities' ability to degrade propionate and acetate (**Paper II**).
3) To explore the biological mechanisms underlying ammonia tolerance of the syntrophic propionate oxidising community (**Paper III**).
4) To develop tools and methods for visual monitoring of the interactions and cell aggregation of the syntrophic communities at both macro- and microscopic scales (**Paper II, III, IV**).

2. Anaerobic Digestion

2.1 History of the AD process

Anaerobic digestion is the microbial degradation of organic material in the absence of oxygen. It is a web of complex interactions between a consortium of microbes where the end product of one organism serves as the substrate of another, leading to the successive conversion of larger organic molecules to smaller ones, ultimately resulting in formation of carbon dioxide (CO_2) and methane (CH_4). This process occurs naturally in oxygen-depleted environments rich in organic material such as swamps, rice paddies, and gastrointestinal tracts. The formation of flammable gases in wetlands and swamps has likely been known for a long time, as suggested by historical accounts of their spontaneous ignition, a phenomenon termed *ignis fatuus* by the Romans or *will-o-wisp* by the English (Gunnerson and Stuckey, 1986; Roels and Verstraete, 2001). However, it was not until the 1770s that Alessandro Volta, through his studies of gases from wetlands, identified methane as the compound responsible for the flammability of the gas (Abbasi et al., 2012). The first "modern" well-documented production of biogas through AD comes from digesters constructed in India and New Zeeland in the mid-19th century (Fowler, 1934; Buswell, 1939; Bond and Templeton, 2011). By putting organic material in sealed containers, so-called digesters or bioreactors, exposure to oxygen is limited which creates the opportunity for the AD process to begin. In Exeter, England, gases from sewage systems was used for street lighting 1896 (Buswell, 1939). Large-scale AD facilities were developed in the 1930s, primarily for the treatment of municipal sewage sludge produced during wastewater processing (Khanal, 2008).

A unique aspect of the AD process is its reliance on a mixed microbial community, unlike most engineered biotechnological systems that typically employ a single organism to produce a specific target compound. The biogas reactor can be seen as an ecosystem, where the microbial community is shaped by the feedstock and the microbes that come with it, and the process parameters at which the reactor is operated. While these factors can influence

the community structure, it is not possible to fully control or synthetically construct the emergent consortium.

2.2 Modern applications of the AD process

The AD process is a versatile technology that combines waste treatment, renewable energy production and nutrient recycling within a single system, aspects which all are needed in the transition to a circular and carbon-neutral economy.

2.2.1 Biomethane – Renewable energy while reducing methane emissions

The gas formed during AD is a mixture made up of methane (60–70%), carbon dioxide (30–40%) and trace amounts of hydrogen sulphide, ammonia, hydrogen, and water vapour. This gas mixture can be immediately combusted for heating or to generate electricity. It can also be upgraded for use as vehicle fuel, for industrial applications, or injected into gas grids as a substitute for fossil natural gas. The upgrading includes the removal of all gases except the methane, and then either compression (200–250 bar) or the liquefying of the methane by cooling the gas to around −162°C, processes which both greatly increase the energy density of the end product. Methane is a potent greenhouse gas and is after CO_2 emissions regarded as the biggest contributor to the observed global warming that has occurred since pre-industrial times, and of the global methane emissions 60% are thought to be anthropogenic (Saunois et al., 2020). The AD process has the potential to capture some of these anthropogenic emissions, by using the organic sources giving rise to these emissions as a feedstock, thus capturing the methane in the controlled environment of the AD-reactor (Bumharter et al., 2023).

2.2.2 Digestate as a fertiliser

The organic residues of the AD process, known as the digestate, retains most of the nutrients originally present in the feedstock. As such, digestate can be applied to farmland as a fertiliser, promoting nutrient recycling and reducing the use of mineral fertilisers. Mineral fertilisers include the elements nitrogen (N), phosphorous (P) and potassium (K), the use of which is a double-edged sword. On one hand, they have been instrumental in increasing agricultural productivity and are fundamental to the modern food systems. On the other

hand, the leaching of these nutrients into water streams cause eutrophication, threatening aquatic ecosystems (Withers et al., 2014). Furthermore, there are problems associated with the production and extraction of the fertilisers in themselves. In the case of nitrogenous fertilisers, the majority is converted from atmospheric nitrogen gas through the energy demanding Haber–Bosch process, estimated to compromise 1–2% of global energy consumption (International Energy Agency, 2021). In addition, the use of fertilisers is the main anthropogenic source of nitrous gas emissions, contributing to air pollution and climate change, which could potentially be mitigated through the use of organic alternatives like digestate (Pan et al., 2022).

Both potassium and phosphorous used in mineral fertilisers are mined from geological deposits, primarily in the form of potash and phosphate rock. Easily accessible deposits, particularly for phosphorous, may be depleting (Cordell et al., 2009; Al Rawashdeh, 2020), with some estimates suggesting that peak production, the point at which extraction reaches its maximum before a steady decline, could occur as early as 2030. Calculations of peak production are highly uncertain, relying on estimates of readily accessible deposits, mining costs, and annual global demand (Cordell and White, 2011). Regardless, it is unsettling to realise that it might be a possibility that, in the grand timeline of human history, we have rapidly depleted the easily accessible mineral resources upon which our agricultural system and current population size depends. Therefore, irrespective of the remaining mineral deposits of phosphorus and potassium or the feasibility of mining them, recycling of nutrient already within the food system must be a central goal for long-term agricultural sustainability.

2.2.3 Biogas production in Europe and Sweden

The landscape of biogas production and utilisation varies both in terms of scale, the feedstock used and how the resulting biogas is utilised (Scarlat et al., 2018). In 2022, total biogas production in Europe reached 625 PJ, with Germany as the main producer accounting for over half of total output (50 %), followed by Italy (14%), France (9%) and Denmark (4%) (EurObserv'ER, 2022). Most of these countries have well-established biogas sectors with widespread anaerobic digestion facilities, whereas others such as Portugal, produce a significant share of their biogas from landfill gas recovery (EurObserv'ER, 2022). The primary use of the produced biogas also

varies across regions. In most of the EU countries, biogas is mainly used for electricity and heat generation in combined heat and power plants. In contrast, Sweden is unique in that a large fraction of the biogas produced is upgraded (68%) for use as a transportation fuel or in industrial processes (Energimyndigheten and Energigas Sverige, 2024). Europe aims to increase biomethane production by approximately 50% to reach 84.7 TWh by 2030, compared to the 2021 level of 56.6 TWh, driven both by climate considerations and the need to reduce European reliance on Russian gas, a vulnerability made evident by the war in Ukraine (EurObserv'ER, 2022).

In Sweden, total biogas production in 2023 was 2.3 TWh (Energimyndigheten and Energigas Sverige, 2024). Around half of this was produced in co-digestion plants (1155 GWh), followed by wastewater sewage sludge treatment plants (715 GWh), plants associated with industrial processes (152 GWh) and, finally, small farm scale plants (132 GWh). In recent years, the production of upgraded and liquefied biomethane has also grown significantly, reaching approximately 180 GWh, up from 40 GWh in 2019 (Energimyndigheten and Energigas Sverige, 2024). It has been estimated that Sweden could increase its production to 7–10 TWh, with the largest potential coming from agricultural residues, mostly manure (Regeringskansliet, 2019).

2.2.4 Process parameters and substrate composition

Reactor design and operational modes

There is a wide variety of bioreactor types, with key differences in factors such as process mode (batch vs continuous), reactor complexity (single-stage vs multistage), solid content of the material fed to the reactor (wet vs dry), and stirring mode (Van et al., 2020). Commonly used reactor types relevant to biogas production include continuous stirred-tank reactor (CSTR) (Sarker et al., 2014), plug flow reactors (Jagadish et al., 1998; Perman et al., 2024), and anaerobic membrane reactors (Saddoud et al., 2007), though a range of other configurations is also in use (Sarker et al., 2019). The choice of reactor or process type depends on factors such as the characteristics of the substrate, technical constrains related to pumping of the substrate, volume of organic waste required to be treated per reactor volume, investment costs, etc. The overall microbial community that develops in reactors is shaped by several

key factors, including reactor type, process parameters, feedstock composition, and the inoculum used during start-up of the reactor (Liu et al., 2018). Accordingly, these process parameters will be regarded more in detail below as they play a pivotal role in shaping the composition and activity of microorganisms with key roles in AD, including species converting intermediate compounds such as acetate and propionate to methane.

Mixing

There are several reasons for mixing the material within the reactor. It enhances mass transfer rates, redistributes heat, homogenises both the substrate and the microorganisms, increases the contact between microorganisms and the substrate, reduces substrate particle size, and promotes gas release from the sludge, which helps prevent foaming. Mixing can be achieved through mechanical means (e.g., impellers), hydraulically (e.g., liquid recirculation), or pneumatically (e.g., gas recirculation). It can occur either continuously or periodically, with varying intensity. In general, mixed processes tend to achieve higher methane production than those with no mixing, although this is not always the case. There are downsides to mixing. First, mixing is an energy intensive process which increases operational costs. Uniformity is not always optimal and often in stark contrast to the stratified environment where AD processes naturally occur. In some microbial processes, proximity between cooperating microorganisms is required, like syntrophic acid oxidation, and mixing risks disrupting those microbial interactions (Kariyama et al., 2018; Singh et al., 2019, **Paper II**). **Paper II** aimed to assess how mixing disrupted syntrophic propionate and acetate oxidation under high-ammonia conditions. This was achieved by subjecting mesophilic enrichment cultures to different mixing conditions (magnetic stirring and orbital shaking) and analysing how these mixing conditions impacted degradation dynamics, microbial community composition, and gene expression. Furthermore, harsh mechanical mixing that induces shear stress can disrupt the establishment of cell-to-cell interactions between cooperating cells by counteract the formation of cellular biofilms, and other aggregations (**Paper II)**.

Hydraulic retention time (HRT) and the organic loading rate (OLR)

The hydraulic retention time (HRT) is the average time sludge remains in a continuously fed reactors before exiting, calculated as the system volume divided by the flow rate. It is dependent on the feeding rate (substrate input rate) and the organic loading rate (OLR), which quantifies the amount of

organic material added per reactor volume and time. In mesophilic processes, HRT typically ranges from 15–30 days, whereas thermophilic processes, which have higher metabolic activity, can operate at shorter HRTs of 10–20 days (Angelidaki et al., 2011). In continuous or semi-continuous processes microbial biomass is constantly lost due to the continuous outflow of reactor contents. If the HRT is shorter than the doubling time of a microorganism, there is a risk that the microorganisms are being washed out of the system. This is a problem for slow-growing organisms with long lag phases, such as methanogens and syntrophic acid oxidisers (**Papers I–III**). To counteract this, a strategy is to increase the solids retention time (SRT), the average time solids particles spend in the reactor, by decoupling it from the HRT. This can be done by biomass retention techniques such as biofilm carriers or granule formation, or by recirculating the biomass-containing solids fraction of the outgoing sludge (Ji et al., 2020; Kiani Deh Kiani et al., 2022; Perman et al., 2024).

Substrate

A wide range of substrates can be used for AD, including agricultural waste, municipal solid waste, industrial waste, aquatic biomass, and energy crops (Atelge et al., 2020). The different feedstocks vary considerably in composition, biodegradability, rheology, and dry matter content. In general terms the feedstock comprises a mixture of three primary macromolecules: carbohydrates, lipids, and proteins, with some constituents less readily degradable than other. Lignin, one of the main constituents in wood, is for example from the AD perspective almost non-degradable, whereas some sugars and volatile fatty acids can be degraded within hours under non-inhibiting conditions (Steffen et al., 1998). The feedstock can also contain various compounds which are inhibitory or toxic to the microbes of the AD process.

A parameter of importance during AD is the carbon-to-nitrogen ratio (C:N), where the ideal ratio is generally considered to be between 20:1 and 30:1 for microbial growth and activity, although AD processes operating outside of this range exist (Ward et al., 2008; Schnürer and Jarvis, 2018). Higher C:N ratios, typical of plant-derived fibrous feedstocks such as grass and straw, leads to a process limited by nitrogen availability, and thus negatively affect process performance. Conversely, lower C:N ratios, typical of protein-rich feedstocks such as manure, sewage sludge, and slaughterhouse waste, leads excess nitrogen which can result in ammonia accumulation and inhibit

members of the microbial community. To mitigate this, substrates are often combined to achieve a more balanced C:N ratio, in a practice known as co-digestion (Ward et al., 2008; Sarker et al., 2019).

Formation of ammonia – NH_3 in the biogas process and its impact on the performance

Ammonia is formed through the degradation of nitrogenous matter, primarily proteins and their constituents amino-acids, with elevated levels observed in the degradation of feedstocks that are protein-rich or have a low C:N ratio. In the aqueous phase it exists in two forms: the ionised ammonium ion (NH_4^+) and the ammonia form (NH_3). Their sum concentration is referred to as total ammonia nitrogen (TAN). These forms exist in an equilibrium, with their ratio dependent on pH and temperature according to equation 1 (Emerson et al., 1975):

$$NH_3\text{-}N = \frac{NH_4^+\text{-}N}{1 + \frac{10^{-pH}}{10^{-\left(0.09018 + \frac{2729.92}{T}\right)}}} \quad (1)$$

From equation 1 it can be inferred that high temperature and/or high pH causes a shift towards ammonia (NH_3). The ammonia form is considered to be the most toxic form to microorganisms, but the susceptibility differs between microorganisms. The details and mechanisms of this ammonia toxicity is discussed at length in Chapter 4. From a process perspective, microbial inhibition due to ammonia toxicity results in reduced process performance and has been shown to cause shifts in microbial communities. A common consequence of ammonia-induced microbial inhibition is acetate accumulation, triggering the build-up of other VFA such as propionate, which can lower the pH of processes with restricted buffer capacity. In the context of ammonia inhibition, this pH decrease partially alleviate the ammonia toxicity, by shifting the equilibrium towards ammonium (Kougias and Angelidaki, 2018). But acetoclastic methanogens are not the only microorganisms effected by increased ammonia levels, and effects can be seen on the entire microbial community (De Vrieze et al., 2015; Bonk et al., 2018; Fischer et al., 2019; Wang et al., 2022). These changes and shifts in microbial communities have effects on the overall process performance of the AD process. In **Paper III**, the effect of ammonia stress on propionate-degrading

microbial cultures was studied, which is described further in chapter 4. The experiment, on which **Paper II** is based, involved spiking syntrophic propionate degrading cultures with ammonium chloride or sodium chloride and analysing the immediate gene expression response (1 hour) or sustained gene expression responses (3 days).

Temperature and pH

Operation at higher temperature, as long as it does not kill or stress the microorganism, tends to increase the metabolic activity (Angelidaki and Sanders, 2004). AD reactors are commonly operated in the mesophilic (30– 40°C) or thermophilic (50–60°C) temperature range (Sarker et al., 2019). Given the increased metabolic activity, thermophilic processes can therefore tolerate a higher loading rate of substrate, i.e., higher OLR or the reactors can be made smaller while keeping the same capacity as mesophilic counterparts. Furthermore, higher temperatures decrease the viscosity of the digestate which makes mixing less energy demanding, and the raised temperature increases pathogen elimination (Seeton, 2006; Álvarez-Fraga et al., 2025). However, this efficiency comes at price, both in terms of the energy required for heating and an increased susceptibility to process disturbances. Thermophilic processes are particularly sensitive to ammonia toxicity as higher temperatures shift the ammonia-ammonium equilibrium toward the toxic free ammonia form. These processes often exhibit higher pH than mesophilic ones (Labatut et al., 2014), explained by reduced CO_2 solubility and increased ammonia concentrations due to elevated protein degradation rates. Different AD processes operate at different pH, typically in the range of 5.5–8.5. While the microbial community of the AD process can adapt and thrive across a range of pH levels, fluctuations in pH can negatively impact process performance. Furthermore, microbes partaking in different stages of the AD process can have different pH optima. An example is the initial degradation of larger macromolecules which could be favoured by lower pH (Zhang et al., 2005; Moestedt et al., 2016). Methanogens generally prefer neutral pH (~7), though some species remain active, and even thrive, under acidic or alkaline conditions (Whitman et al., 2006).

As microbial composition is tightly linked to process parameters shift in conditions such ammonia levels can disrupt established populations and lead to process disturbances, which leaves opportunities for better suited organism to emerge and take over. The next chapter explores the overall microbiology

of the AD process before focusing on the specific microbes that become crucial for converting propionate and acetate when the initially dominant populations responsible for these conversions are inhibited by ammonia

2.3 Microbiology of the AD process

The microbial degradation process in AD consists of several interconnected steps often divided into the four main stages: hydrolysis, acidogenesis, anaerobic oxidation (including acetogenesis), and methanogenesis (Figure 1). Each stage involves distinct biochemical transformations that collectively enable the conversion of complex substrates into methane and carbon dioxide.

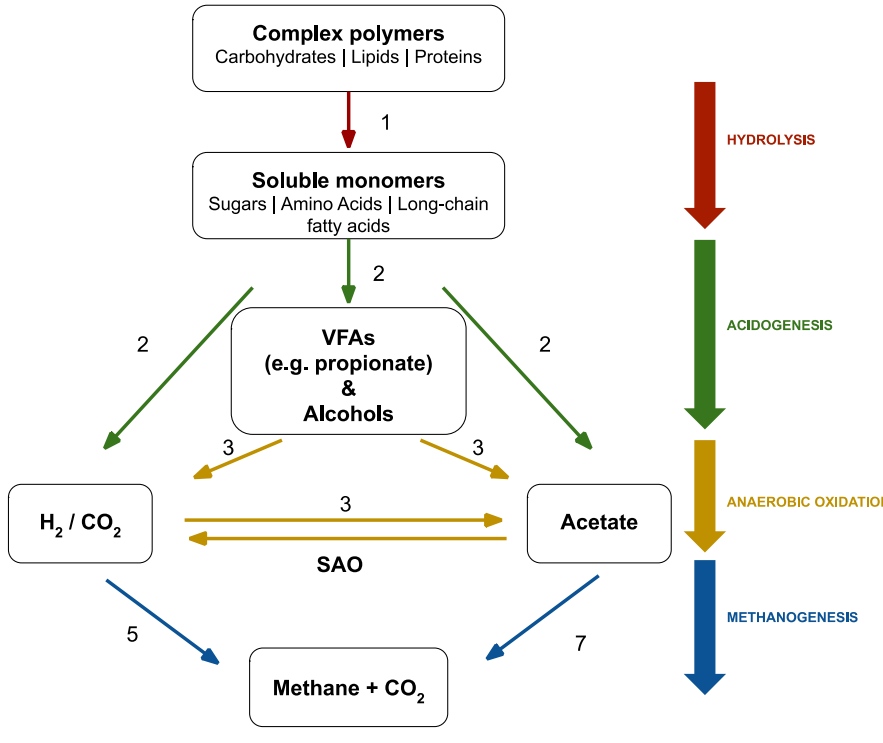

Figure 1: The four main stages of anaerobic digestion, in which complex organic material is converted into carbon dioxide and methane. Syntrophic propionate oxidation (SPO) is part of anaerobic oxidation but not shown. SAO – Syntrophic acetate oxidation

Hydrolysis

The substrate added to AD systems primarily consist of large, complex organic molecules such as carbohydrates, lipids, and proteins. In the first AD stage, these organic molecules are hydrolysed to soluble oligomers and monomers by extracellular enzymes produced by hydrolytic microorganisms. This step is crucial for reducing the size of organic material to a level that allows cellular uptake and further intracellular processing. Hydrolytic microbes can be either generalists, capable of degrading a wide range of organic polymers, or specialists, focusing on a narrower range of substrates. The rate of hydrolysis is influenced by the structural complexity of the organic material, and can for some recalcitrant materials (lignocellulosic material, sewage sludge etc.) be the rate limiting step of the overall AD process (Pavlostathis and Giraldo-Gomez, 1991; Adekunle and Okolie, 2015; Borja and Rincón, 2017).

Acidogenesis

Following hydrolysis, fermentative microorganisms convert the hydrolytic products into a range of intermediate products including VFAs, alcohols, hydrogen gas, carbon dioxide, and ammonia, sometimes called intermediate products. This stage is characterised by a high microbial diversity and involves various fermentation pathways that generate a mixture of metabolic end-products (Schnürer and Jarvis, 2018).

Anaerobic oxidation (Acetogenesis)

Most intermediates from acidogenesis cannot be directly converted to methane by methanogens. As such, anaerobic oxidation (acetogenesis) is the bridging step between acidogenesis and methanogenesis, through the conversion of various intermediate fermentation products such as VFAs (excluding acetate) and alcohols which are further oxidised into acetate, hydrogen and carbon dioxide (Angelidaki et al., 2011).

Methanogenesis

The final stage of the AD process is carried out by methanogens, a phylogenetically diverse group within the archaeal domain. These microorganisms thrive in anaerobic environments where alternative electron acceptors with low redox potentials are scarce (e.g., nitrate, sulphate, or ferric iron). Methanogenesis occurs through three known pathways. The first is hydrogenotrophic methanogenesis, in which carbon dioxide is reduced , typically

using hydrogen as electron donor. The second is acetoclastic methanogenesis, where acetate is disproportionated into methane and carbon dioxide. The third pathway, methylotrophic methanogenesis, involves the conversion of methylated compounds such as methyl sulphides, methanol, and methylamines (Thauer et al., 2008). Among these pathways, acetoclastic and hydrogenotrophic methanogenesis are the most relevant to the AD process, as the substrates required for methylotrophic methanogenesis are generally not readily available (Conrad, 2020). During mesophilic, low-ammonia conditions, approximately 50–75% of methane production originates from the acetoclastic pathway (Jiang et al., 2018). However, as ammonia concentrations increase, the hydrogenotrophic pathway becomes more significant due to the higher ammonia tolerance of hydrogenotrophic methanogens (Koster and Lettinga, 1984; Angelidaki and Ahring, 1993; De Vrieze et al., 2015; Fischer et al., 2019; Wang et al., 2022). Methanogenesis is often considered the rate-limiting step in AD processes that operate on easily degradable substrates, such as food waste, municipal wastewater, and stillage, where hydrolysis is not the limiting factor (Yuan and Zhu, 2016). This limitation is attributed to the low growth rates of methanogenic communities (Kleinsteuber, 2018).

2.4 Syntrophic acid oxidation in the AD system

Syntrophy is a termed used for microbial relationship, in which both partners depend on each other to catabolise a substrate that cannot be catabolised be either one alone (Morris et al., 2013). Such obligate relationship is crucial for converting acids with three or more carbons such as propionate and butyrate formed as intermediates in AD into compounds suitable for methanogenesis (acetate, CO_2, H_2). Here, syntrophic bacteria convert the acids into substrates suitable for methanogenesis (acetate, CO_2, H_2). Acetate a two-carbon acid, which is also produced during acidogenesis, serves as a direct substrate for acetoclastic methanogens under stable, low ammonia-conditions.

However, as discussed in Section 2.2.4, elevated ammonia levels have inhibitory effects on the entire AD microbial community, with acetoclastic methanogens being particularly susceptible. This inhibition leads to a build-up of acetate and can also impair the breakdown of other VFAs such as propionate and butyrate (Westerholm et al., 2015). The resulting VFA build-up

exacerbates process instability, reduces methane yield and can under severe conditions lead to complete process failure. Not all organisms are as adversely affected by ammonia toxicity. Some thrive in the ecological niche that emerges when acetoclastic methanogens are impaired. In systems acclimated to high ammonia levels, syntrophic acetate oxidation (SAO), involving a syntrophic acetate oxidising bacteria (SAOB) and a hydrogenotrophic methanogen, often becomes the dominant pathway for acetate conversion (Westerholm et al., 2016; Ruiz-Sánchez et al., 2018; Buhlmann et al., 2019; Singh et al., 2023). In methanogenic systems, propionate is degraded by a syntrophic propionate oxidising bacterium (SPOB) in cooperation with a hydrogenotrophic methanogen and an acetate-utilising microorganism (Müller et al., 2010). This degradation, unlike acetate degradation, is invariably a syntrophic process. However, the specific microbial species involved often vary depending on ammonia levels (Bonk et al., 2018; Singh et al., 2021, 2023). These syntrophic communities are characterised by slow growth rates and limited energy availability, as the available energy must be shared between the syntrophic partners (**Paper I**). Consequently, if an AD system that have not been exposed to elevated ammonia levels suddenly experience a drastic increase in ammonia, the ammonia-tolerant communities required for syntrophic acetate and propionate oxidation may not be sufficiently abundant and active to sustain the overall metabolic flow and maintain process efficiency.

2.5 Syntrophy, thermodynamics, and interspecies electron transfer

What makes a chemical reaction a viable energy source from which energy can be extracted to fuel cellular activity and growth? At the heart of this question is the thermodynamical concept of Gibbs free energy, which defines the portion of a system's energy available to perform work. The total energy of a system, known as the enthalpy (H) is the sum of the free energy (G) and the unusable energy known as the entropy (S) multiplied by the temperature. The total energy of a system, or enthalpy (H), is the sum of its free energy and the unusable energy component, expressed as entropy (S) multiplied by temperature (T), represented as:

$$H = G + TS \tag{2}$$

The difference in free energy (ΔG) for a chemical reaction is the difference in free energy of the products and the reactants:

$$\Delta G = G_{products} - G_{reactants} \quad (3)$$

At constant temperature, this can be expressed in terms of changes in enthalpy and entropy:

$$\Delta G = \Delta H - T\Delta S \quad (4)$$

The sign and magnitude of ΔG determine the thermodynamic favourability of a reaction. If ΔG < 0, the reaction is exergonic, meaning it releases energy and can proceed spontaneously. If ΔG > 0, it is endergonic, requiring energy input. When ΔG = 0, the system is at thermodynamic equilibrium, with no net energy change (Sadava et al., 2014). Gibbs free energy is typically calculated under biochemical standard conditions (ΔG°′): 25 °C, a pressure of 100 kPa , solute concentrations of 1M, gases at partial pressure of 100 kPa, and a pH of 7 (Thauer et al., 1977). In **Paper I**, ΔG°′ was determined for syntrophic propionate oxidation and syntrophic acetate oxidation and hydrogenotrophic methanogenesis:

Propionate oxidation to acetate, carbon dioxide and hydrogen:

$$CH_3CH_2COO^- + 2H_2O \rightarrow CH_3COO^- + CO_2 + 3H_2 (\Delta G^{\circ\prime} = +73.7 kJ/mol) \quad (5)$$

Acetate oxidation to carbon dioxide and hydrogen:

$$CH_3COO^- + H^+ + 2H_2O \rightarrow 2CO_2 + 4H_2 (\Delta G^{\circ\prime} = +54.9 kJ/mol) \quad (6)$$

Hydrogenotrophic methanogenesis:

$$4H_2 + CO_2 \rightarrow CH_4 + 2H_2O (\Delta G^{\circ\prime} = -130.8 kJ/mol) \quad (7)$$

Standard conditions do not accurately represent the environmental conditions under which microbial metabolism typically occurs. Therefore thermodynamic calculations must be readjusted to account for the actual temperature and concentrations or partial pressures of all chemical species involved in the reaction (Dolfing, 2016). This is achieved by first correcting for

temperature using the Gibbs–Helmholtz equation (not shown), followed by adjusting for the concentrations or partial pressures of the chemical species involved, as illustrated in equation 8 for acetate oxidation:

$$\Delta G = \Delta G^{\circ\prime} + RT\ln\frac{[CO_2]^2 * [H_2]^4}{[CH_3COO^-] * [H_2O]^2} \quad (8)$$

Here, activates are indicated by square brackets (e.g., $[H_2]$), which is approximated by the concentration/partial pressure, except for water which has an activity of 1.

Acetate oxidation is endergonic under standard conditions, but by increasing substrate concentration or decreasing product concentration it can be rendered exergonic. This principle underlies the syntrophic relationship between acid-oxidising bacteria and hydrogenotrophic methanogens, which consume H_2 and thereby drive the overall reaction forward. Another way of looking at it is that when combined, the two separate reactions (hydrogenotrophic methanogenesis and SAO) is overall exergonic. The syntrophic partners must navigate a delicate metabolic balance as they have opposite requirements in regard to the concentration of H_2. The acid oxidiser requires low concentrations, whereas the hydrogenotrophic methanogen benefit from higher concentrations. The balance between these conflicting interests defines a narrow concentration range within which both organisms can have exergonic reactions, known as the window of opportunity (Dolfing et al., 2008). On a similar note, some syntrophic microorganisms employ a mechanism known as electron bifurcation to overcome energetic limitations associated with transferring electrons from high- to low-potential donors. In this process the electron pair (or two) from an intermediate potential electron donor is split: an exergonic electron transfer to a high-potential acceptor is directly coupled to an endergonic transfer to a low-potential acceptor. This coupling enables otherwise unfavourable redox reactions to proceed without external energy input, thus allowing cells to conserve energy (Peters et al., 2016; Buckel and Thauer, 2018).

An exergonic reaction is a reaction that releases energy that in principle could be harnessed to perform biological work. But this energy is of no use if the

organism doesn't manage to capture or conserve it. Cells typically capture this energy in high-energy molecules like ATP or by generating ion gradients across membranes, enabling its use in cellular and anabolic processes. Energy conserving mechanisms also decouples catabolic and anabolic reactions, which otherwise would need to occur simultaneously and locally, limiting metabolic flexibility. But what is the minimal amount of free energy a reaction can give of while still being conserved? This threshold is known as the biological energy quantum (BEQ). The biological energy quantum (BEQ) is the estimated energetic cost of pumping one proton across a membrane (12-15kJ). This value is derived from the free energy of ATP hydrolysis divided by the number of protons used by the proton-translocating ATPase to synthesise one ATP molecule (3-4) (Schink, 1997; Schink and Stams, 2002). Experimental validations show that many syntrophic reactions operate close to these thermodynamics limits (Schink et al., 2019). Furthermore, not all conserved energy supports growth; some is required for maintenance energy (ME), the energy spent on cellular processes that does not directly contribute to growth like cellular repair, homeostasis and protein turnover, etc. (Harder, 1997; van Bodegom, 2007; Hoehler and Jørgensen, 2013). ME is not static and can increase if the organism is subjected to a dynamic environment where it needs to adjust for fluctuations in temperature, osmolarity, etc. For energy constrained organisms, where the energy gained from catabolic reactions are close to the BEQ, as is the case for the syntrophic partners, even modest environmental changes can increase ME demands beyond the available energy supply, rendering the environment uninhabitable for their continued survival (Hoehler, 2007).

2.5.1 Transfer of reducing equivalents

As stated in the previous sections, syntrophic acid oxidisers can, by partnering with a hydrogenotrophic methanogen that scavenges H_2, maintain low enough concentrations of these compounds to enable acid oxidation to proceed. However, this is a simplified representation. More specifically, the syntrophic acid oxidisers generate an excess of electrons, temporary held by intracellular electron carriers such NADH, FADH and ferredoxin. These need to be reoxidised in order to be available for subsequent reactions and to sustain the metabolism. Contrary to the acid oxidisers, the hydrogenotrophic methanogen uses electron carriers (ferredoxin, coenzyme F_{420}) to reduce CO_2 to methane. This creates complementary metabolic needs, while acid

oxidisers require electron removal to sustain oxidation, hydrogenotrophic methanogens require electrons for methanogenesis. At the core of this syntrophic relationship is interspecies electron transfer (IET), where electrons are transferred from the syntrophic acid oxidiser (electron producer) to the hydrogenotrophic methanogen (electron consumer). However, the intracellular electron carriers (e.g., NADH, $FADH_2$, ferredoxin) are not directly exchanged between cells. Instead, their redox states are maintained through external electron transfer mechanisms that facilitate electron flow between the syntrophic partners. This electron exchange occurs via two primary mechanisms: mediated interspecies electron transfer (MIET), which involves electron-shuttling compounds and direct interspecies electron transfer (DIET) (Su et al., 2023).

2.5.2 Mediated interspecies electron transfer

In MIET, the electrons produced by the acid oxidisers are transferred to soluble electron–shuttling molecules, such as hydrogen or formate (**Papers I–III**). These molecules diffuse through the environment and are subsequently taken up and used as source of electrons by the methanogen. Hydrogen was first proposed as the main mechanism of interspecies electron transfer (Iannotti et al., 1973), and the role of formate was later highlighted (Boone et al., 1989). Theoretically, any molecule with a redox potential between that of the donor and acceptor could serve as a mediating molecule. Sulphur compounds, cysteine, quinones and riboflavins have all been reported to be involved in MIET (Biebl and Pfennig, 1977; Smith et al., 2015; Zhuang et al., 2017; Huang et al., 2020; Su et al., 2023). Formate has been suggested to be a more suitable carrier than H_2 when the intracellular distances are long, due to the combination of formate having higher solubility and lower diffusivity as compared to hydrogen, which allows for greater concentration gradients surrounding the producer (de Bok et al., 2004; Batstone et al., 2006).

2.5.3 Direct interspecies electron transfer

In DIET, on the other hand, electrons can be directly transferred between partners via conductive pili, membrane-bound electron transport proteins, or abiotic conductive materials such as magnetite, granular activated carbon, or biochar (Lovley, 2017; Park et al., 2018). Unlike MIET through H_2 or formate, where electrons and protons are transported together as H_2/formate, DIET separates these fluxes, only electrons are transferred via conductive

structures while protons diffuse independently. This uncoupling requires the electron-accepting partner to actively import protons to maintain charge balance (Holmes et al., 2018). Compared to MIET, DIET may reduce energy losses by bypassing the need to synthesise, transport, and perform redox transformations of mediating compounds, steps that can lead to wasteful energy dissipation (Lovley, 2011; Cheng and Call, 2016). Moreover, the mediating compound can diffuse away and be lost to the surrounding environment. However, DIET is not entirely free from energy losses as the energy is dissipated during electron transfer between redox cofactors, a process known as activation loss. Modeling by Storck et al. (2016) suggest that activation losses account for the majority (93%) of DIET-related energy losses. Additionally, electrical resistance within biological conductive nanowires and solution resistance due to ion migration between cells contribute further energy losses (Storck et al., 2016). The extent to which DIET occurs during syntrophic acid oxidation is currently unclear**.** Beyond interspecies electron transfer, syntrophic acid oxidisers could theoretically also dispose excess electrons on extracellular electron acceptors such as iron (Fe^{3+}) or sulphate (SO_4^{-2}) if present. These would provide an alternative electron sink, allowing acid oxidation to proceed as there is extracellular acceptors left to reduce.

Determining the free energy gain in reactions relying on DIET is less straightforward than for the MIET counterpart (Dolfing, 2024). Unlike MIET, where feasibility depends on the concentration of mediating compounds such as H_2, DIET reactions are independent of these, being primarily driven by voltage differences between the syntrophic half-reactions. DIET is also more sensitive to pH fluctuations, as protons are required to maintain charge balance and must diffuse between the DIET partners. Additionally, the actual energy gain depends on the interspecies reduction potential, which can vary between microbial partners and must be determined to accurately quantify the energy gained by the syntrophic partners (Cheng and Call, 2016).

2.6 Identifying and studying ammonia-tolerant communities

As previous sections have concluded, the syntrophic community involved in acid oxidation is characterised by overall low energy yields shared among syntrophic partners, often operating close to thermodynamic equilibrium resulting in low growth rates. Current knowledge of these ammonia-tolerant syntrophic communities remains limited. Several factors hinder their study, both in full-scale AD processes and through cultivation-based approaches. These include the low abundance of syntrophic populations within microbial communities, challenges in isolating syntrophs due to their obligate metabolic dependencies, and limitations in molecular techniques arising from insufficient representation in sequencing data. These factors and alternatives to overcome the challenges will be discussed in the following sections.

2.6.1 Challenges

Studying syntrophic communities presents numerous challenges. First, the AD process is a complex microbial ecosystem in which the syntrophic community constitutes only a minor fraction (Campanaro et al., 2020). This makes it difficult to distinguish their specific interactions from those of the broader microbial population. This scarcity also means they are often "drowned out" by the activity and presence of other microbes, making it difficult to achieve sufficient sequencing depth, as sequencing resources are "wasted" on non-syntrophic organisms. Furthermore, the syntrophic nature of these microorganisms makes isolation and cultivation in pure cultures challenging, if not impossible. Their metabolism depend on intricate interactions with partner organisms, that are difficult to recreate under laboratory conditions if disrupted (Kapinusova et al., 2023; Geesink et al., 2024). Still, co-cultures have been successfully reconstructed, where one syntrophic acid oxidising bacterium cooperate with a hydrogenotrophic methanogen bringing significant knowledge into the area (Hidalgo-Ahumada et al., 2018; Sedano-Núñez et al., 2018; Doloman et al., 2024). Still, given that molecular analyses indicate that many syntrophic organisms remain uncultured (Kim et al., 2022; Cheng et al., 2025), alternative methods to study these syntrophic interactions is needed. Consequently, significant insights into syntrophic metabolism can also been gained from molecular and cultivation studies using defined enrichment cultures (Singh 2023, **Paper I–III**). This reduces some

of the complexity compared to examining them in context of full the AD process.

In molecular in studies of microorganisms, which metabolism has not been comprehensively studied, such as syntrophic organisms, present several bio-informatic challenges. These include a high proportion of uncharacterised proteins and a lack of well-defined reference pathways. These challenges complicate functional predictions and metabolic reconstructions based on metagenomic and transcriptomic data, making it difficult to infer the precise roles of the syntrophic partners and the mechanisms underlying their cooperation. Furthermore, the reactions involved in syntrophic interactions often occur near thermodynamic equilibrium, further complicating efforts to determine the directionality of the metabolic process. While transcriptome-based analyses can reveal the expression of genes associated with a particular pathway, they do not necessarily indicate the direction in which the pathway is operating. This problem is exemplified in **Papers I–III** in which two abundant microorganisms, believed not to be directly involved in the syntrophic acid degradation. This is further discussed in section xx.

The SPO in high ammonia systems necessitates SAO for the complete conversion of propionate into methane and CO_2. Thus, the microbial interactions for the syntrophic propionate degrading enrichment community at minimum requires interactions or exchange of products between: SPOB:methanogen, SPOB:SAOB and SAOB:methanogen. The complex interplay makes it difficult to disentangle the individual syntrophic interactions.

2.6.2 Source of the enrichment culture

Enrichment culturing is a technique used to selectively promote the growth of specific microorganism(s) from a mixed community by controlling growth conditions to favour their proliferation. This can be achieved through various cultivation methods, including continuous or sequential batch cultivations. All the work in this thesis has been conducted on two enrichment cultures previously developed in our research group as part of earlier studies, derived from laboratory-scale CSTRs (Singh et al., 2021). In short, these reactors were inoculated with sludge obtained from a high-ammonia (5.4 g L^{-1} NH_4^+-N) biogas reactor degrading food waste supplemented with albumin. The enrichment CSTRs were then continuously supplied with a bicarbonate-

buffered basal medium containing 0.3M ammonium chloride and either 0.1 M sodium propionate or sodium acetate as the carbon source. The enrichment CSTRs were operated for over 144 days before the enrichment culture was withdrawn and transferred to anaerobic serum bottles. Once transferred to serum bottles, they have been grown in bicarbonate-buffered medium supplemented with 0.3M ammonium chloride with either acetate or propionate as substrate through multiple sequential transfers. In anaerobic culture medium yeast extract is normally included to provide essential nutrients that certain microorganisms are not able to synthetise themselves, such as certain amino acids, vitamins and nucelotides (Groher and Weuster-Botz, 2016; Hendriks et al., 2018). However, in **Papers II–III** yeast extract was omitted to further enrich the systems for the organisms involved in the syntrophic degradation. This essentially removed all carbon sources except for the substrate (acetate/propionate) and cysteine, which is added as a reducing agent. The removal of yeast extract resulted in longer lag phases, but the enrichment cultures have so far managed to survive repeated transfers over multiple years.

2.7 Methods of studying anaerobic microorganisms

2.7.1 Cultivation of anaerobic microorganism

Much of the methodology for cultivating anaerobic microorganism are based on the work of Hungate (1969). In short, the microorganisms are grown in an air-tight container of which there exists many variants, but that typically is made of glass and sealed with butyl rubber stoppers held in place with screwcaps or aluminium seals that are crimped in place (Hanišáková et al., 2022). In this thesis work, serum bottles made of glass with butyl rubber stopper, sealed with aluminium screw caps have been used (**Papers I–III**). Although numerous formulations of anaerobic growth media exist (Hendriks?), a bicarbonate-buffered medium was used in this study prepared as described by Westerholm et. al (2010). This resemble anaerobic medium used in co-cultivation of syntrophic microorganisms, with some modifications (Stams et al., 1993; Hidalgo-Ahumada et al., 2018). In the medium preparation, several steps are taken to ensure that the medium and cultivation vessel is anaerobic, including: boiling of the medium to reduce the amount

of oxygen, transferring the boiled medium while flushing serum bottles and the medium with N_2-gas, exchanging the gas phase of the sealed bottles to a mixture of N_2/CO_2 in 80/20 v/v ratio. Then the reducing agents L-cysteine HCl (0.5 g L^{-1}) and Na_2S (0.24 g L^{-1}) are added to remove trace amount of oxygen still present in the bottle (**Paper I**).

The classic method for cultivating anaerobic microorganisms involves batch cultivation in serum bottles, where substrate is added to the culture and allowed to degrade completely. Additional substrate may be introduced once once the initial supply is depleted, creating a semi-batch setup (**Paper I–II**). This approach offers several advantages: it is simple, cost-effective, and allows for a high number of replicates compared to the more resource-intensive CSTRs. However, the non-steady-state conditions in batch systems, such as varying substrate levels and formation of high levels of products, can be a contrasting parameter to the relatively stable conditions maintained in CSTRs. Batch cultures also follow well-defined growth phases (lag, exponential, stationary, death). This provide insight into microbial dynamic but may not occur in the same extent in continuously-fed industrial AD processes. To minimise inherent heterogeneity of replicate batch cultivation in **Papers I–III** substrate initially supplemented was allowed to be fully degraded before additional substrate was introduced (spiked). This approach ensured that cultures were at a comparable stage of degradation prior to experimental procedures, such as RNA extractions. Despite this precaution, variations in degradation rates were still observed across identical experimental setups, even after the second substrate addition (**Papers I–II**). These variations in degradation rates were likely influenced by the duration of the preceding starvation phase, which may have affected the activity of the syntrophic community.

2.7.2 Imaging microbial interactions and aggregation

Observation of microbial aggregation in serum bottles is limited to macromorphological observations. To follow the dynamics of microbial growth in the serum bottles at a macro-scale, a time-lapse system was constructed and the observations were linked to the acid degradation dynamics (**Paper IV**) (See section 4.2). Nevertheless, to observe the microbial interactions on a cell-to-cell basis in these cultures samples need to be withdrawn from the bottles and analysed by placed on microscope slides for direct observation.

However, this only gives a snapshot of a dying microbial community exposed to oxygen, disrupted by the sampling procedure. One possibility would have been to perform this work in an anaerobic glove box. However, most microscopes are not compatible with standard anaerobic workstations due to space constraints. In addition, such systems often contain hydrogen in their atmosphere to scavenge residual oxygen, which could interfere with the syntrophic acid oxidation. Microfluidic systems have been highly successful in aerobic microbiology, enabling real time observations of single-cell behaviour under strictly controlled conditions. However, their use in anoxic conditions remains limited due to the technical difficulty of maintaining strict oxygen-free environments (Keating et al., 2024). Despite this, a few notable studies have adapted microfluidic setups to study strict anaerobes. For example, a highly oxygen-sensitive methanogen was cultivated in a polydimethylsiloxane-based microfluidic device enclosed within a sealed, nitrogen-flushed chamber (Steinhaus et al., 2007). In that study, this setup was periodically transferred to an inverted microscope for imaging, allowing the authors to identify optimal growth conditions, including pH, shear stress, and total ammonia concentration. In a similar approach, an oxygen-sensitive sulphate-reducing bacteria was grown in a custom-built, gas-tight microscopy chamber designed for continuous live-cell observation (Fievet et al., 2015). Here, cells were placed on a glass coverslip and overlaid with a thin layer of solidified growth medium, forming an agar pad. The chamber was then sealed to preserve anoxic conditions during imaging. Dujany et al. (2025) demonstrated that 3D-printed laboratory-scale reactors can achieve methane yields comparable to those of conventional designs, highlighting the potential of 3D printing in AD research.

Part of the work of this thesis was the construction of 3D-printed bioreactors with transparent surfaces compatible with microscopy. The aim was to be able to cultivate the microbes in these reactors and to follow the microbial interaction and formation of cellular aggregates in real time, using either a microscope (Lumascope LS720, Etaluma) or at a meso-scale using an in-house built automated time-lapse imaging system for screening purposes (**Paper IV**). Keeping the 3D-printed reactors anaerobic proved a significant challenge. First of all, it is hard to determine whether the bioreactors are anaerobic or not. The growth medium contains a redox indicator (Resazurin) that turns pink when oxidised in the presence of oxygen. However, this

colour shift was hard to detect in the small volume of the reactors, thus the methanogenic activity (F_{420} autofluorescence) was used as a proxy for microbial activity and thus maintained anaerobic conditions. Both the manual assembly and 3D-printing quality introduced variation in the quality of the finished reactors where some immediately became oxygenated. The best-performing reactors showed methanogenic activity after 40 days into the experiment. This however, in the timeframe of the slow-growing syntrophic communities, is not sufficient.

2.7.3 16S rRNA gene amplicon sequencing

To identify the microbial species present in the enrichment cultures and track changes in community composition over time and under different experimental conditions, 16S rRNA gene amplicon sequencing was used in **Papers I–II.** With the rise of sequencing technologies it was discovered that phylogenetic relationships could be determined by comparing conserved genetic regions (Woese et al., 1985; Woese, 1987), later to be known as phylogenetic or taxonomic markers. The 16S rRNA gene soon became the dominant gene to be used as a taxonomic marker, due to it being universally present in both bacteria and archaea and having a mix of both highly conserved and variable regions (Clarridge, 2004). The conserved regions allow for design of broad-range primers that almost universally binds to these regions, while the variable regions facilitate taxonomic differentiation (Clarridge, 2004). Numerous databases containing reference sequences and their corresponding taxonomic affiliation are publicly available including GTDB, SILVA, Greengenes, NCBI GenBank and the WWTP/AD specialised database MIDAS (DeSantis et al., 2006; Quast et al., 2013; Clark et al., 2016; Parks et al., 2022; Dueholm et al., 2024). By comparing the sequencing reads from a microbial sample against these databases the microbial composition of a sample can be determined.

In **Paper I**, the microbial community and syntrophic actors of a syntrophic acetate-degrading enrichment culture were compared to those of a propionate-degrading culture, both originating from the same inoculum. The SAOB and methanogen were found to be the same in both systems. By comparing the community profiles of cultures fed either propionate or acetate, the likely key oxidisers for each substrate were identified based on shifts in relative abundance and later confirmed through meta-omics analysis. In **Paper II**, exploring the impact of mixing on syntrophic acid oxidation, a shift in

microbial composition was observed in acetate-oxidising enrichment cultures after a second acetate addition, marked by an increased abundance of an unclassified species belonging to the genus *Alkaliphilus*.

It should be emphasised that several biases can be introduced in the workflow, including DNA extraction (which may differentially extract DNA from certain taxa, leading to under-representation of some groups) and primer design (as mismatches between primers and target sequences can lead to preferential amplification of certain taxa). Furthermore, differences in 16S rRNA gene copy number across species can lead to over- or underestimation of their abundance. In **Papers I–III,** the high methanogenic transcriptional activity was in stark contrast to the low relative abundance of the methanogen observed in the 16S rRNA gene amplicon sequencing data. Archaea have for example been shown to have lower copy number of the 16S rRNA gene than bacteria, leading to underestimation of their relative abundance (Dyksma et al., 2020; Pan et al., 2023). Furthermore, the universal primer pair (515f/805r) (Herlemann et al., 2011) used in **Paper I–II**, has been shown to have restricted specificity of archaeal 16S rRNA gene, further contributing to the under-representation of the archaeal community (Merkel et al., 2019).

All sequencing data, including 16S rRNA gene data, are compositional in nature, meaning they reflect relative rather than absolute abundances (Gloor et al., 2017). This is because sequencing instruments capture only a fraction of the total DNA or RNA molecules present in a sample. As a result, an increase in one taxon's absolute abundance can cause other taxa to appear reduced in relative terms, even if their actual abundance remains unchanged. Therefore, when discussing 16S rRNA gene abundances, it is important to recognise that they are inherently relative measures. To complement relative abundance estimates from sequencing data, quantitative PCR (qPCR) can be used to measure the absolute abundance of target genes, including the 16S rRNA gene (Ginzinger, 2002). qPCR amplifies a specific DNA target while simultaneously and continuously measuring fluorescence, which increases in manner directly proportional to starting amount of the gene in the sample. In **Paper I,** qPCR was used to quantify the absolute abundance (copies/ng DNA) with primers specific for the identified SAOB and primers for the order to which the main methanogen belonged, interfered from the 16S rRNA gene sequencing. In **Paper II**, the primers targeting this methanogenic group

were used to quantify and compare the methanogenic absolute abundance to that of total bacteria, based on universal bacterial primers described by Maeda et al. (2003).

Analysing a single gene, such as the 16S rRNA gene, provides valuable taxonomic information but does not capture the full metabolic potential of an organism. Whole-genome analysis (metagenomics), on the other hand, allows for the identification of functional genes and metabolic pathways, and provides a more comprehensive understanding of microbial capabilities beyond taxonomy. Additionally, 16S rRNA gene-based taxonomic profiling often lacks the resolution needed to reliably differentiate taxa at the species level which can be resolved using when taking the whole genome into account (Janda and Abbott, 2007; Poretsky et al., 2014).

2.7.4 Whole-genome sequencing and metagenomics

Metagenomics is the untargeted sequencing of all DNA present in a mixed microbial community sample. The approach to metagenomics has evolved alongside advancements in sequencing technology. Early metagenomic approaches involved extracting DNA from environmental samples, fragmenting it into large segments, and inserting these into readily culturable host organisms such as *Escherichia coli*, where the DNA was cloned and amplified prior to sequencing (Handelsman et al., 1998). As sequencing techniques improved over time, the need for amplification through cloning was eliminated. In so-called shotgun sequencing, the DNA is randomly broken up into smaller fragments and subsequently sequenced (Quince et al., 2017). The result of this is a computational puzzle of great proportions, with millions of partly overlapping DNA reads originating from multiple species. To reconstruct the original genomic sequences and make sense of this complex mixture, a bioinformatic workflow is applied. It typically involves several steps, including the assembly of the reads into larger overlapping consensus sequences (*contigs*), often using k-mer-based approaches (Pevzner et al., 2001). A common problem is that assemblies often produce many disconnected contigs that cannot be joined into complete genomes. This fragmentation problem arises from several factors. Low-abundance microbes often exhibit restricted sequencing depth, which can result in gaps in their genome coverage, preventing the assembly of contiguous regions. Additionally, repetitive sequences, both within a species (intra-genomic repeats) and

between species (inter-genomic repeats), pose significant difficulties for correct contig assembly and scaffolding (Quince et al., 2021; Benoit et al., 2024). Sequencing technologies that generate longer reads can help bridge these problematic regions and scaffold contigs. However, these long-read technologies often exhibit higher error rates, which has led to the development of hybrid assembly approaches that combine the accuracy of short-read technologies with the bridging capabilities of long-read sequencing. Following assembly of contigs, the next step is binning, which aims to group assembled contigs that are likely to originate from the same species. This process relies on computational methods that use sequence composition, coverage patterns, and other genomic features to cluster contigs accurately (Quince et al., 2017). This enables the recovery of metagenome-assembled genomes (MAGs), which are reconstructed from metagenomic sequencing data and provide valuable insights into uncultivated microorganisms.

In **Paper I**, high-molecular-weight DNA was extracted from the enrichment culture degrading either acetate or propionate under high-ammonia, mesophilic conditions. Metagenomes were constructed using long-read sequencing with a MinION device (Oxford Nanopore Technologies), resulting in the recovery of ten genomes from the acetate-degrading culture and nine genomes from the propionate-degrading culture.

2.7.5 Metatranscriptomic analyses of syntrophic microorganisms

While metagenomics provides insight into an organism's genetic potential, it does not reveal which genes are actively expressed at a given moment. Transcriptomics, on the other hand, focuses on the study of mRNA transcripts, which gives a snapshot of the gene expression in a specific moment. When extended to all transcripts in a microbial community, the approach is called metatranscriptomics and gives insight into the functional activity of the microbes within the environment.

RNA extraction and isolation are challenging due to RNA's inherent instability and the ubiquitous presence of RNases, enzymes that rapidly degrade RNA. These enzymes are found in nearly all biological environments, including cells, body fluids, and lab surfaces, making RNA degradation a major concern. The most common extraction method involves cell lysis

(mechanical or enzymatic) followed by guanidinium thiocyanate/phenol/chloroform extraction. Guanidinium thiocyanate inhibits RNase activity, while phenol/chloroform-based extraction separates RNA from other cellular components (Chomczynski and Sacchi, 1987; Ian, 2005). The phenol/chloroform approach was used for RNA extraction in **Paper I–III**. Other common approaches for separating the RNA include spin column purification and magnetic bead-based methods (Thermo Fisher Scientific, 2021). The isolated RNA is a mixture of all the types of RNA molecules present in the cells (total RNA), of which the mRNA of interest only constitutes a minor fraction. In bacteria, the majority of total RNA is made up of rRNA (80–90%) (Wahl et al., 2022). Thus, a common approach is to deplete the rRNA in the samples through various methods, effectively enriching the fraction of mRNA (Cheng et al., 2021; Wahl et al., 2022). This makes more of the sequencing resources devoted to sequencing of the mRNA transcripts instead of being wasted on rRNA molecules.

Once isolated, mRNA is analysed using two main approaches, both of which begin with reverse transcription to generate complementary DNA (cDNA). The microarray approach involves hybridizing cDNA to probes on a chip, enabling fluorescence-based detection of known target genes (Lowe et al., 2017). However, this method is less suitable for metatranscriptomics due to its reliance on predefined sequences. Instead, RNA sequencing (RNA-seq) has become the preferred method, as it sequences all transcripts in a sample without requiring prior knowledge, making it a more flexible and comprehensive tool for metatranscriptomic analysis. RNA-seq library preparation typically includes mRNA fragmentation before cDNA synthesis, as transcript lengths often exceed sequencing read lengths. The cDNA is then amplified using PCR to increase the library yield and to ensure sufficient material for sequencing, although PCR-free approaches also exist. Sequencing can be performed in a single direction (single-end) or both directions (paired-end) (Martin and Wang, 2011). In **Papers I–III**, the RNA extraction followed the protocol by Weng and Perman (2024). Initially, obtaining sufficient RNA for sequencing was challenging, with adequate yields only achieved during later stages of batch degradation when biomass concentrations were higher. This necessitated large sample volumes (150 mL per extraction). Consequently, RNA was extracted after the second substrate addition, as earlier time points lacked sufficient biomass. Additionally, due to the

large sample volumes, repeated extractions from the same bottle were unfeasible. In **Paper III**, studying the effect of salt addition (NaCl or NH_4Cl) on syntrophic acid oxidation was assessed both 1 hour and 3 days post-addition to capture early and sustained transcriptional responses. Multiple technical replicates were included to ensure robust analysis of gene expression dynamics across stress phases. Another challenge working with mRNA is that the half-life of mRNA molecules can be in the order of seconds to minutes (Mp, 2006; Carvalhais et al., 2012). Furthermore, the degradation rates can vary between different groups of genes with similar function, housekeeping genes have for example been shown to have lower degradation rates, which could lead to an artificial overrepresentation of these genes (Carvalhais et al., 2012). A common procedure to minimise changes in mRNA profile present at the moment of sampling, is to snap-freeze sample in liquid nitrogen or to transfer them into RNA preserving solution, within seconds of sampling. This poses a problem for the RNA extraction of the enrichment cultures in **Papers I–III**. Since 150 mL sample was used for each sample, they first needed to be centrifuged (4°C, 5500 RPM for 30 minutes), before the cell pellets were transferred to RNA preserving guanidinium thiocyanate-containing solution. Although the transfer from anaerobic serum bottles to 50 mL Falcon tubes was performed under continuous N_2 flushing and the tubes were centrifuged with closed lids, some oxygen exposure was unavoidable. As a result, transcriptional activity likely continued for up to 30 minutes after sampling, potentially altering gene expression compared to the strictly anaerobic conditions in the culture bottles. In order to minimise the impact of this treatment the centrifugation tubes were cooled on ice during pouring and centrifugation was conducted on low temperature. Furthermore, the conditions were identical for all samples, which in theory should be accounted for in the differential expression analysis.

Bioinformatic analysis of transcriptomic data begins with pre-processing, including quality control to remove low-quality reads and primer sequences. It is also common to in-silico filter out rRNA transcripts that made it past the rRNA depletion step, using tools like SortMeRNA (Kopylova et al., 2012). The next step is transcriptome assembly, where fragmented reads are reconstructed into transcripts (Martin and Wang, 2011; Raghavan et al., 2022). This can either be done in a reference-based approach, using pre-existing reference genome(s) which the reference reads are mapped against, or,

alternatively, in the de novo assembly approach, where transcripts are reconstructed from reads based on sequence overlap using k-mer based methods (Grabherr et al., 2011). Because de novo assembly lacks functional annotations from reference genomes, assembled transcripts must be annotated using external databases to infer biological functions. Reference-based assembly requires less sequencing depth and provides direct functional insights. Since metagenomes had been assembled from the enrichment culture (**Paper I**), a reference-based approach was used in **Papers I–III**, quantifying reads against the constructed metagenomes using the pseudo-alignment tool Salmon (Patro et al., 2017). This resulted in transcript counts, representing the number of sequencing reads that originated from a particular gene in each sample. It is typically presented as matrix where each row is a gene and the columns samples, known as a count-matrix. By comparing these gene expression levels across experimental sample groups, genes that are differentially expressed (DE), i.e., statistically up- or down-regulated between the conditions compared, can be identified. This allows for insights into the biological processes and pathways that are affected by the experimental conditions. Since there can be a big biological variation in gene expression and for statistical power in the differential expression analysis, biological replicates are needed for the analysis. Before comparison of the experimental groups the count data has to be normalised to account for factors such as differences in library size, gene length etc. One of the more commonly used tools is DESeq2, which was used in **Paper I–III**. It performs differential expression analysis by modelling read counts using a negative binomial distribution, normalising for library size and dispersion, through so-called median of ratios normalisation. In short, the row-wise geometric mean is calculated for each gene, the ratio of each gene's raw count to this reference is computed for each sample and the median of these ratios per sample is taken as the size factor, and raw counts are divided by their respective size factors to obtain the normalised counts.

What additionally complicates metatranscriptomic studies is the difficulty in distinguishing whether an observed changed is due to changes in expression activity or changes in the abundance of the microbe in question (Klingenberg and Meinicke, 2017; Chung et al., 2021). In Papers **I–III** the normalisation was therefore performed on a per-genome level, through the partitioning of the count matrix into row sections containing the genes from a specific

genome, which was separately normalised and then merged back together. Most of the metatranscriptomic tools have been developed for the analysis of single-organism datasets in mind.
Gene expression is characterised by a large degree of biological variability, and the DE-analysis requires replicates for statistical power in the analysis. In **Paper I,** only a single merged sample was taken from each condition, which restricted the use of this data to verify what biological pathways that were expressed by the organisms. However, in **Paper II** (only propionate samples) and **Paper III** (all samples) included technical replicates, which made it possible to apply differential expression analysis.

To gain a broader biological understanding, gene set enrichment or pathway enrichment analysis (also called over-representation analysis) was applied in **Paper III**. Instead of focusing on individual genes, these approaches groups genes into sets, such as those involved in specific metabolic pathways. By comparing the expression patterns of entire gene sets across conditions, it becomes possible to identify pathways that are collectively up- or downregulated, aiding the biological interpretation of the results. This is often done using methods like gene set enrichment analysis (GSEA), which ranks all genes by their expression change and tests whether pathway genes cluster at the top or bottom of the list (Subramanian et al., 2005), or through pathway enrichment analysis which tests if a pathway contains more significant genes than expected by chance (Maleki et al., 2020). Still, when working with novel uncharacterised organisms, such analyses are complicated by incomplete or missing pathway annotations, limited reference genomes, and functional gene annotations that may be inaccurate or absent (Liu et al., 2022). Relying on comparisons to known pathways from model organisms can also be limiting, as it risks overlooking novel or species-specific pathways that are not represented in existing databases.

2.7.6 Working with low biomass cultures – single cell transcriptomics

The use of 150 mL of culture volume for RNA extraction aligns with previous studies on methanogenic syntrophic co-cultures, which typically employ volumes ranging from 100 to 500 mL (Men et al., 2012; Liu and Lu, 2018; Doloman et al., 2024). These volumes are notably larger than those used in studies involving non-syntrophic anaerobic batch cultures, which often rely on volumes of just 5–40 mL (Men et al., 2017; Viacava et al., 2022). This

substantial increase in culture volume likely reflects the inherently slow growth rates and low biomass yields characteristic of syntrophic communities. However, the need for large volumes poses several practical limitations. It disrupts the cultivation process and effectively restricts each bottle to a single RNA extraction. Moreover, the high volume complicates rapid sample preservation as cells cannot be promptly snap-frozen or stabilised in RNA-preserving solutions without prior centrifugation to obtain a concentrated pellet. To address these limitations, this section explores a technique capable of detecting and analysing the minute quantities of RNA found in individual cells, called single-cell RNA sequencing (scRNA-seq). While none of the work presented in this thesis employed scRNA-seq, the technique is a promising direction for future research. In addition of being a technique that works with miniscule RNA amounts, scRNA-seq enables the study of gene expression at the level of individual cell(s) and provides insights into population heterogeneity that are often masked in traditional bulk RNA sequencing (Haque et al., 2017). Unlike bulk RNA sequencing, which averages gene expression across a population, scRNA-seq uncovers differences in gene activity among cells of the same type or species, enabling the discovery of rare cell populations and dynamic cellular states. The process begins with isolating single cells, typically using methods such as fluorescence-activated cell sorting or microfluidic droplet-based systems. Once isolated, the cells are lysed, and their RNA is captured and enriched. For eukaryotic cells, this typically involves poly-A tail enrichment, whereas prokaryotic cells, lacking poly-A tails, require alternative RNA capture techniques. The captured RNA is then reverse transcribed into complementary DNA (cDNA), barcoded, amplified, and sequenced. The unique barcodes allow sequencing reads to be traced back to their respective cell of origin. Compared to eukaryotic organisms, bacteria present several challenges for scRNA-seq, including significantly lower RNA content (approximately 100 times less than typical eukaryotic cells), reduced RNA stability, difficulties in cell lysis due to rigidity and toughness of bacterial cell walls, the absence of polyadenylation, and generally lower mRNA copy numbers (Homberger et al., 2022). Therefore, specialised or modified scRNA-seq approaches are required for studying bacterial (prokaryotic) communities (Sheng et al., 2017; Blattman et al., 2020; Kuchina et al., 2021; Ma et al., 2023; McNulty et al., 2023; Wang et al., 2023).

2.8 Definition of a species

The definition of a eukaryotic species is typically based on reproductive isolation, where barriers to gene flow define species boundaries (Mayr, 1942). This definition does not apply to prokaryotes, which reproduce asexually and exchange genetic material through horizontal gene transfer, enabling gene flow across distantly related lineages and blurring species boundaries. Consequently, a so-called polyphasic approach is used for prokaryotic taxonomy, integrating phenotypic, genotypic, and phylogenetic data (Vandamme et al., 1996). Traditionally, DNA–DNA hybridization (DDH) has been the standard method for assessing genome sequence similarity, with a 70% similarity threshold used to define species boundaries (Wayne et al., 1987). This method is labour-intensive, and with the advent of high-throughput sequencing technologies, alternative approaches that offer faster and more cost-effective analyses were adopted. The 16S rRNA gene is widely used as a molecular marker for bacterial taxonomy, as discussed in the section 2.7.3. A sequence similarity threshold of 98.65% has been proposed for species demarcation (Kim et al., 2014), however, its applicability is debated, as many bacterial taxa do not conform to this threshold, highlighting the gene's limited resolution for species demarcation (Rossi-Tamisier et al., 2015). When whole-genome data are available a higher resolution for species classification can be obtained. Common approaches are digital DNA–DNA hybridisation (dDDH) with a species demarcation threshold of 70% (Goris et al., 2007). Another widely used metric is average nucleotide identity (ANI), which assesses nucleotide-level similarity in homologous genomic regions, with a suggested species demarcation threshold of 95% (Konstantinidis and Tiedje, 2005; Varghese et al., 2015).

Advances in sequencing technologies have revealed a vast diversity of microbes, most of which remain uncultivated. However, under the International Code of Nomenclature of Prokaryotes (ICNP), a taxon name is only validly published if the organism is isolated and cultivated in pure culture. To address the classification of uncultivated microbes identified through genomic and ecological data, Murray and Schleifer (1994) proposed the *Candidatus* designation as a provisional category. The 2022 ICNP revision maintains the requirement for pure cultures in validly published nomenclature but acknowledges *Candidatus* as a useful designation for yet uncultivated taxa supported by genomic data (Oren et al., 2023). When proposing a

Candidatus taxon, genomic information, phylogenetic placement, and relevant biological data, such as morphology, physiology, metabolism, reproductive features, and environmental context, must be included. The name *Candidatus* is italicised and followed by the taxon name, adhering to ICNP naming conventions (Oren et al., 2023). In **Paper I**, a novel hydrogenotrophic methanogen was identified from metagenomic data and given the provisional name '*Candidatus* Methanoculleus ammoniitolerans'. Its genome was 90.7% complete and exhibited an ANI of 83% and a dDDH of 28% compared to the nearest sequenced *Methanoculleus* species. In addition to genomic data, the paper also characterised the morphology, physiology, metabolism and environmental context of the microbe.

As genome-based taxonomy gains traction, debates continue on whether genome sequences alone should suffice to formally name an organism in the absence of pure cultures, and whether the provisional *Candidatus* category should be regarded in official nomenclature and given priority, i.e., the principle that the first validly published name of an organism should take precedence over later names, which currently does not apply to the *Candidatus* status. Proponents argue for a more inclusive and comprehensive taxonomy that reflects the vast diversity of microbial life, much of which remains inaccessible through cultivation-based methods (Sutcliffe, 2015; Whitman, 2016; Konstantinidis et al., 2017; Whitman et al., 2019; Rossello-Mora et al., 2020). Opponents emphasise the need to integrate both genomic and phenotypic data, cautioning that reliance on sequence-based classification alone could lead to nomenclatural instability, misclassification due to technological limitations in genome assembly, and a lack of ecological and functional insights (Bisgaard et al., 2019; Overmann et al., 2019).

3. Syntrophic Metabolic cooperation

This section will discuss the syntrophic acid degrading community, the taxonomy and metabolic pathways used by the SPOB, the SAOB and their methanogenic partners, with an emphasis on the organisms identified in the enrichment study laying ground for **Papers I–III**. The following section also explores the potential role of two other microorganisms that were found to be both abundant and transcriptionally active in the syntrophic enrichment cultures.

3.1 Taxonomy and metabolic pathways

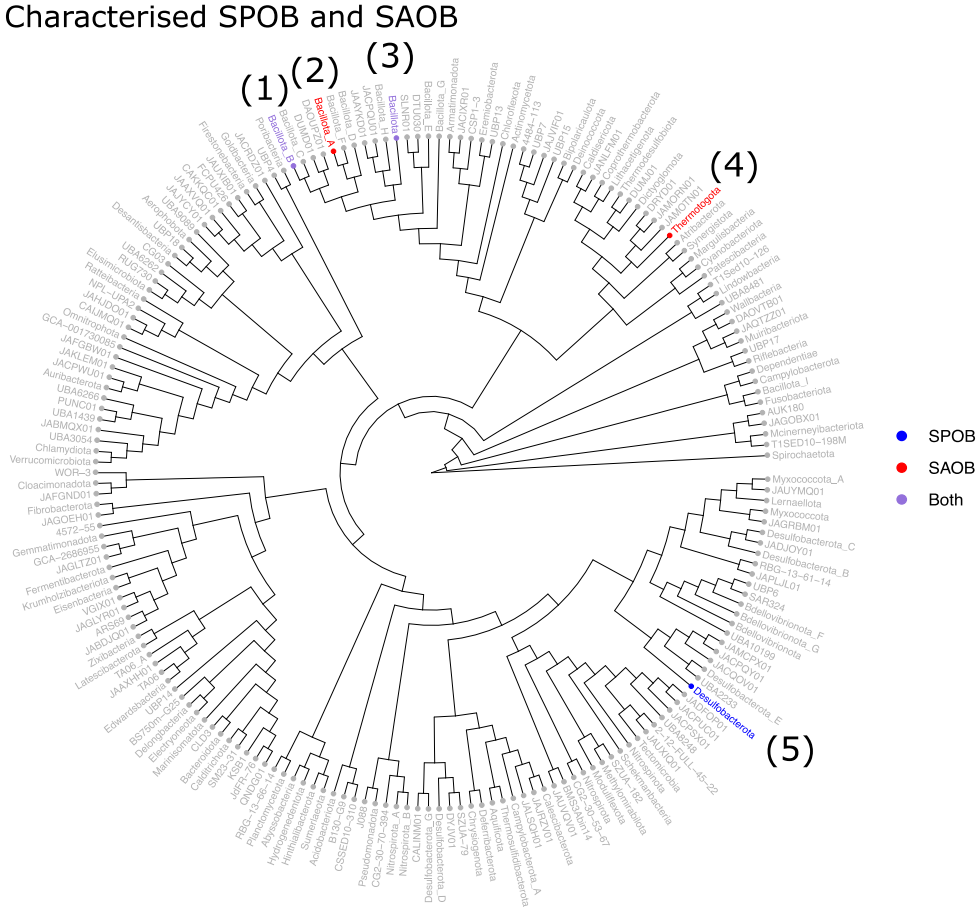

Figure 2: Phylogenetic tree at the phylum level, illustrating the placement of all characterised SAOB and SPOB: (1) *Bacillota_B*, (2) *Bacillota_A*, (3) *Bacillota*, (4) *Thermotogota*, (5) *Desulfobacterota*. Based on the GTDB 120 release.

3.1.1 The phylogeny and pathways of SPOB

To date, several SPOB have been isolated and characterised, while others remain known only through metagenomic data. A vast majority of the characterised species have been isolated from engineered systems, although some have been isolated from environmental methanogenic ecosystems, such as oil reservoirs, rice paddies, and aquatic sediments (Westerholm et al., 2022).

Characterised SPOB include the genera *Pelotomaculum* and *Desulfofundulus* (phylum *Bacillota*_B, Figure 2 label 1), as well as *Smithella*, *Syntrophobacter*, and *Syntrophobacterium* (phylum *Desulfobacterota,* Figure 2 label 5). Meta-omic studies have revealed new linages with the potential to oxidise propionate, in some cases branching outside the taxa of currently characterised SPOB (Figure 2). Examples include '*Ca*. Propionivorax syntrophicum' identified in a propionate enrichment from a full-scale anaerobic digester treating wastewater sludge (Hao et al., 2020) or the new phylum *Cloacimonetes*, members of which have been identified in both mesophilic and thermophilic reactors (Pelletier et al., 2008; Dyksma and Gallert, 2019). Of particular interest to this thesis, is the active SPOB in the enrichment culture, '*Ca*. Syntrophopropionicum ammoniitolerans' (Singh et al., 2021), belonging to the phylum of *Bacillota*_B (Figure 2, label 1). It was detected in a lab-scale mesophilic high-ammonia CSTR, through molecular analysis in comparison with parallel operating acetate-fed reactors. In **Paper I**, the use of 16S rRNA gene amplicon sequencing and meta-omic sequencing methologies were used to confirm that this species was the active SPOB in the enrichment culture.

A vast majority of SPOB, including '*Ca*. S. ammoniitolerans', utilise the methylmalonyl-CoA pathway (mmc pathway) for propionate oxidation (Kosaka et al., 2006; Singh et al., 2021; Westerholm et al., 2022)(**Papers I-III**). The mmc pathway includes 11 steps, in which propionate is activated by the addition of a CoA group and ultimately transformed to acetate through the intermediaries methylmalonyl-CoA, succinyl-CoA, succinate, fumarate, malate, oxaloacetate and pyruvate, acetyl-CoA (Figure 3). One net ATP is predicted to be generated by substrate-level phosphorylation per propionate molecule degraded as well as the release of three electron-pairs (Sieber et al., 2018).

The only other known pathway to be used for SPO is the dismutation pathway, only observed by one species in the genus *Smithella*. In this pathway, two propionate molecules are combined forming a 6-carbon intermediary that is dismutated into an acetate and butyrate molecule. The butyrate molecule is then further converted to two molecules of acetate using β-oxidation (Liu et al., 1999). Propionate conversion either via lactate or

hydroxypropionyl-CoA have been suggested on a theoretical basis, but have not been confirmed experimentally (Patón et al., 2020).

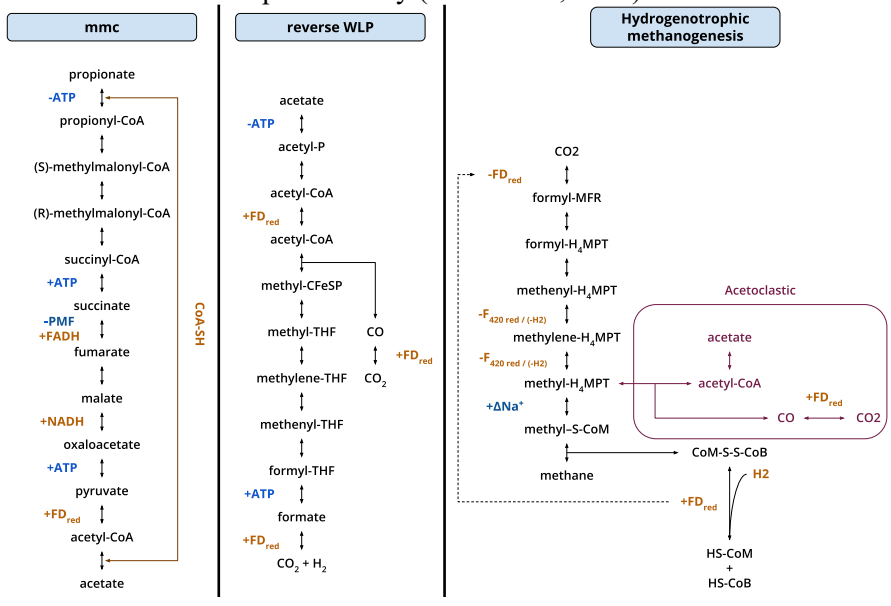

Figure 3: Schematic representation of the main metabolic pathways. Methylmalonyl-CoA pathway (mmc–pathway) (Left), reverse Wood–Ljungdahl pathway (reverse-WLP, middle), Hydrogenotrophic methanogenesis (right).

3.1.2 The phylogeny and pathways of SAOB

To date, five syntrophic acetate oxidising species have been isolated and characterised. Two are thermophilic: *Pseudothermotoga lettingae* and *Thermacetogenium phaeum* (Hattori et al., 2000; Balk et al., 2002) . The remaining three are meophilic: *Tepidanaerobacter acetatoxydans, Schnuerera ultunensis, and Syntrophaceticus schinkii* (Schnürer et al., 1997; Westerholm et al., 2010, 2011). In addition to these isolated and characterised SAOB, potential candidates have been identified through molecular methods including '*Ca*. Syntrophonatronum acetioxidans' (Timmers et al., 2018) and various studies have identified SAOB candidates based on genomic potential (Zeng et al., 2024; Cheng et al., 2025). In **Paper I**, *S. schinkii* was identified as the active SAOB in the enrichment cultures, based on 16S rRNA, metagenomic, and metatranscriptomic data.

Among the characterised SAOB, *T. phaeum, S. schinkii*, and *T. acetatoxydans* oxidise acetate via the Wood–Ljungdahl pathway (WLP), a well-established route for acetogenic metabolism (Figure 3). This ancient pathway enables the autotrophic acetate production of acetate from CO_2 and H_2. During SAO, the pathway is operated "reverse" direction, which is thermodynamically unfavourable under standard conditions, enabled by the consumption of H_2 by the hydrogenotrophic partner. In contrast, *S. ultunense* and *P. lettingae* lack key genes for the WLP, suggesting they rely on alternative metabolic routes, currently not determined. One proposed alternative route, suggested for several taxa (Zhu et al., 2020; Zeng et al., 2024), is the glycine synthase reductase pathway (GSRP), in which the glycine cleavage system (GCS) is used in conjunction with part of the enzymatic machinery of the WLP, with glycine as a key intermediary. However, the GSRP has never been experimentally confirmed to function in this theoretical acetate-oxidising direction and should be interpreted with caution until experimentally verified.

3.1.3 The phylogeny and pathways of the hydrogenotrophic methanogens

Methanogenic activity, i.e., the production of methane as a by-product of energy metabolism under anaerobic conditions, was for a long time believed to be exclusive to the phylum of *Methanobacteriota* comprising the orders *Methanobacteriales, Methanomicrobiales, Methanococcales, Methanopyrales, Methanosarcinales*, and *Methanomassiliicoccales* (Thauer et al., 2008). However, recent genomic studies have expanded our understanding of methanogen diversity, revealing methane metabolism-related genes in other archaeal lineages with multiple example within the phylum of *Thermoproteota* (Evans et al., 2015; Borrel et al., 2016; Vanwonterghem et al., 2016; Berghuis et al., 2019). These findings suggest that methanogenesis may have evolved earlier than previously assumed and is more widespread across the archaeal domain, though uncertainty remains as most non-*Methanobacteriota* candidates lack experimental validation of methanogenic activity. These lineages are less relevant to the AD process, although they have been detected in some reactors. For example, *Thermoproteota*-affiliated metagenomes have been detected in AD systems, where they were suggested to exhibit hydrolytic activity (Maus et al., 2018).

The major methanogenic taxa in AD systems, however, belong primarily to the *Methanobacteriota*. A study that reconstructed metagenome-assembled genomes (MAGs) from publicly available metagenomic datasets of AD systems revealed that 35% of the MAGs contained complete or near complete pathways for acetoclastic methanogenesis, primarily from the classes *Methanomicrobia* (72%) and *Methanobacteria* (24%). Additionally, 36% of the genomes harboured complete or near-complete pathways for hydrogenotrophic methanogenesis, with the vast majority (76%) belonging to *Methanomicrobia* (Centurion et al., 2024). In **Paper I**, the methanogen in the enrichment culture was identified to belong to the genus *Methanoculleus* of the order *Methanomicrobiales.* Whole genome comparisons to other member of the genera showed that it was sufficiently different to qualify as a novel species, and the provisional name '*Ca*. Methanoculleus ammonitolerans' was proposed.

Methanogens perform methane production via three primary pathways: hydrogenotrophic (CO_2 reducing), acetoclastic, and methylotrophic methanogenesis, all of which converge on the final, methane forming conserved step catalysed by the enzyme methyl-coenzyme M reductase (MCR) (Kurth et al., 2020; Garcia et al., 2022). Of these, the hydrogenotrophic and acetoclastic are of most relevance to the AD process. Hydrogenotrophic methanogenesis follows a series of enzymatic steps that overlap with the methyl branch of the WLP (Figure 3), but with archaeal homologous enzymes. However, it differs in the specific methyl carriers and cofactors involved, particularly the use of tetrahydromethanopterin (H_4MPT) instead of tetrahydrofolate (H_4F) (Fuchs, 2011). The process begins with the reduction of CO_2 to formyl (HCO^-), which is then bound to methanofuran (MFR) in a reaction catalysed by formylmethanofuran dehydrogenase (Fwd). The HCO^-group is then transferred to tetrahydromethanopterin (H_4MPT) by a formyl transferase (Ftr) to form HCO-H_4MPT. Through successive reductions, HCO-H_4MPT is converted into methenyl-H_4MPT (Mch), methylene-H_4MPT (Mtd), and methyl-H_4MPT (Mer) (Shima et al., 2020). Conversely, in acetoclastic methanogenesis which is exclusive to the order *Methanosarcinales,* acetate is activated to acetyl-CoA, which is then cleaved into a carbonyl and a methyl group. The methyl group is transferred to tetrahydromethanopterin (H_4MPT) forming methyl-H_4MPT, while the carbonyl group is oxidised to CO_2 (Garcia et al., 2022). In both pathways, the methyl-H_4MPT is transferred to

coenzyme M (CoM) by methyl-H_4MPT:CoM methyltransferase (Mtr), forming methyl-CoM. The methyl group is then reduced to methane using coenzyme B as electron donor, producing a heterodisulfide (CoM-S-S-CoB). The carbonyl group formed in acetoclastic methanogens are oxidised to CO_2 with electrons transferred to ferredoxin. For both types of methanogenic metabolism, energy is conserved during the exergonic transfer of the methyl group to CoM, a process that is coupled with sodium ion translocation across the membrane. This generates a sodium motive force, which can then be utilised to drive ATP synthesis (Thauer et al., 2008; Evans et al., 2019; Garcia et al., 2022).

In **Paper I**, '*Ca*. M. ammonitolerans' was demonstrated to express all genes for the hydrogenotrophic methanogenesis pathway. In this pathway, the electron carriers ferredoxin and coenzyme F_{420} are used during the reduction of CO_2. In order to sustain methanogenesis these carriers need to be re-reduced, typically with electrons from H_2 or formate. This is the reason why the methanogen can act as electron sink, for the excess of reducing equivalents generated by the syntrophic acid oxidising partner. F_{420} is regenerated either by H_2 via hydrogenases (with variant depending on Ni availability, see section 3.2.1) or by formate through the action of a F_{420} dependent formate dehydrogenase (Wood et al., 2003; Thauer et al., 2010). However, ferredoxin has a lower redox potential than H_2 and therefore cannot be reduced using H_2 (or formate) alone. It therefore has to be driven by some other exergonic process. The reduction of heterodisulfide using H_2 is such a process, and by coupling these two redox reactions the overall reaction is made feasible. This is achieved by electron bifurcation, where the electron pair donated by H_2 is split, with one of the electrons going to ferredoxin and the other to cleave the disulfide bond (Buckel and Thauer, 2018). The cleavage of CoM-S-S-CoB driving the reduction of ferredoxin used at the initial step, renders the entire pathway a cyclical process, called the Wolfe cycle (Rouvière and Wolfe, 1988; Kaster et al., 2011; Thauer, 2012).

Cyclical processes like this have an intrinsic problem. If intermediaries are lost, for example when used for anabolic processes or where the coupling of the first and last step are not fully efficient, the process would eventually grind to a halt as there are no means to replenish the ferredoxin. Therefore, there must exist other ways to replenish the ferredoxin. This can be done

through the hydrogenases Ech or Eha, that utilise either a sodium or proton gradient to drive the unfavourable ferredoxin reduction using hydrogen (Thauer, 2012). In **Paper II,** the identified methanogen '*Ca.* M. ammoniitolerans' was shown to harbour several genes encoding for Fwd, the enzyme catalysing the step where reduced ferredoxin is consumed. Interestingly these *fwd* genes were found at multiple genomic locations, next to different electron donating systems including the bifurcating "Hdr-Mvh" and the hydrogenases Eha and Ech. Additionally, *fwd* genes located next to a formate dehydrogenase, the implication of which is unclear. Formate has a similar reduction potential as hydrogen, and as such cannot reduce ferredoxin on its own.

3.1.4 Other abundant and active taxa

In addition to the primary syntrophic partners, two other microorganisms, an *Acetomicrobium sp.* and an *Alkaliphilus sp.*, were consistently abundant and transcriptionally active in the enrichment cultures, suggesting supporting or alternative roles **(Papers I–III).**

The *Acetomicrobium sp.* was present across all studies, showing low but persistent relative abundance or transcriptional activity, with abundance increasing towards the end of degradation (**Papers I–III**). In **Paper I**, the closest characterized species was show to be *Acetomicrobium mobile*, first isolated from wool-scouring wastewater treatment sludge (Menes and Muxí, 2002). **Paper I** showed that the *Acetomicrobium sp.* lacked key genes for the Wood-Ljungdahl pathway and initial acetate activation, suggesting it is not a conventional syntrophic acetate oxidiser via this pathway. It did however express gene for the glycine synthase reductase pathway (GSRP). The *Alkaliphilus sp.* had low activity in propionate fed cultures. In **Paper II** the species was shown to be in low abundance in propionate fed cultures. However in acetate-fed cultures it increased drastically in relative abundance during the later stage of degradation following the second additions of substrate. Similarly to the *Acetomicrobium sp.* it expressed all the genes for the GSRP while lacking key genes of reverse-WLP. Members of the genera *Acetomicrobium* and *Alkaliphilus*, are commonly found in biogas systems rich in acetate, often co-occurring with syntrophic microbes and hydrogenotrophic methanogens (Kovács et al., 2015; Dyksma et al., 2020; Li et al., 2022) [67–

69]. They have also been reported in power-to-gas experiments involving hydrogen injection(Kamravamanesh et al., 2023), though their exact function in such contexts is still uncertain.

3.2 Hydrogenases and formate dehydrogenases

Hydrogenases and formate dehydrogenases catalyse redox reactions involving simple inorganic substrates (H_2 and formate). By mediating electron flow in response to cellular conditions, they play a crucial role in redox homeostasis, either dissipating excess reducing power or supplying electrons for metabolic processes.

3.2.1 Hydrogenases

Hydrogenases are metalloenzymes that catalyse the simple and reversible oxidation of molecular hydrogen (H_2) into protons and electrons:

$$H_2 \rightleftharpoons 2H^+ + 2e^- \tag{9}$$

These enzymes exist within all domains of life and are classified based on the metal composition of their active sites into [Fe]-, [FeFe]-, and [NiFe]-hydrogenases (Lubitz et al., 2014). Within these groups, further classification into subgroups is based on phylogeny, genetic organisation, and functional properties (Calusinska et al., 2010; Peters et al., 2015; Søndergaard et al., 2016).

[FeFe]- and [NiFe]-hydrogenases

[FeFe]- and [NiFe]-hydrogenases are examples of convergent evolution, as they share structural and mechanistic similarities despite distinct evolutionary origins (Meyer, 2007). Both classes use cyanide (CN^-) ligands to coordinate the metal centre and contain iron-sulphur (Fe–S) clusters that facilitate electron transfer within the enzyme. Mechanistically, [NiFe]- and [FeFe]-hydrogenase cleave the H_2 into a hydride (H^-) and proton (H^+), with sequential transfer of electrons from the hydride to the accepting compound via Fe-S clusters. [FeFe] hydrogenases do in general exhibit high catalytic efficiency and are primarily involved in H_2 production, whereas [NiFe] hydrogenases predominantly function in H_2 oxidation, though exceptions exist (Vignais and Billoud, 2007).

In **Paper I**, hydrogenases were identified in the assembled metagenomes of the enrichment cultures using the hydrogenase-annotating tool HydDB and a regular expression-based method looking for typical hydrogenase motifs, amino acid/nucleic acid patterns specific to hydrogenases (Vignais and

Billoud, 2007; Calusinska et al., 2010; Søndergaard et al., 2016). The SPOB only had [FeFe]-type hydrogenases, including several bifurcating type A3 variants, one of which was located near a type C3 hydrogenase that may act as a H_2 sensor and gene regulator. The type A3 hydrogenase reversibly bifurcates electrons from H_2 to NAD and Fd_{ox} (Schut and Adams, 2009; Søndergaard et al., 2016), which would serve as an outlet for some of the electron carriers formed during the propionate oxidation. The absence of [NiFe] hydrogenases is a characteristic of the genus *Desulfofundulus,* to which the SPOB in **Paper I** belongs (Westerholm et al., 2022).

In **Paper I**, the SAOB was shown expressed a bifurcating [FeFe]-type A3 hydrogenase alongside multiple [NiFe] hydrogenases: a periplasmic type 1a potentially capable of reducing extracellular inorganic electron acceptors; a NADP-coupled type 3b facilitating H_2 production from NADP. Furthermore, the SAOB also expressed a membrane-bound type 4e (Ech) complex that generates H_2 from reduced ferredoxin while translocating protons or sodium ions. The methanogen expressed only [NiFe] hydrogenases, including a bifurcating type 3c involved in the Wolfe cycle (coupling ferredoxin and heterodisulfide reduction using H_2); a type 3a for coenzyme F_{420} re-reduction; two membrane-bound hydrogenases, types 4e (Ech) and 4a (Eha), both catalysing the endergonic reduction of ferredoxin with H_2, powered by the transmembrane ion gradient. The SAOB exhibits a diverse array of hydrogenases, likely enabling both H_2 uptake and generation.

In **Paper II**, orbital shaking caused a downregulation of the [NiFe]-type 4a hydrogenase in the methanogen. When comparing acetate- and propionate-fed cultures, the SAOB downregulated both the ion-translocating [NiFe] 4e hydrogenase and the NADP-coupled [NiFe] 3b hydrogenase, while also downregulating multiple formate dehydrogenases and transporters, suggesting alternate routes of electron transfers or overall reduced flux between syntrophic partners. In **Paper III** SPOB upregulated a bifurcating [FeFe]-type 3a hydrogenase as sustained response after spiking with NaCl, whereas *Acetomicrobium* sp upregulated a NAD-coupled [NiFe] 3d hydrogenase.

[Fe]-hydrogenases

The [Fe]-hydrogenase, also known as H_2-forming methylene-H_4MPT dehydrogenase (Hmd), is found exclusively in methanogenic archaea and is distinct from the other two hydrogenase classes. It catalyses the reversible

reduction of methenyl-H_4MPT using H_2 under nickel-limited conditions. When nickel is available, methanogens rely on a F_{420}-reducing [NiFe]-hydrogenase (Frh) to generate reduced coenzyme F_{420}, which is required for methylene-H_4MPT and methenyl-H_4MPT reduction (Thauer et al., 2010; Shima et al., 2020). Working in concert with the [Fe]-hydrogenase, Mtd (methylene-H_4MPT dehydrogenase) can be used to regenerate reduced F_{420} needed for the reduction methenyl-H_4MPT (Afting et al., 1998). Unlike the other hydrogenases, [Fe]-hydrogenase lacks Fe–S clusters and CN^- ligands and instead contains a unique iron-containing Fe–GP cofactor. Notably, H_2 cleavage in [Fe]-hydrogenase results in direct hydride transfer to methenyl-H_4MPT, rather than electron transfer through Fe–S clusters. In **Paper I**, '*Ca.* M. ammoniitolerans' genes encoding [Fe]-hydrogenase were not detected in its metagenome. Consequently, the species relies on Mtd for the reduction of methenyl-H_4MPT and on the [NiFe]-hydrogenase Frh for F_{420} reduction. It also encodes a F_{420}-dependent formate dehydrogenase, which may serve as an alternative route for F_{420} reduction. The absence of [Fe]-hydrogenase may indicate a greater sensitivity to nickel limitation. However, studies on *Methanoculleus bourgensis* have demonstrated that nickel limitation had a limited impact on its methane production (Neubeck et al., 2016).

Hydrogenase maturation and oxygen sensitivity

Most hydrogenases are highly sensitive to oxygen, often causing irreversible damage, with [FeFe]-hydrogenases regarded as the most sensitive, although oxygen-tolerant variants do exist (Morra, 2022). [NiFe]- and [Fe]- hydrogenases are somewhat more robust, with examples of either oxygen-tolerant variants or variants that switch to an inactive yet reversible state. Hydrogenases require intricate maturation processes to assemble their catalytic metal centres, with [NiFe]- and [FeFe]-hydrogenases undergoing particularly complex pathways involving metal insertion, ligand biosynthesis (CO, CN^-), and specialised chaperones. In contrast, [Fe]-hydrogenase follows a simpler maturation route, relying only on Fe insertion and FeGP cofactor assembly. In **Paper III**, the SPOB was shown to downregulate several H-cluster maturation factors of bifurcating type [FeFe]-A3 hydrogenase predominantly in the late response to addition to NaCl and NH_4Cl. Interestingly, the catalytic subunit itself was not differentially expressed, while the adjacent NADH-quinone oxidoreductase (Nuo) subunits were upregulated during the early responses and in the late sodium-specific response.

3.2.2 Formate dehydrogenases

Formate dehydrogenases (FDHs) catalyse the reversible oxidation of formate ($HCOO^-$) to carbon dioxide (CO_2), proton and electrons:

$$HCOO^- \rightleftharpoons CO_2 + 2e^- + H^+ \quad (10)$$

FDHs are classified into two major groups: metal-dependant and metal-free FDHs (Kobayashi et al., 2023). NAD(P)-dependent FDHs, lack metals in their active site and directly transfer a hydride to NAD^+ (or in some variants $NADP^+$). They typically catalyse oxidation of formate (i.e., stripping electron from formate) and are oxygen-tolerant. Metal-dependent formate dehydrogenases feature a molybdenum or tungsten centre at their active site, coordinated by cysteine or selenocysteine residues, along with a metal-binding pterin guanidine dinucleotide cofactor and a small ligand, typically oxygen or sulphur. Metal-dependent FDHs are structurally diverse and may also incorporate various cofactors such as iron–sulphur clusters, FMN, FAD, or heme-groups. They utilise a diverse range of electron acceptors, including NAD^+, cytochromes, ferredoxins, quinones, and coenzyme F_{420} (Kobayashi et al., 2023; Maier et al., 2024). Metal-dependent FDHs are sensitive to oxygen, as oxygen oxidises the catalytic site, specifically the metal centre and its ligands, leading to inactivation. Some molybdenum-containing FDHs have structural adaptations that provide partial oxygen tolerance (Hartmann and Leimkühler, 2013).

In **Paper I** it was shown that the SPOB expressed a periplasmic NAD^+/$NADP^+$-dependent FDH, a coenzyme F_{420}-dependent FDH, and a $NADP^+$-linked FDH that was associated with a formate transporter and the nuoEF complex, which is involved in electron transfer. The SAOB expressed similar FDHs including a periplasmic FDH and a coenzyme F_{420}-dependent FDH linked to a hydrogenase and heterodisulfide reductase (HdrABC). The methanogen utilised a membrane-bound formate dehydrogenase, enabling the direct uptake of formate-derived electrons for methanogenesis, as well as a F_{420}-dependent formate dehydrogenase. In the stressful conditions associated with magnetic stirring (**Paper II)** and sudden salt stress (**Paper III**) the SPOB upregulated the periplasmic FDH (*only DE compared to orbital shaking). Furthermore, all the FDH of the SPOB was somehow differentially expressed, either up or down in response to the salt addition of **Paper III**.

The methanogen upregulated a formate transporter (FdhC) in repsponse to both motions in **Paper II** and to sodium stress in **Paper III**, possibly indicating greater reliance on formate MIET under stressful conditions.

As mentioned in section 2.5.2, formate is considered a better carrier than H_2 when intracellular distances are long. However, in **Paper II** where intracellular distances were increased by mechanically disrupting cellular aggregates, the majority of formate dehydrogenases and hydrogenases showed no change in expression in response to the agitative motions, with the exception a membrane-bound formate dehydrogenase that was downregulated in response to both agitative motions. These results were contrary the initial hypothesis, that increased cellular distances would lead to a shift in transfer mechanisms towards formate mediated interspecies electron transfer.

All in all, the transfer of reducing equivalents is likely not binary, meaning that syntrophic organisms are not solemnly relying on one compound for transfer of reducing equivalents. This is supported by the concurrent expression of both hydrogenases and formate dehydrogenases by all the syntrophic partners, observed in studies (**Paper I–III**). Furthermore, alternative carriers in addition to hydrogen and formate could be used, although I currently do not have any evidence that this is the case. To confirm this possibility, further studies are required that combine chemical measurements of extracellular compounds believed to be involved in electron transfer with omics data, enabling a more comprehensive understanding of the compounds exchanged between syntrophic organisms. In addition to this, DIET, either cell–cell or abiotically mediated, could also serve as an outlet. Determining the exact pathways of electron flow between syntrophic partners remains challenging, but the findings presented here could serve as valuable starting points for future studies.

3.3 Other interspecies cooperation

In both natural and engineered microbial systems, syntrophic interactions represent only a subset of the diverse interspecies relationships shaping community dynamics. Microbes continuously release extracellular molecules including metabolites, toxins, siderophores, signalling compounds, and exoenzymes, that influence their surroundings (Fritts et al., 2021). Additionally,

they interact through physical cell–cell interaction and alter their immediate surrounding by creating shielded environments, such as biofilms or aggregates, that may either be attached or free-floating, and mono or multispecies in composition (Flemming et al., 2016; Doloman and Sousa, 2024).

3.3.1 Cross-feeding

Syntrophy is a niche case of a broader concept known as cross-feeding. Cross-feeding encompasses diverse metabolic exchanges, from unidirectional by-product consumption to bidirectional cooperative trade of costly metabolites such as amino acids, vitamins, or electron carriers (D'Souza et al., 2018). Cross-feeding can arise due to metabolic constraints, energetic efficiency, or gene loss, often explained by the Black Queen Hypothesis (Morris et al., 2012). The hypothesis proposes that microbes can streamline their genomes, to reduce metabolic costs and enhance replication efficiency, by losing genes for metabolite production if other community members supply these compounds as public goods. Metabolites end up as public goods for multiples reasons, including the release of metabolic by-products, the unintentional leakage of metabolites into the shared environment, cell lysis and the extracellular degradation of high-molecular weight molecules (Culp and Goodman, 2023). This shapes the microbial community and creates metabolic dependencies. Furthermore, much like the economic theory of comparative advantages, which explains how trade can be mutually beneficial when parties specialise based on their relative production efficiencies, microbes may also benefit from the bi-directional exchange of metabolites. By trading metabolites instead of producing everything independently, trading microbes can achieve greater overall metabolic efficiency than if it were to function in isolation (D'Souza et al., 2018). This exchange dynamic promotes specialisation and cooperative interactions within microbial communities.

One key reason why metabolic specialisation can be advantageous is the presence of metabolic trade-offs, where enhancing the efficiency of one pathway comes at the expense of another (Johnson et al., 2012). Over the long haul, these dynamics cause auxotrophies, the inability of an organism to synthesise essential compounds, necessitating uptake from its environment. Auxotrophies are widespread in nature, where exchanged compounds include many of the intermediaries in AD process (sugars, VFAs, alcohols, amino acids, H_2, etc.) and compounds such as vitamins, cofactors, and iron

compounds (heme and sidephores). For example, pathway analysis of microbial genomes suggest that a large fraction of sequenced bacterial species lack the capability to synthesise at least one amino acid (24%–98%) (Mee and Wang, 2012; D'Souza et al., 2014; Culp and Goodman, 2023). In **Paper II,** the potential of the investigated the SPOB, the SAOB, the hydrogenotrophic methanogen and the *Acetomicrobium* sp. were analysed by screening their metagenomes for genes involved in production of amino acids. This analysis indicated that all species were auxotrophic. This, in combination with the growth medium not containing any amino acids (except for cysteine), suggest that cross-feeding on amino acids is occurring. Since the SAOB *S. schiinki* requires addition of yeast extract when grown in pure culture (Westerholm et al., 2010), this would be interesting to analyse further by comparing transcriptomic data of this species in pure and syntrophic cultivation. Some caution is needed when interpreting metabolic pathway analysis results suggesting amino acid auxotrophies, as studies have shown that they sometimes overpredict auxotrophies (Price et al., 2018; Tramontano et al., 2018). Moreover, high genome completeness is crucial for the analysis. In **Paper II**, the expression pattern of these identified amino acid-producing genes were compared between acetate- and propionate-fed cultures, using a pathway enrichment analysis approach with the differentially-expressed genes. The aim was to find if the changes in the microbial community, i.e., mostly the increased abundance of the SPOB in the propionate-fed cultures, would alter amino acid expressions of the other community members, indicating amino acid cross-feeding. The results showed that the SAOB *S. schinkii* downregulated expression of genes for synthesis of branched amino acid (leucine/isoleucine) in propionate-fed cultures. The SPOB had the capability of producing these amino acids, thus one explanation could be that the SPOB is providing these amino acids to the SAOB. These changes in gene expression might not necessarily be due to auxotrophies; they could also be the result of varying levels of acetate or propionate. For instance, *E. coli* can synthesise isoleucine by converting propionate to 2-ketobutyrate through an alternate pathway under anaerobic conditions in the presence of propionate (Cotton et al., 2020). Chemical measurements of extracellular compound concentrations, such as amino acids, would aid in disentangling what compounds besides those essential to the syntrophic degradation (acetate, CO_2, H_2, formate) that are being exchanged between the syntrophic community members. Furthermore, community scale metabolic models (Cerk et al., 2024) can help identify

potential exchanged compounds between community members, that could inform future experiments. These models simulate the combined metabolism of multiple organisms by integrating genome-scale models into a shared environment, enabling predictions of metabolite production, consumption, and exchange based on defined nutrient inputs and target molecules to be produced.

3.3.2 Biofilms and aggregates

Prokaryotic organisms gathering in aggregated communities is the rule rather than the exception (Flemming and Wuertz, 2019). Rather than existing as solitary (planktonic) cells, they frequently adhere to surfaces and/or to each other. These aggregated states span a wide range of forms, from surface-attached variants such as small cell clusters on soil particles, extensive microbial mats and thin cell layers at air–water interfaces to free-floating variants like flocs and marine snow, as well as dense layered granules found in wastewater treatment plants. Theses aggregated states can consist of single microbial species (auto-aggregation) or of different microbial species (co-aggregation). Most microbes in aggregated states produce an extracellular matrix that encapsulates the cells, a hydro-gel consisting of extracellular polymeric substances (EPS) like polysaccharides, proteins, lipids and extracellular DNA (Flemming et al., 2023). Depending on the definition used these variants can all be considered biofilms, although biofilm research has traditionally studied disease-associated aerobic bacteria that typically form surface-attached biofilms (Sauer et al., 2022). From here on the term floc, will be used to refer to free-floating cellular aggregate that were observed in the syntrophic enrichment culture (**Paper I–IV,** see section below) and surface-attached biofilm for the thin surface-attached layer that formed on the bottom of culture bottles.

So, what are the advantages of living in an aggregated state rather than as free-floating planktonic cells? First, it provides physical protection from shear forces and from harsh environmental conditions by buffering against fluctuations in pH, oxygen levels, and other stressors like ammonia etc (Jefferson, 2004; Carvalho and R, 2018). Biofilms and aggregates also enhance resistance to antibiotics and toxins, and prevents the community members from drying out (Liu et al., 2024). Beyond protection, communal living facilitates cooperative behaviours such as cross-feeding and division of labour

by keeping partners in close proximity, and it also creates opportunities for the exchange of genetic material (Evans et al., 2020; Michaelis and Grohmann, 2023). By attaching to solid surfaces, biofilms allow communities to remain in favourable environments minimising the risk of being dislodged. Similarly, microbial aggregation on suspended organic particles enables cells to remain in close proximity while also benefiting from the nutrients and shelter these particles provide. Embedment in a EPS matrix also enables the localised production of extracellular enzymes, allowing microbes to degrade complex substrates while remain near the released nutrients (Flemming et al., 2021).

The enrichment culture used in **Papers I–IV**, formed distinct flocs. In **Paper IV,** the macromorphological behaviour of this aggregation was captured using the robotic time lapse imaging system over the course of acid degradation. Both propionate- and acetate-degrading cultures formed flocs, with the first flocs being visible from day 12. At the point of peak acid degradation, VFA sampling triggered a notable change in aggregation. Over the course of a week, a large floc formed as smaller flocs merged into it. During this process, the flocs displayed dynamic movement, often changing position between images, colliding and aggregating, to create increasingly larger flocs. The flocs were at some points positively buoyant, floating up from the bottom, possibly due to formation of gas within the aggregates. At this stage, it is unclear whether the observed motion is biologically driven or a result of fluid dynamics within the bottle, perhaps due to gas formation within the flocs. In addition, in both cultures a thin surface-attached biofilm with a sheet-like structure was formed that fragmented into multiple sheets following VFA sampling. This structure was more pronounced in acetate cultures.

Microscopic inspection of the enrichment culture revealed that the majority of methanogens resided within large aggregates, that seemed to also contain non-methanogenic species (Figure 4).

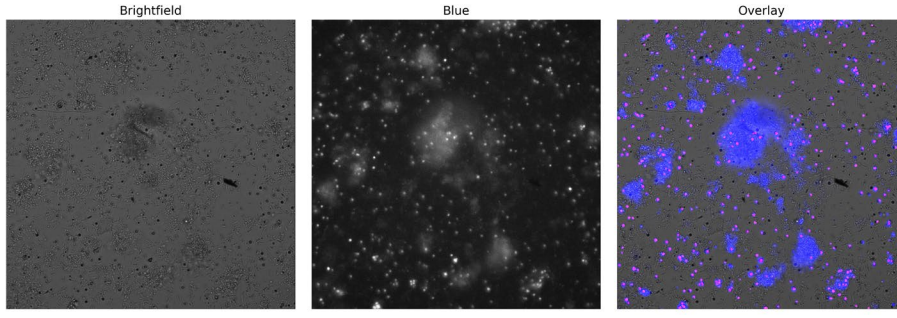

Figure 4: Micrographs of a syntrophic culture captured in brightfield (left) and blue light spectrum (middle). The compound image (right) combines a thresholded blue light image (shown in blue) with an additional highlight of bright circular spots in the blue light image (shown in pink) identified using top-hat filtering and shape analysis to highlight likely methanogenic cells**.**

The large-scale aggregates exhibit ambient autofluorescence, likely due to the high presence of methanogens and the majority of the floc being out of focus, as it is too large to fit within the focal plane. The smaller floc in the bottom right corner is a clear example of where methanogens are intermingled with non-methanogenic species, some of which are rod-shaped. In **Paper III**, magnetic stirring was shown to disrupt the formation of macromorphological flocs, while shaking promoted their formation. Stirring substantially hindered the initiation of propionate degradation whereas acetate degradation was less affected. Although no macromorphological flocs could be observed in the stirred cultures, microscopical flocs could still be observed, even in the cultures that were unable to initiate propionate degradation.

Mechanisms of aggregate formation

Biofilm formation follows a five-stage cycle: reversible attachment, irreversible attachment, maturation I & II, and dispersion (Sauer et al., 2022; Sharma et al., 2023). Surface contact initiates attachment, with bacteria initially adhering via appendages such as flagella, pili and/or through physical forces. Irreversible attachment is marked by reduced flagellar gene expression, and the production biofilm matrix. Maturation I involves early microcolony formation, while Maturation II results in fully developed, matrix-embedded biofilms. Dispersion occurs with the degradation of matrix components, releasing motile cells to restart the cycle. The secondary messenger cyclic di-GMP is a one of the key regulators in the transition between planktonic and sessile lifestyles, with high levels promoting biofilm formation and

low levels favouring planktonic and dispersed cells (Valentini and Filloux, 2016). The formation of non-surface-attached biofilms like flocs lacks a comparable stepwise definition comparable to the attached biofilms, though several strong efforts have been made to describe the formation process (Cai, 2020; Kragh et al., 2023; Doloman and Sousa, 2024). At a minimum, their development can be broken down into partner recognition and the regulation of EPS production.

In short, the initial cell–cell contact is mediated by external cell appendages like adhesins, lectins, flagella and pili (Trunk et al., 2018; Doloman and Sousa, 2024). For instance the propionate oxidiser *P. thermopropionicum* have been suggested to initiate contact with its methanogenic partner through the flagellar cap protein FliD, and presence of the protein alone triggered expression of genes related to methanogenesis in the methanogenic partner (Shimoyama et al., 2009). In **Paper III**, the *Acetomicrobium* sp. exhibited upregulation of this gene in both the early and late response to addition of salts (NH_3 and NaCl). Furthermore, the SPOB upregulated flagellar genes in the early ammonia response and downregulated in the late sodium response. In **Paper II**, orbital shaking induced the SAOB to upregulate tight adherence and pilus assembly proteins, resembling genes linked to the ability of marine bacteria to colonise the mucus layer around phytoplankton (Isaac et al., 2021), suggesting potential involvement in floc formation. Furthermore, both the SAOB and *Acetomicrobium* sp. downregulated pilus and twitching motility proteins in response to both shaking and stirring motion.

The regulatory mechanism controlling the transition from planktonic to a sessile is controlled by intracellular messengers like c-di-GMP in bacteria. In archaea, regulatory mechanisms remain less understood (van Wolferen et al., 2018), and is likely more complex and tightly regulated than bacterial counterparts as suggested by proteomic study of the halophilic archaeon *Halobacterium salinarum* showing significant proteome shifts between planktonic and sessile states (Losensky et al., 2017) and a transcriptional study of the methanogen *Methanospirillum hungatei* in co-culture with the SPOB *Syntrophobacterium fumaroxidans*, revealing differential expression of 160 genes between early and one-year old aggregates, including upregulation of archaeal type IV pili in mature aggregates (Doloman et al., 2024). The increased levels of c-di-GMP causes downregulation of motility-associated

genes like pilus/flagella and the initiation of EPS production (Doloman and Sousa, 2024). In **Paper II**, the *Acetomicrobium* sp. downregulated a diguanylate cyclase (c-di-GMP-producing enzyme) in response to stirring in an operon containing several glycine cleavage related genes, indicating a potential link between glycine cleavage activity and flocculation status. Some of these glycine cleavage genes were upregulated in the late response to NH_4Cl addition in **Paper III**, although the diguanylate cyclase showed no change in expression. Furthermore, in **Paper III,** the SPOB downregulated a diguanylate cyclase in response to additions of both salts, while simultaneously upregulating the antagonistic c-di-GMP phosphodiesterase (c-di-GMP-degrading), indicating a rapid turnover and strict regulation of the c-di-GMP pool.

Knowledge of EPS biosynthesis pathways is largely based on aerobic microbes, and include well defined pathways (Schmid et al., 2015; Whitfield et al., 2020), while EPS production and composition of anaerobic co-aggregates and archaeal organisms remains less studied. Cross-feeding of EPS precursors (nucleotide sugars) has been hypothesised to promote granulation, where filamentous cyanobacteria supply EPS precursors to a co-aggregating partner, which incorporate them into EPS, facilitating granule formation and development (Kong et al., 2023).

In summary, **Paper II** demonstrated that disrupting floc formation through stirring significantly impeded the initiation of SPO, while SAO remained largely unaffected. This raises the question of whether the enrichment cultures aggregating tendencies are essential for syntrophic acid oxidation or primarily serve as a defence mechanism against the high ammonia conditions under which the cells are cultivated, conditions that impose osmotic stress, disrupt enzyme function, and inhibit cell growth. These effects, along with microbial responses to ammonia and salt stress, will be explored in the next chapter.

4. Ammonia toxicity and stress

Ammonia (NH_3) serves as a key nitrogen source for many microorganisms and is often considered the preferred form of nitrogen for bacteria (Merrick and Edwards, 1995). It exists in equilibrium between ionised (ammonium, NH_4^+) and unionised (ammonia, NH_3) forms, and as a weak base it can also buffer and stabilise pH in AD processes (Procházka et al., 2012). However, as discussed in section 2.2.4 it can also exert toxic effects on microorganisms. This toxicity is observed for all domains of life from microbes to multicellular organisms. In the context of the AD process seminal studies from the 1960s examining the impact of various salts (Ca, P, Mg, Na, NH_3) on methane production found that ammonium salts were the most inhibitory to methane yield, especially at low pH (McCarty and McKinney, 1961; Kugelman and McCarty, 1965). These findings pointed to a mode of inhibition more complex than mere osmotic stress, likely involving the dissociation of ammonium to free ammonia. This equilibrium between ionised and unionised forms introduces two distinct routes of toxicity: a general osmotic stress associated with elevated salt concentrations, and a specific inhibitory effect linked to free ammonia. The following chapter delves into the mechanisms of ammonia toxicity, beginning with nonspecific salt stress and advancing to microbial strategies for coping with both osmotic pressure and ammonia-specific inhibition.

4.1 Generic salt stress

Differences in solutes that cannot readily cross the cell membrane (e.g., NH_4^+, Na^+) drive water flux toward regions of higher osmolality, that is, toward areas of lower water activity (i.e., less freely available water.) (Wood, 2011; Bremer and Krämer, 2019). This can lead to swelling and potential lysis under hypoosmotic stress, where the external solute concentration is lower than inside the cell, or to plasmolysis and dehydration under hyperosmotic stress, where the external solute concentration is higher. To counteract these effects, cells must tightly regulate their internal solute concentration, a process known as osmoregulation, to maintain osmotic balance and avoid structural damage. Most microorganisms maintain a positive turgor pressure, meaning they sustain a slightly higher internal solute concentration relative to their surroundings (Kempf and Bremer, 1998). External osmolality can

shift rapidly, causing water fluxes in the timescale of milliseconds, which puts microorganisms under a constant pressure to be able to both sense and rapidly adjust their internal osmolality, or else risk structural damage (Wood, 1999).

4.1.1 Osmosensing

Microorganisms rely on specialised osmosensors to detect fluctuations in external osmolarity and initiate compensatory responses. These sensors do not recognise specific molecules but instead detect changes in physicochemical properties such as membrane tension, ionic strength, protein or macromolecular crowding (Wood, 2011; Bremer and Krämer, 2019). While many of the underlying mechanisms remain poorly understood, notable examples include:

- **Mechanosensitive channels,** are channels that sense the mechanical force associated with membrane stretch that under hypoosmotic stress enables the quick release of intracellular solutes out of the cell, preventing osmotic bursting of the cell (Cox et al., 2018). First described in *E. coli*, the different types are classified according to their conductance capacity according to mini, small, and large conductance (mscM, mscS, mscL) (Perozo and Rees, 2003). In **Paper III**, genes encoding mechano sensitive channels was upregulated in response to addition of both salts (NH_4Cl, NaCl) in the methanogen (mscS) and for the addition of NaCl for the SPOB (mscL). Additionally, a moderate conductive mechanosensitive channel ybiO known to protect *E. coli* when exposed to hyperosmotic stress (Edwards et al., 2012), was upregulated in late response to NaCl addition for the SPOB, located next to genes needed for the synthesis of the compatible solute N^{ε}-acetyl-β-lysine (see section 4.1.2)

- **Osmosensory transporters**, doubles as both osmotic sensors and osmoregulators by transporting osmolytes (see section 4.1.2). Well-studied examples include BetP of *Corynebacterium glutamicum*, ProP of *E. coli*, and OpuA of *Lactococcus lactis* (Racher et al., 1999; Rübenhagen et al., 2000; van der Heide and Poolman, 2000). Although the exact molecular mechanisms of sensing remain unclear, studies have indicated that BetP senses membrane tension and

cytoplasmic K^+ levels, OpuA responds to changes in internal ionic strength, and ProP sensen membrane alterations caused by cellular dehydration (Wood, 2006; Bremer and Krämer, 2019).

- **Two-component sensor kinases** are signal transduction systems that detect osmotic changes and regulate gene expression in response. These systems consist of a membrane-bound sensor kinase that detects osmotic stress and a cytoplasmic response regulator that mediates transcriptional changes. A well-characterised example is the EnvZ/OmpR system in *E. coli*, which regulates porin expression in response to osmolarity shifts, although the nature of the stimuli is not known (Foo et al., 2015).

4.1.2 Osmoadaption

Microorganisms cannot actively pump water in or out of the cell to counteract osmotic water fluxes; no such mechanisms are known, nor would such a strategy be energetically viable. As a result, the only effective strategy is to modulate intracellular osmolality to match the surrounding environment. To cope with elevated external osmolality, microorganisms primarily employ two strategies: the salt-in and salt-out approaches, or a combination of both.

Salt-in strategy

In the salt-in strategy, common among halophilic species such as members of the archaeal class of *Halobacteria*, cells accumulate high concentrations of inorganic ions, most commonly potassium (K^+) and chloride (Cl^-) to balance high external osmotic pressure while maintaining intracellular net charge(Sleator and Hill, 2002). Simultaneously, sodium (Na^+) is exported from the cell. For most organisms, such high intracellular salt concentrations pose a risk of protein denaturation and disruption of essential cellular functions (Jungwirth and Winter, 2008). In contrast, the proteins of these salt-in specialist are uniquely adapted that they exhibit an increased frequency of acidic amino acids (aspartate and glutamate) which enhance protein solubility and stability in high-salt environments. As a result, these organisms often require high salinity for growth and few members of *Halobacteria* manage to grow below their optimum salt concentration (Sleator and Hill, 2002; Gunde-Cimerman et al., 2018). In *Halobacteria*, the accumulation of K^+ and Cl^- is maintained at the expense of energy. Na^+/H^+ antiporters expel Na^+ from

the cell. K^+ accumulation is generally thought to be driven by an overall negative-inside membrane potential and the expulsion of sodium ions. In addition, active K^+ transport through high affinity, ATP-consuming transport systems have also been observed (Oren, 2013). For bacteria (not only halophilic variants), two well-established K^+ systems have been described, the low-affinity (Trk) system active in high K^+ environments, and the ATP-driven high-affinity (Kdp) system (Epstein, 1986; Whatmore et al., 1990). In **Paper III**, homologous genes to the low-affinity Trk-system were expressed for all species, but expression was unaffected by the addition of salts, except for a single gene in the *Acetomicrobium* sp. The high-affinity Kdp variant was identified only in the SPOB and expression was not affected by the addition of salts. Several different Na^+/H^+ antiporters were identified as differentially expressed, with responses varying between community members, suggesting distinct adaptive strategies. The SPOB upregulated a Na^+/H^+ antiporter in the late sodium response, while downregulating a cation:H^+ antiporter in both the early and late sodium response. The SAOB upregulated a "Na-translocating system protein MpsC family protein" under all conditions, though the functional directionality of this protein is elusive. The *Acetomicrobium* sp, downregulated a Na^+/H^+ antiporter in the early response for both salts.

Salt-out strategy

In the salt-out strategy, microorganisms accumulate organic molecules to counteract external osmotic pressure. These organic molecules, known as osmolytes, compatible solutes, or osmoprotectants are typically small, highly soluble, and polar, with many being zwitterionic. Crucially, they can accumulate to high intracellular concentrations without interfering with cellular processes, hence the term compatible (Sleator and Hill, 2002; Roberts, 2005). One widely supported explanation is preferential exclusion, where osmolytes are excluded from the surface of proteins due to their unfavourable interactions with the protein backbone. This exclusion preserves the protein's hydration shell, an organised layer of water molecules that stabilises the folded structure through hydrogen bonding and polar interactions. By maintaining this shell compatible solutes shift the equilibrium toward the native state, effectively enhancing protein stability (Mojtabavi et al., 2019). Compatible solutes can either be synthesised de-novo or taken up from the external surroundings. Common examples include proline, glycine betaine, trehalose, ectoine, glutamate, and the archaeal osmolyte N^{ε}(6)-acetyl-β-L-lysine(da Costa et al., 1998). Compared to the salt-in strategy, the synthesis

of these compounds is energetically costly, but it avoids the need for protein structural adaptations and offers greater flexibility in the range of salt concentrations that can be tolerated (Gunde-Cimerman et al., 2018).

Paper III showed that none of the major species synthesised glycine betaine de novo, but that most of the core members upregulated its uptake in response to spiking of the salts. The SPOB consistently upregulated the ABC transporter ProU (OpuA homolog in *E. Coli*), while *Acetomicrobium* upregulated genes of the OpuA system, along with genes for the glycine cleavage. Trehalose synthesis genes were expressed by the *Acetomicrobium* sp. and the methanogen, with key genes upregulated under late ammonia or sodium stress. N^{ε}-acetyl-β-lysine synthesis was strongly upregulated in the SPOB in both early and late sodium cultures, while the methanogen and SAOB showed partial or alternative expression patterns. Polyamine synthesis, especially putrescine, was generally downregulated early on, whereas spermidine synthesis was upregulated in the SPOB under prolonged sodium stress.

Hyperosmotic shock – A combined approach

In response to sudden hyperosmotic shock, many microorganisms employ a biphasic strategy that combines both the salt in and salt out strategies (Sleator and Hill, 2002; Gunde-Cimerman et al., 2018). This involves the rapid uptake of K^+ to quickly counteract water loss, typically balanced by the accumulation of glutamate as a counterion. This immediate response is followed by a delayed response characterised by the synthesis or uptake of compatible solutes, which gradually substitute the osmotic role of K^+, enabling its intracellular concentration to decline.

4.2 The elusive NH_3 molecule

Being a small uncharged molecule, ammonia (NH_3) can freely pass through the cell membrane (Kleiner, 1981). At neutral pH the ammonia–ammonium equilibrium is heavily shifted (>99%) toward ammonium (NH_4^+), but this balance moves toward ammonia with increasing pH or temperature. Several mechanisms have been proposed to explain the specific toxicity of ammonia. Early studies revealed that exposure to ammonia triggered a rapid loss of intracellular potassium (K^+) in methanogens, particularly under alkaline conditions (Sprott et al., 1984). This effect was attributed to the diffusion of NH_3 into the cell, where its protonation to NH_4^+ consumes intracellular protons, elevating the cytoplasmic pH and triggering K^+ efflux via a K^+/H^+ antiporter to restore pH balance. Later studies suggested that NH_4^+ might also exert a direct inhibitory effect on methanogenic enzymes by interfering with extracellular Mg^{2+}/Ca^{2+} binding sites (Sprott et al., 1985). In *E. coli*, a distinct mechanism of ammonia toxicity has been proposed, involving futile NH_4^+ cycling. Due to its similarity to K^+ in charge and ionic radius, NH_4^+ is mistakenly taken up by ATP-dependent K^+ transporters. Once inside the cell, NH_4^+ can dissociate into membrane-permeable NH_3, which diffuses out, prompting further NH_4^+ uptake and resulting in an energetically costly futile cycle (Buurman et al., 1991).

Beyond osmotically driven responses (section 4.1.2), microbes employ several strategies to mitigate ammonia specific toxicity. One of the most widespread is ammonia assimilation, i.e., the rapid conversion of ammonia into less toxic organic compounds, primarily amino acids. The two principal pathways for ammonia assimilation are the ATP-consuming glutamine synthetase/glutamate synthase (GS/GOGAT) system and the glutamate dehydrogenase (GDH) pathway (Merrick and Edwards, 1995; Yuan et al., 2009). In the GS/GOGAT system, GS catalyses the ATP-dependent conversion of glutamate and NH_3 into glutamine, which GOGAT then combines with α-ketoglutarate, forming two molecules of glutamate. This high-affinity pathway operates efficiently under low ammonium concentrations. In contrast, GDH directly incorporates ammonium with α-ketoglutarate to form glutamate, without consumption of ATP, and is typically active when ammonium is abundant. Both pathways consume α-ketoglutarate, a key intermediary in the Krebs cycle and could potentially lead to depletion of carbon intermediaries (Yuan et al., 2009; Sánchez-Cañizares et al., 2020). In **Paper III**, the

SPOB upregulated GS during the late sodium response, while GOGAT was downregulated under all conditions. The methanogen also downregulated GOGAT during the late ammonia response. For the GDH pathway, the SPOB upregulated GDH in the early sodium response and downregulated it late in the ammonia response, with changes occurring in distinct operons. Other assimilatory pathways could exist, many eukaryotic organisms for example deal with excess ammonia by converting it into urea or uric acid. The ammonia-oxidising archaea '*Candidatus* Nitrosocosmicus agrestis' was shown to upregulate genes involved in arginine and polyamine synthesis and export under high-ammonia conditions, suggesting this as a mechanism for ammonia tolerance (Liu et al., 2021). However, in **Paper III**, polyamine putrescine synthesis genes were downregulated in the early response for both the SPOB and *Acetomicrobium*, and in late ammonia response for the SPOB. The *speD* gene, required for synthesis of the polyamine spermidine, was downregulated in all ammonia cultures but upregulated in the late sodium response for the SPOB. This suggests an immediate suppression of polyamine synthesis, with a potential shift toward spermidine production during long-term sodium adaptation.

As previously described, ammonia is the preferred nitrogen source for many microorganisms. Because passive diffusion of NH_3 is often insufficient to meet cellular nitrogen demands, microbes express high-affinity ammonium transporters belonging to the Amt/Mep/Rh superfamily (Bizior et al., 2023). However, in high-ammonia environments these transport systems can become detrimental by causing excessive ammonia influx and energy-wasting futile cycles. To prevent this, many bacteria and archaea regulate ammonium uptake through the protein GlnK, which binds and blocks AmtB transporters under nitrogen-rich conditions (Conroy et al., 2007). The previously mentioned study on the ammonia-oxidising archaea '*Ca.* Nitrosocosmicus agrestis' also reported the downregulation of the ammonium transporter gene *amtB* under high-ammonia conditions (Liu et al., 2021). In **Paper III**, none of the microbial community members were shown to contain Amt-family ammonium transporters nor the regulatory GlnK, which could be an adaption to a life in elevated ammonia conditions.

Additionally, general stress-related genes like chaperones, were commonly observed in response to the salt addition. A study showed that exposure to

elevated ammonia levels induced the expression of the molecular chaperone hsp70 (dnaK) and a regulatory gene of potassium transport, in *M. mazeii* (Lange et al., 1997).

4.3 Floc formation as a response to osmotic shock

In **Papers I-III**, the syntrophic enrichment culture was shown to form large flocs. This raised the question whether it was essential for the syntrophic interactions by facilitating transfer of reducing equivalent, enabling cross feeding etc among the syntrophic partner or wethter it occurred for some other reason. An alternative reason could be flocculation as a protective response against the elevated ammonia levels at which the enrichment culture was grown. Elevated ammonia levels have for example been shown to induce biofilm formation in the aerobic denitrifier Enterobacter cloacae by reducing motility and upregulating EPS biosynthesis pathways (Weng et al., 2022). Furhtermore generic osmotic stress caused by NaCl have been shown to induce EPS production in the acetogen *Clostridium ljungdahlii* (Philips et al., 2017). In **Paper III,** where the culture was subjected to a sudden upshock in salt of either NaCl or NH_4Cl, microscopic time lapse images on over a 24-hour period with (Figure 5). These microscopical observations showed that the addition of NH_4Cl and NaCl significantly promoted cellular aggregation. This effect was noticeable around 8 hours after the salts were added, as cells started forming larger multicellular assemblies instead of remaining isolated or in small, scattered clusters, as seen in the control and during the initial post-inoculation phase.

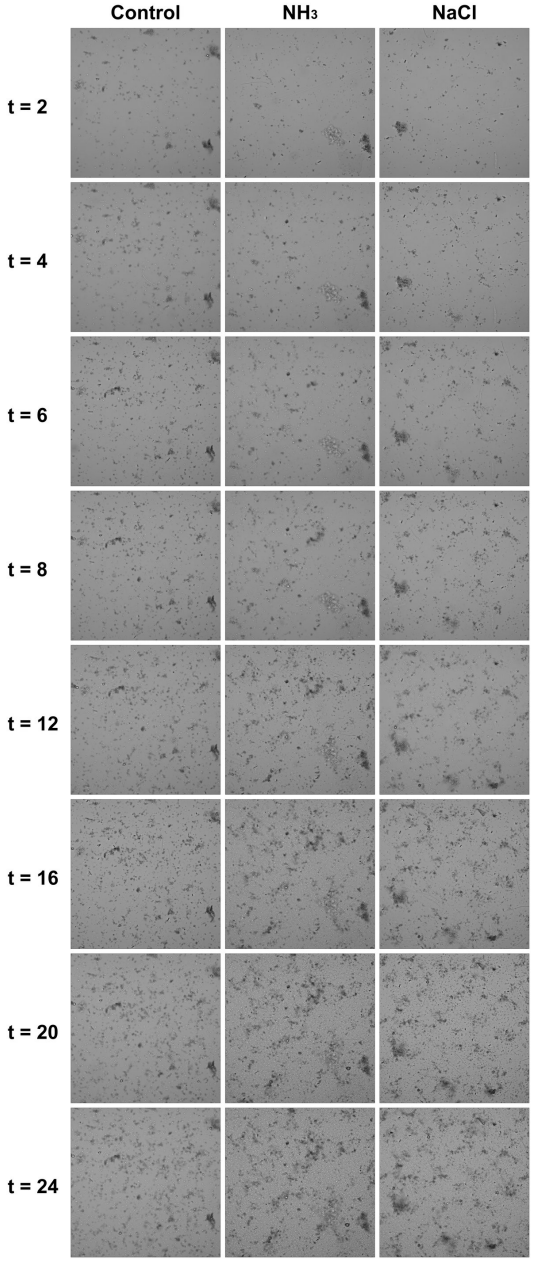

Figure 5: Time-resolved microscopy showing cellular aggregation in response to NaCl and ammonia addition. Brightfield microscopy images showing cellular aggregation over 24 hours following addition of NH_4Cl (middle column) or NaCl (right column) compared to an control without addition (left column). Images are shown at 2-hour intervals

In **Paper III** transcriptomic responses indicated condition-specific regulation of motility systems, particularly in the SPOB and *Acetomicrobium* sp. The SPOB downregulated key flagellar genes in the late sodium response, while upregulating others under early and late ammonia conditions, suggesting dynamic control of motility. The *Acetomicrobium* sp. consistently upregulated fliD, potentially facilitating interspecies interactions. Type IV pilus genes were broadly downregulated in the SPOB and *Acetomicrobium* sp., implying reduced twitching motility in the sustained response. In contrast, the SAOB upregulated pilus assembly components under all conditions. In the SPOB, one diguanylate cyclase (c-di-GMP forming) operon was upregulated under all conditions and another specifically as an early response. A phosphodiesterase (c-di-GMP degrading) was also consistently upregulated, indicating active turnover and tight regulation of intracellular c-di-GMP levels. These genes were however not co-localised with biofilm associated genes.

5. Conclusion and future perspective

Syntrophic oxidation of propionate and acetate plays a crucial role in the AD process, particularly under high-ammonia conditions where conventional degraders of these intermediates are inhibited. In such environments, the coordinated activity of propionate- and acetate-oxidising bacteria, along with hydrogenotrophic methanogens, is essential to sustain methane production.
The overarching goal of this thesis was to increase knowledge on syntrophic propionate oxidation in high-ammonia systems and specifically aimed to: (1) Investigate the metabolic pathways and interactions involved in syntrophic acid oxidation; (2) Asses how physical disturbance affects acid degradation, aggregation, and microbial activity; (3) Investigate the mechanisms underlying ammonia tolerance within syntrophic propionate degrading community; (4) Develop tools for real-time visualisation of microbial aggregation and interactions. These objectives were explored through four interrelated studies, of which the key outcomes are summarised below.

Paper I identified the metabolic pathways and interspecies interaction between key syntrophic partners of the studied enrichment culture: *'Ca.* Syntrophopropionicum ammoniitolerans', *Syntrophaceticus schinkii*, and the novel hydrogenotrophic methanogen for which the name *'Ca* Methanoculleus ammoniitolerans*'* was proposed. The study showed that electron transfer between the syntrophic acid oxidisers and the hydrogenotrophic partner was mediated both through H_2 and formate. Thermodynamic calculations confirmed that both propionate oxidation, acetate oxidation, and hydrogenotrophic methanogenesis were thermodynamically viable throughout cultivation. Despite this propionate degradation exhibited a biphasic degradation pattern. The study generated metagenomes foundational for the other papers.

Paper II investigated the impact of physical disturbance on syntrophic acid oxidation by examining how different mixing regimes affected degradation performance, microbial aggregation, and gene expression. The study found that disruption of microbial aggregation through stirring significantly delayed or inhibited propionate degradation, whereas acetate degradation was less affected. Despite the mechanical disturbance, the microbial community composition remained relatively stable and was instead shaped by substrate

type and progress of degradation. Metatranscriptomic analysis showed that stirring resulted in downregulation of genes involved in motility, surface sensing, and biofilm formation, particularly in the SAOB. The most pronounced transcriptional changes were found in the methanogen, the most notable of which suggested reliance on energy conserving coupling between the initial and final steps of hydrogenotrophic methanogenesis. In the SPOB, the elevated expression of an oxalate–formate antiporter in aggregated states suggested that its activity depends on cellular proximity and may serve as an indicator of a well-functioning SPOB community.

Paper III explored the immediate and sustained response of the syntrophic community members to exposure to NH_4Cl and NaCl. Visual and microscopical inspection showed that both salts induced flocculation. The immediate gene expression responses for most microorganisms were similar for both salts, suggesting an immediate non-specific osmotic stress response. In contrast, the sustained response varied between the two salts, reflecting salt-specific adaptations. The microbes employed both salt-in and compatible solute strategies, with SPOB and the methanogen showing pronounced ion transport regulation and osmolyte synthesis. Sustained adaptations included changes in motility, expression of biofilm-related genes, and solute uptake, highlighting species- and salt-dependent responses.

Paper IV presented a set of tools for the visual monitoring of microbial aggregation under anaerobic conditions. These tools allowed for in-situ, real-time monitoring of microbial aggregation at micro-, meso-, and macro-scales an essential, but previously inaccessible, aspect of studying syntrophic interactions. The micro- and meso-scale systems utilised 3D-printed anaerobic bioreactors, designed with embedded glass slides to allow compatibility with microscopy. The most successful reactors allowed for anaerobic cultivation up to 40 days.

5.1 Future perspectives

Knowledge and understanding of syntrophic propionate oxidation and its influence on process performance and stability is still limited and more

research is needed. Several promising avenues can be explored to advance this field, including:

- Although the microscopical monitoring of flocculation and cellular interactions made possible by the method development in **Paper IV,** it is currently not possible to identify most microorganisms involved except for the methanogen, which can be detected due to its auto-fluorescent properties. Employing fluorescence in situ hybridization variants suitable for anaerobic conditions (Harris et al., 2022), could be used with probes designed for the other core enrichment community members. This would allow for answering questions such: What is the microbial composition of the flocs? Which microorganism initiate the floc formation?
- Development of RNA extraction protocols. As noted in section 2.7.5 the current RNA extraction protocol requires a relatively large sample volume (150 ml) and involves a time delay between sampling and RNA stabilisation due to the need of centrifugation. Reducing the sample volume would enable sequential RNA sampling from the same cultivation bottle. Increasing the RNA yield would allow gene expression to be captured at early stages of aggregation, before syntrophic interactions have been established, allowing for direct comparison of gene expression before and after these interactions occur. Finally, alternative extraction methods, such as suction filtration followed by immediate freezing of the filter in liquid nitrogen, could improve RNA preservation.
- Isolation of the currently uncultured syntrophic enrichment community members ('*Ca*. S. ammoniitolerans', '*Ca*. M. ammoniitolerans') would enable detailed physiological and metabolic characterisation, providing deeper insights into their specific roles in syntrophic interactions.
- The use of genome-scale metabolic models could help identify candidate compounds exchanged between syntrophic community members. This information could guide future experiments, where chemical analyses, such as NMR may be used to verify the presence of these compounds in the extracellular medium. This combined approach could help to increase the understanding of the complex and interconnected nature of syntrophic interactions.

- Studying syntrophic interactions in enriched cultures reduces complexity and allows for easier investigation of metabolic pathways, gene expression, and cooperative behaviour. However, such simplified systems may overlook how these organisms function within more diverse communities, such as those found in anaerobic digesters, where both cooperation and competition with additional microbes can influence their activity. Studying their activity and ecological role in more complex systems could yield more representative insights into their function in anaerobic digestion and guide development of operational strategies to optimise their performance.

Overall, the goal of this thesis was to deepen the understanding of archaeal–bacterial interactions. Such insights could inform strategies to enhance the efficiency and stability of AD systems while also contributing fundamental knowledge relevant to other biotechnological processes.

References

Abbasi, T., Tauseef, S. M., and Abbasi, S. A. (2012). "A Brief History of Anaerobic Digestion and 'Biogas,'" in *Biogas Energy*, eds. T. Abbasi, S. M. Tauseef, and S. A. Abbasi (New York, NY: Springer), 11–23. doi: 10.1007/978-1-4614-1040-9_2

Adekunle, K. F., and Okolie, J. A. (2015). A Review of Biochemical Process of Anaerobic Digestion. *Advances in Bioscience and Biotechnology* 6, 205–212. doi: 10.4236/abb.2015.63020

Afting, C., Hochheimer, A., and Thauer, R. K. (1998). Function of H_2-forming methylenetetrahydromethanopterin dehydrogenase from *Methanobacterium thermoautotrophicum* in coenzyme F_{420} reduction with H_2. *Arch Microbiol* 169, 206–210. doi: 10.1007/s002030050562

Al Rawashdeh, R. (2020). World peak potash: An analytical study. *Resources Policy* 69, 101834. doi: 10.1016/j.resourpol.2020.101834

Álvarez-Fraga, L., Capson-Tojo, G., Sanglier, M., Hamelin, J., Escudié, R., Wéry, N., et al. (2025). A meta-analysis of pathogen reduction data in anaerobic digestion. *Renewable and Sustainable Energy Reviews* 207, 114982. doi: 10.1016/j.rser.2024.114982

Angelidaki, I., and Ahring, B. K. (1993). Thermophilic anaerobic digestion of livestock waste: the effect of ammonia. *Appl Microbiol Biotechnol* 38, 560–564. doi: 10.1007/BF00242955

Angelidaki, I., Karakashev, D., Batstone, D. J., Plugge, C. M., and Stams, A. J. M. (2011). "Biomethanation and Its Potential," in *Methods in Enzymology*, eds. A. C. Rosenzweig and S. W. Ragsdale (Academic Press), 327–351. doi: 10.1016/B978-0-12-385112-3.00016-0

Angelidaki, I., and Sanders, W. (2004). Assessment of the anaerobic biodegradability of macropollutants. *Rev Environ Sci Biotechnol* 3, 117–129. doi: 10.1007/s11157-004-2502-3

Atelge, M. R., Krisa, D., Kumar, G., Eskicioglu, C., Nguyen, D. D., Chang, S. W., et al. (2020). Biogas Production from Organic Waste: Recent

Progress and Perspectives. *Waste Biomass Valor* 11, 1019–1040. doi: 10.1007/s12649-018-00546-0

Balk, M., Weijma, J., and Stams, A. J. M. (2002). *Thermotoga lettingae* sp. nov., a novel thermophilic, methanol-degrading bacterium isolated from a thermophilic anaerobic reactor. *Int J Syst Evol Microbiol* 52, 1361–1368. doi: 10.1099/00207713-52-4-1361

Batstone, D. J., Picioreanu, C., and van Loosdrecht, M. C. M. (2006). Multidimensional modelling to investigate interspecies hydrogen transfer in anaerobic biofilms. *Water Research* 40, 3099–3108. doi: 10.1016/j.watres.2006.06.014

Benoit, G., Raguideau, S., James, R., Phillippy, A. M., Chikhi, R., and Quince, C. (2024). High-quality metagenome assembly from long accurate reads with metaMDBG. *Nat Biotechnol* 42, 1378–1383. doi: 10.1038/s41587-023-01983-6

Berghuis, B. A., Yu, F. B., Schulz, F., Blainey, P. C., Woyke, T., and Quake, S. R. (2019). Hydrogenotrophic methanogenesis in archaeal phylum *Verstraetearchaeota* reveals the shared ancestry of all methanogens. *Proc Natl Acad Sci U S A* 116, 5037–5044. doi: 10.1073/pnas.1815631116

Biebl, H., and Pfennig, N. (1977). Growth of sulfate-reducing bacteria with sulfur as electron acceptor. *Arch. Microbiol.* 112, 115–117. doi: 10.1007/BF00446664

Bisgaard, M., Christensen, H., Clermont, D., Dijkshoorn, L., Janda, J. M., Moore, E. R. B., et al. (2019). The use of genomic DNA sequences as type material for valid publication of bacterial species names will have severe implications for clinical microbiology and related disciplines. *Diagnostic Microbiology and Infectious Disease* 95, 102–103. doi: 10.1016/j.diagmicrobio.2019.03.007

Bizior, A., Williamson, G., Harris, T., Hoskisson, P. A., and Javelle, A. (2023). Prokaryotic ammonium transporters: what has three decades of research revealed? *Microbiology (Reading)* 169, 001360. doi: 10.1099/mic.0.001360

Blattman, S. B., Jiang, W., Oikonomou, P., and Tavazoie, S. (2020). Prokaryotic single-cell RNA sequencing by in situ combinatorial indexing. *Nat Microbiol* 5, 1192–1201. doi: 10.1038/s41564-020-0729-6

Bond, T., and Templeton, M. R. (2011). History and future of domestic biogas plants in the developing world. *Energy for Sustainable Development* 15, 347–354. doi: 10.1016/j.esd.2011.09.003

Bonk, F., Popp, D., Weinrich, S., Sträuber, H., Kleinsteuber, S., Harms, H., et al. (2018). Ammonia Inhibition of Anaerobic Volatile Fatty Acid Degrading Microbial Communities. *Front. Microbiol.* 9. doi: 10.3389/fmicb.2018.02921

Boone, D. R., Johnson, R. L., and Liu, Y. (1989). Diffusion of the Interspecies Electron Carriers H_2 and Formate in Methanogenic Ecosystems and Its Implications in the Measurement of Km for H_2 or Formate Uptake. *Appl Environ Microbiol* 55, 1735–1741.

Borja, R., and Rincón, B. (2017). "Biogas Production," in *Reference Module in Life Sciences*, (Elsevier). doi: 10.1016/B978-0-12-809633-8.09105-6

Borrel, G., Adam, P. S., and Gribaldo, S. (2016). Methanogenesis and the Wood–Ljungdahl Pathway: An Ancient, Versatile, and Fragile Association. *Genome Biology and Evolution* 8, 1706–1711. doi: 10.1093/gbe/evw114

Bremer, E., and Krämer, R. (2019). Responses of Microorganisms to Osmotic Stress. *Annual Review of Microbiology* 73, 313–334. doi: 10.1146/annurev-micro-020518-115504

Buckel, W., and Thauer, R. K. (2018). Flavin-Based Electron Bifurcation, Ferredoxin, Flavodoxin, and Anaerobic Respiration With Protons (Ech) or NAD^+ (Rnf) as Electron Acceptors: A Historical Review. *Frontiers in Microbiology* 9. Available at: https://www.frontiersin.org/articles/10.3389/fmicb.2018.00401 (Accessed February 27, 2023).

Buhlmann, C. H., Mickan, B. S., Jenkins, S. N., Tait, S., Kahandawala, T. K. A., and Bahri, P. A. (2019). Ammonia stress on a resilient mesophilic anaerobic inoculum: Methane production, microbial

community, and putative metabolic pathways. *Bioresource Technology* 275, 70–77. doi: 10.1016/j.biortech.2018.12.012

Bumharter, C., Bolonio, D., Amez, I., García Martínez, M. J., and Ortega, M. F. (2023). New opportunities for the European Biogas industry: A review on current installation development, production potentials and yield improvements for manure and agricultural waste mixtures. *Journal of Cleaner Production* 388, 135867. doi: 10.1016/j.jclepro.2023.135867

Buswell, A. M. (1939). Anaerobic fermentations. *Bulletin (Illinois State Water Survey) no. 32*.

Buurman, E. T., Joost Teixeira de Mattos, M., and Neijssel, O. M. (1991). Futile cycling of ammonium ions via the high affinity potassium uptake system (Kdp) of *Escherichia coli*. *Arch. Microbiol.* 155, 391–395. doi: 10.1007/BF00243460

Cai, Y.-M. (2020). Non-surface Attached Bacterial Aggregates: A Ubiquitous Third Lifestyle. *Front Microbiol* 11, 557035. doi: 10.3389/fmicb.2020.557035

Calusinska, M., Happe, T., Joris, B., and Wilmotte, A. (2010). The surprising diversity of clostridial hydrogenases: a comparative genomic perspective. *Microbiology (Reading)* 156, 1575–1588. doi: 10.1099/mic.0.032771-0

Campanaro, S., Treu, L., Rodriguez-R, L. M., Kovalovszki, A., Ziels, R. M., Maus, I., et al. (2020). New insights from the biogas microbiome by comprehensive genome-resolved metagenomics of nearly 1600 species originating from multiple anaerobic digesters. *Biotechnol Biofuels* 13, 25. doi: 10.1186/s13068-020-01679-y

Carvalhais, L. C., Dennis, P. G., Tyson, G. W., and Schenk, P. M. (2012). Application of metatranscriptomics to soil environments. *Journal of Microbiological Methods* 91, 246–251. doi: 10.1016/j.mimet.2012.08.011

Carvalho, D., and R, C. C. C. (2018). Marine Biofilms: A Successful Microbial Strategy With Economic Implications. *Front. Mar. Sci.* 5. doi: 10.3389/fmars.2018.00126

Centurion, V. B., Rossi, A., Orellana, E., Ghiotto, G., Kakuk, B., Morlino, M. S., et al. (2024). A unified compendium of prokaryotic and viral genomes from over 300 anaerobic digestion microbiomes. *Environmental Microbiome* 19, 1. doi: 10.1186/s40793-023-00545-2

Cerk, K., Ugalde-Salas, P., Nedjad, C. G., Lecomte, M., Muller, C., Sherman, D. J., et al. (2024). Community-scale models of microbiomes: Articulating metabolic modelling and metagenome sequencing. *Microbial Biotechnology* 17, e14396. doi: 10.1111/1751-7915.14396

Cheng, G. B., Bongcam-Rudloff, E., and Schnürer, A. (2025). Metagenomic Exploration Uncovers Several Novel 'Candidatus' Species Involved in Acetate Metabolism in High-Ammonia Thermophilic Biogas Processes. *Microbial Biotechnology* 18, e70133. doi: 10.1111/1751-7915.70133

Cheng, M.-Y., Tao, W.-B., Yuan, B.-F., and Feng, Y.-Q. (2021). Methods for isolation of messenger RNA from biological samples. *Anal. Methods* 13, 289–298. doi: 10.1039/D0AY01912G

Cheng, Q., and Call, D. F. (2016). Hardwiring microbes via direct interspecies electron transfer: mechanisms and applications. *Environ. Sci.: Processes Impacts* 18, 968–980. doi: 10.1039/C6EM00219F

Chomczynski, P., and Sacchi, N. (1987). Single-step method of RNA isolation by acid guanidinium thiocyanate-phenol-chloroform extraction. *Analytical Biochemistry* 162, 156–159. doi: 10.1016/0003-2697(87)90021-2

Chung, M., Bruno, V. M., Rasko, D. A., Cuomo, C. A., Muñoz, J. F., Livny, J., et al. (2021). Best practices on the differential expression analysis of multi-species RNA-seq. *Genome Biology* 22, 121. doi: 10.1186/s13059-021-02337-8

Clark, K., Karsch-Mizrachi, I., Lipman, D. J., Ostell, J., and Sayers, E. W. (2016). GenBank. *Nucleic Acids Res* 44, D67–D72. doi: 10.1093/nar/gkv1276

Clarridge, J. E. (2004). Impact of 16S rRNA Gene Sequence Analysis for Identification of Bacteria on Clinical Microbiology and Infectious Diseases. *Clin Microbiol Rev* 17, 840–862. doi: 10.1128/CMR.17.4.840-862.2004

Conrad, R. (2020). Importance of hydrogenotrophic, aceticlastic and methylotrophic methanogenesis for methane production in terrestrial, aquatic and other anoxic environments: A mini review. *Pedosphere* 30, 25–39. doi: 10.1016/S1002-0160(18)60052-9

Conroy, M. J., Durand, A., Lupo, D., Li, X.-D., Bullough, P. A., Winkler, F. K., et al. (2007). The crystal structure of the *Escherichia coli* AmtB–GlnK complex reveals how GlnK regulates the ammonia channel. *Proceedings of the National Academy of Sciences* 104, 1213–1218. doi: 10.1073/pnas.0610348104

Cordell, D., Drangert, J.-O., and White, S. (2009). The story of phosphorus: Global food security and food for thought. *Global Environmental Change* 19, 292–305. doi: 10.1016/j.gloenvcha.2008.10.009

Cordell, D., Rosemarin, A., Schröder, J. J., and Smit, A. L. (2011). Towards global phosphorus security: A systems framework for phosphorus recovery and reuse options. *Chemosphere* 84, 747–758. doi: 10.1016/j.chemosphere.2011.02.032

Cordell, D., and White, S. (2011). Peak Phosphorus: Clarifying the Key Issues of a Vigorous Debate about Long-Term Phosphorus Security. *Sustainability* 3, 2027–2049. doi: 10.3390/su3102027

Cotton, C. A., Bernhardsgrütter, I., He, H., Burgener, S., Schulz, L., Paczia, N., et al. (2020). Underground isoleucine biosynthesis pathways in *E. coli*. *eLife* 9, e54207. doi: 10.7554/eLife.54207

Cox, C. D., Bavi, N., and Martinac, B. (2018). Bacterial Mechanosensors. *Annu Rev Physiol* 80, 71–93. doi: 10.1146/annurev-physiol-021317-121351

Culp, E. J., and Goodman, A. L. (2023). Cross-feeding in the gut microbiome: Ecology and mechanisms. *Cell Host & Microbe* 31, 485–499. doi: 10.1016/j.chom.2023.03.016

da Costa, M. S., Santos, H., and Galinski, E. A. (1998). An overview of the role and diversity of compatible solutes in Bacteria and Archaea. *Adv Biochem Eng Biotechnol* 61, 117–153. doi: 10.1007/BFb0102291

De Bernardini, N., Basile, A., Zampieri, G., Kovalovszki, A., De Diego Diaz, B., Offer, E., et al. (2022). Integrating metagenomic binning with

flux balance analysis to unravel syntrophies in anaerobic CO_2 methanation. *Microbiome* 10, 117. doi: 10.1186/s40168-022-01311-1

de Bok, F. A. M., Plugge, C. M., and Stams, A. J. M. (2004). Interspecies electron transfer in methanogenic propionate degrading consortia. *Water Res* 38, 1368–1375. doi: 10.1016/j.watres.2003.11.028

De Vrieze, J., Saunders, A. M., He, Y., Fang, J., Nielsen, P. H., Verstraete, W., et al. (2015). Ammonia and temperature determine potential clustering in the anaerobic digestion microbiome. *Water Res* 75, 312–323. doi: 10.1016/j.watres.2015.02.025

DeSantis, T. Z., Hugenholtz, P., Larsen, N., Rojas, M., Brodie, E. L., Keller, K., et al. (2006). Greengenes, a Chimera-Checked 16S rRNA Gene Database and Workbench Compatible with ARB. *Appl Environ Microbiol* 72, 5069–5072. doi: 10.1128/AEM.03006-05

Dolfing, J. (2016). "Protocols for Calculating Reaction Kinetics and Thermodynamics," in *Hydrocarbon and Lipid Microbiology Protocols: Statistics, Data Analysis, Bioinformatics and Modelling*, eds. T. J. McGenity, K. N. Timmis, and B. Nogales Fernández (Berlin, Heidelberg: Springer), 155–163. doi: 10.1007/8623_2015_109

Dolfing, J. (2024). Thermodynamic constraints on the window of opportunity for direct interspecies electron transfer (DIET). *Microb Biotechnol* 17, e70019. doi: 10.1111/1751-7915.70019

Dolfing, J., Larter, S. R., and Head, I. M. (2008). Thermodynamic constraints on methanogenic crude oil biodegradation. *ISME J* 2, 442–452. doi: 10.1038/ismej.2007.111

Doloman, A., Besteman, M. S., Sanders, M. G., and Sousa, D. Z. (2024). Methanogenic partner influences cell aggregation and signalling of *Syntrophobacterium fumaroxidans*. *Appl Microbiol Biotechnol* 108, 127. doi: 10.1007/s00253-023-12955-w

Doloman, A., and Sousa, D. Z. (2024). Mechanisms of microbial co-aggregation in mixed anaerobic cultures. *Appl Microbiol Biotechnol* 108, 407. doi: 10.1007/s00253-024-13246-8

D'Souza, G., Shitut, S., Preussger, D., Yousif, G., Waschina, S., and Kost, C. (2018). Ecology and evolution of metabolic cross-feeding interactions in bacteria. *Nat. Prod. Rep.* 35, 455–488. doi: 10.1039/C8NP00009C

D'Souza, G., Waschina, S., Pande, S., Bohl, K., Kaleta, C., and Kost, C. (2014). Less is more: selective advantages can explain the prevalent loss of biosynthetic genes in bacteria. *Evolution* 68, 2559–2570. doi: 10.1111/evo.12468

Dueholm, M. K. D., Andersen, K. S., Korntved, A.-K. C., Rudkjøbing, V., Alves, M., Bajón-Fernández, Y., et al. (2024). MiDAS 5: Global diversity of bacteria and archaea in anaerobic digesters. *Nat Commun* 15, 5361. doi: 10.1038/s41467-024-49641-y

Dujany, A., Otaola, F., André, L., Naji, A., Luart, D., Leturia, M., et al. (2025). Batch Reactor Design and Conception at Laboratory Scale for Solid-State Anaerobic Digestion: Practical Comparison Between 3D-Printed Digesters and Conventional Methods. *Fermentation* 11, 41. doi: 10.3390/fermentation11010041

Dyksma, S., and Gallert, C. (2019). *Candidatus* Syntrophosphaera thermopropionivorans: a novel player in syntrophic propionate oxidation during anaerobic digestion. *Environmental Microbiology Reports* 11, 558–570. doi: 10.1111/1758-2229.12759

Dyksma, S., Jansen, L., and Gallert, C. (2020). Syntrophic acetate oxidation replaces acetoclastic methanogenesis during thermophilic digestion of biowaste. *Microbiome* 8, 105. doi: 10.1186/s40168-020-00862-5

Edwards, M. D., Black, S., Rasmussen, T., Rasmussen, A., Stokes, N. R., Stephen, T.-L., et al. (2012). Characterization of three novel mechanosensitive channel activities in *Escherichia coli*. *Channels* 6, 272–281. doi: 10.4161/chan.20998

Ehmann, A., Thumm, U., and Lewandowski, I. (2018). Fertilizing Potential of Separated Biogas Digestates in Annual and Perennial Biomass Production Systems. *Front. Sustain. Food Syst.* 2. doi: 10.3389/fsufs.2018.00012

Emerson, K., Russo, R. C., Lund, R. E., and Thurston, R. V. (1975). Aqueous Ammonia Equilibrium Calculations: Effect of pH and Temperature.

Journal of the Fisheries Research Board of Canada 32, 2379–2383. doi: 10.1139/f75-274

Energimyndigheten, and Energigas Sverige (2024). Produktion av biogas och rötrester och dess användning år 2023. Energigas Sverige. Available at: https://www.energigas.se/Media/v32n3skg/biogasstatistik-rapport_2023_slutversion-240930-sammanfogad.pdf

Epstein, W. (1986). Osmoregulation by potassium transport in *Escherichia coli*. *FEMS Microbiology Reviews* 2, 73–78. doi: 10.1111/j.1574-6968.1986.tb01845.x

EurObserv'ER (2022). 21st annual overview barometer. Available at: https://www.eurobserv-er.org/21st-annual-overview-barometer/ (Accessed July 10, 2023).

Evans, C. R., Kempes, C. P., Price-Whelan, A., and Dietrich, L. E. P. (2020). Metabolic Heterogeneity and Cross-Feeding in Bacterial Multicellular Systems. *Trends in Microbiology* 28, 732–743. doi: 10.1016/j.tim.2020.03.008

Evans, P. N., Boyd, J. A., Leu, A. O., Woodcroft, B. J., Parks, D. H., Hugenholtz, P., et al. (2019). An evolving view of methane metabolism in the Archaea. *Nat Rev Microbiol* 17, 219–232. doi: 10.1038/s41579-018-0136-7

Evans, P. N., Parks, D. H., Chadwick, G. L., Robbins, S. J., Orphan, V. J., Golding, S. D., et al. (2015). Methane metabolism in the archaeal phylum *Bathyarchaeota* revealed by genome-centric metagenomics. *Science* 350, 434–438. doi: 10.1126/science.aac7745

Fievet, A., Ducret, A., Mignot, T., Valette, O., Robert, L., Pardoux, R., et al. (2015). Single-Cell Analysis of Growth and Cell Division of the Anaerobe *Desulfovibrio vulgaris* Hildenborough. *Front. Microbiol.* 6. doi: 10.3389/fmicb.2015.01378

Fischer, M. A., Ulbricht, A., Neulinger, S. C., Refai, S., Waßmann, K., Künzel, S., et al. (2019). Immediate Effects of Ammonia Shock on Transcription and Composition of a Biogas Reactor Microbiome. *Front. Microbiol.* 10, 2064. doi: 10.3389/fmicb.2019.02064

Flemming, H.-C., Baveye, P., Neu, T. R., Stoodley, P., Szewzyk, U., Wingender, J., et al. (2021). Who put the film in biofilm? The migration of a term from wastewater engineering to medicine and beyond. *npj Biofilms Microbiomes* 7, 10. doi: 10.1038/s41522-020-00183-3

Flemming, H.-C., van Hullebusch, E. D., Neu, T. R., Nielsen, P. H., Seviour, T., Stoodley, P., et al. (2023). The biofilm matrix: multitasking in a shared space. *Nat Rev Microbiol* 21, 70–86. doi: 10.1038/s41579-022-00791-0

Flemming, H.-C., Wingender, J., Szewzyk, U., Steinberg, P., Rice, S. A., and Kjelleberg, S. (2016). Biofilms: an emergent form of bacterial life. *Nat Rev Microbiol* 14, 563–575. doi: 10.1038/nrmicro.2016.94

Flemming, H.-C., and Wuertz, S. (2019). Bacteria and archaea on Earth and their abundance in biofilms. *Nat Rev Microbiol* 17, 247–260. doi: 10.1038/s41579-019-0158-9

Foo, Y. H., Gao, Y., Zhang, H., and Kenney, L. J. (2015). Cytoplasmic sensing by the inner membrane histidine kinase EnvZ. *Prog Biophys Mol Biol* 118, 119–129. doi: 10.1016/j.pbiomolbio.2015.04.005

Fowler, G. J. (1934). An Introduction to the Biochemistry of Nitrogen Conservation.

Fritts, R. K., McCully, A. L., and McKinlay, J. B. (2021). Extracellular Metabolism Sets the Table for Microbial Cross-Feeding. *Microbiol Mol Biol Rev* 85, e00135-20. doi: 10.1128/MMBR.00135-20

Fuchs, G. (2011). Alternative pathways of carbon dioxide fixation: insights into the early evolution of life? *Annu Rev Microbiol* 65, 631–658. doi: 10.1146/annurev-micro-090110-102801

Garcia, P. S., Gribaldo, S., and Borrel, G. (2022). Diversity and Evolution of Methane-Related Pathways in Archaea. *Annual Review of Microbiology* 76, 727–755. doi: 10.1146/annurev-micro-041020-024935

Geesink, P., ter Horst, J., and Ettema, T. J. G. (2024). More than the sum of its parts: uncovering emerging effects of microbial interactions in complex communities. *FEMS Microbiology Ecology* 100, fiae029. doi: 10.1093/femsec/fiae029

Ginzinger, D. G. (2002). Gene quantification using real-time quantitative PCR: An emerging technology hits the mainstream. *Experimental Hematology* 30, 503–512. doi: 10.1016/S0301-472X(02)00806-8

Gloor, G. B., Macklaim, J. M., Pawlowsky-Glahn, V., and Egozcue, J. J. (2017). Microbiome Datasets Are Compositional: And This Is Not Optional. *Front. Microbiol.* 8. doi: 10.3389/fmicb.2017.02224

Goris, J., Konstantinidis, K. T., Klappenbach, J. A., Coenye, T., Vandamme, P., and Tiedje, J. M. (2007). DNA–DNA hybridization values and their relationship to whole-genome sequence similarities. *International Journal of Systematic and Evolutionary Microbiology* 57, 81–91. doi: 10.1099/ijs.0.64483-0

Grabherr, M. G., Haas, B. J., Yassour, M., Levin, J. Z., Thompson, D. A., Amit, I., et al. (2011). Full-length transcriptome assembly from RNA-Seq data without a reference genome. *Nat Biotechnol* 29, 644–652. doi: 10.1038/nbt.1883

Groher, A., and Weuster-Botz, D. (2016). General medium for the autotrophic cultivation of acetogens. *Bioprocess Biosyst Eng* 39, 1645–1650. doi: 10.1007/s00449-016-1634-5

Gunde-Cimerman, N., Plemenitaš, A., and Oren, A. (2018). Strategies of adaptation of microorganisms of the three domains of life to high salt concentrations. *FEMS Microbiology Reviews* 42, 353–375. doi: 10.1093/femsre/fuy009

Gunnerson, C. G., and Stuckey, D. C. (1986). Anaerobic digestion: principles and practices for biogas systems. World Bank technical paper. International Bank for Reconstruction and Development, Washington, DC (USA). Available at: https://www.osti.gov/biblio/5582401 (Accessed January 29, 2025).

Handelsman, J., Rondon, M. R., Brady, S. F., Clardy, J., and Goodman, R. M. (1998). Molecular biological access to the chemistry of unknown soil microbes: a new frontier for natural products. *Chemistry & Biology* 5, R245–R249. doi: 10.1016/S1074-5521(98)90108-9

Hanišáková, N., Vítězová, M., and Rittmann, S. K.-M. R. (2022). The Historical Development of Cultivation Techniques for Methanogens and Other Strict Anaerobes and Their Application in Modern

Microbiology. *Microorganisms* 10, 412. doi: 10.3390/microorganisms10020412

Hao, L., Michaelsen, T. Y., Singleton, C. M., Dottorini, G., Kirkegaard, R. H., Albertsen, M., et al. (2020). Novel syntrophic bacteria in full-scale anaerobic digesters revealed by genome-centric metatranscriptomics. *ISME J* 14, 906–918. doi: 10.1038/s41396-019-0571-0

Haque, A., Engel, J., Teichmann, S. A., and Lönnberg, T. (2017). A practical guide to single-cell RNA-sequencing for biomedical research and clinical applications. *Genome Medicine* 9, 75. doi: 10.1186/s13073-017-0467-4

Harder, J. (1997). Species-independent maintenance energy and natural population sizes. *FEMS Microbiology Ecology* 23, 39–44. doi: 10.1111/j.1574-6941.1997.tb00389.x

Hari, A. R., Katuri, K. P., Logan, B. E., and Saikaly, P. E. (2016). Set anode potentials affect the electron fluxes and microbial community structure in propionate-fed microbial electrolysis cells. *Scientific reports* 6, 38690.

Harris, R. L., Vetter, M. C. Y. L., van Heerden, E., Cason, E., Vermeulen, J.-G., Taneja, A., et al. (2022). FISH-TAMB, a Fixation-Free mRNA Fluorescent Labeling Technique to Target Transcriptionally Active Members in Microbial Communities. *Microb Ecol* 84, 182–197. doi: 10.1007/s00248-021-01809-5

Hartmann, T., and Leimkühler, S. (2013). The oxygen-tolerant and NAD^+-dependent formate dehydrogenase from *Rhodobacter capsulatus* is able to catalyze the reduction of CO_2 to formate. *The FEBS Journal* 280, 6083–6096. doi: 10.1111/febs.12528

Hattori, S., Kamagata, Y., Hanada, S., and Shoun, H. (2000). *Thermacetogenium phaeum* gen. nov., sp. nov., a strictly anaerobic, thermophilic, syntrophic acetate-oxidizing bacterium. *Int J Syst Evol Microbiol* 50 Pt 4, 1601–1609. doi: 10.1099/00207713-50-4-1601

Hendriks, A. T. W. M., van Lier, J. B., and de Kreuk, M. K. (2018). Growth media in anaerobic fermentative processes: The underestimated potential of thermophilic fermentation and anaerobic digestion.

Biotechnology Advances 36, 1–13. doi: 10.1016/j.biotechadv.2017.08.004

Herlemann, D. P., Labrenz, M., Jürgens, K., Bertilsson, S., Waniek, J. J., and Andersson, A. F. (2011). Transitions in bacterial communities along the 2000 km salinity gradient of the Baltic Sea. *ISME J* 5, 1571–1579. doi: 10.1038/ismej.2011.41

Hidalgo-Ahumada, C. A. P., Nobu, M. K., Narihiro, T., Tamaki, H., Liu, W.-T., Kamagata, Y., et al. (2018). Novel energy conservation strategies and behaviour of *Pelotomaculum schinkii* driving syntrophic propionate catabolism. *Environ Microbiol* 20, 4503–4511. doi: 10.1111/1462-2920.14388

Hoehler, T. M. (2007). An Energy Balance Concept for Habitability. *Astrobiology* 7, 824–838. doi: 10.1089/ast.2006.0095

Hoehler, T. M., and Jørgensen, B. B. (2013). Microbial life under extreme energy limitation. *Nat Rev Microbiol* 11, 83–94. doi: 10.1038/nrmicro2939

Holmes, D. E., Rotaru, A.-E., Ueki, T., Shrestha, P. M., Ferry, J. G., and Lovley, D. R. (2018). Electron and Proton Flux for Carbon Dioxide Reduction in *Methanosarcina barkeri* During Direct Interspecies Electron Transfer. *Front. Microbiol.* 9. doi: 10.3389/fmicb.2018.03109

Homberger, C., Barquist, L., and Vogel, J. (2022). Ushering in a new era of single-cell transcriptomics in bacteria. *microLife* 3, uqac020. doi: 10.1093/femsml/uqac020

Huang, L., Liu, X., Ye, Y., Chen, M., and Zhou, S. (2020). Evidence for the coexistence of direct and riboflavin-mediated interspecies electron transfer in *Geobacter* co-culture. *Environmental Microbiology* 22, 243–254. doi: 10.1111/1462-2920.14842

Hungate, R. E. (1969). "A Roll Tube Method for Cultivation of Strict Anaerobes," in *Methods in Microbiology*, eds. J. R. Norris and D. W. Ribbons (New York: Academic Press), 117–132.

Ian, B. M. (2005). "Extraction of RNA From Cells and Tissue," in *Hypertension: Methods and Protocols*, eds. J. P. Fennell and A. H. Baker

(Totowa, NJ: Humana Press), 139–148. doi: 10.1385/1-59259-850-1:139

Iannotti, E. L., Kafkewitz, D., Wolin, M. J., and Bryant, M. P. (1973). Glucose Fermentation Products of *Ruminococcus albus* Grown in Continuous Culture with *Vibrio succinogenes*: Changes Caused by Interspecies Transfer of H_2. *J Bacteriol* 114, 1231–1240.

International Energy Agency (2021). Ammonia Technology Roadmap. Available at: https://www.iea.org/reports/ammonia-technology-roadmap

Isaac, A., Francis, B., Amann, R. I., and Amin, S. A. (2021). Tight Adherence (Tad) Pilus Genes Indicate Putative Niche Differentiation in Phytoplankton Bloom Associated *Rhodobacterales*. *Front Microbiol* 12, 718297. doi: 10.3389/fmicb.2021.718297

Jagadish, K. S., Chanakya, H. N., Rajabapaiah, P., and Anand, V. (1998). Plug flow digestors for biogas generation from leaf biomass. *Biomass and Bioenergy* 14, 415–423. doi: 10.1016/S0961-9534(98)00003-8

Janda, J. M., and Abbott, S. L. (2007). 16S rRNA Gene Sequencing for Bacterial Identification in the Diagnostic Laboratory: Pluses, Perils, and Pitfalls. *J Clin Microbiol* 45, 2761–2764. doi: 10.1128/JCM.01228-07

Jefferson, K. K. (2004). What drives bacteria to produce a biofilm? *FEMS Microbiol Lett* 236, 163–173. doi: 10.1016/j.femsle.2004.06.005

Ji, J., Kakade, A., Yu, Z., Khan, A., Liu, P., and Li, X. (2020). Anaerobic membrane bioreactors for treatment of emerging contaminants: A review. *Journal of Environmental Management* 270, 110913. doi: 10.1016/j.jenvman.2020.110913

Jiang, Y., Banks, C., Zhang, Y., Heaven, S., and Longhurst, P. (2018). Quantifying the percentage of methane formation via acetoclastic and syntrophic acetate oxidation pathways in anaerobic digesters. *Waste Management* 71, 749–756. doi: 10.1016/j.wasman.2017.04.005

Johnson, D. R., Goldschmidt, F., Lilja, E. E., and Ackermann, M. (2012). Metabolic specialization and the assembly of microbial communities. *ISME J* 6, 1985–1991. doi: 10.1038/ismej.2012.46

Jungwirth, P., and Winter, B. (2008). Ions at aqueous interfaces: from water surface to hydrated proteins. *Annu Rev Phys Chem* 59, 343–366. doi: 10.1146/annurev.physchem.59.032607.093749

Kamravamanesh, D., Rinta Kanto, J. M., Ali-Loytty, H., Myllärinen, A., Saalasti, M., Rintala, J., et al. (2023). *Ex-situ* biological hydrogen methanation in trickle bed reactors: Integration into biogas production facilities. *Chem Eng Sci* 269, 118498. doi: 10.1016/j.ces.2023.118498

Kapinusova, G., Lopez Marin, M. A., and Uhlik, O. (2023). Reaching unreachables: Obstacles and successes of microbial cultivation and their reasons. *Front. Microbiol.* 14. doi: 10.3389/fmicb.2023.1089630

Kariyama, I. D., Zhai, X., and Wu, B. (2018). Influence of mixing on anaerobic digestion efficiency in stirred tank digesters: A review. *Water Research* 143, 503–517. doi: 10.1016/j.watres.2018.06.065

Kaster, A.-K., Moll, J., Parey, K., and Thauer, R. K. (2011). Coupling of ferredoxin and heterodisulfide reduction via electron bifurcation in hydrogenotrophic methanogenic archaea. *Proceedings of the National Academy of Sciences* 108, 2981–2986. doi: 10.1073/pnas.1016761108

Keating, C., Fiege, K., Diender, M., Sousa, D. Z., and Villanueva, L. (2024). Microbial single-cell applications under anoxic conditions. *Applied and Environmental Microbiology* 90, e01321-24. doi: 10.1128/aem.01321-24

Kempf, B., and Bremer, E. (1998). Uptake and synthesis of compatible solutes as microbial stress responses to high-osmolality environments. *Arch Microbiol* 170, 319–330. doi: 10.1007/s002030050649

Khanal, S. K. (2008). “Overview of Anaerobic Biotechnology,” in *Anaerobic Biotechnology for Bioenergy Production*, (John Wiley & Sons, Ltd), 1–27. doi: 10.1002/9780813804545.ch1

Kiani Deh Kiani, M., Parsaee, M., Safieddin Ardebili, S. M., Reyes, I. P., Fuess, L. T., and Karimi, K. (2022). Different bioreactor configurations for biogas production from sugarcane vinasse: A comprehensive review. *Biomass and Bioenergy* 161, 106446. doi: 10.1016/j.biombioe.2022.106446

Kim, M., Oh, H.-S., Park, S.-C., and Chun, J. (2014). Towards a taxonomic coherence between average nucleotide identity and 16S rRNA gene sequence similarity for species demarcation of prokaryotes. *International Journal of Systematic and Evolutionary Microbiology* 64, 346–351. doi: 10.1099/ijs.0.059774-0

Kim, M., Rhee, C., Wells, M., Shin, J., Lee, J., and Shin, S. G. (2022). Key players in syntrophic propionate oxidation revealed by metagenome-assembled genomes from anaerobic digesters bioaugmented with propionic acid enriched microbial consortia. *Front. Microbiol.* 13. doi: 10.3389/fmicb.2022.968416

Kleiner, D. (1981). The transport of NH_3 and NH_4^+ across biological membranes. *Biochim Biophys Acta* 639, 41–52. doi: 10.1016/0304-4173(81)90004-5

Kleinsteuber, S. (2018). "Metagenomics of Methanogenic Communities in Anaerobic Digesters," in *Biogenesis of Hydrocarbons*, eds. A. J. M. Stams and D. Sousa (Cham: Springer International Publishing), 1–23. doi: 10.1007/978-3-319-53114-4_16-1

Klingenberg, H., and Meinicke, P. (2017). How to normalize metatranscriptomic count data for differential expression analysis. *PeerJ* 5, e3859. doi: 10.7717/peerj.3859

Kobayashi, A., Taketa, M., Sowa, K., Kano, K., Higuchi, Y., and Ogata, H. (2023). Structure and function relationship of formate de-hydrogenases: an overview of recent progress. *IUCrJ* 10, 544–554. doi: 10.1107/S2052252523006437

Kong, L., Feng, Y., Du, W., Zheng, R., Sun, J., Rong, K., et al. (2023). Cross-Feeding between Filamentous Cyanobacteria and Symbiotic Bacteria Favors Rapid Photogranulation. *Environ Sci Technol* 57, 16953–16963. doi: 10.1021/acs.est.3c04867

Konstantinidis, K. T., Rosselló-Móra, R., and Amann, R. (2017). Uncultivated microbes in need of their own taxonomy. *ISME J* 11, 2399–2406. doi: 10.1038/ismej.2017.113

Konstantinidis, K. T., and Tiedje, J. M. (2005). Genomic insights that advance the species definition for prokaryotes. *Proceedings of the National Academy of Sciences* 102, 2567–2572. doi: 10.1073/pnas.0409727102

Kopylova, E., Noé, L., and Touzet, H. (2012). SortMeRNA: fast and accurate filtering of ribosomal RNAs in metatranscriptomic data. *Bioinformatics* 28, 3211–3217. doi: 10.1093/bioinformatics/bts611

Kosaka, T., Uchiyama, T., Ishii, S., Enoki, M., Imachi, H., Kamagata, Y., et al. (2006). Reconstruction and Regulation of the Central Catabolic Pathway in the Thermophilic Propionate-Oxidizing Syntroph Pelotomaculum thermopropionicum. *Journal of Bacteriology* 188, 202–210. doi: 10.1128/jb.188.1.202-210.2006

Koster, I. W., and Lettinga, G. (1984). The influence of ammonium-nitrogen on the specific activity of pelletized methanogenic sludge. *Agricultural Wastes* 9, 205–216. doi: 10.1016/0141-4607(84)90080-5

Kougias, P. G., and Angelidaki, I. (2018). Biogas and its opportunities—A review. *Front. Environ. Sci. Eng.* 12, 14. doi: 10.1007/s11783-018-1037-8

Kovács, E., Wirth, R., Maróti, G., Bagi, Z., Nagy, K., Minárovits, J., et al. (2015). Augmented biogas production from protein-rich substrates and associated metagenomic changes. *Bioresour Technol* 178, 254–261. doi: 10.1016/j.biortech.2014.08.111

Kragh, K. N., Tolker-Nielsen, T., and Lichtenberg, M. (2023). The non-attached biofilm aggregate. *Commun Biol* 6, 1–13. doi: 10.1038/s42003-023-05281-4

Kuchina, A., Brettner, L. M., Paleologu, L., Roco, C. M., Rosenberg, A. B., Carignano, A., et al. (2021). Microbial single-cell RNA sequencing by split-pool barcoding. *Science* 371, eaba5257. doi: 10.1126/science.aba5257

Kugelman, I. J., and McCarty, P. L. (1965). Cation Toxicity and Stimulation in Anaerobic Waste Treatment. *Journal (Water Pollution Control Federation)* 37, 97–116.

Kurth, J. M., Op den Camp, H. J. M., and Welte, C. U. (2020). Several ways one goal—methanogenesis from unconventional substrates. *Appl Microbiol Biotechnol* 104, 6839–6854. doi: 10.1007/s00253-020-10724-7

Labatut, R. A., Angenent, L. T., and Scott, N. R. (2014). Conventional mesophilic vs. thermophilic anaerobic digestion: A trade-off between performance and stability? *Water Research* 53, 249–258. doi: 10.1016/j.watres.2014.01.035

Lange, M., Macario, A. J. L., Ahring, B. K., and Conway de Macario, E. (1997). Increased transcripts of the dnaK locus genes in *Methanosarcina mazei* S-6 exposed to supraoptimal concentrations of ammonia. *FEMS Microbiology Letters* 152, 379–384. doi: 10.1111/j.1574-6968.1997.tb10455.x

Li, C., He, P., Hao, L., Lü, F., Shao, L., and Zhang, H. (2022). Diverse acetate-oxidizing syntrophs contributing to biogas production from food waste in full-scale anaerobic digesters in China. *Renew Energy* 193, 240–250. doi: 10.1016/j.renene.2022.04.143

Liu, H. Y., Prentice, E. L., and Webber, M. A. (2024). Mechanisms of antimicrobial resistance in biofilms. *npj Antimicrob Resist* 2, 1–10. doi: 10.1038/s44259-024-00046-3

Liu, L., Liu, M., Jiang, Y., Lin, W., and Luo, J. (2021). Production and Excretion of Polyamines To Tolerate High Ammonia, a Case Study on Soil Ammonia-Oxidizing Archaeon "*Candidatus* Nitrosocosmicus agrestis." *mSystems* 6, 10.1128/msystems.01003-20. doi: 10.1128/msystems.01003-20

Liu, P., and Lu, Y. (2018). Concerted Metabolic Shifts Give New Insights Into the Syntrophic Mechanism Between Propionate-Fermenting *Pelotomaculum thermopropionicum* and Hydrogenotrophic *Methanocella conradii*. *Front. Microbiol.* 9. doi: 10.3389/fmicb.2018.01551

Liu, S., Moon, C. D., Zheng, N., Huws, S., Zhao, S., and Wang, J. (2022). Opportunities and challenges of using metagenomic data to bring uncultured microbes into cultivation. *Microbiome* 10, 76. doi: 10.1186/s40168-022-01272-5

Liu, T., Sun, L., Nordberg, Å., and Schnürer, A. (2018). Substrate-Induced Response in Biogas Process Performance and Microbial Community Relates Back to Inoculum Source. *Microorganisms* 6, 80. doi: 10.3390/microorganisms6030080

Liu, Y., Balkwill, D. L., Aldrich, H. C., Drake, G. R., and Boone, D. R. (1999). Characterization of the anaerobic propionate-degrading syntrophs *Smithella propionica* gen. nov., sp. nov. and *Syntrophobacter wolinii*. *International Journal of Systematic and Evolutionary Microbiology* 49, 545–556. doi: 10.1099/00207713-49-2-545

Losensky, G., Jung, K., Urlaub, H., Pfeifer, F., Fröls, S., and Lenz, C. (2017). Shedding light on biofilm formation of *Halobacterium salinarum* R1 by SWATH-LC/MS/MS analysis of planktonic and sessile cells. *Proteomics* 17. doi: 10.1002/pmic.201600111

Lovley, D. R. (2011). Powering microbes with electricity: direct electron transfer from electrodes to microbes. *Environmental Microbiology Reports* 3, 27–35. doi: 10.1111/j.1758-2229.2010.00211.x

Lovley, D. R. (2017). Syntrophy Goes Electric: Direct Interspecies Electron Transfer. *Annual Review of Microbiology* 71, 643–664. doi: 10.1146/annurev-micro-030117-020420

Lowe, R., Shirley, N., Bleackley, M., Dolan, S., and Shafee, T. (2017). Transcriptomics technologies. *PLoS Comput Biol* 13, e1005457. doi: 10.1371/journal.pcbi.1005457

Lubitz, W., Ogata, H., Rüdiger, O., and Reijerse, E. (2014). Hydrogenases. *Chem. Rev.* 114, 4081–4148. doi: 10.1021/cr4005814

Ma, P., Amemiya, H. M., He, L. L., Gandhi, S. J., Nicol, R., Bhattacharyya, R. P., et al. (2023). Bacterial droplet-based single-cell RNA-seq reveals antibiotic-associated heterogeneous cellular states. *Cell* 186, 877-891.e14. doi: 10.1016/j.cell.2023.01.002

Maeda, H., Fujimoto, C., Haruki, Y., Maeda, T., Kokeguchi, S., Petelin, M., et al. (2003). Quantitative real-time PCR using TaqMan and SYBR Green for Actinobacillus actinomycetemcomitans, Porphyromonas gingivalis, Prevotella intermedia, tetQ gene and total bacteria. *FEMS Immunol Med Microbiol* 39, 81–86. doi: 10.1016/S0928-8244(03)00224-4

Maier, A., Mguni, L. M., Ngo, A. C. R., and Tischler, D. (2024). Formate Dehydrogenase: Recent Developments for NADH and NADPH Recycling in Biocatalysis. *ChemCatChem* 16, e202401021. doi: 10.1002/cctc.202401021

Maleki, F., Ovens, K., Hogan, D. J., and Kusalik, A. J. (2020). Gene Set Analysis: Challenges, Opportunities, and Future Research. *Front. Genet.* 11. doi: 10.3389/fgene.2020.00654

Martin, J. A., and Wang, Z. (2011). Next-generation transcriptome assembly. *Nat Rev Genet* 12, 671–682. doi: 10.1038/nrg3068

Maus, I., Rumming, M., Bergmann, I., Heeg, K., Pohl, M., Nettmann, E., et al. (2018). Characterization of *Bathyarchaeota* genomes assembled from metagenomes of biofilms residing in mesophilic and thermophilic biogas reactors. *Biotechnol Biofuels* 11, 167. doi: 10.1186/s13068-018-1162-4

Mayr, E. (1942). *Systematics and the Origin of Species*. New York: Columbia University Press.

McCarty, P. L., and McKinney, R. E. (1961). Salt Toxicity in Anaerobic Digestion. *Journal (Water Pollution Control Federation)* 33, 399–415.

McNulty, R., Sritharan, D., Pahng, S. H., Meisch, J. P., Liu, S., Brennan, M. A., et al. (2023). Probe-based bacterial single-cell RNA sequencing predicts toxin regulation. *Nat Microbiol* 8, 934–945. doi: 10.1038/s41564-023-01348-4

Mee, M. T., and Wang, H. H. (2012). Engineering ecosystems and synthetic ecologies. *Mol. BioSyst.* 8, 2470–2483. doi: 10.1039/C2MB25133G

Men, Y., Feil, H., VerBerkmoes, N. C., Shah, M. B., Johnson, D. R., Lee, P. K. H., et al. (2012). Sustainable syntrophic growth of *Dehalococcoides ethenogenes* strain 195 with *Desulfovibrio vulgaris*

Hildenborough and *Methanobacterium congolense*: global transcriptomic and proteomic analyses. *The ISME Journal* 6, 410–421. doi: 10.1038/ismej.2011.111

Men, Y., Yu, K., Bælum, J., Gao, Y., Tremblay, J., Prestat, E., et al. (2017). Metagenomic and Metatranscriptomic Analyses Reveal the Structure and Dynamics of a Dechlorinating Community Containing *Dehalococcoides mccartyi* and Corrinoid-Providing Microorganisms under Cobalamin-Limited Conditions. *Applied and Environmental Microbiology* 83, e03508-16. doi: 10.1128/AEM.03508-16

Menes, R. J., and Muxí, L. (2002). *Anaerobaculum mobile* sp. nov., a novel anaerobic, moderately thermophilic, peptide-fermenting bacterium that uses crotonate as an electron acceptor, and emended description of the genus *Anaerobaculum*. *International Journal of Systematic and Evolutionary Microbiology* 52, 157–164. doi: 10.1099/00207713-52-1-157

Merkel, A. Yu., Tarnovetskii, I. Yu., Podosokorskaya, O. A., and Toshchakov, S. V. (2019). Analysis of 16S rRNA Primer Systems for Profiling of Thermophilic Microbial Communities. *Microbiology* 88, 671–680. doi: 10.1134/S0026261719060110

Merrick, M. J., and Edwards, R. A. (1995). Nitrogen control in bacteria. *Microbiol Rev* 59, 604–622.

Meyer, J. (2007). [FeFe] hydrogenases and their evolution: a genomic perspective. *Cell Mol Life Sci* 64, 1063–1084. doi: 10.1007/s00018-007-6477-4

Michaelis, C., and Grohmann, E. (2023). Horizontal Gene Transfer of Antibiotic Resistance Genes in Biofilms. *Antibiotics (Basel)* 12, 328. doi: 10.3390/antibiotics12020328

Moestedt, J., Nordell, E., Hallin, S., and Schnürer, A. (2016). Two-stage anaerobic digestion for reduced hydrogen sulphide production. *Journal of Chemical Technology & Biotechnology* 91, 1055–1062. doi: 10.1002/jctb.4682

Mojtabavi, S., Samadi, N., and Faramarzi, M. A. (2019). Osmolyte-Induced Folding and Stability of Proteins: Concepts and Characterization. *Iran J Pharm Res* 18, 13–30. doi: 10.22037/ijpr.2020.112621.13857

Morra, S. (2022). Fantastic [FeFe]-Hydrogenases and Where to Find Them. *Frontiers in Microbiology* 13. Available at: https://www.frontiersin.org/articles/10.3389/fmicb.2022.853626 (Accessed November 7, 2022).

Morris, B. E. L., Henneberger, R., Huber, H., and Moissl-Eichinger, C. (2013). Microbial syntrophy: interaction for the common good. *FEMS Microbiol Rev* 37, 384–406. doi: 10.1111/1574-6976.12019

Morris, J. J., Lenski, R. E., and Zinser, E. R. (2012). The Black Queen Hypothesis: Evolution of Dependencies through Adaptive Gene Loss. *mBio* 3, e00036-12. doi: 10.1128/mBio.00036-12

Mp, D. (2006). Degradation of RNA in bacteria: comparison of mRNA and stable RNA. *Nucleic acids research* 34. doi: 10.1093/nar/gkj472

Müller, N., Worm, P., Schink, B., Stams, A. J. M., and Plugge, C. M. (2010). Syntrophic butyrate and propionate oxidation processes: from genomes to reaction mechanisms. *Environ Microbiol Rep* 2, 489–499. doi: 10.1111/j.1758-2229.2010.00147.x

Murray, R. G., and Schleifer, K. H. (1994). Taxonomic notes: a proposal for recording the properties of putative taxa of procaryotes. *Int J Syst Bacteriol* 44, 174–176. doi: 10.1099/00207713-44-1-174

Neubeck, A., Sjöberg, S., Price, A., Callac, N., and Schnürer, A. (2016). Effect of Nickel Levels on Hydrogen Partial Pressure and Methane Production in Methanogens. *PLoS One* 11, e0168357. doi: 10.1371/journal.pone.0168357

Oren, A. (2013). "Life at High Salt Concentrations," in *The Prokaryotes: Prokaryotic Communities and Ecophysiology*, eds. E. Rosenberg, E. F. DeLong, S. Lory, E. Stackebrandt, and F. Thompson (Berlin, Heidelberg: Springer), 421–440. doi: 10.1007/978-3-642-30123-0_57

Oren, A., Arahal, D. R., Göker, M., Moore, E. R. B., Rossello-Mora, R., and Sutcliffe, I. C. (2023). International Code of Nomenclature of Prokaryotes. Prokaryotic Code (2022 Revision). *International Journal of Systematic and Evolutionary Microbiology* 73, 005585. doi: 10.1099/ijsem.0.005585

Overmann, J., Huang, S., Nübel, U., Hahnke, R. L., and Tindall, B. J. (2019). Relevance of phenotypic information for the taxonomy of not-yet-cultured microorganisms. *Systematic and Applied Microbiology* 42, 22–29. doi: 10.1016/j.syapm.2018.08.009

Pan, P., Gu, Y., Sun, D.-L., Wu, Q. L., and Zhou, N.-Y. (2023). Microbial Diversity Biased Estimation Caused by Intragenomic Heterogeneity and Interspecific Conservation of 16S rRNA Genes. *Applied and Environmental Microbiology* 89, e02108-22. doi: 10.1128/aem.02108-22

Pan, S.-Y., He, K.-H., Lin, K.-T., Fan, C., and Chang, C.-T. (2022). Addressing nitrogenous gases from croplands toward low-emission agriculture. *npj Clim Atmos Sci* 5, 1–18. doi: 10.1038/s41612-022-00265-3

Park, J.-H., Kang, H.-J., Park, K.-H., and Park, H.-D. (2018). Direct interspecies electron transfer via conductive materials: A perspective for anaerobic digestion applications. *Bioresource Technology* 254, 300–311. doi: 10.1016/j.biortech.2018.01.095

Parks, D. H., Chuvochina, M., Rinke, C., Mussig, A. J., Chaumeil, P.-A., and Hugenholtz, P. (2022). GTDB: an ongoing census of bacterial and archaeal diversity through a phylogenetically consistent, rank normalized and complete genome-based taxonomy. *Nucleic Acids Research* 50, D785–D794. doi: 10.1093/nar/gkab776

Patón, M., Hernández, H. H., and Rodríguez, J. (2020). Comprehensive Bioenergetic Evaluation of Microbial Pathway Variants in Syntrophic Propionate Oxidation. *mSystems* 5, e00814-20. doi: 10.1128/mSystems.00814-20

Patro, R., Duggal, G., Love, M. I., Irizarry, R. A., and Kingsford, C. (2017). Salmon provides fast and bias-aware quantification of transcript expression. *Nat Methods* 14, 417–419. doi: 10.1038/nmeth.4197

Pavlostathis, S. G., and Giraldo-Gomez, E. (1991). Kinetics of anaerobic treatment: A critical review. *Critical Reviews in Environmental Control* 21, 411–490. doi: 10.1080/10643389109388424

Pelletier, E., Kreimeyer, A., Bocs, S., Rouy, Z., Gyapay, G., Chouari, R., et al. (2008). "*Candidatus* Cloacamonas Acidaminovorans": Genome Sequence Reconstruction Provides a First Glimpse of a New

Bacterial Division. *Journal of Bacteriology* 190, 2572–2579. doi: 10.1128/jb.01248-07

Perman, E., Karlsson, A., Westerholm, M., Isaksson, S., and Schnürer, A. (2024). High-solid digestion – A comparison of completely stirred and plug-flow reactor systems. *Waste Manage* 189, 265–275. doi: 10.1016/j.wasman.2024.08.025

Perozo, E., and Rees, D. C. (2003). Structure and mechanism in prokaryotic mechanosensitive channels. *Current Opinion in Structural Biology* 13, 432–442. doi: 10.1016/S0959-440X(03)00106-4

Peters, J. W., Miller, A.-F., Jones, A. K., King, P. W., and Adams, M. W. (2016). Electron bifurcation. *Current Opinion in Chemical Biology* 31, 146–152. doi: 10.1016/j.cbpa.2016.03.007

Peters, J. W., Schut, G. J., Boyd, E. S., Mulder, D. W., Shepard, E. M., Broderick, J. B., et al. (2015). [FeFe]- and [NiFe]-hydrogenase diversity, mechanism, and maturation. *Biochimica et Biophysica Acta (BBA) - Molecular Cell Research* 1853, 1350–1369. doi: 10.1016/j.bbamcr.2014.11.021

Pevzner, P. A., Tang, H., and Waterman, M. S. (2001). An Eulerian path approach to DNA fragment assembly. *Proc Natl Acad Sci U S A* 98, 9748–9753. doi: 10.1073/pnas.171285098

Philips, J., Rabaey, K., Lovley, D. R., and Vargas, M. (2017). Biofilm Formation by *Clostridium ljungdahlii* Is Induced by Sodium Chloride Stress: Experimental Evaluation and Transcriptome Analysis. *PLOS ONE* 12, e0170406. doi: 10.1371/journal.pone.0170406

Poretsky, R., Rodriguez-R, L. M., Luo, C., Tsementzi, D., and Konstantinidis, K. T. (2014). Strengths and Limitations of 16S rRNA Gene Amplicon Sequencing in Revealing Temporal Microbial Community Dynamics. *PLoS One* 9, e93827. doi: 10.1371/journal.pone.0093827

Price, M. N., Zane, G. M., Kuehl, J. V., Melnyk, R. A., Wall, J. D., Deutschbauer, A. M., et al. (2018). Filling gaps in bacterial amino acid biosynthesis pathways with high-throughput genetics. *PLOS Genetics* 14, e1007147. doi: 10.1371/journal.pgen.1007147

Procházka, J., Dolejš, P., Máca, J., and Dohányos, M. (2012). Stability and inhibition of anaerobic processes caused by insufficiency or excess of ammonia nitrogen. *Appl Microbiol Biotechnol* 93, 439–447. doi: 10.1007/s00253-011-3625-4

Quast, C., Pruesse, E., Yilmaz, P., Gerken, J., Schweer, T., Yarza, P., et al. (2013). The SILVA ribosomal RNA gene database project: improved data processing and web-based tools. *Nucleic Acids Res* 41, D590–D596. doi: 10.1093/nar/gks1219

Quince, C., Nurk, S., Raguideau, S., James, R., Soyer, O. S., Summers, J. K., et al. (2021). STRONG: metagenomics strain resolution on assembly graphs. *Genome Biology* 22, 214. doi: 10.1186/s13059-021-02419-7

Quince, C., Walker, A. W., Simpson, J. T., Loman, N. J., and Segata, N. (2017). Shotgun metagenomics, from sampling to analysis. *Nat Biotechnol* 35, 833–844. doi: 10.1038/nbt.3935

Racher, K. I., Voegele, R. T., Marshall, E. V., Culham, D. E., Wood, J. M., Jung, H., et al. (1999). Purification and Reconstitution of an Osmosensor: Transporter ProP of *Escherichia coli* Senses and Responds to Osmotic Shifts. *Biochemistry* 38, 1676–1684. doi: 10.1021/bi981279n

Raghavan, V., Kraft, L., Mesny, F., and Rigerte, L. (2022). A simple guide to de novo transcriptome assembly and annotation. *Briefings in Bioinformatics* 23, bbab563. doi: 10.1093/bib/bbab563

Rajagopal, R., Massé, D. I., and Singh, G. (2013). A critical review on inhibition of anaerobic digestion process by excess ammonia. *Bioresour Technol* 143, 632–641. doi: 10.1016/j.biortech.2013.06.030

Regeringskansliet, R. och (2019). Mer biogas! För ett hållbart Sverige. *Regeringskansliet*. Available at: https://www.regeringen.se/rattsligadokument/statens-offentliga-utredningar/2019/12/sou-201963/ (Accessed January 31, 2025).

Robazza, A., Baleeiro, F. C. F., Kleinsteuber, S., and Neumann, A. (2024). Two-stage conversion of syngas and pyrolysis aqueous condensate into L-malate. *Biotechnology for Biofuels and Bioproducts* 17, 85. doi: 10.1186/s13068-024-02532-2

Roberts, M. F. (2005). Organic compatible solutes of halotolerant and halophilic microorganisms. *Saline Systems* 1, 5. doi: 10.1186/1746-1448-1-5

Roels, J., and Verstraete, W. (2001). Biological formation of volatile phosphorus compounds. *Bioresour Technol* 79, 243–250. doi: 10.1016/s0960-8524(01)00032-3

Rossello-Mora, R., Konstantinidis, K. T., Sutcliffe, I., and Whitman, W. (2020). Opinion: Response to concerns about the use of DNA sequences as types in the nomenclature of prokaryotes. *Syst Appl Microbiol* 43, 126070. doi: 10.1016/j.syapm.2020.126070

Rossi-Tamisier, M., Benamar, S., Raoult, D., and Fournier, P.-E. (2015). Cautionary tale of using 16S rRNA gene sequence similarity values in identification of human-associated bacterial species. *Int J Syst Evol Microbiol* 65, 1929–1934. doi: 10.1099/ijs.0.000161

Rouvière, P. E., and Wolfe, R. S. (1988). Novel biochemistry of methanogenesis. *J Biol Chem* 263, 7913–7916.

Rübenhagen, R., Rönsch, H., Jung, H., Krämer, R., and Morbach, S. (2000). Osmosensor and Osmoregulator Properties of the Betaine Carrier BetP from *Corynebacterium glutamicum* in Proteoliposomes *. *Journal of Biological Chemistry* 275, 735–741. doi: 10.1074/jbc.275.2.735

Ruiz-Sánchez, J., Campanaro, S., Guivernau, M., Fernández, B., and Prenafeta-Boldú, F. X. (2018). Effect of ammonia on the active microbiome and metagenome from stable full-scale digesters. *Bioresource Technology* 250, 513–522. doi: 10.1016/j.biortech.2017.11.068

Sadava, D., Hillis, D. M., Heller, H. C., and Berenbaum, M. R. (2014). *Life: The Science of Biology*., 10th Edn. Basingstoke, UK: Macmillan Education.

Saddoud, A., Hassaïri, I., and Sayadi, S. (2007). Anaerobic membrane reactor with phase separation for the treatment of cheese whey. *Bioresource Technology* 98, 2102–2108. doi: 10.1016/j.biortech.2006.08.013

Sánchez-Cañizares, C., Prell, J., Pini, F., Rutten, P., Kraxner, K., Wynands, B., et al. (2020). Global control of bacterial nitrogen and carbon metabolism by a PTSNtr-regulated switch. *Proceedings of the National Academy of Sciences* 117, 10234–10245. doi: 10.1073/pnas.1917471117

Sancho Navarro, S., Cimpoia, R., Bruant, G., and Guiot, S. R. (2016). Biomethanation of Syngas Using Anaerobic Sludge: Shift in the Catabolic Routes with the CO Partial Pressure Increase. *Front. Microbiol.* 7. doi: 10.3389/fmicb.2016.01188

Sarker, S., Lamb, J. J., Hjelme, D. R., and Lien, K. M. (2019). A Review of the Role of Critical Parameters in the Design and Operation of Biogas Production Plants. *Applied Sciences* 9, 1915. doi: 10.3390/app9091915

Sarker, S., Møller, H. B., and Bruhn, A. (2014). Influence of variable feeding on mesophilic and thermophilic co-digestion of *Laminaria digitata* and cattle manure. *Energy Conversion and Management* 87, 513–520. doi: 10.1016/j.enconman.2014.07.039

Sauer, K., Stoodley, P., Goeres, D. M., Hall-Stoodley, L., Burmølle, M., Stewart, P. S., et al. (2022). The biofilm life cycle: expanding the conceptual model of biofilm formation. *Nat Rev Microbiol* 20, 608–620. doi: 10.1038/s41579-022-00767-0

Saunois, M., Stavert, A. R., Poulter, B., Bousquet, P., Canadell, J. G., Jackson, R. B., et al. (2020). The Global Methane Budget 2000–2017. *Earth System Science Data* 12, 1561–1623. doi: 10.5194/essd-12-1561-2020

Scarlat, N., Dallemand, J.-F., and Fahl, F. (2018). Biogas: Developments and perspectives in Europe. *Renew Energy* 129, 457–472. doi: 10.1016/j.renene.2018.03.006

Schink, B. (1997). Energetics of syntrophic cooperation in methanogenic degradation. *Microbiol Mol Biol Rev* 61, 262–280. doi: 10.1128/mmbr.61.2.262-280.1997

Schink, B., McInerney, M. J., Hoehler, T., and Gunsalus, R. P. (2019). "Introduction to Microbial Hydrocarbon Production: Bioenergetics," in *Biogenesis of Hydrocarbons*, eds. A. J. M. Stams and D. Z. Sousa

(Cham: Springer International Publishing), 1–17. doi: 10.1007/978-3-319-78108-2_1

Schink, B., and Stams, A. J. M. (2002). "Syntrophism among prokaryotes," in *The prokaryotes*, (Springer), 471–493. doi: 10.1007/978-3-642-30123-0_59

Schmid, J., Sieber, V., and Rehm, B. (2015). Bacterial exopolysaccharides: biosynthesis pathways and engineering strategies. *Front Microbiol* 6, 496. doi: 10.3389/fmicb.2015.00496

Schnürer, A., and Jarvis, Å. (2018). *Microbiology of the biogas process*. Swedish Waste Management.

Schnürer, A., Svensson, B. H., and Schink, B. (1997). Enzyme activities in and energetics of acetate metabolism by the mesophilic syntrophically acetate-oxidizing anaerobe *Clostridium ultunense*. *FEMS Microbiology Letters* 154, 331–336. doi: 10.1016/S0378-1097(97)00350-9

Schut, G. J., and Adams, M. W. W. (2009). The iron-hydrogenase of *Thermotoga maritima* utilizes ferredoxin and NADH synergistically: a new perspective on anaerobic hydrogen production. *J Bacteriol* 191, 4451–4457. doi: 10.1128/JB.01582-08

Sedano-Núñez, V. T., Boeren, S., Stams, A. J. M., and Plugge, C. M. (2018). Comparative proteome analysis of propionate degradation by *Syntrophobacter fumaroxidans* in pure culture and in coculture with methanogens. *Environ Microbiol* 20, 1842–1856. doi: 10.1111/1462-2920.14119

Seeton, C. J. (2006). Viscosity–temperature correlation for liquids. *Tribol Lett* 22, 67–78. doi: 10.1007/s11249-006-9071-2

Sharma, S., Mohler, J., Mahajan, S. D., Schwartz, S. A., Bruggemann, L., and Aalinkeel, R. (2023). Microbial Biofilm: A Review on Formation, Infection, Antibiotic Resistance, Control Measures, and Innovative Treatment. *Microorganisms* 11, 1614. doi: 10.3390/microorganisms11061614

Sheng, K., Cao, W., Niu, Y., Deng, Q., and Zong, C. (2017). Effective detection of variation in single-cell transcriptomes using MATQ-seq. *Nat Methods* 14, 267–270. doi: 10.1038/nmeth.4145

Shima, S., Huang, G., Wagner, T., and Ermler, U. (2020). Structural Basis of Hydrogenotrophic Methanogenesis. *Annu Rev Microbiol* 74, 713–733. doi: 10.1146/annurev-micro-011720-122807

Shimoyama, T., Kato, S., Ishii, S., and Watanabe, K. (2009). Flagellum Mediates Symbiosis. *Science* 323, 1574–1574. doi: 10.1126/science.1170086

Sieber, J. R., McInerney, M. J., Müller, N., Schink, B., Gunsalus, R. P., and Plugge, C. M. (2018). "Methanogens: Syntrophic Metabolism," in *Biogenesis of Hydrocarbons*, eds. A. J. M. Stams and D. Sousa (Cham: Springer International Publishing), 1–31. doi: 10.1007/978-3-319-53114-4_2-1

Singh, A., Schnürer, A., Dolfing, J., and Westerholm, M. (2023). Syntrophic entanglements for propionate and acetate oxidation under thermophilic and high-ammonia conditions. *ISME J* 17, 1966–1978. doi: 10.1038/s41396-023-01504-y

Singh, A., Schnürer, A., and Westerholm, M. (2021). Enrichment and description of novel bacteria performing syntrophic propionate oxidation at high ammonia level. *Environ Microbiol.* 23, 1620–1637. doi: 10.1111/1462-2920.15388

Singh, B., Szamosi, Z., and Siménfalvi, Z. (2019). State of the art on mixing in an anaerobic digester: A review. *Renewable Energy* 141, 922–936. doi: 10.1016/j.renene.2019.04.072

Sleator, R. D., and Hill, C. (2002). Bacterial osmoadaptation: the role of osmolytes in bacterial stress and virulence. *FEMS Microbiol Rev* 26, 49–71. doi: 10.1111/j.1574-6976.2002.tb00598.x

Smith, C., Hill, A. K., and Torrente-Murciano, L. (2020). Current and future role of Haber–Bosch ammonia in a carbon-free energy landscape. *Energy Environ. Sci.* 13, 331–344. doi: 10.1039/C9EE02873K

Smith, J. A., Nevin, K. P., and Lovley, D. R. (2015). Syntrophic growth via quinone-mediated interspecies electron transfer. *Front. Microbiol.* 6. doi: 10.3389/fmicb.2015.00121

Søndergaard, D., Pedersen, C. N. S., and Greening, C. (2016). HydDB: A web tool for hydrogenase classification and analysis. *Sci Rep* 6, 34212. doi: 10.1038/srep34212

Sprott, G. D., Shaw, K. M., and Jarrell, K. F. (1984). Ammonia/potassium exchange in methanogenic bacteria. *Journal of Biological Chemistry* 259, 12602–12608. doi: 10.1016/S0021-9258(18)90789-1

Sprott, G. D., Shaw, K. M., and Jarrell, K. F. (1985). Methanogenesis and the K^+ transport system are activated by divalent cations in ammonia-treated cells of *Methanospirillum hungatei*. *Journal of Biological Chemistry* 260, 9244–9250. doi: 10.1016/S0021-9258(17)39359-6

Stams, A. J. M., Van Dijk, J. B., Dijkema, C., and Plugge, C. M. (1993). Growth of Syntrophic Propionate-Oxidizing Bacteria with Fumarate in the Absence of Methanogenic Bacteria. *Appl Environ Microbiol* 59, 1114–1119.

Steffen, R., Szolar, O., and Braun, R. (1998). *Feedstocks for Anaerobic Digestion*. Vienna, Austria: Institute for Agrobiotechnology Tulln, University of Agricultural Sciences. Available at: https://citeseerx.ist.psu.edu/document?repid=rep1&type=pdf&doi=293ea2a9a8d8315548b8d749f60e4b28378d9dfa

Steinhaus, B., Garcia, M. L., Shen, A. Q., and Angenent, L. T. (2007). A Portable Anaerobic Microbioreactor Reveals Optimum Growth Conditions for the *Methanogen Methanosaeta* concilii. *Appl Environ Microbiol* 73, 1653–1658. doi: 10.1128/AEM.01827-06

Storck, T., Virdis, B., and Batstone, D. J. (2016). Modelling extracellular limitations for mediated versus direct interspecies electron transfer. *ISME J* 10, 621–631. doi: 10.1038/ismej.2015.139

Su, K., Li, L., Wang, Q., and Cao, R. (2023). A Review on the Interspecies Electron Transfer of Methane Production in Anaerobic Digestion System. *Fermentation* 9, 467. doi: 10.3390/fermentation9050467

Subramanian, A., Tamayo, P., Mootha, V. K., Mukherjee, S., Ebert, B. L., Gillette, M. A., et al. (2005). Gene set enrichment analysis: A knowledge-based approach for interpreting genome-wide expression profiles. *Proceedings of the National Academy of Sciences* 102, 15545–15550. doi: 10.1073/pnas.0506580102

Sutcliffe, I. C. (2015). Challenging the anthropocentric emphasis on phenotypic testing in prokaryotic species descriptions: rip it up and start again. *Front. Genet.* 6. doi: 10.3389/fgene.2015.00218

Tampio, E., Laaksonen, I., Rimhanen, K., Honkala, N., Laakso, J., Soinne, H., et al. (2024). Effect of manure co-digestion on methane production, carbon retention, and fertilizer value of digestate. *Science of The Total Environment* 927, 172083. doi: 10.1016/j.scitotenv.2024.172083

Thauer, R. K. (2012). The Wolfe cycle comes full circle. *Proceedings of the National Academy of Sciences* 109, 15084–15085. doi: 10.1073/pnas.1213193109

Thauer, R. K., Jungermann, K., and Decker, K. (1977). Energy conservation in chemotrophic anaerobic bacteria. *Bacteriol Rev* 41, 100–180. doi: 10.1128/br.41.1.100-180.1977

Thauer, R. K., Kaster, A.-K., Goenrich, M., Schick, M., Hiromoto, T., and Shima, S. (2010). Hydrogenases from Methanogenic Archaea, Nickel, a Novel Cofactor, and H_2 Storage. *Annu. Rev. Biochem.* 79, 507–536. doi: 10.1146/annurev.biochem.030508.152103

Thauer, R. K., Kaster, A.-K., Seedorf, H., Buckel, W., and Hedderich, R. (2008). Methanogenic archaea: ecologically relevant differences in energy conservation. *Nat Rev Microbiol* 6, 579–591. doi: 10.1038/nrmicro1931

Thermo Fisher Scientific (2021). The Basics of RNA Isolation. Available at: https://www.thermofisher.com/se/en/home/references/ambion-tech-support/rna-isolation/general-articles/the-basics-rna-isolation.html

Timmers, P. H. A., Vavourakis, C. D., Kleerebezem, R., Damsté, J. S. S., Muyzer, G., Stams, A. J. M., et al. (2018). Metabolism and Occurrence of Methanogenic and Sulfate-Reducing Syntrophic Acetate Oxidizing Communities in Haloalkaline Environments. *Frontiers in*

Microbiology 9. Available at: https://www.frontiersin.org/articles/10.3389/fmicb.2018.03039 (Accessed May 29, 2023).

Tramontano, M., Andrejev, S., Pruteanu, M., Klünemann, M., Kuhn, M., Galardini, M., et al. (2018). Nutritional preferences of human gut bacteria reveal their metabolic idiosyncrasies. *Nat Microbiol* 3, 514–522. doi: 10.1038/s41564-018-0123-9

Trunk, T., Khalil, H. S., Leo, J. C., Trunk, T., Khalil, H. S., and Leo, J. C. (2018). Bacterial autoaggregation. *AIMSMICRO* 4, 140–164. doi: 10.3934/microbiol.2018.1.140

Valentini, M., and Filloux, A. (2016). Biofilms and Cyclic di-GMP (c-di-GMP) Signaling: Lessons from *Pseudomonas aeruginosa* and Other Bacteria. *J Biol Chem* 291, 12547–12555. doi: 10.1074/jbc.R115.711507

van Bodegom, P. (2007). Microbial Maintenance: A Critical Review on Its Quantification. *Microb Ecol* 53, 513–523. doi: 10.1007/s00248-006-9049-5

Van, D. P., Fujiwara, T., Tho, B. L., Toan, P. P. S., and Minh, G. H. (2020). A review of anaerobic digestion systems for biodegradable waste: Configurations, operating parameters, and current trends. *Environmental Engineering Research* 25, 1–17. doi: 10.4491/eer.2018.334

van der Heide, T., and Poolman, B. (2000). Osmoregulated ABC-transport system of *Lactococcus lactis* senses water stress via changes in the physical state of the membrane. *Proceedings of the National Academy of Sciences* 97, 7102–7106. doi: 10.1073/pnas.97.13.7102

van Wolferen, M., Orell, A., and Albers, S.-V. (2018). Archaeal biofilm formation. *Nat Rev Microbiol* 16, 699–713. doi: 10.1038/s41579-018-0058-4

Vandamme, P., Pot, B., Gillis, M., de Vos, P., Kersters, K., and Swings, J. (1996). Polyphasic taxonomy, a consensus approach to bacterial systematics. *Microbiological Reviews* 60, 407–438. doi: 10.1128/mr.60.2.407-438.1996

Vanwonterghem, I., Evans, P. N., Parks, D. H., Jensen, P. D., Woodcroft, B. J., Hugenholtz, P., et al. (2016). Methylotrophic methanogenesis

discovered in the archaeal phylum *Verstraetearchaeota*. *Nat Microbiol* 1, 1–9. doi: 10.1038/nmicrobiol.2016.170

Varghese, N. J., Mukherjee, S., Ivanova, N., Konstantinidis, K. T., Mavrommatis, K., Kyrpides, N. C., et al. (2015). Microbial species delineation using whole genome sequences. *Nucleic Acids Res* 43, 6761–6771. doi: 10.1093/nar/gkv657

Viacava, K., Qiao, J., Janowczyk, A., Poudel, S., Jacquemin, N., Meibom, K. L., et al. (2022). Meta-omics-aided isolation of an elusive anaerobic arsenic-methylating soil bacterium. *The ISME Journal* 16, 1740–1749. doi: 10.1038/s41396-022-01220-z

Vignais, P. M., and Billoud, B. (2007). Occurrence, Classification, and Biological Function of Hydrogenases: An Overview. *Chem. Rev.* 107, 4206–4272. doi: 10.1021/cr050196r

Wahl, A., Huptas, C., and Neuhaus, K. (2022). Comparison of rRNA depletion methods for efficient bacterial mRNA sequencing. *Sci Rep* 12, 5765. doi: 10.1038/s41598-022-09710-y

Wang, B., Lin, A. E., Yuan, J., Novak, K. E., Koch, M. D., Wingreen, N. S., et al. (2023). Single-cell massively-parallel multiplexed microbial sequencing (M3-seq) identifies rare bacterial populations and profiles phage infection. *Nat Microbiol* 8, 1846–1862. doi: 10.1038/s41564-023-01462-3

Wang, Z., Wang, S., Hu, Y., Du, B., Meng, J., Wu, G., et al. (2022). Distinguishing responses of acetoclastic and hydrogenotrophic methanogens to ammonia stress in mesophilic mixed cultures. *Water Res* 224, 119029. doi: 10.1016/j.watres.2022.119029

Ward, A. J., Hobbs, P. J., Holliman, P. J., and Jones, D. L. (2008). Optimisation of the anaerobic digestion of agricultural resources. *Bioresource Technology* 99, 7928–7940. doi: 10.1016/j.biortech.2008.02.044

Wayne, L. G., Brenner, D. J., Colwell, R. R., Grimont, P. A. D., Kandler, O., Krichevsky, M. I., et al. (1987). Report of the Ad Hoc Committee on Reconciliation of Approaches to Bacterial Systematics. *International Journal of Systematic and Evolutionary Microbiology* 37, 463–464. doi: 10.1099/00207713-37-4-463

Weng, N., and Perman, E. (2024). RNA extraction & depletion. *Protocols.io.* doi: dx.doi.org/10.17504/protocols.io.36wgq3y6klk5/v1

Weng, X., Mao, Z., Fu, H.-M., Chen, Y.-P., Guo, J.-S., Fang, F., et al. (2022). Biofilm formation during wastewater treatment: Motility and physiological response of aerobic denitrifying bacteria under ammonia stress based on surface plasmon resonance imaging. *Bioresour Technol* 361, 127712. doi: 10.1016/j.biortech.2022.127712

Westerholm, M., Calusinska, M., and Dolfing, J. (2022). Syntrophic propionate-oxidizing bacteria in methanogenic systems. *FEMS Microbiology Reviews* 46, fuab057. doi: 10.1093/femsre/fuab057

Westerholm, M., Liu, T., and Schnürer, A. (2020). Comparative study of industrial-scale high-solid biogas production from food waste: Process operation and microbiology. *Bioresour Technol* 304, 122981. doi: 10.1016/j.biortech.2020.122981

Westerholm, M., Moestedt, J., and Schnürer, A. (2016). Biogas production through syntrophic acetate oxidation and deliberate operating strategies for improved digester performance. *Applied Energy* 179, 124–135. doi: 10.1016/j.apenergy.2016.06.061

Westerholm, M., Müller, B., Isaksson, S., and Schnürer, A. (2015). Trace element and temperature effects on microbial communities and links to biogas digester performance at high ammonia levels. *Biotechnol Biofuels* 8, 154. doi: 10.1186/s13068-015-0328-6

Westerholm, M., Roos, S., and Schnürer, A. (2010). *Syntrophaceticus schinkii* gen. nov., sp. nov., an anaerobic, syntrophic acetate-oxidizing bacterium isolated from a mesophilic anaerobic filter. *FEMS Microbiol Lett* 309, 100–104. doi: 10.1111/j.1574-6968.2010.02023.x

Westerholm, M., Roos, S., and Schnürer, A. (2011). *Tepidanaerobacter acetatoxydans* sp. nov., an anaerobic, syntrophic acetate-oxidizing bacterium isolated from two ammonium-enriched mesophilic methanogenic processes. *Systematic and Applied Microbiology* 34, 260–266. doi: 10.1016/j.syapm.2010.11.018

Whatmore, A. M., Chudek, J. A., and Reed, R. H. (1990). The effects of osmotic upshock on the intracellular solute pools of *Bacillus subtilis*.

J Gen Microbiol 136, 2527–2535. doi: 10.1099/00221287-136-12-2527

Whitfield, C., Wear, S. S., and Sande, C. (2020). Assembly of Bacterial Capsular Polysaccharides and Exopolysaccharides. *Annu Rev Microbiol* 74, 521–543. doi: 10.1146/annurev-micro-011420-075607

Whitman, W. B. (2016). Modest proposals to expand the type material for naming of prokaryotes. *Int J Syst Evol Microbiol* 66, 2108–2112. doi: 10.1099/ijsem.0.000980

Whitman, W. B., Bowen, T. L., and Boone, D. R. (2006). "The Methanogenic Bacteria," in *The Prokaryotes: An Evolving Electronic Resource for the Microbiological Community*, ed. M. Dworkin (New York: Springer). Available at: http://link.springer-ny.com/link/service/books/10125

Whitman, W. B., Sutcliffe, I. C., and Rossello-Mora, R. (2019). Proposal for changes in the International Code of Nomenclature of Prokaryotes: granting priority to Candidatus names. *Int J Syst Evol Microbiol* 69, 2174–2175. doi: 10.1099/ijsem.0.003419

Withers, P. J. A., Neal, C., Jarvie, H. P., and Doody, D. G. (2014). Agriculture and Eutrophication: Where Do We Go from Here? *Sustainability* 6, 5853–5875. doi: 10.3390/su6095853

Woese, C. R. (1987). Bacterial evolution. *Microbiol Rev* 51, 221–271.

Woese, C. R., Stackebrandt, E., Macke, T. J., and Fox, G. E. (1985). A Phylogenetic Definition of the Major Eubacterial Taxa. *Systematic and Applied Microbiology* 6, 143–151. doi: 10.1016/S0723-2020(85)80047-3

Wood, G. E., Haydock, A. K., and Leigh, J. A. (2003). Function and Regulation of the Formate Dehydrogenase Genes of the Methanogenic Archaeon *Methanococcus maripaludis*. *J Bacteriol* 185, 2548–2554. doi: 10.1128/JB.185.8.2548-2554.2003

Wood, J. M. (1999). Osmosensing by Bacteria: Signals and Membrane-Based Sensors. *Microbiol Mol Biol Rev* 63, 230–262.

Wood, J. M. (2006). Osmosensing by Bacteria. *Science's STKE* 2006, pe43–pe43. doi: 10.1126/stke.3572006pe43

Wood, J. M. (2011). Bacterial osmoregulation: a paradigm for the study of cellular homeostasis. *Annu Rev Microbiol* 65, 215–238. doi: 10.1146/annurev-micro-090110-102815

World Biogas Association (2019). World Biogas Association (WBA): Global Potential of Biogas. Available at: https://www.worldbiogasassociation.org/wp-content/uploads/2019/09/WBA-execsummary-4ppa4_digital-Sept-2019.pdf (Accessed July 10, 2023).

Yenigün, O., and Demirel, B. (2013). Ammonia inhibition in anaerobic digestion: A review. *Process Biochemistry* 48, 901–911. doi: 10.1016/j.procbio.2013.04.012

Yuan, H., and Zhu, N. (2016). Progress in inhibition mechanisms and process control of intermediates and by-products in sewage sludge anaerobic digestion. *Renewable and Sustainable Energy Reviews* 58, 429–438. doi: 10.1016/j.rser.2015.12.261

Yuan, J., Doucette, C. D., Fowler, W. U., Feng, X.-J., Piazza, M., Rabitz, H. A., et al. (2009). Metabolomics-driven quantitative analysis of ammonia assimilation in E. coli. *Mol Syst Biol* 5, 302. doi: 10.1038/msb.2009.60

Zeng, Y., Zheng, D., Li, L.-P., Wang, M., Gou, M., Kamagata, Y., et al. (2024). Metabolism of novel potential syntrophic acetate-oxidizing bacteria in thermophilic methanogenic chemostats. *Applied and Environmental Microbiology* 90, e01090-23. doi: 10.1128/aem.01090-23

Zhang, B., Zhang, L. L., Zhang, S. C., Shi, H. Z., and Cai, W. M. (2005). The influence of pH on hydrolysis and acidogenesis of kitchen wastes in two-phase anaerobic digestion. *Environ Technol* 26, 329–339. doi: 10.1080/09593332608618563

Zhu, X., Campanaro, S., Treu, L., Seshadri, R., Ivanova, N., Kougias, P. G., et al. (2020). Metabolic dependencies govern microbial syntrophies during methanogenesis in an anaerobic digestion ecosystem. *Microbiome* 8, 22. doi: 10.1186/s40168-019-0780-9

Zhuang, L., Ma, J., Tang, J., Tang, Z., and Zhou, S. (2017). Cysteine-Accelerated Methanogenic Propionate Degradation in Paddy Soil Enrichment. *Microb Ecol* 73, 916–924. doi: 10.1007/s00248-016-0882-x

Popular science summary

Climate change is one of the greatest challenges of our time. Our use of fossil energy sources, such as coal and oil, has released enormous amounts of carbon dioxide (CO_2) into the atmosphere. There, the carbon dioxide contributes to global warming by acting like a blanket, reflecting the Earth's heat radiation back toward the surface of the earth. To avoid further contributing to this warming, we must essentially stop using these fossil fuels. To achieve that, we need to turn to alternative energy sources such as solar, hydro, wind, and bioenergy. Biogas (a mixture of methane and carbon dioxide) is one such alternative. Biogas is produced by microorganisms (bacteria and archaea) through the anaerobic digestion process, which occurs in oxygen-deprived environments rich in organic (carbon-containing) material. Examples of such environments include wetlands, lakebeds, and digestive tracts. When anaerobic digestion occurs in natural settings, it contributes to methane emissions, which like carbon dioxide, also intensify global warming. However, by conducting this biological process in a controlled space (a bioreactor), the resulting biogas can be captured. This biotechnological process, aimed at producing biogas, will hereafter be referred to as the biogas process. The biogas can be used directly as heat to power generators and produce electricity, or it can be upgraded for use as vehicle fuel among other uses. In theory, most organic materials can be used in the biogas process. One of the biogas process greatest advantages is its ability to convert organic waste, such as food waste, manure, and residues from industry and agriculture, into energy. In addition to the biogas produced, the process yields a nutrient-rich residue called digestate. This is the material exiting the bioreactor that has not been converted to gas. It contains the nutrients originally present in the organic waste and can be used as an organic fertilizer. This versatility is a key strength of the biogas process. It recovers energy, handles waste, recycles nutrients, and in some cases prevents methane emissions if the waste would otherwise have been left to decompose freely. The biogas process will by no means be able replace fossil fuels on its own. Achieving this will likely require a combination of energy sources. However, it is one of the best, if not the best technology for addressing all these problems at once.

One of the more common issues with the biogas process is the inhibition of microorganisms due to ammonia accumulation, which is formed during the

degradation of protein-rich waste. Using such protein-rich waste has several advantages. It yields a high amount of biogas per unit weight and results in a nutrient-rich digestate. However, the ammonia-induced inhibition can, in the worst case, cause the biogas process to fail. Some systems, however, that gradually acclimate to ammonia can continue to function undisturbed even at elevated ammonia levels. Understanding how these systems work is the focus of the research in this thesis.

In order to be able to delve into those details, we must first explain how the biogas process works at the microbial level. As mentioned earlier, the conversion of organic material is performed by microorganisms. An entire ecosystem of microbes is required to break down large molecules like fats, sugars, and proteins into biogas. This degradation occurs sequentially, with the waste (product) of one microorganism serving as the food (substrate) for the next. The exact microorganisms involved vary between reactors and systems, but they are generally categorized into groups based on their functional roles. To understand the research in this thesis, one must understand the final steps of the biogas process where methane is formed. The very last step is carried out by a group of microorganism called methanogens. There are two main types of methanogens: those that convert acetate into methane (acetoclastic methanogens) and those that convert carbon dioxide and hydrogen into methane (hydrogenotrophic methanogens). In typical low ammonia biogas systems, acetoclastic methanogens account for most of the methane produced. However, these methanogens are highly sensitive to ammonia and are thereby inhibited at elevated ammonia levels. This results in a build-up of acetate, which then inhibits microbes earlier in the degradation chain. Furthermore, the usual organisms responsible for converting propionate (a molecule similar to acetate but with one additional carbon) are also sensitive to ammonia and are located just above the methanogens in the sequential steps of degradations. In systems adapted to high ammonia concentrations, an alternative pathway is used for the conversion of acetate and propionate. Hydrogenotrophic methanogens are generally less sensitive to ammonia, and by converting the accumulated acetate and propionate into forms that these methanogens can use, namely hydrogen and carbon dioxide, the biogas process can continue. There is one group of bacteria that can convert acetate into hydrogen and carbon dioxide (SAOB), and another group that can convert propionate into hydrogen, carbon dioxide, and acetate (SPOB), after which

the acetate is converted by SAOB. The issue with these conversions is that they yield very little energy, and the bacteria accumulate excess electrons that they must dispose of. They cannot carry out these conversions unless they closely cooperate with a hydrogenotrophic methanogen that can rapidly accept these electrons, typically in the form of hydrogen, which the methanogen needs in order to convert carbon dioxide into methane. In fact, none of these three organisms could perform this conversion on their own, a mutual dependency called syntrophy. Syntrophic organisms gain very little energy performing these reactions. In simple terms, they must share the energy that is available, which results in slow growth and low abundance in the the biogas ecosystem. Therefore, they are often insufficient if ammonia levels suddenly increase in a typical low-ammonia system. Their low abundance also makes them difficult to study, as they are hidden within the immense diversity of the other microorganisms present in biogas systems.

This thesis investigates these syntrophic organisms through a so-called enrichment culture derived from a high-ammonia bioreactor that has been fed propionate or acetate over a long period, enriching for the syntrophic organisms. The aim of the thesis is to characterize this culture and answer questions such as: Which organisms are present? How do they convert propionate and acetate? What does their cooperation look like? Do they employ any strategies to cope with high ammonia levels? To answer these questions, the microorganisms were analysed using methods that examine their genetic material to identify which organisms and genes are present, as well as which genes are actively expressed. This provided vital clues about which proteins the organisms produced, that is, the molecular machines they use to perform nearly all cellular functions. Additionally, this thesis included the development of small 3D-printed bioreactors that enabled microscopic observation of microorganisms over time in an oxygen-free environment, something previously not possible.

In summary, this thesis identified the syntrophic organisms involved in syntrophic propionate oxidation in the enrichment culture, one of which was a previously unknown hydrogenotrophic methanogen. These syntrophic organisms appeared to use multiple pathways for disposal of excess electrons. Beyond hydrogen, formate also was used. The overarching goal of this thesis and the knowledge it contributes is to develop strategies for managing biogas

reactors to make them more resilient to ammonia-induced disturbances. It also aims to provide general insight into microbial interactions, which may be valuable in other biotechnological systems.

Populärvetenskaplig sammanfattning

Klimatet är en av vår tids största utmaningar. Vårt användande av fossila energikällor, såsom kol och olja, har frisläppt enorma mängder koldioxid (CO_2) i atmosfären. Där bidrar koldioxiden till jordens uppvärmning genom att, likt ett täcke, reflektera tillbaka jordens värmestrålning. För att inte ytterligare bidra till denna uppvärmning måste vi i princip sluta använda dessa fossila energikällor, och för att göra detta behöver vi använda oss av alternativa energikällor såsom sol, vatten, vind och bioenergi. Biogas (en blandning av metan och koldioxid) är en sådan alternativ energikälla. Biogas produceras av mikroorganismer (bakterier och bakterieliknande arkéer) i den så kallade rötningsprocessen, som sker i syrefattiga miljöer där det finns gott om organiskt material (kolinnehållande). Exempel på sådana miljöer är träskmarker, sjöbottnar och mag-tarmkanaler. När rötningsprocessen sker i naturliga miljöer bidrar det till utsläpp av metan, som likt koldioxid också bidrar till jordens uppvärmning. Men genom att låta denna biologiska process istället ske i ett kontrollerat utrymme (bioreaktor) kan man samla in den biogas som bildas. Denna bioteknologiska process, med syftet att producera biogas, kommer hädanefter benämnas biogasprocessen. Biogasen kan sedan användas direkt som värme för att driva generatorer och skapa el, eller uppgraderas så att den kan användas som bränsle, till exempel för bilar. Teoretiskt kan det mesta organiska material användas i biogasprocessen, men en av dess största styrkor är att den kan ta organiskt avfall såsom matavfall, gödsel, rester från industri och jordbruk och omvandla det till energi. Utöver den biogas som bildas skapas även en näringsrik så kallad rötrest, vilket är det material som kommer ut från bioreaktorn och som inte omvandlats till gas. Den innehåller de näringsämnen som fanns i det organiska avfallet som stoppades in i bioreaktorn och kan användas som ett organiskt gödsel. Denna mångsidighet är biogasprocessens styrka. Den utvinner energi, hanterar avfall, återvinner näringsämnen och förhindrar i vissa fall utsläpp av metan om avfallet annars hade hamnat ute i det fria. Biogasprocessen kommer inte på långa vägar kunna ersätta de fossila bränslena. För detta krävs troligtvis en kombination av olika källor. Men det är en, om inte den bästa, teknologin för att lösa alla dessa problem samtidigt.

Ett av de vanligare problemen för biogasprocessen är hämning av mikroorganismer på grund av ammoniak, som bildas vid nedbrytning av proteinrikt

avfall. Att använda denna typ av avfall har flera fördelar. Det ger mycket biogas per viktenhet och en mycket näringsrik rötrest. Men hämningen det kan orsaka kan i värsta fall leda till att biogasprocessen stannar. Vissa system som gradvis får vänja sig vid ammoniak kan däremot fungera obehindrat. Det är hur dessa system fungerar som forskningen i denna avhandling handlar om. Men för att kunna gå in på dessa detaljer behöver vi förklara hur biogasprocessen fungerar på mikroorganismernas nivå. Som tidigare nämnt sker omvandlingen av organiskt material av mikroorganismer. Ett helt ekosystem av mikroorganismer krävs för att bryta ner större molekyler såsom fett, socker och proteiner till biogas. Nedbrytningen sker sekventiellt, där restprodukten (avföringen) från en mikroorganism blir substratet (maten) för nästa. Exakt vilka mikroorganismer som utför nedbrytningen varierar mellan bioreaktorer och system, men de brukar delas in efter roller eller grupper som utför typiska omvandlingar. För att förstå forskningen i denna avhandling måste man förstå de sista stegen i biogasprocessen där metan bildas. Det absolut sista steget i processen utförs av så kallade metanogener. Det finns två huvudsakliga typer av metanogener: de som omvandlar ättiksyra (acetat) till metan (acetoklastiska metanogener), och de som omvandlar koldioxid och vätgas till metan (hydrogenotrofa metanogener). I vanliga biogassystem står de acetatkonsumerande metanogenerna för det mesta av den bildade biogasen. Men dessa metanogener är väldigt känsliga för ammoniak och hämmas därav. Det leder till att de inte kan konsumera acetat, vilket då ackumuleras och i sin tur hämmar mikroorganismer högre upp i nedbrytningsledet. Vidare är de normala organismerna för omvandlingen av propionat (som acetat fast med ett extra kol) också känsliga för ammoniak, och de står direkt ovanför metanogenerna i kedjan.

I processer som har vant sig vid höga ammoniaknivåer används en alternativ väg för omvandlingen av acetat och propionat. De hydrogenotrofa metanogenerna är oftast inte lika känsliga för ammoniak, och genom att omvandla de ackumulerade restprodukterna acetat och propionat till en form som de hydrogenotrofa metanogenerna kan använda, det vill säga vätgas och koldioxid, kan biogasprocessen fortlöpa. Det finns en viss grupp bakterier som kan omvandla acetat till vätgas och koldioxid (SAOB). Det finns en annan grupp som kan omvandla propionat till vätgas, koldioxid och acetat (SPOB), varefter acetatet omvandlas av SAOB. Problemet med dessa omvandlingar är att de ger väldigt lite energi och bakterierna får ett överskott av elektroner

som de måste göra sig av med. De kan inte utföra denna omvandling om de inte samarbetar tätt med en hydrogenotrof metanogen som snabbt kan ta upp dessa elektroner, vanligen i form av vätgas, vilka metanogenen behöver för att kunna omvandla koldioxid till metan. Faktum är att ingen av dessa tre organismer skulle kunna utföra detta på egen hand, utan de kräver varandras hjälp. Ett fenomen som kallas syntrofi. Problemet med denna syntrofa trio är att de får väldigt lite energi. Förenklat sett måste de dela på den energi som finns tillgänglig, vilket gör att de växer långsamt och har låg förekomst i hela ekosystemet i biogasprocessen. De räcker därför oftast inte till om ammoniaknivåerna plötsligt skulle öka i en normal process med låg ammoniaknivå. Deras låga förekomst gör dem dessutom svåra att studera, då de försvinner i det enorma antalet mikroorganismer som finns i biogassystemet.

Denna avhandling studerar dessa syntrofa organismer genom en så kallad anrikningskultur som kommer från en bioreaktor med hög ammoniaknivå, som har matats med propionat och acetat under en längre tid, vilket har anrikat de syntrofa organismerna. Syftet med avhandlingen är att beskriva denna kultur och svara på frågor såsom: Vilka är organismerna som finns där? Hur gör de för att omvandla propionat och acetat? Hur ser deras samarbete ut? Gör de något för att hantera den höga ammoniaknivån? För att besvara dessa frågor har mikroorganismerna analyserats med metoder som undersöker deras arvsmassa för att få ledtrådar om vilka organismer och gener som finns där, men också vilka gener som faktiskt uttrycks. Det ger viktiga ledtrådar kring vilka proteiner organismerna tillverkar, alltså de små molekylära maskiner som mikroorganismerna använder för att utföra i stort sett alla sysslor. Vidare innebär denna avhandling framtagandet av små 3D-printade bioreaktorer som gjort det möjligt att studera mikroorganismerna i mikroskop över tid i en syrefri miljö, något som tidigare inte varit möjligt.

Sammanfattningsvis har denna avhandling identifierat de syntrofa organismerna i en propionat nedbrytande anrikningskultur, varav en var en tidigare okänd hydrogenotrof metanogen. De syntrofa organismerna verkade använda olika vägar för att göra sig av med överskotts-elektroner. Utöver vätgas användes även format. Det övergripande målet med denna avhandling och den kunskap den bidrar med är att kunna hitta strategier för att sköta biogasreaktorer så att de blir mer tåliga mot ammoniakstörningar. Den syftar

också till att bidra med generell kunskap om mikroorganismers samspel, vilket kan vara värdefullt i andra bioteknologiska system.

Acknowledgements

Först och främst, tack Maria Westerholm för att du gav mig möjligheten att påbörja denna resa, och för ett varm välkomnande till Uppsala och till forskningsgruppen. Tack för ditt tålamod, din kunskap, och all din ovärderliga hjälp under dessa år. Utan dig hade jag aldrig klarat detta. Din glädje och passion för området lyser verkligen igenom och inspirerar.

Tack Jonas A. Ohlsson, för din handledning. För dina alltid så insiktsfulla och konkreta kommentarer och idéer, de har förbättrat många av mina arbeten. Tack för ditt stöd och din positiva attityd, och vetskapen att du alltid ställer upp och finns där. För alla intressanta tankar och idéer som gör alla luncher lite roligare!

Thank you Abhijet Singh, for your always positive attitude and willingness to help. I have really appreciated your guidance throughout these years.

Thank you Jan Dolfing, for interesting and though provoking mail-threads. I really admire the clarity in which you formulate your ideas, it is a quality I aspire to develop in my own writing.

Tack Simon, för att du likt Atlas håller uppe labbet på dina axlar och får allt att friktionsfritt rulla på. För alla analyser du har hjälpt till med genom åren. Men framför allt tack för dina härliga energi och den glädje du sprider på jobbet. Jag är tacksam för alla fina frisbee rundor vi har haft genom åren.

Tack Dries, min härliga rumskamrat för din fina och nyfikna energi. Tack för att du har stått ut med mitt stundvis dåliga humör, och för all support, och input dy har gett som har hjälp mig genom många problem genom åren.

Thank you Eduardo my fellow PhD companion with whom I started this journey. Thank you for your open hearted way of sharing yourself and your thoughts.

Thank you to all current and former members of the AMB group. I truly see you all as my friends. Each of you has been a big part of what made these four years of my PhD worthwhile.

Till min älskade familj, Ánimo, Peter och Kicki. Tack för att ni alltid finns där för mig. Jag är så tacksam för all den fina tid vi har haft tillsammans.

Till Julia! Du är utan tvekan det bästa och finaste som dessa år har gett mig. Jag är så glad att tacksam att jag får ha dig i mitt liv. Jag älskar dig.

I

frontiers | Frontiers in Microbiology

TYPE Original Research
PUBLISHED 05 June 2024
DOI 10.3389/fmicb.2024.1389257

OPEN ACCESS

EDITED BY
Decai Jin,
Chinese Academy of Sciences (CAS), China

REVIEWED BY
Sabine Kleinsteuber,
Helmholtz Association of German Research Centres (HZ), Germany
Anna Doloman,
Wageningen University and Research, Netherlands

*CORRESPONDENCE
Maria Westerholm
maria.westerholm@slu.se

RECEIVED 21 February 2024
ACCEPTED 23 May 2024
PUBLISHED 05 June 2024

CITATION
Weng N, Singh A, Ohlsson JA, Dolfing J and Westerholm M (2024) Catabolism and interactions of syntrophic propionate- and acetate oxidizing microorganisms under mesophilic, high-ammonia conditions. *Front. Microbiol.* 15:1389257. doi: 10.3389/fmicb.2024.1389257

Catabolism and interactions of syntrophic propionate- and acetate oxidizing microorganisms under mesophilic, high-ammonia conditions

Nils Weng[1], Abhijeet Singh[2], Jonas A. Ohlsson[1], Jan Dolfing[3] and Maria Westerholm[1]*

[1]Department of Molecular Sciences, Swedish University of Agricultural Sciences, Uppsala, Sweden, [2]Palaeobiology, Department of Earth Sciences, Uppsala University, Uppsala, Sweden, [3]Faculty of Energy and Environment, Northumbria University, Newcastle upon Tyne, United Kingdom

Microbial inhibition by high ammonia concentrations is a recurring problem that significantly restricts methane formation from intermediate acids, i.e., propionate and acetate, during anaerobic digestion of protein-rich waste material. Studying the syntrophic communities that perform acid conversion is challenging, due to their relatively low abundance within the microbial communities typically found in biogas processes and disruption of their cooperative behavior in pure cultures. To overcome these limitations, this study examined growth parameters and microbial community dynamics of highly enriched mesophilic and ammonia-tolerant syntrophic propionate and acetate-oxidizing communities and analyzed their metabolic activity and cooperative behavior using metagenomic and metatranscriptomic approaches. Cultivation in batch set-up demonstrated biphasic utilization of propionate, wherein acetate accumulated and underwent oxidation before complete degradation of propionate. Three key species for syntrophic acid degradation were inferred from genomic sequence information and gene expression: a syntrophic propionate-oxidizing bacterium (SPOB) "*Candidatus* Syntrophopropionicum ammoniitolerans", a syntrophic acetate-oxidizing bacterium (SAOB) *Syntrophaceticus schinkii* and a novel hydrogenotrophic methanogen, for which we propose the provisional name "*Candidatus* Methanoculleus ammoniitolerans". The results revealed consistent transcriptional profiles of the SAOB and the methanogen both during propionate and acetate oxidation, regardless of the presence of an active propionate oxidizer. Gene expression indicated versatile capabilities of the two syntrophic bacteria, utilizing both molecular hydrogen and formate as an outlet for reducing equivalents formed during acid oxidation, while conserving energy through build-up of sodium/proton motive force. The methanogen used hydrogen and formate as electron sources. Furthermore, results of the present study provided a framework for future research into ammonia tolerance, mobility, aggregate formation and interspecies cooperation.

KEYWORDS

syntrophic propionate oxidation, syntrophic acetate oxidation, hydrogenotrophic methanogenesis, ammonia tolerance, anaerobic degradation, biogas production, syntrophy

Introduction

Anaerobic digestion (AD) is a waste management and renewable energy production technology which provides environmental benefits through substitution of fossil fuels and generation of nutrient-rich residual material that can be used as fertilizer. The AD sector has considerable expansion potential and can be one of the tools needed to prevent further climate change (World Biogas Association, 2019; EurObserv'ER, 2022). In AD, organic matter is degraded through a series of consecutive and parallel reactions by a consortium of cooperating microorganisms, eventually resulting in production of methane and carbon dioxide (CO_2). Substrate composition and operating parameters have crucial impacts on the structure and activity of the microbial community, and thereby on overall process performance (Westerholm et al., 2019b). One of the most common process challenges is high ammonia levels arising from anaerobic degradation of protein-rich materials (e.g., slaughterhouse waste, food waste and animal manure) (Westerholm et al., 2022). High ammonia levels inhibit various members of the AD community, including acetate-utilizing methanogens (De Vrieze et al., 2015; Fischer et al., 2019; Wang et al., 2022), leading to lower methane yields and accumulation of the organic intermediates propionate and acetate (Westerholm et al., 2015). This acid accumulation leads to process instability and can halt upstream microbial activities, ultimately causing process failure if not managed properly.

Satisfactory methane yields and relatively stable operating conditions can still be achieved under high-ammonia conditions. In AD processes stressed by high ammonia or high temperature, syntrophic acid-oxidizing reactions have been shown to offer important routes for propionate and acetate conversion (Westerholm et al., 2016; Ruiz-Sánchez et al., 2018; Buhlmann et al., 2019; Singh et al., 2023). Within those routes, acetate is oxidized by syntrophic acetate-oxidizing bacteria (SAOB) that operate the Wood-Ljungdahl pathway (WLP) in reverse to form CO_2 and hydrogen (H_2) (or formate) (Schnürer et al., 1997; Hattori et al., 2005; Manzoor et al., 2016a). Propionate is metabolized by syntrophic propionate-oxidizing bacteria (SPOB), most often via the methylmalonyl-CoA (mmc) pathway which yields acetate, H_2 and CO_2 as products. This propionate conversion route occurs both in low- and high-ammonia conditions, although the bacterial species involved differ (Westerholm et al., 2022; Singh et al., 2023). A characteristic in common to both SAOB and SPOB is the need to establish tight mutualistic interaction with a hydrogenotrophic methanogen, which makes the acid oxidation reactions thermodynamically feasible by maintaining H_2/formate at low levels. These mutualistic interactions and the thermodynamic restrictions underpinning them have been suggested to restrict acid degradation rates (Dolfing, 1992; Ishii et al., 2005; McInerney et al., 2009; Leng et al., 2018). Ammonia concentrations above certain levels can also affect cell growth and acid degradation rates despite the communities being ammonia-tolerant, ultimately leading to acid accumulation in AD processes (Westerholm et al., 2019a). To prevent acid accumulation and improve process disturbances, there is a need to increase understanding of the complex interactions that drive syntrophic acid oxidation in high-ammonia conditions, and the underlying principles. To date, transcriptomic activities of syntrophic propionate and acetate conversion to methane have only been studied in thermophilic enrichment cultures (Singh et al., 2023), while the growth characteristics and gene expression involved in syntrophic relationships between mesophilic acid oxidizers and their methanogenic partners remain underexplored.

The aim of this study was therefore to investigate mesophilic enrichment cultures of both acetate- and propionate-degrading communities during batch cultivation in high-ammonia conditions. Previous studies by our research group have shown that the mesophilic SAOB and SPOB co-exist in propionate-degrading communities under high-ammonia conditions (Singh et al., 2021, 2023). This raises the question of whether syntrophic acetate- and propionate-oxidizing bacteria employ similar strategies to cooperate with their hydrogenotrophic partner, and whether the behavior of SAOB is affected by the presence of SPOB. To study the interplay and growth of the syntrophic enrichment cultures, substrate consumption, product formation and pH during growth were monitored and thermodynamic constraints were calculated. Microbial composition over time in the cultures was explored using 16S rRNA gene profiling and metagenomics. Microbial activity was analyzed using metatranscriptomics, in order to reveal mutual and species-specific mechanisms that underpin the syntrophic cooperation.

Materials and methods

Source of microbial community

The enrichment cultures used originated from laboratory-scale continuous stirred-tank reactors (CSTRs) described previously (Singh et al., 2021). In brief, the CSTRs were inoculated with sludge from a biogas reactor degrading food waste supplemented with albumin and the resulting enrichment cultures were continuously fed with bicarbonate-buffered basal medium supplemented with ammonium chloride (0.3 M) and either 0.1 M sodium propionate or 0.1 M sodium acetate as substrate (Westerholm et al., 2015). The CSTRs were operated for more than 144 days before withdrawal of enrichment culture.

Batch cultivation

Bicarbonate-buffered basal medium was prepared as described elsewhere (Westerholm et al., 2010) and supplemented with yeast extract (0.2 g/L) and ammonium chloride (0.3 M NH_4Cl). The medium was then supplied with substrate, comprising either acetate (A) to an initial concentration of 50 mM (aA50, A50, AM) or propionate (P) to an initial concentration of 50 or 100 mM (P50, P100, PM) (Figure 1). Cultivation batches were prepared in serum bottles (1 L) sealed with butyl rubber stoppers. Each bottle contained a medium volume of either 0.5 L (degradation dynamics cultures) or 0.7 L (meta-omics cultures, PM, AM) and was autoclaved at 121°C for 20 min. After autoclaving, vitamins and trace elements were added, together with the reducing agents L-cysteine HCl (0.5 g/L) and Na_2S (0.24 g/L) to remove traces of oxygen. All batches except aA50 were inoculated with 25–35 mL (5% of culture volume) of enrichment culture originating from the propionate-fed CSTR described above, while aA50 was inoculated with enrichment culture originating from the acetate-fed CSTR (denoted by lowercase "a" in batch name) (Figure 1). The pH of the medium after inoculation was 7.1–7.3. Triplicate samples were prepared for degradation dynamics cultures (aA50, A50,

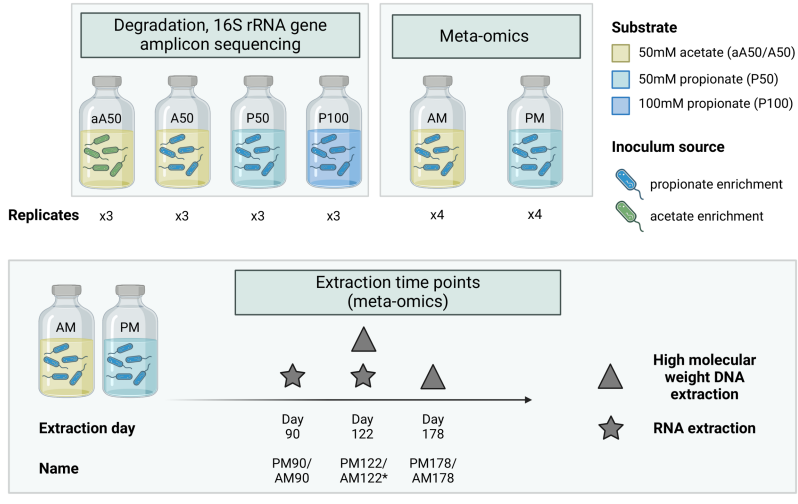

FIGURE 1
Experimental set-up used in batch cultivations. Triplicate cultures were prepared for assessment of acid conversion rates, 16S rRNA gene amplicon-based microbial community composition and thermodynamic calculations. Quadruplicate cultures were prepared for whole genome sequencing (WGS) and gene expression analysis, with an initial substrate concentration of either 50 mM acetate (AM) or 50 mM propionate (PM). A and P in batch names signify the provision of acetate or propionate as feedstock, respectively whereas 50 and 100 indicate the initial concentration in mM. The lowercase a in aA50 indicates inoculation with an enrichment culture originating from acetate-fed CSTR acetate, whereas other cultures were inoculated with an enrichment culture originating from a propionate-fed CSTR. *No RNA extraction conducted at day 122 in the acetate culture (AM), only DNA extraction.

P50, P100) and quadruple samples for meta-omics cultures (AM, PM). Incubation proceeded under stationary conditions at 37°C in darkness.

To prevent accidental bursting of butyl rubber stoppers from the serum bottles due to overpressure, when the head-space gas pressure reached >1,000 mbar it was reduced to around 100 mbar above atmospheric pressure. The amount of methane released was accounted for by measuring gas composition and pressure before and after gas release.

In the batch assays used for meta-omics analysis VFA was sampled at day 0, 13, 62, 70 and 90 for the acetate fed culture (AM) and at day 0, 13, 62, 70, 90, 107 and 122 for the propionate fed culture (PM) (Supplementary Figure S1) The frequency of sampling was kept low to minimize disruption of syntrophic growth. At day 70, additional substrate was added to increase cell biomass for subsequent RNA extraction.

Chemical analytical methods

For chemical and molecular analyses, weekly samples of gas (1 mL) and liquid (4 mL) were extracted from the batch assays employing syringes. Of the 4 mL liquid sample, 2 mL were allocated for pH measurements, while the remaining half was promptly frozen for subsequent utilization in VFA and molecular analyses. The pH was measured directly after sampling, using a pH electrode with an integrated temperature probe (InLab Expert Pro-ISM, Mettler Toledo, Ohio, United States). To quantify the concentrations of short-chain volatile fatty acid (VFA, acetate, propionate, butyrate, isobutyrate, valerate, isovalerate, caproate, isocaproate) the frozen 2 mL liquid sample underwent thawing and centrifugation (at 9000 *g*). The supernatant was subsequently injected into a high-performance liquid chromatography (HPLC) (Westerholm et al., 2010). Methane and CO_2 levels in the headspace of the culture bottles were measured by gas chromatography as described previously (Westerholm et al., 2012). The H_2 concentration in the headspace was measured using a gas chromatograph equipped with a reducing compound photometer detector (Peak Performer 1 Reduced Gas Analyzer PP1, Peak Laboratories, CA, USA) as described previously (Westerholm et al., 2019a). Pressure measurements of the headspace were conducted each time gas samples were taken using a handheld pressure meter (GMH 3111, Gresinger). For thermodynamic calculations, gas concentration measurements (CO_2, CH_4, H_2) were converted to partial pressure by multiplication of the total headspace pressure. Total ammonia nitrogen (g NH_3-N/L) was calculated for batch assays (aA50, A50, P50, P100) as a function of temperate and pH, as described by Hansen et al. (1998). The assumption was made that all of the initially supplemented ammonia (0.3 M) remained in the ammonia/ammonium form and was not converted to other compounds.

Methanogenic cell morphology was examined and micrographs were taken using a fluorescence microscope (Lumascope LS720 (Etaluma) at 60x magnification) and F420 autofluorescence of methanogens was visualized with a 370–410 nm excitation filter and a 429–462 nm emission filter.

Thermodynamic calculations

The following equations were used in thermodynamic calculations: Acetate oxidation to carbon dioxide and hydrogen:

$$CH_3COO^- + H^+ + 2H_2O \rightarrow 2CO_2 + 4H_2 \Delta G^{o\prime} = +54.9kJ / mol \quad (1)$$

Propionate oxidation to acetate, carbon dioxide and hydrogen:

$$CH_3CH_2COO^- + 2H_2O \rightarrow CH_3COO^- + CO_2 + 3H_2 \Delta G^{o\prime} = +73.7kJ / mol \quad (2)$$

Hydrogenotrophic methanogenesis:

$$4H_2 + CO_2 \rightarrow CH_4 + 2H_2O \left(\Delta G^{o\prime} = -130.8kJ / mol\right) \quad (3)$$

Values for the standard free energy of formation (G_f) and the standard enthalpy of formation (H_f) used for determining standard free energy change (ΔG_0) for the reactions were based on values from Shock and Helgeson (Shock and Helgeson, 1990) for acetate/propionate and Hanselmann (Hanselmann, 1991) for the remaining species (H_2, H^+, CO_2, H_2O, CH_4, Supplementary Data SE1). Free energy values for the reactions under nonstandard conditions, using the weekly VFA, gas and pH measurements were calculated as described elsewhere (Dolfing, 2016). The Gibbs-Helmholtz equation was applied to determine free energy at 310.15 K (37°C) in otherwise standard conditions:

$$\Delta G^{\circ}_{T_{310.15K}} = \Delta G^{\circ}_{T_{298.15K}} \times \left(\frac{T_{310.15K}}{T_{298.15K}}\right) + \Delta H^{\circ}_{T_{298.15K}} \times \left(\frac{T_{298.15K} \times T_{310.15K}}{T_{298.15K}}\right) \quad (4)$$

where T is temperature in Kelvin, $\Delta G^{\circ}_{T\,298.15K}$ is free energy of the reaction in standard conditions, $\Delta H^{\circ}_{T\,298.15K}$ is enthalpy of the reaction in standard conditions and $\Delta G^{\circ}_{T\,310.15K}$ is free energy of the reaction at 310.15 K (37°C) in otherwise standard conditions.

ΔG values were then calculated for the actual concentrations measured in cultures as:

$$\Delta G = \Delta G^{\circ}_{T_{310.15K}} + RTlnQ \quad (5)$$

where $\Delta G_{0\,T\,310.15K}$ is free energy in standard state conditions at 310.15 K (37°C), R is the gas constant, T is temperature in Kelvin and Q is the reaction quotient.

16S rRNA gene amplicon sequencing and data analyses

To investigate changes in the microbial community structure over time, the frozen 2 mL liquid samples taken weekly from the batch assays aA50, A50, P50, P100 and stored in −20°C were used for 16S rRNA gene amplicon sequencing. After thawing the samples were centrifuged (at 9000 *g*) and the pellets were used for sequencing and the supernatant was used for VFA analysis as described above. The DNA extraction was conducted using the FastDNA soil kit from MP Biomedicals (France) according to the manufacturer's instructions. 16S rRNA gene amplicon libraries were constructed using primers 515F (GTGBCAGCMGCCGCGGTAA) and 805R (GACTACHVG GGTATCTAATCC) (Herlemann et al., 2011), and Illumina sequencing of the 16S rRNA gene amplicon libraries was performed as described by Müller et al. (2016). Paired-end sequencing was performed using Illumina MiSeq (Eurofins, Germany).

Raw paired-end reads were trimmed of primer sequences and Illumina adapters using Cutadapt (v 4.1) (Martin, 2011) and sequences with a maximum length of 300 bp were used in further processing. For generation of amplicon sequence variants, taxonomic assignment and abundance tables, the package dada2 (v 1.24.0) (Callahan et al., 2016) in R (v 4.2.1) (R Core Team, 2022) was used. In the DADA2 pipeline, forward and reverse sequences were cut to 159 and 191 bp, respectively, with a quality threshold of truncQ = 20, maxEE = (1,2), with cut lengths informed by calculations using the open-source software Figaro (Weinstein et al., 2019). For taxonomic assignment, a DADA2 formatted version of Genome taxonomy database (GTDB) release 207 was used as a reference rRNA database (Parks et al., 2018, 2020; Alishum, 2021). The R package phyloseq (v 1.40) (McMurdie and Holmes, 2013) was used for visualization of microbial community structure.

DNA extraction and metagenomic assembly, binning, and functional analysis

For extraction of high molecular weight DNA suitable for long read sequencing, samples were taken toward the later stage of acid degradation at two occasions (day 122 and 178) for both meta-omic cultures (AM/PM, Figure 1). At day 122, 5 mL sample was sampled and pooled from each of the four biological replicates for both the AM or PM culture (total volume 20 mL for each setup) and at day 178, 20 mL sample was sampled from two out of the four biological replicates for both the AM and PM culture (total volume 40 mL from each setup). Samples were stored at −20°C until DNA extraction. Upon extraction, samples were thawed, centrifuged (at 4000 g, 4°C, for 20 min) and the supernatant removed, and pellets of biological replicates were pooled at this stage. DNA extraction was performed using NucleoBond® AXG as described previously (Sun et al., 2020). The extracted DNA was barcoded using the ligation kit SQK-LSK109 together with the native barcoding expansion 1–12 (EXP-NBD104, Oxford Nanopore Technologies, Oxford, Great Britain) according to the manufacturer's instructions. DNA concentration was determined using a 2,100 BioAnalyzer from Agilent. The extracted DNA was sequenced using a MinION device (Oxford Nanopore Technologies).

Raw Nanopore sequencing data were base-called and demultiplexed using guppy (v 5.0.7–1) (Wick et al., 2019) and filtered using filtlong (v 0.2.0) (Wick, 2022). Reads from the two different timepoints were merged and treated as a single acetate or propionate sample. Genome construction was performed using flye (v 2.8.3) (Kolmogorov et al., 2019) and subsequently polished using racon (v 1.4.20) (Vaser et al.,

2017) and medaka (v 1.4.3) (Oxford Nanopore Technologies, 2024). Read mapping for polishing was performed with minmap2 (v 2.17) (Li, 2018). Binning was performed using three separate binning tools, Metabat2 (v 2.13) (Kang et al., 2019), concoct (v 1.1.0) (Alneberg et al., 2014) and Maxbin2 (v 2.2.7) (Wu et al., 2016). The bins generated from each tool were then consolidated to refined bins, using the bin_refinement module in metaWRAP (v 1.2.2) (Uritskiy et al., 2018), and the quality of the resulting bins was assessed using CheckM (v 1.0.18) (Parks et al., 2015). Bacterial metagenome assembled genome (MAG) annotations were conducted using Bakta (v 1.2.2) (Schwengers et al., 2021) and annotation of the archaeal MAG using Prokka (v 1.14.6) (Seemann, 2014). In addition, both archaeal and bacterial metagenomes were annotated, using GhostKoala (Kanehisa et al., 2016). Taxonomic assignments of MAGs were made using Sourmash (v 4.2.0) (Brown and Irber, 2016) against a reference database prepared from the Genome Taxonomy Database (GTDB, Release 202) (Parks et al., 2022).

In cases where MAGs from the acetate (AM) and propionate (PM) cultures were annotated as the same species, the highest-quality MAG was chosen for further studies. For higher-resolution annotation of hydrogenases, all coding sequences identified were classified against the curated hydrogenase database HydDB (Søndergaard et al., 2016) and true positives were identified by regular expressions searching for FeFe- or NiFe-binding motifs associated with hydrogenases (Vignais and Billoud, 2007; Calusinska et al., 2010) using Python (v 3.10.2). Regular expressions used for finding hydrogenase motifs are listed in Supplementary Data SE2. Any FeFe type A hydrogenases found residing in close genomic proximity (within 5 coding sequences) to a gene encoding NuoF were classified as bifurcating type A3 hydrogenases (Søndergaard et al., 2016). For comparison of the repertoire of hydrogenases for species closely related to the MAGs, protein FASTA files for those species were downloaded from RefSeq and annotated for hydrogenases as described above.

Prediction of signal peptides in all coding sequences was carried out using SignalP 6.0 (Teufel et al., 2022) and prediction of alpha and beta transmembrane proteins based on amino acid sequence using DeepTMHMM (v 1.0.24) (Hallgren et al., 2022). Species trees of MAGs were created using the species tree inference from all genes (STAG method) implemented in Orthofinder (v 2.5.4) (Emms and Kelly, 2017, 2019). For comparison of MAGs to their closest relatives, genome-to-genome distance was calculated using the Genome-to-Genome Distance Calculator (v 3.0) (Meier-Kolthoff et al., 2022) and whole genome average nucleotide identity (ANI) was determined using the python module PyAni (v0.2.9) (Pritchard et al., 2015), all with default parameters.

RNA extraction, sequencing, and data analysis

For the acetate-containing cultures (AM, Figure 1), RNA was extracted at day 90 (AM90) toward the end of acetate degradation, when the acetate concentration was around 4 mM. For the propionate-containing cultures (PM), RNA was extracted on two occasions: on day 90 (PM90), when propionate was being degraded but was still present in high concentrations (40 mM), and on day 122 (PM122) when the propionate level was 11 mM. These specific sampling points were selected due to insufficient RNA yield during attempts at earlier stages of growth. RNA was extracted at day 122 (PM122) to ensure a time point with concurrent acetate and propionate degradation. Samples were taken from each of the four biological replicates and pooled prior to rRNA depletion, resulting in a total of three RNA samples being sequenced (AM90, PM90, PM122). To sample the flocs formed during cultivation, bottles were inverted prior to sampling to allow the flocs to sediment (approx. 5 min before sampling). Triplicate 50 mL culture broth samples were then collected from each bottle (including flocs), transferred to Falcon tubes pre-flushed with N_2 and kept on ice. The Falcon tubes were immediately centrifuged at 4°C and 5,000 × *g* for 30 min. The supernatant was discarded and the triplicate cell pellets were pooled and dissolved in 1 mL chilled Trizol (TRIzol Reagent, Thermo Fisher Scientific, Massachusetts, United States) and 0.2 mL chloroform. Total RNA was then extracted using Quick-RNA Fecal/Soil Microbe Microprep Kit (Zymo Research, California, United States) with an additional DNase I depletion step. The biological replicates from RNA extraction were pooled, resulting in a total of three samples (AM90, PM90, and PM122). Ribosomal RNA was depleted using pan-prokaryote riboPOOL probes and streptavidin-coated Dynabeads (MyOne Streptavidin C1, Invitrogen #65001) according to the manufacturer's protocol. The rRNA-depleted RNA was paired end sequenced (2× 75 bp) on a MiSeq v3 flow cell at the SNP&SEQ platform (SciLifeLab, Uppsala, Sweden).

RNA sequences were trimmed from adapters using Cutadapt (v 4.0) (Martin, 2011) and filtered for quality using Trimmomatic (v 0.39–2) (Bolger et al., 2014). Ribosomal RNA was filtered out *in silico* using SortMeRNA (v 2.1b) (Kopylova et al., 2012). Quality controlled and trimmed reads were then quantified by mapping against taxonomically distinct MAGs using Salmon (v 1.8.0) (Patro et al., 2017). Quantification results were reported as raw counts and normalized by the median of ratios method, using the R package DESeq2 (v 1.36.0) (Love et al., 2014). Further analyses and visualization of quantified expression were performed using the R packages pheatmap (Kolde, 2019) and ggplot2 (Wickham, 2016) and Python (v 3.10.2).

Quantitative PCR

Quantitative PCR (qPCR) analyses were conducted in samples from the propionate enrichment batches P50 and P100. The qPCR was conducted using primers THACf (5′-ATCAACCCCATCTGTGCC-3′) and THACr (5′-CAGAATTCGCAGGATGTC-3′) (Westerholm et al., 2011) to quantify the 16S rRNA genes of *S. schinkii* and the primers MMBf (5′-ATCGRTACGGGTTGTGGG-3′) and MMBr (5′-CACCTAACGCRCATHGTTTAC-3′) (Yu et al., 2005) to determine the 16S rRNA gene level of methanogens of the order Methanomicrobiales. The qPCRs were performed in a 20 µL reaction mixture that consisted of 3 µL DNA sample, 10 µL iQ™ SYBR® Green Supermix (Bio-Rad), 1 µL of each primer (10 µM). The qPCR protocol for quantification was as follows: 7 min at 95°C, 40 cycles of 95°C for 40 s, annealing at 66 or 61°C (for the order Methanomicrobiales and *S. schinkii*, respectively) for 1 min and 72°C for 40 s, and melting curve analysis at 95°C for 15 s, followed by 1 min at 55°C and finally at 95°C for 1 s. All reactions were carried out in QuantStudio™ 5 (ThermoFisher).

Results and discussion

Biphasic propionate utilization and elevated relative abundance of syntrophic microorganisms

During all batch cultivations of the propionate enrichment culture, propionate degradation followed essentially the same pattern, irrespective of the starting concentration of propionate (50 or 100 mM). This pattern comprised a lag phase, initial propionate degradation with subsequent acetate accumulation, a plateau phase during which no propionate was degraded, and a second propionate degradation phase with concurrent acetate consumption (Figures 2A,B). For the 100 mM setup a second acetate peak was observed (17 mM at day 224) whereas minor acetate accumulation was observed for the 50 mM setup. This discrepancy could be explained by the longer plateau phase, in which the acetate oxidizing community is starved on substrate, as well as overall greater net conversion of propionate 100 mM setup. The findings from the 16S rRNA gene amplicon sequencing demonstrated the initial dominance of two members from the Tissierellaceae family (Supplementary Figure S2) within the Clostridia class (Supplementary Figure S3). Given the gradual decline in the relative abundance of Tissierellaceae over time, it's plausible that these community members were not directly engaged in acid degradation. Instead, they likely converted compounds found in the yeast extract or the reducing agent cysteine.

Furthermore, the results showed that initiation of propionate degradation by day 22 in P50 and day 30 in P100 was associated with 2% increased relative abundance of "*Ca.* Syntrophopropionicum". The maximum relative abundance of "*Ca.* Syntrophopropionicum" was 22% in P50 (day 177) and 18% in P100 (day 60) (Figures 2C,D; Supplementary Figure S2). During the initial propionate degradation phase, acetate accumulated stoichiometrically in approximately 1:1 ratio with propionate degradation (Figures 2A,B; Supplementary Data SE3), indicating that no acetate was consumed during the initial phase of propionate degradation. Subsequent cessation of propionate degradation and a decline in acetate levels (P50: day 81, P100: day 71) coincided with an increase in relative abundance of a bacterium of the genus *Syntrophaceticus* up to a maximum of 58 and 71% for P50 (day 81) and P100 (day 263), respectively (Figures 2A–D). The qPCR results

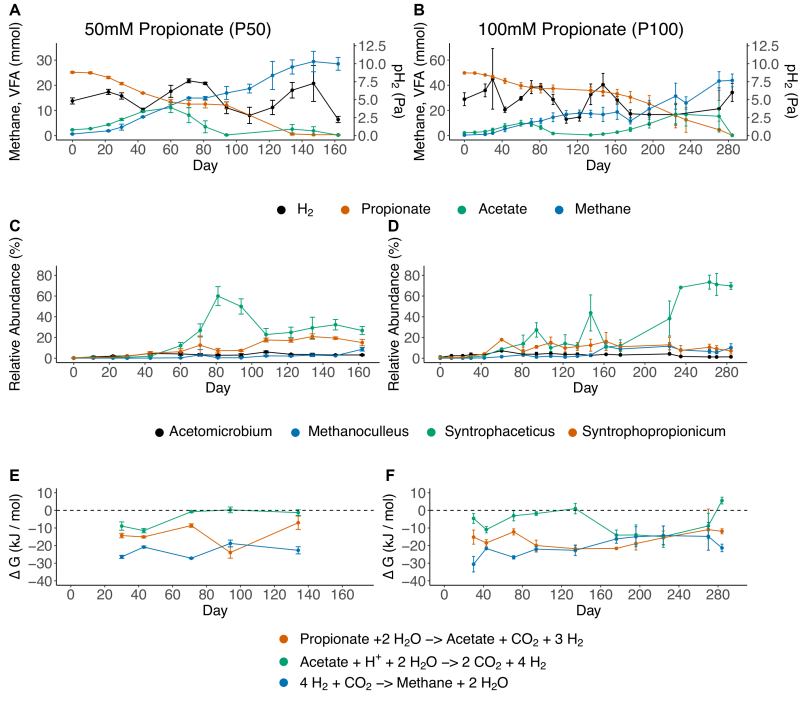

FIGURE 2
Overview of the propionate-degrading batch cultures, showing **(A,B)** substrate and product concentrations, **(C,D)** dynamics of genera that increased in relative abundance over the course of degradation and **(E,F)** change in Gibbs free energy (ΔG, kJ mol^{-1}). Panels on the left refer to batches initiated with 50 mM propionate (P50), and panels on the right refer to batches initiated with 100 mM propionate (P100). Error bars indicate standard deviation of triplicates.

revealed *S. schinkii* 16S rRNA gene abundance of 10^6 copies/ng DNA during the first 80 days in P50 and P100. In accordance with the amplicon sequencing, a decrease in *S. schinkii* copy numbers (by a factor of ten) was observed as acetate levels declined (between days 94–134 in P50 and days 94–162 in P100, Figure 1; Supplementary Figure S4). However, as the experiment progressed, the counts gradually increased, ultimately reaching their initial levels. The methanogenic community initially accounted for less than 0.02% of total reads and consisted of a single species belonging to the genus *Methanoculleus*. The relative abundance increased over time, reaching a final value of 10–13% (Figures 2C,D). To compensate for restricted primer specificity of methanogens by the Illumina sequencing primers, qPCR analysis of the order Methanomicrobiales was conducted. The result demonstrated an average level of 10^8 16S rRNA gene copies/ng DNA during the initial experimental period (day 0 to 94/134). Similar to the SAOB, the gene copy numbers decreased tenfold between days 94–134/162 in P50 and P100, followed by a subsequent increase to initial levels (Supplementary Figure S4).

To investigate degradation of acetate by the microbial community enriched for either acetate (aA50) or simultaneous propionate and acetate degradation (A50), batch cultures with acetate as substrate were prepared and inoculated with either acetate (aA50) or propionate (A50) CSTR enrichment cultures (Figure 1). Similar to P50 (and P100 cultures), acetate degradation in A50 coincided with a rapid increase in the genus *Syntrophaceticus* (Figure 3A). In aA50, on the other hand, the genus *Syntrophaceticus* remained relatively constant over the course of degradation. After acetate depletion in aA50 (<0.2 g/L, day 72) (Figure 3), a drastic shift in community structure was observed and members of the genera *Alkaliphilus* and *Clostridium* increased to relative abundance of 70 and 10%, respectively. The cause of this change in the microbial community remains unknown and requires further investigation. A similar shift was not seen in the A50 community. No methanogenic amplicon sequence variants were identified in these cultures. Other bacteria present in all propionate- and acetate-fed batches over the course of degradation were members of the genera *Tepidanaerobacter* and *Acetomicrobium*, each representing relative abundance of 1–9% of the total community at the end of the trials (Figure 3, Supplementary Figure S5). Of the approximately 24% of the total community not classified at genus levels, a majority (73%) were affiliated to the Clostrida class (data not shown). For the acetate fed batches 20% lacked classification at genus level, and of the unclassified 52% were Clostridia, 12% Campylobacteria, 9% Bacterioidia. Notable difference between the acetate-fed batches was the presence of fewer different genera in the A50 culture than in the aA50 culture (Figure 3). This could relate to the long starvation time for the acetate-consuming populations during previous batch cultivations of A50 (i.e., before enough acetate is formed from the propionate degradation) or because propionate itself had an inhibitory effect on some of the species that thrive on yeast extract, cysteine or other compounds in the cultivation medium (Han et al., 2020).

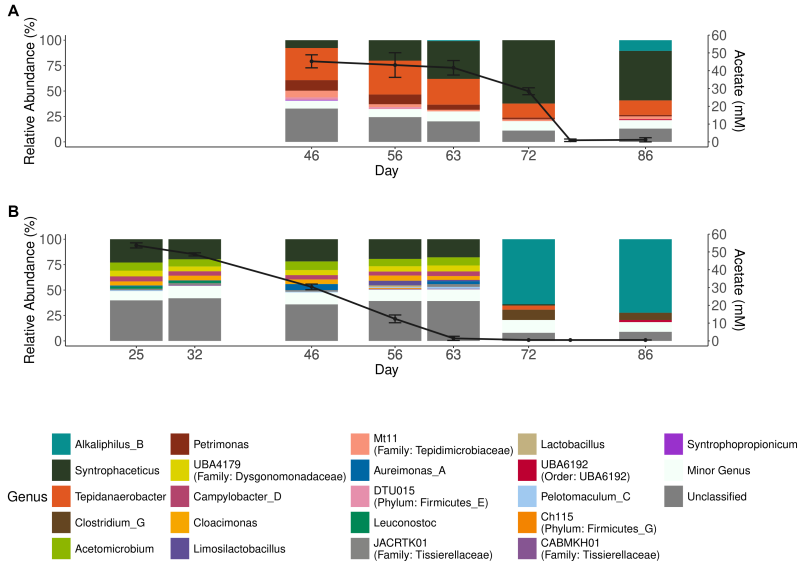

FIGURE 3
Acetate concentration and microbial community structure of the acetate-degrading batch cultures. Acetate concentration (black lines, right axis) and relative abundance (>2.5%) of microbial communities (bar plots, left axis) in batches inoculated with enrichment culture from **(A)** propionate-fed CSTR (A50) and **(B)** acetate-fed CSTR (aA50). Error bars indicate standard deviation of triplicate samples.

Thermodynamic calculations indicate low impact of acetate levels on propionate degradation

The free energy of VFA oxidation and methanogenesis under the non-standard conditions, calculated based on weekly measures of gas composition, VFA, pH and temperature, remained exergonic throughout the cultivation period (Figures 2E,F; Supplementary Data SE3). One exception was that acetate oxidation (equation 1) reached slightly positive ΔG values both during low and high propionate settings (+0.25 kJ/mol / +5.5 kJ/mol), when acetate levels were very low (at day 94 in P50 and day 134/280 in P100). The ΔG values for propionate oxidation (equation 2) fluctuated between −25 kJ/mol and − 10 kJ/mol during the experiment. The ΔG values for hydrogenotrophic methanogenesis (equation 3) fluctuated between −30 kJ/mol and − 10 kJ/mol throughout cultivation.

Even though propionate oxidation was exergonic (> −10 kJ/mol throughout cultivation) a halt in propionate degradation was observed coinciding with increasing acetate levels. Therefore, potential acetate inhibition was analyzed using thermodynamic calculations. The critical acetate concentration needed to reach thermodynamic equilibrium (ΔG = 0) for propionate degradation was calculated using fixed values for propionate (58 mM), pH_2 (5.3 Pa) and pCO_2 (26,700 Pa) (equations 4,5). These fixed values were based on the mean experimental conditions during the plateau phase of propionate degradation (P100, day 81–134). The critical acetate concentration needed for propionate oxidation to become endergonic was around 4.3 M, i.e., orders of magnitude higher than the actual acetate concentrations in the experimental set-up (Supplementary Data SE4). Therefore, from a thermodynamic point of view the halt in propionate degradation was not explained by increasing acetate level.

As the stoichiometric coefficient for H_2 during syntrophic acetate and propionate oxidation is 4 and 3, respectively (equations 2, 3), the H_2 partial pressure has a distinctly greater impact on the ΔG values of these reactions as compared to other reactants and products (as their coefficients are lower). Thus, it is critical that H_2 concentrations are kept low by a syntrophic partner. To confirm that this is the case in the observations, the Pearson correlation of H_2 partial pressure and acetate degradation rates (based on slope of linear model fitted through the particular day in question) was analyzed. Pearson correlation coefficient of −0.30 ($p < 0.01$) was found, indicating a significant negative impact of H_2 partial pressure on acetate degradation rates, which was expected given the stoichiometry of acetate oxidation (equation 1).

Despite several similarities between the 50 mM and the 100 mM cultures in terms of community and degradation profiles, notable differences complicate drawing overarching conclusions. In the 50 mM setup, the cessation of propionate degradation could potentially be attributed to a biological interplay between methanogens and the two acid oxidizers. This speculation stems from the observation that the halt in propionate degradation and lowering of acetate levels coincide with an increase in *Syntrophaceticus* abundance, accompanied by a rise in hydrogen partial pressure (Figure 1). It is plausible that the additional hydrogen and/or formate (or other reducing equivalents) from an increased activity of the SAOB exceed the capacity of the existing methanogenic population, resulting in elevated hydrogen levels, which could have become detrimental to propionate degradation. Subsequently, once all acetate is consumed and hydrogen levels decline, propionate oxidation resumes without acetate accumulation. Although the transition shows similar dynamics, in the 100 mM setup propionate oxidation does not resume directly after acetate gets depleted. Instead it took 40 days before propionate degradation recommenced. The qPCR results also indicated that the gene abundance of Methanomicrobiales required somewhat longer levels to return to 10^8 16S rRNA gene copies/ng DNA after the intermediate decrease (Supplementary Figure S4), which further point to a biological interplay between methanogens and the two acid oxidizers. Labeling experiments and metaproteomics could potentially provide further information to reveal the underlying mechanisms giving rise to this turn-taking behavior.

Description of the four transcriptionally active MAGs obtained from the syntrophic enrichment culture

Metagenomic binning resulted in ten and nine MAGs (>72% completeness) from the acetate and propionate cultures, respectively. Five of the MAGs retrieved from the acetate- and propionate-fed batches had identical taxonomic assignments, while four MAGs lacked taxonomic assignment on superkingdom level (Supplementary Data SE5). In the metatranscriptomic data, around 41% of the reads were removed as rRNA. The majority of the remaining reads were mapped against MAG17 (61%), followed by MAG18 (23%), MAG16 (4.7%) and MAG15 (3.7%). Based on microbial community structure (Figure 2), the taxonomic placement of the MAGs (Supplementary Table S1) and metatranscriptomic mapping (Supplementary Figure S6), MAG15, MAG17 and MAG18 were identified as most important for the metabolic activities of the communities (Figure 4). Of the transcriptionally active metagenomes MAG16 and MAG17 were of high quality (completeness >90%, contamination <5%) while MAG15 and MAG18 were of medium quality (completeness >80%, contamination <10%) (Supplementary Table S2). A detailed description of the characteristics of these MAGs, their functional activities and pathways is provided below.

The putative SPOB *Ca.* "Syntrophopropionicum ammoniitolerans" (MAG15)

Taxonomic analysis identified MAG15 as the putative SPOB "*Candidatus* Syntrophopropionicum ammoniitolerans" (family *Pelotomaculaceae*, ANI 99.4%) (Supplementary Table S1; Supplementary Figure S7). This bacterium was previously characterized in an in-depth study of the high-ammonia reactors that supplied the inoculum used in the present study (Singh et al., 2021). The present study confirmed that genes for all steps of the conventional methylmalonyl-CoA pathway were expressed by MAG15 in the propionate cultures, whereas little or no expression was shown in the acetate culture (Figure 5; Supplementary Data SE6). These results strongly indicate that MAG15 is the main propionate oxidizer in the community representing the SPOB candidate "*Ca.* S. ammoniitolerans".

As reported for all known SPOB in the family Pelotomaculaceae (Kato et al., 2009), most of the genes coding for enzymes in the methylmalonyl-CoA pathway formed an operon-like cluster in

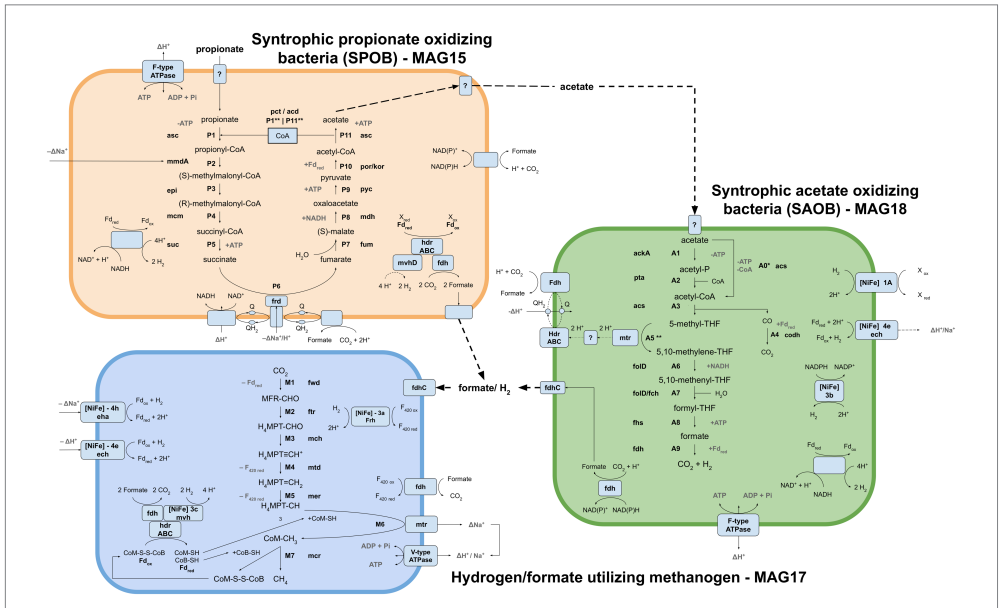

FIGURE 4
Visualization of the metabolic pathways and interplays employed for propionate oxidation by the syntrophic propionate-oxidizing bacteria (SPOB, MAG15) via acetate assimilation by the syntrophic acetate-oxidizing bacteria (SAOB, MAG18) and hydrogen/formate conversion to methane by the hydrogenotrophic methanogen (MAG17) under mesophilic and high-ammonia conditions. SPOB: asc acetyl-CoA synthetase, pct propionate CoA-transferase, acd acetate CoA ligase, mmdA methylmalonyl CoA decarboxylase, epi methylmalonyl CoA/ethylmalonyl CoA epimerase, mcm methylmalonyl-CoA mutase, suc succinyl-CoA synthetase, frd succinate dehydrogenase, fum fumarate hydratase, mdh malate dehydrogenase, pyc pyruvate carboxylase, por/kor pyruvate ferredoxin oxidoreductase/2-oxoglutarate/2-oxoacid ferredoxin oxidoreductase. SAOB: ackA acetate kinase, pta phosphate acetyltransferase, codh anaerobic carbon-monoxide dehydrogenase, fold methylenetetrahydrofolate dehydrogenase, fch methenyltetrahydrofolate cyclohydrolase, fhs formate-tetrahydrofolate ligase. Methanogen: fwd formylmethanofuran dehydrogenase, ftr formylmethanofuran-tetrahydromethanopterin N-formyltransferase, mch methenyltetrahydromethanopterin cyclohydrolase, mtd methylenetetrahydromethanopterin dehydrogenase, mer 5,10-methylenetetrahydromethanopterin reductase, mtr tetrahydromethanopterin S-methyltransferase, mcr methyl-coenzyme M reductase, eha energy-converting hydrogenase, ech ech hydrogenase, Frh NiFe type 3a hydrogenase. Generic: Fd ferredoxin, hdr heterodisulfide reductase, mvhD F_{420}-non-reducing hydrogenase, fdh formate dehydrogenase, Q quinone, NuO NADH:ubiquinone oxidoreductase, fdhC formate transporter.

MAG15 (except the genes for steps P1, P6 and P11; see Figure 4 and Supplementary Data SE6). The transcriptomic data revealed that MAG15 exhibited relatively low expression of genes for CoA transferases in comparison with the highly expressed AMP-dependent acetyl-CoA synthetase (acs). This indicates that, as reported for several other SPOBs (Kato et al., 2009; Hidalgo-Ahumada et al., 2018; Hao et al., 2020; Singh et al., 2023), "*Ca.* S. ammoniitolerans" MAG15 connects the first step of endergonic propionate activation (P1) (Sofeo et al., 2019) with the last step of exergonic acetyl-CoA de-activation (P11). For the subsequent step involving endergonic addition of a carboxyl group to propionyl-CoA (P2), two catalytic paths have been proposed. One involves coupling of this step with the downstream exergonic decarboxylation of oxaloacetate (P9) catalyzed by methylmalonyl-CoA carboxyltransferase. In the other option, methylmalonyl-CoA decarboxylase (mmdA) driven by sodium import catalyzes the reaction, which is most likely the case for MAG15 based on its expression of mmdA, located in the aforementioned operon-like cluster (Supplementary Data SE6, Locus: BGEMGI_09260).

Expression of pyruvate carboxylase subunit B (pycB) and an adjacent gene annotated as oadA located in the MMC operon-like cluster indicated their involvement in step P9. In the SPOB candidate "*Ca.* Propionivorax syntrophicum", conversion of oxaloacetate to pyruvate has been proposed to proceed through extrusion of two sodium ions by oxaloacetate decarboxylase (oad) (Hao et al., 2020). However, "*Ca.* S. ammoniitolerans" MAG15 only encoded and expressed the oadA subunit, and BlastP suggested similarities of this gene with pycB, suggesting that it did not employ sodium ion extrusion at this step and instead relied on the ATP forming pyruvate carboxylase. Detailed descriptions of gene expression by MAG15 for the remaining reaction steps in the MMC pathway are given in Supplementary Note 1.

The SAOB *Syntrophaceticus schinkii* (MAG18)

Genomic analysis of MAG18 indicated 98.6% ANI to the SAOB *Syntrophaceticus schinkii* (Supplementary Table S1), previously isolated from a high ammonia mesophilic biogas digester (Westerholm et al., 2010). The metatranscriptomic results showed that MAG18 had the second most abundant expression level (after

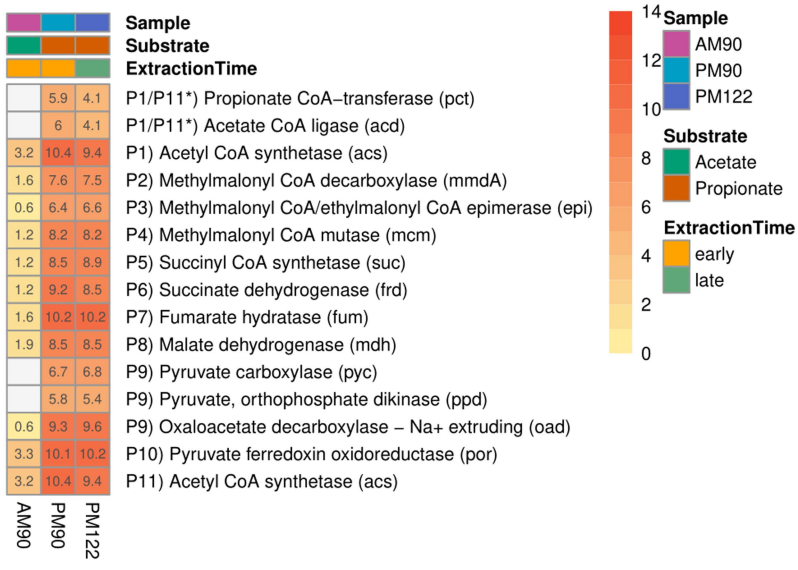

FIGURE 5
Expression of genes involved in the methylmalonyl-CoA pathway by the putative propionate oxidizer "*Ca.* S. ammoniitolerans" (MAG15) in propionate (PM90, PM122) and acetate batch assays (AM90). Heatmap values are aggregated log2-transformed deseq2 normalized count, of all copies and subunits for each respective gene. Genes not expressed are shown in gray. *Putative coupling between step P1 and P11 for propionate activation.

the methanogen) in both the acetate-fed and propionate-fed batches (Supplementary Figure S6). These results demonstrate that MAG18 is the previously known SAOB *S. schinkii* and the main acetate oxidizer in both the AM and PM enrichment communities. The Wood-Ljungdahl Pathway (WLP) is believed to operate in the reverse direction during syntrophic acetate oxidation in the presence of a reducing equivalents-consuming partner. In MAG18, all genes involved in the WLP were expressed in both the acetate- and propionate-fed batches (Figure 6). The gene expression pattern found for MAG18 was in agreement with previous findings for *S. schinkii* (Schnürer et al., 1997; Hattori et al., 2005; Oehler et al., 2012; Manzoor et al., 2016a), showing initial endergonic activation of acetate to acetyl-CoA by an ATP-consuming acetate kinase (ack) followed by exchanging the phosphate group for a CoA group using phosphate acetyltransferase (pta) (Figures 4, 6 steps A1-A2). MAG18 also expressed acetyl-CoA synthetase, enabling direct activation of acetate to acetyl-CoA, although the gene expression was lower than that of *ack* and *pta*. The thermophilic SAOB *T. phaeum* has been suggested to activate acetate through an ATP-independent aldehyde ferredoxin oxidoreductase followed by oxidation of acetaldehyde to acetyl-CoA (Keller et al., 2019), which would allow the bacterium to balance the overall ATP budget. However, low transcript levels of the corresponding genes compared with that of acetate kinase in MAG18 (Supplementary Data SE6) indicated that ATP was consumed in this first step, as shown previously for a thermophilic ammonia-tolerant SAOB candidate (Singh et al., 2023).

For the carbonyl branch, MAG18 expressed genes for the ferredoxin-dependent carbon monoxide dehydrogenase (CODH) reducing carbon monoxide to carbon dioxide (Figures 4, 6; step A4). The CODH was encoded in close proximity to the methylenetetrahydrofolate reductase (MTHFR) and dehydrogenase required for the methyl branch of the WLP (steps, A5-A7; Figures 4, 6). MAG18 also expressed genes for heterodisulphide reductase-like protein (hdrABC), with subunit A located within the CODH operon and the methyl-branched genes and subunits B-C located roughly 30 coding sequences upstream of this operon (Supplementary Figure S8). Notably, many of the interposed genes coded for heme and ubiquinone synthesis, both typical electron carriers, and their expression by MAG18 could be an indication of their involvement in the methyl branch. A second hdrABC-containing gene cluster was located next to those for a formate dehydrogenase and a methyl viologen-reducing hydrogenase (mvhD). Similar gene organization has been reported for *T. phaeum* (Keller et al., 2019), with the exception that no genes for mvhD were located next to the formate dehydrogenase in *T. phaeum* (Supplementary Figure S8). In SAOB, the presence of the endergonic methyl-THF oxidation (step A5) remains an enigma, as it releases electrons with a redox potential of −200 mV, which cannot be directly transferred to NADH (redox potential of −320 mV) (Thauer et al., 1977). In *T. phaeum*, methyl-THF oxidation has been suggested to be linked with formate formation, through a (reversed) electron transport chain involving hdrABC, a quinone pool and membrane-bound formate dehydrogenase, where the endergonic threshold is surmounted by a proton motive force. For *T. phaeum*, such a proton gradient may be created through ATP hydrolysis, since the species was able to achieve acetate activation without ATP investment, thus netting 1 ATP for each acetate oxidized. As seen for a thermophilic and ammonia-tolerant SAOB candidate (Singh et al., 2023), this is not a

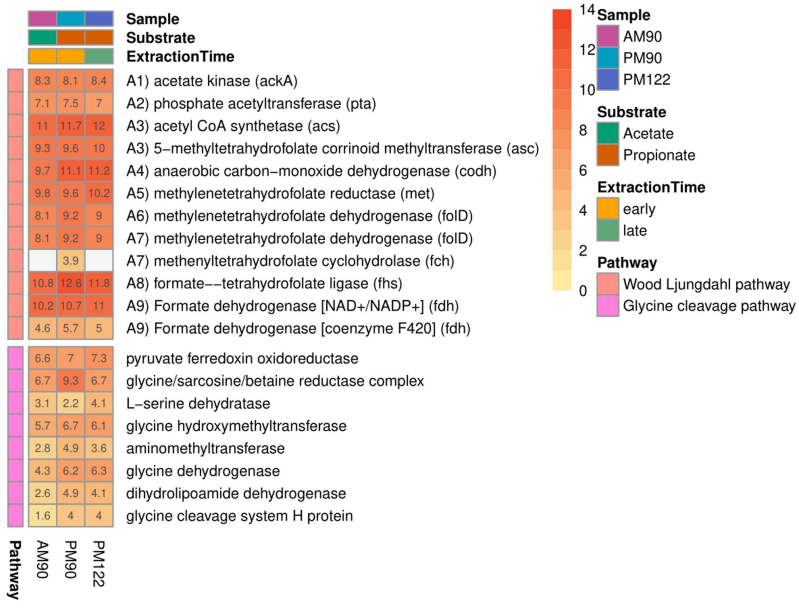

FIGURE 6
Expression of genes in the Wood-Ljungdahl pathway by the syntrophic acetate-oxidizing bacteria (SAOB) *S. schinkii* (MAG18), in propionate (PM90, PM122) and acetate batch assays (AM90). Heatmap values are the aggregated log2-transformed deseq2 normalized count, of all copies and subunits for each respective gene. Genes not expressed are shown in gray.

viable option for MAG18 since ATP investment is needed for the initial acetate activation. However, both MAG18 and the ammonia-tolerant SAOB candidate express a gene for a membrane-bound hydrogenase complex (Ech) that could serve as a potential driver of a proton motive force through cytoplasmic proton consumption. However, irrespective of the source of the proton motive force, the expression profile of MAG18 and the thermophilic ammonia-tolerant SAOB candidate indicated that a mechanism involving hdrABC and formate dehydrogenase, similar to that observed for *T. phaeum*, is utilized for methyl-THF oxidation (step A5, Figures 4, 6). This reinforces the hypothesis put forward by Keller et al. (2019) that a periplasmatically orientated formate dehydrogenase could be key for reversibility of the WLP. However, further research is needed to confirm the metabolic activity underpinning the oxidation of methyl-THF (step A5) in *S. schinkii*, especially with respect to the establishment of a proton gradient.

SPOB exclusively expressed [FeFe]-type hydrogenases, while the SAOB expressed both [FeFe] and [NiFe] hydrogenases for electron transfer

Syntrophs often express multiple variants of hydrogenases and formate dehydrogenases, which serve as an important outlet for re-oxidation of reduced electron carriers formed during VFA oxidation (Sieber et al., 2012). Genes encoding both formate dehydrogenases and hydrogenases were expressed by the SPOB candidate "*Ca.* S. ammoniitolerans" MAG15 and the SAOB *S. schinkii* MAG18, indicating that both use H_2 and formate as outlets for excess reducing equivalents generated during acid oxidation. "*Ca.* S. ammoniitolerans" MAG15 only expressed genes for [FeFe]-type hydrogenases, which were all predicted to be cytoplasmic and included several bifurcating type A3 [FeFe] hydrogenases, one of which was in close genomic proximity to a sensing type C3 [FeFe] hydrogenase. Absence of [NiFe] hydrogenases is a shared characteristic of SPOB in the genus *Desulfofundulus*, whereas SPOB belonging to the genus *Pelotomaculum*, the thermophilic ammonia-tolerant SPOB candidate "*Ca.* T. ammoniitolerans" and *S. fumaroxidans* express both [FeFe] and [NiFe] hydrogenases (Westerholm et al., 2022; Singh et al., 2023).

For acetate oxidation, *S. schinkii* MAG18 expressed a gene for a bifurcating [FeFe]-type A3 hydrogenase. It also expressed genes for multiple [NiFe] hydrogenases, which included a periplasmic type 1a hydrogenase, a NADP-coupled type 3b hydrogenase and a membrane-bound hydrogenase complex (Ech) type 4e hydrogenase (Figure 4). Comparison of the thermophilic SAOB *T. phaeum* with the mesophilic *S. schinkii* MAG18 revealed a similar set of hydrogenases (NiFe 1a, 4e, 3b and FeFe A3), except that *T. phaeum* also had a membrane-bound NiFe 4a formate hydrogenlyase (Supplementary Figure S9).

At this point, it is difficult to draw conclusions from the observed differences (i.e., MAG15 only expressed [FeFe]-type hydrogenases,

MAG18 expressed both [FeFe] and [NiFe] hydrogenases) and similarities (both expressed bifurcating type A3 [FeFe] hydrogenases) within the syntrophic bacteria. [FeFe] hydrogenases are typically involved in H_2 production, whereas [NiFe] hydrogenases tend to be H_2-consuming, although with many exceptions, and several known hydrogenases also operate in a reversible manner (Lubitz et al., 2014). Furthermore, biochemical characterization and detailed insights into structure and reaction mechanisms of hydrogenases from most syntrophic bacteria are lacking. The functional impact in syntrophic culture of the multiple bifurcating hydrogenases produced by the SPOB candidate MAG15, compared with use of only one group of [FeFe] and higher dependence on [NiFe] hydrogenases by the SAOB *S. schinkii* MAG18, is a possible topic for future research.

For formate formation, the SPOB candidate MAG15 expressed a periplasmic $NAD^+/NADP^+$ utilizing formate dehydrogenase, a $NADP^+$-dependent formate dehydrogenase in an operon flanked by genes encoding NADH:ubiquinone oxidoreductase (nuoEF) and formate transporter (fdhC). Nuo is an enzyme complex that transfers electrons from NADH to a quinone pool coupled with proton translocation, where nuoEF forms the NADH binding site (Moparthi and Hägerhäll, 2011). Additional subunits of the Nuo complex (nuoE, F, G, M) were located at other genomic regions in MAG15. A coenzyme F_{420}-dependent formate dehydrogenase was also expressed, together with heterodisulphide reductase (hdrA) and F_{420}-non-reducing hydrogenase (mvhD) in MAG15. For production of formate during acetate oxidation, *S. schinkii* MAG18 expressed a similar genomic region to that found in MAG15, containing a coenzyme F_{420}-dependent formate dehydrogenase-mvhD-hdrABC complex adjacent to a periplasmic formate dehydrogenase ($NAD^+/NADP^+$, Supplementary Figure S8). In addition, the SAOB MAG18 expressed a $NADP^+$-reducing formate dehydrogenase next to genes encoding a molybdate uptake system (mobABC) and a F-type ATPase. Formate cannot passively move over the membrane and several copies of formate transporters (fdhC) were expressed in both the SAOB MAG18 and the SPOB candidate MAG15 (Supplementary Note 2). MAG15 also expressed an oxalate/formate antiporter in close genomic proximity to a formate dehydrogenase (fdh). Of particular interest was a non-annotated gene (Supplementary Data SE6, Locus: BGEMGI_15380) found in the nuoEF-fdhC-fdh containing operon of the SPOB MAG15. This gene was among the most highly expressed genes at both extraction time points in the propionate culture and was predicted to be transmembranal (two passes), containing a bacterial OB-fold domain. Bacterial OB-fold domains locate periplasmically and can function as protein membrane anchors (Ginalski et al., 2004).

The methanogen "*Candidatus* Methanoculleus ammoniitolerans" (MAG17)

MAG17 (90.7% completeness) was taxonomically assigned to the genus *Methanoculleus* (Supplementary Tables S1, S2). The phylogenetic analysis using *Methanoculleus* genomes available at NCBI demonstrated greatest similarity with an uncharacterized *Methanoculleus* species (GCA_013201385.1) (ANI 98%, dDDH 85%; Supplementary Figure S10, Supplementary Table S1) previously identified in the high-ammonia CSTR from which the inoculum used in this study originated (Singh et al., 2021). Based on the genome similarity measurements and the fact that both MAGs were sampled from the same biological source, it is highly likely that the two MAGs represent the same species. However, for the MAG obtained in the previous study, the MAG quality was not sufficiently high for the proposal of a provisional name for this species (Singh et al., 2021).

The second closest species was "*Candidatus* Methanoculleus thermohydrogenotrophicum" (GCA_001512375.1), where the genome comparison revealed values (ANI 83%, DDH of 28%) well below the suggested threshold for species delineation (Goris et al., 2007; Jain et al., 2018). MAG17 had genome size 2.68 Mbp, 58.4% GC content and 3,344 protein coding sequences, which is comparable to the type strain *M. bourgensis* MS_2T (2.79 Mbp, 60.6% GC content, 2,586 protein coding sequences) (Maus et al., 2015). However, the 25% smaller genome size of the closest neighbor "*Ca.* M. thermohydrogenotrophicum" (2.15 Mbp, 59.5% GC content, 2,415 protein coding sequences) indicates that part of that genome is missing, bringing some uncertainties to the comparison of values against that metagenome. Based on the high quality of MAG17 and the genome comparison suggesting that MAG17 [and GCA_013201385.1 (Singh et al., 2021)] will form a novel species when isolated, we propose the provisional name "*Candidatus* Methanoculleus ammoniitolerans".

All genes needed for hydrogenotrophic methanogenesis were expressed by MAG17 (Figure 7). As reported for *M. bourgensis* $MS2^T$ (Maus et al., 2015; Kougias et al., 2017), genes encoding enzymes for steps M1, M2, M6 and M7 (Figures 4, 8) were located in a core-pathway operon in MAG17, whereas the hydrogenotrophic genes for the other steps were scattered throughout the genome. For the first step (M1), involving formylmethanofuran dehydrogenase (Fwd), the reduction of CO2 to formylmethanofuran necessitates reduced ferredoxin. The reduction of ferredoxin is an endergonic reaction and in MAG17 genes encoding Fwd were located at four different loci throughout the genome next to distinct enzymatic systems for reduction of ferredoxin: (i, ii) a membrane-bound [NiFe]-hydrogenase of either type 4e (Ech) or 4 h (Eha) using hydrogen as electron donor and proton or sodium motive force to drive the reaction, respectively; (ii) bifurcative coupling with exergonic reduction of CoM-S-S-CoB using hydrogen as electron donor (Figure 4, Supplementary Data SE6); and (iii) using formate via a membrane-bound formate dehydrogenase (fdhAB). This indicates that MAG17 has flexibility when it comes to the source of reductive power needed to drive the endergonic ferredoxin reduction. This can be advantageous during anabolic growth, since reduced ferredoxin also can be created without coupling to reduction of the heterodisulphide (CoM-S-S-CoB) as part of methanogenesis.

For reduction of coenzyme F_{420} (oxidized in steps M4 and M5), either a cytoplasmic [NiFe] type 3a hydrogenase (Frh) or a membrane-attached formate dehydrogenase was expressed. Comparing the hydrogenase repertoire of MAG17 with that of closely related species (Supplementary Figures S10, S11) revealed that, in contrast to the thermophilic "*Ca.* M. thermohydrogenotrophicum" but similarly to the mesophilic ammonia-tolerant *M. bourgensis*, MAG17 expressed a bifurcating 3c [NiFe] hydrogenase (Supplementary Figure 10). This enzyme is crucial for operating hydrogenotrophic methanogenesis in a circular fashion (i.e., the Wolfe cycle), coupling the reduction of ferredoxin to the reduction of heterodisulphide (CoM-S-S-CoB) (Thauer, 2012). The conjoined expression of Ech and Eha observed for MAG17 in the present study has previously been suggested as a possible explanation for ammonia tolerance in *Methanothermobacter* sp. studied in thermophilic batch reactors (Yan et al., 2020).

In summary, these findings highlight metabolic flexibility in reduction of oxidized electron carriers by "*Ca.* M. ammoniitolerans" MAG17, using both molecular hydrogen and formate as sources of

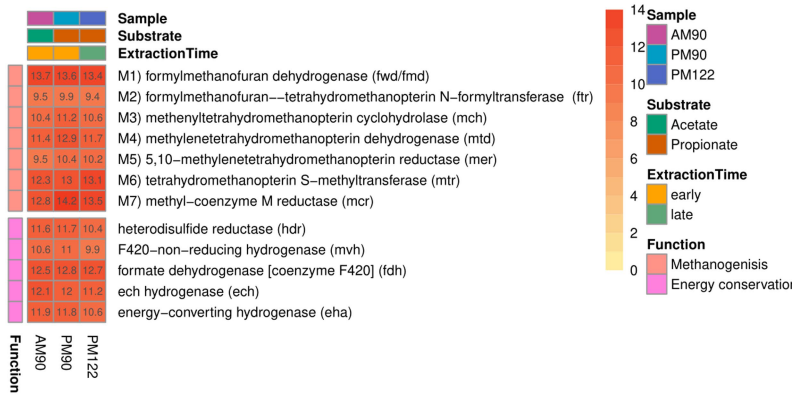

FIGURE 7
Expression of genes in the hydrogenotrophic pathway by the methanogen "*Candidatus* Methanoculleus ammoniitolerans" (MAG17) in propionate (PM90, PM122) and acetate batch assays (AM90). Heatmap values are aggregated log2-transformed deseq2 normalized count, of all copies and subunits for each respective gene.

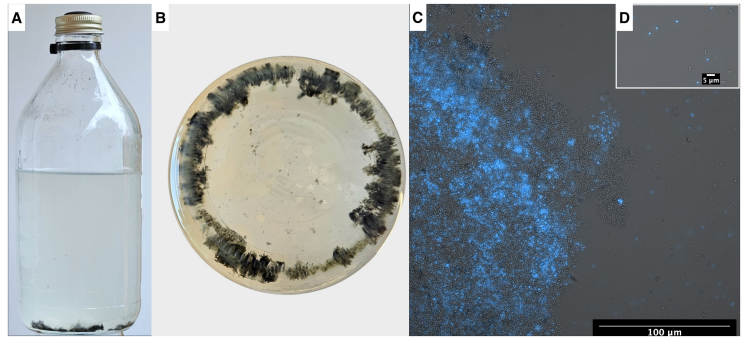

FIGURE 8
(A) Serum bottle containing syntrophic propionate-oxidizing community, **(B)** bottle visualized from below showing the flocs within the microbial community. Fluorescence-brightfield composite micrograph showing autofluorescence of "*Ca.* Methanoculleus ammoniitolerans" **(C)** in floc community and **(D)** as planktonic cells.

reductive power for the reduction of electron carriers needed for hydrogenotrophic methanogenesis.

Despite absence of alcohol in the cultures studied, alcohol dehydrogenase was expressed by the methanogen, in particular in acetate and early propionate batches. Expression of secondary alcohol dehydrogenases in cultures not supplied with alcohol has been reported previously in a hydrogenotrophic methanogen under H_2-limited conditions (Widdel and Wolfe, 1989), indicating that deeper insights could be gained by further study of the role of this protein in hydrogenotrophic methanogens. *Methanoculleus* sp. use minor amounts of acetate for biosynthesis (Schnürer et al., 1999; Maus et al., 2015), and MAG17 expressed Acetyl-CoA synthetase/acetate-CoA ligase (Supplementary Figure 12), which uses ATP for activation of acetate to acetyl-CoA.

Microscopic analyses of the enrichment culture demonstrated presence of cells with autofluorescence in the 420 nm region. The "*Ca.* Methanoculleus ammoniitolerans" cells were identified as irregular cocci with diameter 1–2 µm, with limited motility, and often residing as part of large cellular aggregates (Figure 8C).

Potential function of Acetomicrobium sp. (MAG16) in the syntrophic communities

Since 4.7% of the transcriptomic reads mapped against MAG16 in this study (Supplementary Figure S6), detailed analysis of this MAG was conducted. The results showed that MAG16 belonged to the genus *Acetomicrobium* (class Synergistia, order Synergistales, family

Acetomicrobiaceae) (Supplementary Table S1). The closest characterized species to MAG16 was found to be *Acetomicrobium mobile* (ANI 98%) (Supplementary Figure S13) isolated from an anaerobic lagoon treating wool-scouring wastewater (Menes and Muxí, 2002). The *Acetomicrobium* sp. MAG16 showed similar gene expression level in both the acetate-fed and propionate-fed batches (Supplementary Figure S12). The bacterium lacked key genes needed for the WL pathway, such as acetyl-CoA synthetase and carbon monoxide dehydrogenase, and the complete gene set needed for initial activation of acetate (expression of acetate kinase, but no phosphotransacetylase or an acetyl-CoA synthetase) (Supplementary Figure S12). However, MAG16 expressed genes involved in the reductive glycine pathway. In this CO_2 fixation pathway, CO_2 is reduced to formate and through additional condensation of CO_2 forming intermediates such as glycine, acetyl-P and acetyl-CoA (Sánchez-Andrea et al., 2020). The species expressed all genes needed for the glycine cleavage system except for serine dehydratase, although a threonine dehydratase with similar catalytic function was expressed. The reductive glycine pathway has been proposed to be operated in the oxidative direction (Sánchez-Andrea et al., 2020), in conjunction with the methyl branch of WLP, acting as a hypothesized acetate oxidation pathway, thus competing with the SAOB for available acetate (Zhu et al., 2020; Li et al., 2022; Kieft et al., 2023). However, considering the lack of experimental evidence, this should be viewed as speculative. Since a species belonging to the genus *Acetomicrobium* with a similar activity profile has been observed in a thermophilic syntrophic propionate and acetate-oxidizing culture enriched under high-ammonia conditions in our laboratory (Singh et al., 2023), its activity naturally piqued our interest. Given the sustained activity observed in both acetate and propionate-fed cultures over time, it is conceivable that this species participates in the degradation of either acetate or utilizes formate as a growth substrate. However, considering the wide range of substrates used by members of Acetomicrobium, including organic acids, sugars, amino acids including cysteine (by some members), this bacterium might ferment compounds included in the yeast extract, as well as compounds released from dead cells or possibly grew oxidatively using cysteine as electron acceptor.

Expression of genes potentially related to ammonia tolerance differed between the syntrophic bacteria and the methanogen

As the enrichment cultures were cultivated under high-ammonia (Supplementary Figure S14) conditions and originated from CSTRs operated in high-ammonia conditions, the metatranscriptomic data were used to identify expression of genes known to be involved in microbial strategies to cope with elevated ammonia and the associated osmotic stress (Figure 9). Common strategies to counteract osmotic stress include uptake of cations and synthesis or uptake of compatible solutes, where the latter are low molecular weight organic compounds that accumulate in the cytoplasm to balance the external osmotic stress (Martin et al., 1999; Sleator and Hill, 2002). Expression by the SPOB (MAG15) indicating synthesis of compatible solutes included the genes for lysine 2,3-aminomutase (ablA) and beta-lysine N6-acetyltransferase (ablB) for conversion of lysine to the compatible solute N^{ε}-acetyl-β-lysine first characterized in methanogenic archaea (Sowers et al., 1990). Interestingly, these genes were located adjacent to genes encoding a mechanosensitive channel (ybioO) previously shown to protect *E. coli* cells when exposed to hyperosmotic stress (Edwards et al., 2012). In contrast, the methanogen (MAG17) only expressed the ablB gene and the SAOB (MAG18) only expressed the ablA gene. Furthermore, MAG17 expressed the gene trehalose 6-phosphate synthase for synthesis of the glucose-derived compatible solute trehalose. This compound has been shown to accumulate in members of the domain *Archaea* in response to osmotic stress and genes for trehalose synthase have also been identified in several *Methanoculleus* genomes (Empadinhas and da Costa, 2006; Maus et al., 2015; Chen et al., 2019).

Compatible solutes can also be taken up from the extracellular environment. Both the syntrophic bacteria and the methanogen expressed glycine betaine/proline ABC transporters (Figure 9). Intriguingly, neither of the syntrophic partners nor *Acetomicrobium* sp. (MAG16) had the complete set of genes needed for synthesis of glycine betaine, but all expressed genes needed for the uptake systems (Figure 9, Supplementary Data SE6). It is possible that the compatible solute was synthesized by one of the other species in the culture, despite overall low relative expression level (Yan et al., 2020, 2022).

A common initial response to osmotic stress involves uptake of potassium ions. All three species (MAG15, MAG17, MAG18) expressed the gene for low-affinity potassium uptake protein (trk), but lacked ATP-consuming, high-affinity uptake variants (Sleator and Hill, 2002). None of the organisms expressed ammonia transporters, a trait that can be beneficial to withstand the stress in ammonia-rich environments (Maus et al., 2015; Manzoor et al., 2016b; Singh et al., 2021). Numerous different chaperones (DnaK, DnaJ, archaeal chaperonin, ClpB, ClpC, ClpX) and heat shock proteins (GroEL, HSP20) were expressed by the syntrophic community (Supplementary Figure S15), many of which were coded for by the most highly expressed genes. Chaperones are a common microbial stress response (Hill et al., 2002; Papadimitriou et al., 2016) and high expression of chaperones by the syntrophs could provide protection against protein denaturation and potentially be fundamental to the ability of syntrophic communities to deal with ammonia stress. However, it could also be an artifact of the stress induced during RNA extraction. To gain a deeper understanding of how these syntrophic communities manage ammonia stress, it is imperative to conduct future studies specifically focused on investigating the microbial response to such stressors.

Gene expression of potential importance for mobility, flocculation or interspecies cooperation

Visual inspection of the syntrophic cultures revealed formation of large flocs during the exponential phase of VFA degradation in both the acetate- and propionate-oxidizing cultures (Figure 10). Hence, a specific search was made for gene expression related to microbial aggregation and interaction. Flagella and pili are known to be used for mobility, but have also been shown to facilitate biofilm

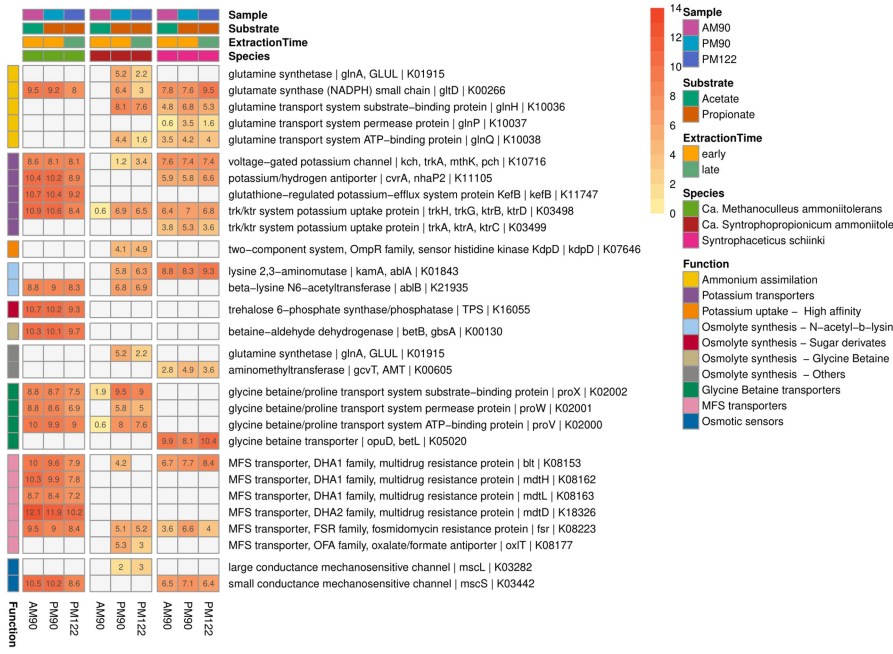

FIGURE 9
Gene expression potentially related to ammonia tolerance activity by the syntrophic propionate-oxidizing bacteria (SPOB) "*Ca.* Syntrophopropionicum ammoniitolerans" (MAG15), the syntrophic acetate-oxidizing bacteria (SAOB) *S. schinkii* (MAG18) and the methanogen "*Ca.* Methanoculleus ammoniitolerans" (MAG17) sampled from propionate and acetate batch assays (AM90, PM90, PM122). Heatmap values are the aggregated log2-transformed deseq2 normalized count, of all copies of each respective gene. Genes not expressed are shown in gray. Annotation of rows is based on KEGG annotations and follows the order: Gene name | Protein Symbol | KO identifier.

formation, cell contact and interspecies cooperation. For instance, the propionate oxidizer *P. thermopropionicum* has been demonstrated to initiate contact with its methanogenic partner through the flagellar cap protein FliD (Shimoyama et al., 2009). The SPOB candidate MAG15 expressed genes encoding a complete flagellum complex, but also expressed pilus-associated genes (pilB, pilC, pilD, pilM) during early propionate degradation, albeit at low levels.

In contrast to the SPOB (MAG15), the SAOB (MAG18) completely lacked flagella-associated genes (Figure 10) but instead expressed pilus genes, especially subunits encoding the motor complex (pilB, pilC, pilT) (Hospenthal et al., 2017), indicating its involvement in motility. Notably, the subunits involved in formation of the secretin complex (pilQ) and alignment complex (pilP) were not present in the genome. The SAOB MAG18 also expressed Flp-type prepilin, which was organized in a characteristic operon containing tight adherence (tad) genes in close proximity. Flp-type pili have been shown to be involved in adherence, twitching motility, DNA uptake and biofilm formation (Cai et al., 2021). The methanogen MAG17 had a limited set of archaeal flagellar genes (flaI, flaJ, flaK), but lacked other critical archaeal flagellar genes needed for motility. The methanogen also expressed genes for archaeal type IV pilus assembly proteins (pilA), some of which resided on an operon together with the aforementioned archaeal flagellar genes found in the genome.

As regards chemotaxis and orchestration of the motility machinery, the SPOB MAG15 expressed genes for methyl-accepting chemotaxis proteins used for recognition of extracellular stimuli, but lacked further signal-transducing genes needed for regulation of flagellar activity (Wadhams and Armitage, 2004) (Figure 10). Although quorum sensing systems have been shown to play an important role in some syntrophic systems (Yin et al., 2020; Doloman et al., 2024) no clear indication of complete quorum sensing machinery was observed based on the KEGG reference pathway analysis for any of the three species.

Both the SAOB and the SPOB expressed genes for phosphodiesterase (ymdB), previously shown to be essential for the formation of nanotubes (small membranous structures that allow for exchange of nutrients and genetic material between cells), which are important for the switch from motile to attached sessile lifestyle in *Bacillus subtilis* (Diethmaier et al., 2011; Dubey et al., 2016). There was a striking similarity between the operon harboring ymdB in the SAOB and the SPOB. The gene was next to that for a 167 aa long hypothetical protein, a stage V sporulation

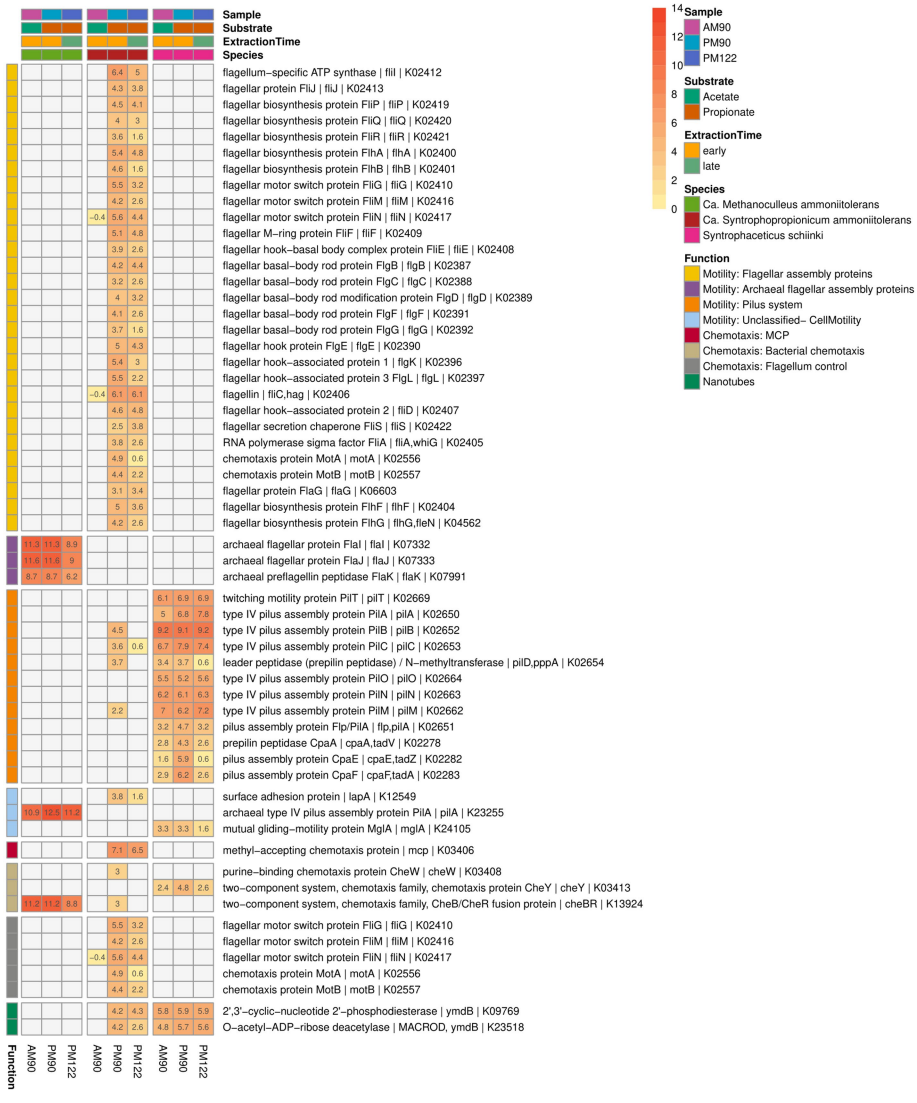

FIGURE 10
Expression of genes potentially related to mobility, biofilm formation, cell contact and interspecies cooperation activity by the syntrophic propionate-oxidizing bacteria (SPOB) "*Ca.* Syntrophopropionicum ammoniitolerans" (MAG15), the syntrophic acetate-oxidizing bacteria (SAOB) *S. schinkii* (MAG18) and the methanogen "*Ca.* Methanoculleus ammoniitolerans" (MAG17) in propionate and acetate batch assays (AM90, PM90, PM122). Heatmap values are shown as log2 of the deseq2 normalized raw counts, where genes with identical KO identifiers are merged. Genes not expressed are shown in gray. Annotation of rows is based on KEGG annotations and follows the order: Gene name | Protein Symbol | KO identifier.

protein S (spoVS) and numerous other shared proteins, including a vesicle-fusing ATPase. This is consistent with findings in a previous study of a thermophilic and anaerobic digester-derived enrichment culture of expression of ymdB by the ammonia-tolerant SPOB and SAOB candidates, indicating that this activity plays an important role in syntrophic cultures at high ammonia levels (Singh et al., 2023). Furthermore, the SPOB MAG15 expressed genes for a surface adhesion protein (lapA),

which has been shown to be a key factor in biofilm formation (Ainelo et al., 2017).

Conclusion

This study elucidates the energetic pathways utilized by the mesophilic SPOB candidate "*Ca. S. ammoniitolerans*", the SAOB *S. schinkii* and a novel hydrogenotrophic methanogenic candidate "*Ca.* M. ammoniitolerans" during syntrophic propionate oxidation at high ammonia conditions. Specifically, the study reveals that the both acid oxidizers share the same methanogenic partner, and that the gene expression by the SAOB and the hydrogenotrophic methanogen was not affected by presence of the SPOB. The SPOB exclusively expressed [FeFe]-type hydrogenases, while the SAOB expressed both [FeFe] and [NiFe] hydrogenases. Both species also expressed bifurcating type A3 [FeFe] hydrogenases, and similar regions encoding formate dehydrogenases. The methanogen expressed a bifurcating 3c [NiFe] hydrogenase, suggesting the operation of hydrogenotrophic methanogenesis in a circular manner (i.e., the Wolfe cycle). Additionally, the concurrent expression of membrane-bound [NiFe]-hydrogenase Ech and Eha by the methanogen reinforces previous association with ammonia tolerance. Furthermore, gene expression profiles by the three syntrophic microorganisms indicated various mechanisms proposed to mitigate ammonia inhibition, including synthesis of compatible solutes or their uptake from the surrounding environment. Further research should be conducted to validate these findings. Floc formation was observed during growth and was postulated to occur as a stress response to high ammonia level or as an act by the cells to foster proximity to the cooperating partner. Gene expression potentially related to flocculating activity included flagella- ("*Ca.* S. ammoniitolerans") and pili-associated (*S. schinkii*, "*Ca.* M. ammoniitolerans") genes and genes encoding proteins previously shown to be essential for formation of nanotubes ("*Ca.* S. ammoniitolerans", *S. schinkii*), a trait shared with thermophilic ammonia-tolerant syntrophic propionate- and acetate-oxidizing bacteria.

Data availability statement

The datasets presented in this study can be found in online repositories. The names of the repository and accession number(s) can be found at: NCBI repository (https://www.ncbi.nlm.nih.gov/), accession numbers: PRJNA1016136, PRJNA1016271, PRJNA1016301, JAVTVG000000000, JAVTVF010000000, JAVTVH010000000, JAVTVI010000000.

Author contributions

NW: Writing – original draft, Data curation, Investigation, Methodology, Software, Visualization. AS: Writing – review & editing, Data curation, Software. JO: Writing – review & editing, Visualization. JD: Writing – review & editing, Formal analysis, Data curation. MW: Writing – review & editing, Conceptualization, Formal analysis, Funding acquisition, Investigation, Methodology, Project administration, Resources, Supervision, Validation.

Funding

The author(s) declare that financial support was received for the research, authorship, and/or publication of this article. Research reported in this publication was supported by the HR2020 ERC – Grant European Research Council (grant number 948138), the Swedish Research Council (VR, grant number 2019-03846) and the Swedish Research Council (Formas, grant number 2018-00928).

Acknowledgments

The authors thank nanozoo GmbH (http://www.nanozoo.com) for the genome reconstruction.

Conflict of interest

The authors declare that the research was conducted in the absence of any commercial or financial relationships that could be construed as a potential conflict of interest.

Publisher's note

Supplementary material

The Supplementary material for this article can be found online at: https://www.frontiersin.org/articles/10.3389/fmicb.2024.1389257/full#supplementary-material

References

Ainelo, H., Lahesaare, A., Teppo, A., Kivisaar, M., and Teras, R. (2017). The promoter region of lapA and its transcriptional regulation by Fis in *Pseudomonas putida*. *PLoS One* 12:e0185482. doi: 10.1371/journal.pone.0185482

Alishum, A. (2021). *DADA2 formatted 16S rRNA gene sequences for both bacteria and archaea*

Alneberg, J., Bjarnason, B. S., de Bruijn, I., Schirmer, M., Quick, J., Ijaz, U. Z., et al. (2014). Binning metagenomic contigs by coverage and composition. *Nat. Methods* 11, 1144–1146. doi: 10.1038/nmeth.3103

Bolger, A. M., Lohse, M., and Usadel, B. (2014). Trimmomatic: a flexible trimmer for Illumina sequence data. *Bioinformatics* 30, 2114–2120. doi: 10.1093/bioinformatics/btu170

Brown, C. T., and Irber, L. (2016). Sourmash: a library for MinHash sketching of DNA. *J. Open Sour. Softw.* 1:27. doi: 10.21105/joss.00027

Buhlmann, C. H., Mickan, B. S., Jenkins, S. N., Tait, S., Kahandawala, T. K. A., and Bahri, P. A. (2019). Ammonia stress on a resilient mesophilic anaerobic inoculum: methane production, microbial community, and putative metabolic pathways. *Bioresour. Technol.* 275, 70–77. doi: 10.1016/j.biortech.2018.12.012

Cai, L., Jain, M., Sena-Vélez, M., Jones, K. M., Fleites, L. A., Heck, M., et al. (2021). Tad pilus-mediated twitching motility is essential for DNA uptake and survival of Liberibacters. *PLoS One* 16:e0258583. doi: 10.1371/journal.pone.0258583

Callahan, B. J., McMurdie, P. J., Rosen, M. J., Han, A. W., Johnson, A. J. A., and Holmes, S. P. (2016). DADA2: high-resolution sample inference from Illumina amplicon data. *Nat. Methods* 13, 581–583. doi: 10.1038/nmeth.3869

Calusinska, M., Happe, T., Joris, B., and Wilmotte, A. (2010). The surprising diversity of clostridial hydrogenases: a comparative genomic perspective. *Microbiology (Reading)* 156, 1575–1588. doi: 10.1099/mic.0.032771-0

Chen, S.-C., Weng, C.-Y., Lai, M.-C., Tamaki, H., and Narihiro, T. (2019). Comparative genomic analyses reveal trehalose synthase genes as the signature in genus Methanoculleus. *Mar. Genomics* 47:100673. doi: 10.1016/j.margen.2019.03.008

De Vrieze, J., Saunders, A. M., He, Y., Fang, J., Nielsen, P. H., Verstraete, W., et al. (2015). Ammonia and temperature determine potential clustering in the anaerobic digestion microbiome. *Water Res.* 75, 312–323. doi: 10.1016/j.watres.2015.02.025

Diethmaier, C., Pietack, N., Gunka, K., Wrede, C., Lehnik-Habrink, M., Herzberg, C., et al. (2011). A novel factor controlling Bistability in *Bacillus subtilis*: the YmdB protein affects Flagellin expression and biofilm formation. *J. Bacteriol.* 193, 5997–6007. doi: 10.1128/jb.05360-11

Dolfing, J. (1992). The energetic consequences of hydrogen gradients in methanogenic ecosystems. *FEMS Microbiol. Lett.* 101, 183–187. doi: 10.1111/j.1574-6968.1992.tb05774.x

Dolfing, J. (2016). "Protocols for calculating reaction kinetics and thermodynamics" in *Hydrocarbon and lipid microbiology protocols: Statistics, data analysis, bioinformatics and modelling*. eds. T. J. McGenity, K. N. Timmis and B. Nogales Fernández (Berlin, Heidelberg: Springer).

Doloman, A., Besteman, M. S., Sanders, M. G., and Sousa, D. Z. (2024). Methanogenic partner influences cell aggregation and signalling of Syntrophobacterium fumaroxidans. *Appl. Microbiol. Biotechnol.* 108:127. doi: 10.1007/s00253-023-12955-w

Dubey, G. P., Malli Mohan, G. B., Dubrovsky, A., Amen, T., Tsipshtein, S., Rouvinski, A., et al. (2016). Architecture and characteristics of bacterial nanotubes. *Dev. Cell* 36, 453–461. doi: 10.1016/j.devcel.2016.01.013

Edwards, M. D., Black, S., Rasmussen, T., Rasmussen, A., Stokes, N. R., Stephen, T.-L., et al. (2012). Characterization of three novel mechanosensitive channel activities in *Escherichia coli*. *Channels* 6, 272–281. doi: 10.4161/chan.20998

Emms, D. M., and Kelly, S. (2017). STRIDE: species tree root inference from gene duplication events. *Mol. Biol. Evol.* 34, 3267–3278. doi: 10.1093/molbev/msx259

Emms, D. M., and Kelly, S. (2019). OrthoFinder: phylogenetic orthology inference for comparative genomics. *Genome Biol.* 20:238. doi: 10.1186/s13059-019-1832-y

Empadinhas, N., and da Costa, M. S. (2006). Diversity and biosynthesis of compatible solutes in hyper/thermophiles. *Int. Microbiol.* 9, 199–206

EurObserv'ER (2022). 21st annual overview barometer. Available at: https://www.eurobserv-er.org/21st-annual-overview-barometer/ (Accessed July 10, 2023).

Fischer, M. A., Ulbricht, A., Neulinger, S. C., Refai, S., Waßmann, K., Künzel, S., et al. (2019). Immediate effects of Ammonia Shock on transcription and composition of a biogas reactor microbiome. *Front. Microbiol.* 10:2064. doi: 10.3389/fmicb.2019.02064

Ginalski, K., Kinch, L., Rychlewski, L., and Grishin, N. V. (2004). BOF: a novel family of bacterial OB-fold proteins. *FEBS Lett.* 567, 297–301. doi: 10.1016/j.febslet.2004.04.086

Goris, J., Konstantinidis, K. T., Klappenbach, J. A., Coenye, T., Vandamme, P., and Tiedje, J. M. (2007). DNA-DNA hybridization values and their relationship to whole-genome sequence similarities. *Int. J. Syst. Evol. Microbiol.* 57, 81–91. doi: 10.1099/ijs.0.64483-0

Hallgren, J., Tsirigos, K. D., Pedersen, M. D., Armenteros, J. J. A., Marcatili, P., Nielsen, H., et al. (2022). DeepTMHMM predicts alpha and beta transmembrane proteins using deep neural networks, 609. doi: 10.1101/2022.04.08.487609

Han, Y., Green, H., and Tao, W. (2020). Reversibility of propionic acid inhibition to anaerobic digestion: inhibition kinetics and microbial mechanism. *Chemosphere* 255:126840. doi: 10.1016/j.chemosphere.2020.126840

Hanselmann, K. W. (1991). Microbial energetics applied to waste repositories. *Experientia* 47, 645–687. doi: 10.1007/BF01958816

Hansen, K. H., Angelidaki, I., and Ahring, B. K. (1998). Anaerobic digestion of swine manure: inhibition by ammonia. *Water Res.* 32, 5–12. doi: 10.1016/S0043-1354(97)00201-7

Hao, L., Michaelsen, T. Y., Singleton, C. M., Dottorini, G., Kirkegaard, R. H., Albertsen, M., et al. (2020). Novel syntrophic bacteria in full-scale anaerobic digesters revealed by genome-centric metatranscriptomics. *ISME J.* 14, 906–918. doi: 10.1038/s41396-019-0571-0

Hattori, S., Galushko, A. S., Kamagata, Y., and Schink, B. (2005). Operation of the CO dehydrogenase/acetyl coenzyme a pathway in both acetate oxidation and acetate formation by the Syntrophically acetate-oxidizing bacterium *Thermacetogenium phaeum*. *J. Bacteriol.* 187, 3471–3476. doi: 10.1128/JB.187.10.3471-3476.2005

Herlemann, D. P., Labrenz, M., Jürgens, K., Bertilsson, S., Waniek, J. J., and Andersson, A. F. (2011). Transitions in bacterial communities along the 2000 km salinity gradient of the Baltic Sea. *ISME J.* 5, 1571–1579. doi: 10.1038/ismej.2011.41

Hidalgo-Ahumada, C. A. P., Nobu, M. K., Narihiro, T., Tamaki, H., Liu, W.-T., Kamagata, Y., et al. (2018). Novel energy conservation strategies and behaviour of *Pelotomaculum schinkii* driving syntrophic propionate catabolism. *Environ. Microbiol.* 20, 4503–4511. doi: 10.1111/1462-2920.14388

Hill, C., Cotter, P. D., Sleator, R. D., and Gahan, C. G. M. (2002). Bacterial stress response in *Listeria monocytogenes*: jumping the hurdles imposed by minimal processing. *Int. Dairy J.* 12, 273–283. doi: 10.1016/S0958-6946(01)00125-X

Hospenthal, M. K., Costa, T. R. D., and Waksman, G. (2017). A comprehensive guide to pilus biogenesis in gram-negative bacteria. *Nat. Rev. Microbiol.* 15, 365–379. doi: 10.1038/nrmicro.2017.40

Ishii, S., Kosaka, T., Hori, K., Hotta, Y., and Watanabe, K. (2005). Coaggregation facilitates interspecies hydrogen transfer between Pelotomaculum thermopropionicum and *Methanothermobacter thermautotrophicus*. *Appl. Environ. Microbiol.* 71, 7838–7845. doi: 10.1128/AEM.71.12.7838-7845.2005

Jain, C., Rodriguez-R, L. M., Phillippy, A. M., Konstantinidis, K. T., and Aluru, S. (2018). High throughput ANI analysis of 90K prokaryotic genomes reveals clear species boundaries. *Nat. Commun.* 9:5114. doi: 10.1038/s41467-018-07641-9

Kanehisa, M., Sato, Y., and Morishima, K. (2016). BlastKOALA and GhostKOALA: KEGG tools for functional characterization of genome and metagenome sequences. *J. Mol. Biol.* 428, 726–731. doi: 10.1016/j.jmb.2015.11.006

Kang, D. D., Li, F., Kirton, E., Thomas, A., Egan, R., An, H., et al. (2019). MetaBAT 2: an adaptive binning algorithm for robust and efficient genome reconstruction from metagenome assemblies. *PeerJ* 7:e7359. doi: 10.7717/peerj.7359

Kato, S., Kosaka, T., and Watanabe, K. (2009). Substrate-dependent transcriptomic shifts in *Pelotomaculum thermopropionicum* grown in syntrophic co-culture with *Methanothermobacter thermautotrophicus*. *Microb. Biotechnol.* 2, 575–584. doi: 10.1111/j.1751-7915.2009.00102.x

Keller, A., Schink, B., and Müller, N. (2019). Energy-conserving enzyme systems active during syntrophic acetate oxidation in the thermophilic bacterium *Thermacetogenium phaeum*. *Front. Microbiol.* 10:2785. doi: 10.3389/fmicb.2019.02785

Kieft, B., Finke, N., McLaughlin, R. J., Nallan, A. N., Krzywinski, M., Crowe, S. A., et al. (2023). Genome-resolved correlation mapping links microbial community structure to metabolic interactions driving methane production from wastewater. *Nat. Commun.* 14:5380. doi: 10.1038/s41467-023-40907-5

Kolde, R. (2019). Pheatmap: pretty Heatmaps. Available at: https://CRAN.R-project.org/package=pheatmap

Kolmogorov, M., Yuan, J., Lin, Y., and Pevzner, P. A. (2019). Assembly of long, error-prone reads using repeat graphs. *Nat. Biotechnol.* 37, 540–546. doi: 10.1038/s41587-019-0072-8

Kopylova, E., Noé, L., and Touzet, H. (2012). SortMeRNA: fast and accurate filtering of ribosomal RNAs in metatranscriptomic data. *Bioinformatics* 28, 3211–3217. doi: 10.1093/bioinformatics/bts611

Kougias, P. G., Campanaro, S., Treu, L., Zhu, X., and Angelidaki, I. (2017). A novel archaeal species belonging to Methanoculleus genus identified via de-novo assembly and metagenomic binning process in biogas reactors. *Anaerobe* 46, 23–32. doi: 10.1016/j.anaerobe.2017.02.009

Leng, L., Yang, P., Singh, S., Zhuang, H., Xu, L., Chen, W.-H., et al. (2018). A review on the bioenergetics of anaerobic microbial metabolism close to the thermodynamic limits and its implications for digestion applications. *Bioresour. Technol.* 247, 1095–1106. doi: 10.1016/j.biortech.2017.09.103

Li, H. (2018). Minimap2: pairwise alignment for nucleotide sequences. *Bioinformatics* 34, 3094–3100. doi: 10.1093/bioinformatics/bty191

Li, C., Hao, L., Lü, F., Duan, H., Zhang, H., and He, P. (2022). Syntrophic acetate-oxidizing microbial consortia enriched from full-scale mesophilic food waste anaerobic digesters showing high biodiversity and functional redundancy 7, e0033922. doi: 10.1128/msystems.00339-22

Love, M. I., Huber, W., and Anders, S. (2014). Moderated estimation of fold change and dispersion for RNA-seq data with DESeq2. *Genome Biol.* 15:550. doi: 10.1186/s13059-014-0550-8

Lubitz, W., Ogata, H., Rüdiger, O., and Reijerse, E. (2014). Hydrogenases. *Chem. Rev.* 114, 4081–4148. doi: 10.1021/cr4005814

Manzoor, S., Bongcam-Rudloff, E., Schnürer, A., and Müller, B. (2016a). Genome-guided analysis and whole transcriptome profiling of the mesophilic syntrophic acetate Oxidising bacterium *Syntrophaceticus schinkii*. *PLoS One* 11:e0166520. doi: 10.1371/journal.pone.0166520

Manzoor, S., Schnürer, A., Bongcam-Rudloff, E., and Müller, B. (2016b). Complete genome sequence of *Methanoculleus bourgensis* strain MAB1, the syntrophic partner of mesophilic acetate-oxidising bacteria (SAOB). *Stand. Genomic Sci.* 11:80. doi: 10.1186/s40793-016-0199-x

Martin, M. (2011). Cutadapt removes adapter sequences from high-throughput sequencing reads. *EMBnet.journal* 17, 10–12. doi: 10.14806/ej.17.1.200

Martin, D. D., Ciulla, R. A., and Roberts, M. F. (1999). Osmoadaptation in Archaea. *Appl. Environ. Microbiol.* 65, 1815–1825. doi: 10.1128/AEM.65.5.1815-1825.1999

Maus, I., Wibberg, D., Stantscheff, R., Stolze, Y., Blom, J., Eikmeyer, F.-G., et al. (2015). Insights into the annotated genome sequence of *Methanoculleus bourgensis* MS2T, related to dominant methanogens in biogas-producing plants. *J. Biotechnol.* 201, 43–53. doi: 10.1016/j.jbiotec.2014.11.020

McInerney, M. J., Sieber, J. R., and Gunsalus, R. P. (2009). Syntrophy in anaerobic global carbon cycles. *Curr. Opin. Biotechnol.* 20, 623–632. doi: 10.1016/j.copbio.2009.10.001

McMurdie, P. J., and Holmes, S. (2013). Phyloseq: an R package for reproducible interactive analysis and graphics of microbiome census data. *PLoS One* 8:e61217. doi: 10.1371/journal.pone.0061217

Meier-Kolthoff, J. P., Carbasse, J. S., Peinado-Olarte, R. L., and Göker, M. (2022). TYGS and LPSN: a database tandem for fast and reliable genome-based classification and nomenclature of prokaryotes. *Nucleic Acids Res.* 50, D801–D807. doi: 10.1093/nar/gkab902

Menes, R. J., and Muxí, L. (2002). *Anaerobaculum mobile* sp. nov., a novel anaerobic, moderately thermophilic, peptide-fermenting bacterium that uses crotonate as an electron acceptor, and emended description of the genus Anaerobaculum. *Int. J. Syst. Evol. Microbiol.* 52, 157–164. doi: 10.1099/00207713-52-1-157

Moparthi, V. K., and Hägerhäll, C. (2011). The evolution of respiratory chain complex I from a smaller last common ancestor consisting of 11 protein subunits. *J. Mol. Evol.* 72, 484–497. doi: 10.1007/s00239-011-9447-2

Müller, B., Sun, L., Westerholm, M., and Schnürer, A. (2016). Bacterial community composition and fhs profiles of low- and high-ammonia biogas digesters reveal novel syntrophic acetate-oxidising bacteria. *Biotechnol. Biofuels* 9:48. doi: 10.1186/s13068-016-0454-9

Oehler, D., Poehlein, A., Leimbach, A., Müller, N., Daniel, R., Gottschalk, G., et al. (2012). Genome-guided analysis of physiological and morphological traits of the fermentative acetate oxidizer *Thermacetogenium phaeum*. *BMC Genomics* 13:723. doi: 10.1186/1471-2164-13-723

Oxford Nanopore Technologies (2024). Medaka: a tool to create consensus sequences and variant calls from nanopore sequencing data. Available at: https://github.com/nanoporetech/medaka (Accessed May 9, 2024).

Papadimitriou, K., Alegría, Á., Bron, P. A., de Angelis, M., Gobbetti, M., Kleerebezem, M., et al. (2016). Stress physiology of lactic acid Bacteria. *Microbiol. Mol. Biol. Rev.* 80, 837–890. doi: 10.1128/MMBR.00076-15

Parks, D. H., Chuvochina, M., Chaumeil, P.-A., Rinke, C., Mussig, A. J., and Hugenholtz, P. (2020). A complete domain-to-species taxonomy for Bacteria and Archaea. *Nat. Biotechnol.* 38, 1079–1086. doi: 10.1038/s41587-020-0501-8

Parks, D. H., Chuvochina, M., Rinke, C., Mussig, A. J., Chaumeil, P.-A., and Hugenholtz, P. (2022). GTDB: an ongoing census of bacterial and archaeal diversity through a phylogenetically consistent, rank normalized and complete genome-based taxonomy. *Nucleic Acids Res.* 50, D785–D794. doi: 10.1093/nar/gkab776

Parks, D. H., Chuvochina, M., Waite, D. W., Rinke, C., Skarshewski, A., Chaumeil, P.-A., et al. (2018). A standardized bacterial taxonomy based on genome phylogeny substantially revises the tree of life. *Nat. Biotechnol.* 36, 996–1004. doi: 10.1038/nbt.4229

Parks, D. H., Imelfort, M., Skennerton, C. T., Hugenholtz, P., and Tyson, G. W. (2015). CheckM: assessing the quality of microbial genomes recovered from isolates, single cells, and metagenomes. *Genome Res.* 25, 1043–1055. doi: 10.1101/gr.186072.114

Patro, R., Duggal, G., Love, M. I., Irizarry, R. A., and Kingsford, C. (2017). Salmon provides fast and bias-aware quantification of transcript expression. *Nat. Methods* 14, 417–419. doi: 10.1038/nmeth.4197

Pritchard, L., Glover, R. H., Humphris, S., Elphinstone, J. G., and Toth, I. K. (2015). Genomics and taxonomy in diagnostics for food security: soft-rotting enterobacterial plant pathogens. *Anal. Methods* 8, 12–24. doi: 10.1039/C5AY02550H

R Core Team (2022). *R: a language and environment for statistical computing*. Vienna, Austria: R Foundation for Statistical Computing.

Ruiz-Sánchez, J., Campanaro, S., Guivernau, M., Fernández, B., and Prenafeta-Boldú, F. X. (2018). Effect of ammonia on the active microbiome and metagenome from stable full-scale digesters. *Bioresour. Technol.* 250, 513–522. doi: 10.1016/j.biortech.2017.11.068

Sánchez-Andrea, I., Guedes, I. A., Hornung, B., Boeren, S., Lawson, C. E., Sousa, D. Z., et al. (2020). The reductive glycine pathway allows autotrophic growth of *Desulfovibrio desulfuricans*. *Nat. Commun.* 11:5090. doi: 10.1038/s41467-020-18906-7

Schnürer, A., Svensson, B. H., and Schink, B. (1997). Enzyme activities in and energetics of acetate metabolism by the mesophilic syntrophically acetate-oxidizing anaerobe *Clostridium ultunense*. *FEMS Microbiol. Lett.* 154, 331–336. doi: 10.1016/S0378-1097(97)00350-9

Schnürer, A., Zellner, G., and Svensson, B. H. (1999). Mesophilic syntrophic acetate oxidation during methane formation in biogas reactors. *FEMS Microbiol. Ecol.* 29, 249–261. doi: 10.1111/j.1574-6941.1999.tb00616.x

Schwengers, O., Jelonek, L., Dieckmann, M. A., Beyvers, S., Blom, J., and Goesmann, A. (2021). Bakta: rapid and standardized annotation of bacterial genomes via alignment-free sequence identification. *Microb. Genom.* 7:000685. doi: 10.1099/mgen.0.000685

Seemann, T. (2014). Prokka: rapid prokaryotic genome annotation. *Bioinformatics* 30, 2068–2069. doi: 10.1093/bioinformatics/btu153

Shimoyama, T., Kato, S., Ishii, S., and Watanabe, K. (2009). Flagellum mediates Symbiosis. *Science* 323:1574. doi: 10.1126/science.1170086

Shock, E. L., and Helgeson, H. C. (1990). Calculation of the thermodynamic and transport properties of aqueous species at high pressures and temperatures: standard partial molal properties of organic species. *Geochim. Cosmochim. Acta* 54, 915–945. doi: 10.1016/0016-7037(90)90429-O

Sieber, J. R., McInerney, M. J., and Gunsalus, R. P. (2012). Genomic insights into Syntrophy: the paradigm for anaerobic metabolic cooperation. *Ann. Rev. Microbiol.* 66, 429–452. doi: 10.1146/annurev-micro-090110-102844

Singh, A., Schnürer, A., Dolfing, J., and Westerholm, M. (2023). Syntrophic entanglements for propionate and acetate oxidation under thermophilic and high-ammonia conditions. *ISME J.* 17, 1966–1978. doi: 10.1038/s41396-023-01504-y

Singh, A., Schnürer, A., and Westerholm, M. (2021). Enrichment and description of novel bacteria performing syntrophic propionate oxidation at high ammonia level. *Environ. Microbiol.* 23, 1620–1637. doi: 10.1111/1462-2920.15388

Sleator, R. D., and Hill, C. (2002). Bacterial osmoadaptation: the role of osmolytes in bacterial stress and virulence. *FEMS Microbiol. Rev.* 26, 49–71. doi: 10.1111/j.1574-6976.2002.tb00598.x

Sofeo, N., Hart, J. H., Butler, B., Oliver, D. J., Yandeau-Nelson, M. D., and Nikolau, B. J. (2019). Altering the substrate specificity of acetyl-CoA Synthetase by rational mutagenesis of the carboxylate binding pocket. *ACS Synth. Biol.* 8, 1325–1336. doi: 10.1021/acssynbio.9b00008

Søndergaard, D., Pedersen, C. N. S., and Greening, C. (2016). HydDB: a web tool for hydrogenase classification and analysis. *Sci. Rep.* 6:34212. doi: 10.1038/srep34212

Sowers, K. R., Robertson, D. E., Noll, D., Gunsalus, R. P., and Roberts, M. F. (1990). N epsilon-acetyl-beta-lysine: an osmolyte synthesized by methanogenic archaebacteria. *Proc. Natl. Acad. Sci. U.S.A.* 87, 9083–9087. doi: 10.1073/pnas.87.23.9083

Sun, H., Brandt, C., and Schnürer, A. (2020). Long-read DNA preparation for bacterial isolates. Protocols.io. Available at: https://www.protocols.io/view/long-read-dna-preparation-for-bacterial-isolates-64ghgtw (Accessed December 5, 2022).

Teufel, F., Almagro Armenteros, J. J., Johansen, A. R., Gíslason, M. H., Pihl, S. I., Tsirigos, K. D., et al. (2022). SignalP 6.0 predicts all five types of signal peptides using protein language models. *Nat. Biotechnol.* 40, 1023–1025. doi: 10.1038/s41587-021-01156-3

Thauer, R. K. (2012). The Wolfe cycle comes full circle. *Proc. Natl. Acad. Sci. U.S.A.* 109, 15084–15085. doi: 10.1073/pnas.1213193109

Thauer, R. K., Jungermann, K., and Decker, K. (1977). Energy conservation in chemotrophic anaerobic bacteria. *Bacteriol. Rev.* 41, 100–180. doi: 10.1128/br.41.1.100-180.1977

Uritskiy, G. V., DiRuggiero, J., and Taylor, J. (2018). MetaWRAP—a flexible pipeline for genome-resolved metagenomic data analysis. *Microbiome* 6:158. doi: 10.1186/s40168-018-0541-1

Vaser, R., Sović, I., Nagarajan, N., and Šikić, M. (2017). Fast and accurate de novo genome assembly from long uncorrected reads. *Genome Res.* 27, 737–746. doi: 10.1101/gr.214270.116

Vignais, P. M., and Billoud, B. (2007). Occurrence, classification, and biological function of hydrogenases: an overview. *Chem. Rev.* 107, 4206–4272. doi: 10.1021/cr050196r

Wadhams, G. H., and Armitage, J. P. (2004). Making sense of it all: bacterial chemotaxis. *Nat. Rev. Mol. Cell Biol.* 5, 1024–1037. doi: 10.1038/nrm1524

Wang, Z., Wang, S., Hu, Y., Du, B., Meng, J., Wu, G., et al. (2022). Distinguishing responses of acetoclastic and hydrogenotrophic methanogens to ammonia stress in mesophilic mixed cultures. *Water Res.* 224:119029. doi: 10.1016/j.watres.2022.119029

Weinstein, M. M., Prem, A., Jin, M., Tang, S., and Bhasin, J. M. (2019). FIGARO: an efficient and objective tool for optimizing microbiome rRNA gene trimming parameters. 610394. doi: 10.1101/610394

Westerholm, M., Calusinska, M., and Dolfing, J. (2022). Syntrophic propionate-oxidizing bacteria in methanogenic systems. *FEMS Microbiol. Rev.* 46:fuab057. doi: 10.1093/femsre/fuab057

Westerholm, M., Dolfing, J., and Schnürer, A. (2019a). Growth characteristics and thermodynamics of syntrophic acetate oxidizers. *Environ. Sci. Technol.* 53, 5512–5520. doi: 10.1021/acs.est.9b00288

Westerholm, M., Dolfing, J., Sherry, A., Gray, N. D., Head, I. M., and Schnürer, A. (2011). Quantification of syntrophic acetate-oxidizing microbial communities in biogas processes. *Environ. Microbiol. Rep.* 3, 500–505. doi: 10.1111/j.1758-2229.2011.00249.x

Westerholm, M., Hansson, M., and Schnürer, A. (2012). Improved biogas production from whole stillage by co-digestion with cattle manure. *Bioresour. Technol.* 114, 314–319. doi: 10.1016/j.biortech.2012.03.005

Westerholm, M., Moestedt, J., and Schnürer, A. (2016). Biogas production through syntrophic acetate oxidation and deliberate operating strategies for improved digester performance. *Appl. Energy* 179, 124–135. doi: 10.1016/j.apenergy.2016.06.061

Westerholm, M., Müller, B., Isaksson, S., and Schnürer, A. (2015). Trace element and temperature effects on microbial communities and links to biogas digester performance at high ammonia levels. *Biotechnol. Biofuels* 8:154. doi: 10.1186/s13068-015-0328-6

Westerholm, M., Roos, S., and Schnürer, A. (2010). *Syntrophaceticus schinkii* gen. Nov., sp. nov., an anaerobic, syntrophic acetate-oxidizing bacterium isolated from a mesophilic anaerobic filter. *FEMS Microbiol. Lett.* 309, 100–104. doi: 10.1111/j.1574-6968.2010.02023.x

Westerholm, M., Schnürer, A., Westerholm, M., and Schnürer, A. (2019b). "Microbial responses to different operating practices for biogas production systems" in *Anaerobic digestion* (IntechOpen).

Wick, R. (2022). rrwick/Filtlong. Available at: https://github.com/rrwick/Filtlong (Accessed December 5, 2022).

Wick, R. R., Judd, L. M., and Holt, K. E. (2019). Performance of neural network basecalling tools for Oxford Nanopore sequencing. *Genome Biol.* 20:129. doi: 10.1186/s13059-019-1727-y

Wickham, H. (2016). *ggplot2: Elegant graphics for data analysis*. New York: Springer-Verlag.

Widdel, F., and Wolfe, R. S. (1989). Expression of secondary alcohol dehydrogenase in methanogenic bacteria and purification of the F420-specific enzyme from Methanogenium thermophilum strain TCI. *Arch. Microbiol.* 152, 322–328. doi: 10.1007/BF00425168

World Biogas Association (2019). World biogas association (WBA): global potential of biogas. Available at: https://www.worldbiogasassociation.org/wp-content/uploads/2019/09/WBA-execsummary-4ppa4_digital-Sept-2019.pdf (Accessed July 10, 2023).

Wu, Y.-W., Simmons, B. A., and Singer, S. W. (2016). MaxBin 2.0: an automated binning algorithm to recover genomes from multiple metagenomic datasets. *Bioinformatics* 32, 605–607. doi: 10.1093/bioinformatics/btv638

Yan, M., Treu, L., Zhu, X., Tian, H., Basile, A., Fotidis, I. A., et al. (2020). Insights into Ammonia adaptation and methanogenic precursor oxidation by genome-centric analysis. *Environ. Sci. Technol.* 54, 12568–12582. doi: 10.1021/acs.est.0c01945

Yan, Y., Yan, M., Angelidaki, I., Fu, D., and Fotidis, I. A. (2022). Osmoprotectants boost adaptation and protect methanogenic microbiome during ammonia toxicity events in continuous processes. *Bioresour. Technol.* 364:128106. doi: 10.1016/j.biortech.2022.128106

Yin, Q., Gu, M., Hermanowicz, S. W., Hu, H., and Wu, G. (2020). Potential interactions between syntrophic bacteria and methanogens via type IV pili and quorum-sensing systems. *Environ. Int.* 138:105650. doi: 10.1016/j.envint.2020.105650

Yu, Y., Lee, C., Kim, J., and Hwang, S. (2005). Group-specific primer and probe sets to detect methanogenic communities using quantitative real-time polymerase chain reaction. *Biotechnol. Bioeng.* 89, 670–679. doi: 10.1002/bit.20347

Zhu, X., Campanaro, S., Treu, L., Seshadri, R., Ivanova, N., Kougias, P. G., et al. (2020). Metabolic dependencies govern microbial syntrophies during methanogenesis in an anaerobic digestion ecosystem. *Microbiome* 8:22. doi: 10.1186/s40168-019-0780-9

II

Weng *et al.*
Biotechnology for Biofuels and Bioproducts (2025) 18:45
https://doi.org/10.1186/s13068-025-02644-3

Biotechnology for Biofuels and Bioproducts

RESEARCH

Open Access

Disruption-induced changes in syntrophic propionate and acetate oxidation: flocculation, cell proximity, and microbial activity

Nils Weng[1], Hossein Nadali Najafabadi[2] and Maria Westerholm[1*]

Abstract

Background Syntrophic propionate- and acetate-oxidising bacteria (SPOB and SAOB) play a crucial role in biogas production, particularly under high ammonia conditions that are common in anaerobic degradation of protein-rich waste streams. These bacteria rely on close interactions with hydrogenotrophic methanogens to facilitate interspecies electron transfer and maintain thermodynamic feasibility. However, the impact of mixing-induced disruption of these essential syntrophic interactions in biogas systems remains largely unexplored. This study investigates how magnetic stirring and orbital shaking influence degradation dynamics, microbial community composition, and gene expression in syntrophic enrichment communities under high-ammonia conditions.

Results Stirring significantly delayed the initiation of propionate degradation in one culture and completely inhibited it in the other two parallel cultures, whereas acetate degradation was less affected. Computational fluid dynamics modelling revealed that stirring generated higher shear rates (~ 20 s^{-1}) and uniform cell distribution, while shaking led to lower shear rates and cell accumulation at the bottom of the culture bottle. Visual observations confirmed that stirring inhibited floc formation, while shaking promoted larger flocs compared to the static control condition, which formed smaller flocs and a sheet-like biofilm. Microbial community analysis identified substrate type and degradation progress as primary drivers of community structure, with motion displaying minimal influence. However, metatranscriptomic analysis revealed that motion-induced gene downregulation was associated with motility, surface sensing, and biofilm formation in SAOB and another bacterial species expressing genes for the glycine synthase reductase pathway. Stirring also suppressed oxalate–formate antiporter expression in SPOB, suggesting its dependence on spatial proximity for this energy-conserving mechanism. The strongest gene expression changes of stirring were observed in methanogens, indicating a coupling of the first and last steps of hydrogenotrophic methanogenesis, likely an adaptive strategy for efficient energy conservation. Other downregulated genes included ferrous iron transporters and electron transfer-associated enzymes.

Conclusions This study highlights that stirring critically disrupts the initial syntrophic connection between SPOB and methanogens, whereas SAOB communities exhibit greater tolerance to shear stress and disruptive conditions that inhibits aggregate formation. These findings emphasize the importance of carefully managing mixing regimes, especially when attempting to reactivate ammonia-tolerant syntrophic propionate degraders in biogas systems experiencing rapid propionate accumulation under high-ammonia conditions.

Keywords Syntrophic propionate-oxidizing bacteria, Syntrophic acetate-oxidizing bacteria, Methanogens, Anaerobic digestion, Mixing, Flocculation, Computational fluid dynamics, Interspecies electron transfer

*Correspondence:
Maria Westerholm
Maria.Westerholm@slu.se
Full list of author information is available at the end of the article

Graphical abstract

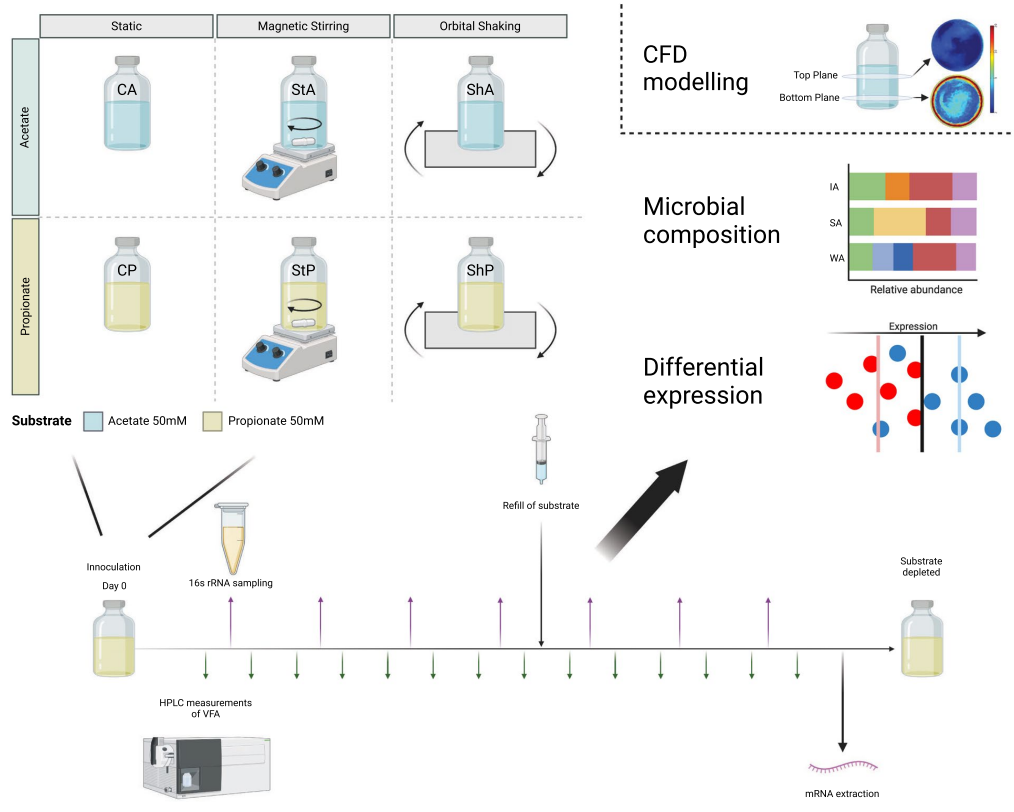

Introduction

To function effectively, biotechnological systems rely on a synergistic interplay between microbiology, chemistry, and technology. An example of this is the anaerobic digestion (AD) process, wherein productivity is directly linked to microbial activity which is, in turn, governed by both chemical conditions and process technology [1]. AD is a well-established biotechnology that converts organic waste into renewable energy (biogas), green chemicals, and sustainable fertiliser [2]. These products are vital components in the transition to a more carbon–neutral society, as they offer sustainable alternatives to fossil-derived fuels and chemicals. In addition, the use of sustainable fertilisers promotes nutrient recycling and reduces the reliance on mineral fertiliser, which is responsible for a significant amount of greenhouse gas emissions during both production and application [3–5].

From a microbial perspective, the AD process involves a continuous interaction between distinct microbial species which are responsible for transforming complex compounds into methane. This process is generally divided into four stages. In the first hydrolytic stage, proteins, fats, and carbohydrates are broken down into amino acids, fatty acids, and sugars. This is followed by the acidogenesis and acetogenesis stages, where these intermediates are further converted into volatile fatty acids (VFA), alcohols, ammonia, carbon dioxide (CO_2), and hydrogen (H_2). During the last step, methane is formed from either acetate (acetoclastic methanogenesis) or by the reduction of CO_2, typically using H_2 or formate as a reducing agent (hydrogenotrophic methanogenesis).

By taking chemistry and process technology into consideration, the microbial interplay becomes more complex, as the various species can be distinctly affected by certain process conditions. This is particularly evident during ammonia inhibition, which frequently occurs in AD processes that degrade protein-rich materials, such as chicken manure or slaughterhouse waste. Although the use of protein-rich substrates offers a high methane yield potential and produces ammonia-rich digestate with a significant value as a fertiliser, elevated ammonia levels can inhibit key members of the microbial community. Acetoclastic methanogens, which convert acetate to methane, are notably sensitive to elevated ammonia concentrations [6–8], and their reduced activity under these conditions leads to an acetate build-up. Moreover, the inhibition of microorganisms that are responsible for degrading other acids, such as propionate, often results in additional VFA accumulation [9]. This further diminishes process performance and methane yield and can, in severe cases, lead to a complete process failure.

At high ammonia levels, an alternative route for acetate conversion to methane frequently emerges, where syntrophic acetate oxidising bacteria (SAOB) oxidise acetate into CO_2 and H_2. For propionate degradation, syntrophic propionate oxidising bacteria (SPOB) convert propionate into acetate, CO_2, and H_2. The formed acetate can then be used by either acetoclastic methanogens in low ammonia conditions [10, 11] or by SAOB under high ammonia conditions [12, 13]. While SAOB are crucial for the AD process under high ammonia conditions, SPOB convert propionate in both low and high ammonia conditions, although the genera of SPOB observed at high ammonia levels typically differ from those that are active under lower ammonia conditions [12, 14].

Both the acetate and propionate oxidation reactions are exothermic under standard conditions and rely on a hydrogenotrophic methanogenic partner to consume the products, thereby making the reaction thermodynamically feasible. This mutualistic cooperation involves the acid oxidiser producing an excess of reducing equivalents during oxidation, which the methanogen uses to reduce CO_2. These reducing equivalents are subsequently transferred through a mediated interspecies electron transfer using either H_2 or formate [15, 16]. Direct electron transfer between cells has also been suggested as a possible mechanism; however, the extent to which this occurs during syntrophic acid oxidation is currently unclear. For mediated transfer, formate is considered to be more efficient than H_2 for electron transfer over longer intracellular distances, due to its higher solubility but lower diffusivity [15, 17]. However, regardless of whether H_2 or formate is used for electron transfer, close proximity between the syntrophic bacteria and the methanogen enhances the efficiency of transferring reducing equivalents between the cells.

The formation of flocs, also referred to as flocculation, is a common microbial strategy to reduce cell-to-cell distance. This has been observed in mesophilic syntrophic acetate and propionate oxidising enrichment cultures under high ammonia conditions [13], as well as in other syntrophic cultures cultivated under mesophilic and low ammonia conditions [18]. The importance of cell proximity was also highlighted in a study of high ammonia mesophilic enrichment cultures, which found a higher abundance of syntrophs within flocs compared to planktonic cells [19]. Furthermore, in low ammonia and thermophilic conditions, microscopic observations revealed that a SPOB and a hydrogenotrophic methanogen grew as free-living cells in monoculture but co-aggregated when cultivated together in a syntrophic propionate degrading coculture [20]. These results raise the question of whether the observed flocculation is primarily driven by its role in syntrophic acid degradation or if it arises from other reasons commonly associated with microbial aggregation, such as protection from environmental stress, nutrient cross-feeding, exchange of genetic material, or attachment to solid surfaces [21–24]. The protective function is particularly relevant in high-ammonia environments, where microbial communities must withstand significant stress. This underscores the importance of integrating microbiological insights with process technology, as reactor mixing can significantly influence microbial flocculation.

In AD, rapid mixing has been suggested to disrupt spatial proximity between hydrogen producers and consumers [25], and it has also been proposed to negatively impact propionate degradation [26]. Although the effects of mixing on the biogas community and process performance [27, 28] has been previously investigated, no studies have specifically examined the impact on syntrophic acid oxidising communities, which are highly reliant on close cell proximity for optimal function. Studying syntrophic interactions within the complex web of microbial interactions of the AD process makes it challenging to isolate the effects of mixing on syntrophic acid oxidation, from those on other stages in the process, such as acid production rates. In addition, the low abundances of the syntrophic community commonly occurring in AD [29] obstructs studying the effects on a molecular level.

The objective of this study is to investigate how disruptive motion affects the activity of syntrophic acid-oxidizing communities under high-ammonia conditions. Specifically, we aimed to determine whether harsh stirring disrupts flocculation, impact on the acid degrading activities, and alters electron transfer mechanisms. We hypothesized that obstructed flocculation would lead to

a lower expression of biofilm-associated genes and a shift in electron transfer mechanisms toward formate-mediated transfer. To test this, we used mesophilic enrichment cultures degrading either acetate or propionate under high-ammonia conditions and subjected them to two different mixing modes: magnetic stirring and orbital shaking. The impact of these conditions on degradation rates, microbial community composition, and microbial metabolic activities were analysed using molecular analyses. Furthermore, computational fluid dynamics (CFD) modelling was employed to assess the hydrodynamic forces and fluid motion generated by different mixing modes. CFD modelling provided insights into variations in shear rates and particle distribution, serving as a proxy for microbial dispersion. Given the essential role of syntrophic communities in preventing VFA accumulation in high-ammonia biogas reactors, understanding their response to mixing can help optimize VFA degradation and improve biogas process stability.

Materials and methods

Source of microbial community and batch cultivation setup

The syntrophic propionate-oxidising and acetate-oxidising enrichment cultures were derived from mesophilic laboratory-scale continuous stirred-tank reactors (CSTRs), previously described by Singh et al. [12]. In short, these CSTRs were inoculated with sludge from a high-ammonia biogas reactor degrading food waste and supplemented with albumin. The CSTRs were continuously fed with a bicarbonate-buffered medium containing ammonium chloride (0.3 M) and sodium propionate (0.1 M) as substrate [9]. The CSTRs were operated for over 144 days before the enrichment cultures were transferred to anaerobic serum bottles.

The anoxic bicarbonate-buffered medium was prepared as described by Westerholm et al. [30] and supplemented with ammonium chloride (0.3 M NH_4Cl). However, unlike previous publications [12, 13, 19] the enrichment cultures in this study were cultivated through multiple sequential transfers into medium without the addition of yeast extract. This repeated transfer process ensured the gradual elimination of all carbon sources except for the acids (excluding the reducing agent cysteine).

For the preparation of cultivation batches for this study, 0.225 L of the medium without yeast extract containing either 50 mM sodium acetate (**A**) (C**A**, St**A**, Sh**A**) or 50mM sodium propionate (**P**) (C**P**, St**P**, Sh**P**) was transferred to serum bottles (0.5 L) while flushing with N_2. At this stage, stirrer magnets were added to the bottles designated for stirring motion (**St**) (**St**P, **St**A). The bottles were each sealed with a butyl stopper and the gas phase was exchanged to N_2/CO_2. The bottles were autoclaved at 121 °C for 20 min, then allowed to cool to room temperature, before adding sterile-filtered solutions containing vitamins, trace elements, and the reducing agents cysteine–HCL (0.5 g/L final concentration) and Na_2S (0.24 g/L final concentration), reaching a working volume of 0.25 L. The batches were inoculated with 12.5 mL (5% v/v) of the aforementioned enrichment culture grown in a medium without yeast extract. Triplicate batches were incubated for each setting in the dark at 37 °C. The control batches (C) were incubated under static conditions. Batches designated for shaking (**Sh**) (**Sh**A, **Sh**P) were placed on an orbital shaker (Orbitron Orbital Schüttler Shaker, Infors HT, Switzerland) with a circular motion radius of 14.5 mm and a frequency of 2Hz (120 rpm). Batches designated for stirring (StA, StP) were placed on magnetic stirrers set to an approximate speed of 700 rpm. The stirring speed was estimated by analysing slow-motion video footage of the magnetic stirrer, counting revolutions, and dividing by the video recording time. The final rotational speed was calculated as the average of three separate recordings. Consequently, in this setup triplicate batches were exposed to either: static (C), gentle shaking under relative mild conditions (Sh) and intense, high-speed stirring conditions (St). Once the initially supplemented substrate was depleted, it was replenished to a concentration of 50 mM on day 111 for acetate-fed cultures, and day 300 for propionate-fed cultures and again incubated under respective conditions.

Chemical analytical methods

For chemical analysis, liquid (2 mL) and gas (1 mL) samples were extracted using syringes. Propionate and acetate levels were measured using high-performance liquid chromatography (HPLC), as previously described by Westerholm et al. [30]. Methane and CO_2 composition of the headspace were measured using gas chromatography as described by Westerholm et al. [31]. Pressure measurements of the headspace were taken each time liquid and gas samples were extracted, using a handheld pressure meter (GMH 3111, Gresinger). Pressure measurements were also regularly taken to monitor whether acid degradation had started during the long lag phases of the batch cultivations.

Optical inspection of floc-formation

Images were taken of the batch assays 56 and 104 days after incubation. Bottles were placed on a sheet of acrylic glass, and images were taken from beneath and from the side of the bottle.

To microscopically visualise aggregates and methanogenic activity (based on F_{420} autofluorescence) a droplet of sample culture was placed on a microscope slide. Micrographs were captured using a fluorescent

microscope (Lumascope LS720, Etaluma) at 60× magnification. F_{420} autofluorescence of methanogens was visualised using a 370–410 nm excitation filter and a 429–462 nm emission filter. Microscopic inspection was performed on all stirred propionate samples, and on a representative replicate from the control and shaking batch assays.

Computational fluid dynamics modelling

A CFD model was constructed to determine the impact of stirring and orbital shaking on the hydrodynamic conditions and cell distribution. Two complementary simulations were constructed for each mode of motion. Light particles (1 µm) were used as a proxy to represent the cells and small-scale aggregates, which were initially homogeneously dispersed throughout the fluid. The cultivation batches in serum bottles were modelled up to the top of the working liquid height using finite element-based solver COMSOL Multiphysics (v 6.2) [32]. The stirring was modelled through a moving mesh with a domain rotation corresponding to 700 rpm. For the shaking motion, the same control volume used for stirring was applied, but without the magnet. Modelling was conducted in COMSOL in Multiphysics using mesh deformation with the following relations:

Mesh displacement in X	$R\cos(2\pi\omega)$
Mesh displacement in Y	0
Mesh displacement in Z	$R\sin(2\pi\omega)$

where R is the radius of rotation and ω the frequency with values of 0.0145 [m] and 2 [Hz], respectively.

The governing equations, conservation of momentum and mass, take the form of Reynolds Averaged Navier–Stokes (RANS) equations for turbulent flow. The Realizable $k-\varepsilon$ model has been used as the turbulence model, which considers two additional transport equations, namely the turbulent kinetic energy and dissipation to be solved along with RANS. This is the most commonly used turbulence model within the community to simulate the hydrodynamic environment in bioreactors [33, 34] and its performance was validated using Particle Image Velocimetry by Sucosky et al. [35]. The calculated Re are 6992 and 1597 for the stirring and orbital shaking table, respectively, which suggests turbulent flow as they are above the critical Re of 1000 [36]. The characteristic lengths used in the model were the length of the magnet stirrer and the translational motion diameter, defined as $2R$ for the orbital shaking-table. The cultivation medium, being an aqueous solution, was treated as water for the CFD analysis, and it was assumed that its density and viscosity were equal to water at 20 °C. A no-slip boundary condition was used for the walls, and in the case of the orbital shaker, the walls followed the frame motion. A symmetry plane was applied at the free surface of the liquid, and gravitational forces were accounted for as volume forces.

To investigate the effect of hydrodynamic forces on floc distribution, a phase transport module was employed to solve for the mass transport of two species; water as liquid and microbes or microbial aggregates as solid particles, with a diameter of 1 µm and 1% heavier than water, purposefully selected to approximate the size and density of microbial cells [13, 37]. The initial volume fraction of heavier particles was set at 0.1, with a homogenous distribution. The Multiphysics coupling between turbulent flow and phase transport was carried out through the Mixture Model from COMSOL Multiphysics. The selected slip and mixture viscosity models are Hadamard-Rybczynski and Krieger, respectively [32].

The computational mesh uses tetrahedral elements for the bulk flow and 4 layers of prism elements to capture the larger gradients near the wall. The grid convergence index [38], based on the volume average of shear rate and velocity, showed a GCI value of less than 1% for a mesh with the control volume consisting of 166,729 elements compared to a finer mesh. The selected mesh had element size distribution ranges from 4.63×10^{-4} to 9.83×10^{-3}. The implicit time-dependent solver was run until the average volume values of velocity and shear rate changed by less than 1% for the last two consecutive times, indicating that the solution had reached a steady state. This was established after 20 s for the magnetic stirring and 50 s for the orbital shaker. For example, in the earlier case, the comparison of volume average shear rate and velocity between times 20 s and 21 s had indicated errors of 0.03% and 0.4%, respectively. The post-processing considered the hydrodynamic force, i.e., contours of shear rate and volume fraction of solid particles, denoting the distribution of microbes or microbial aggregates, which were initially uniform. Two circumferential planes located at the bottom and top of the computational domains were selected to study the effect of stirring or shaking.

16S rRNA gene amplicon sequencing, data analysis and qPCR

16S rRNA gene amplicon sequencing was conducted to monitor the microbial community structure over time. Due to differences in degradation dynamics between experimental setups, liquid samples (5 mL) were taken at various timepoints to obtain samples representing different stages of degradation. The samples were taken as follows: acetate degrading batch cultures (CA, ShA, StA) on days 49, 69, 97, 111, 125, and 139; propionate degrading control and shaking motion batch cultures (CP, ShP) on days 111, 139, 160, 216, 230, 251, 300, 328, and 338;

stirred propionate culture (StP1) on days 196, 216, 230, 251, 280, 300, 328, and 338. Due to the absence of propionate degrading activity, the stirred propionate cultures StP2 and StP3 were sampled only on days 196, 251, and 300. The samples were stored at − 20 °C until DNA extraction. After thawing, total DNA was extracted using the DNAeasy Blood and Tissue Kit (Qiagen) according to the manufacturer's instructions. Construction of 16S rRNA gene amplicon libraries using primers 515F [39] and 805R [40] and Illumina sequencing was performed as described by Muller et al. [41]. Paired-end sequencing was conducted using an Illumina MiSeq instrument (Eurofins, Germany) at SciLifeLab Stockholm, Sweden.

The raw sequencing data underwent a multistep preprocessing pipeline. Due to the initial poor quality of the reverse reads, the first 42 bases were removed from the reverse reads using Trimmomatic (v 0.39) [42]. Subsequently, primer and adapter sequences were removed using Cutadapt (v 4.7) [43]. Amplicon sequence variants and abundance tables were generated in R (v 4.2.1) using the *dada2* package (v 1.24.0) [44]. In the *dada2* pipeline, forward and reverse sequences were cut to 272 and 182 bp, respectively, with a quality threshold of maxEE = (2, 7) and a default value of truncQ = 2. For taxonomic assignment of the amplicon sequence variants, a reference database formatted specifically for *dada2* was utilised [45]. This database was derived from the Genome Taxonomy Database (GTDB) release 207 [46]. The *phyloseq* package (v 1.40) [47] was used for subsequent data handling and visualisation of the microbial community structure. Non-metric Multidimensional Scaling (NMDS) was applied to assess the similarity of the community structure between experimental setups. The distance matrix used for the NMDS was created using Bray–Curtis distance.

To compensate for the restricted specificity of archaeal 16S rRNA genes by the primers used in the present study [48], quantitative PCR (qPCR) analyses were conducted on samples taken from the propionate and acetate enrichment batches at the following timepoints: CA, ShA, and StA on days 49, 69, 126, and 139; CP and ShP on days 139, 196, 251, and 328; and StP1 on days 216, 251, 300, and 328. The qPCR was conducted using primers MMBf (5′-ATCGRTACGGGTTGTGGG-3′) and MMBr (5′-CACCTAACGCRCATHGTTTAC-3′) to determine the 16S rRNA gene level of methanogens of the order *Methanomicrobiales* [49]. Total bacteria were assayed using the forward primer (5′-GTGITGCAIGGIIGTCGTCA-3′) and reverse primer (5′-ACGTCITCCICICCTTCCTC-3′) based on primers described in Maeda et al. [50]. The qPCRs were performed in a 20 µL reaction mixture that consisted of 3 µL DNA sample, 10 µL ORA™ SEE qPCR Green ROX Master Mix (HighQu), 1 µL of each primer (10 µM). The qPCR protocol for quantification was as follows: 7 min at 95 °C, 40 or 55 cycles of 95 °C for 40 s, annealing at 66 or 61 °C (for the order *Methanomicrobiales* and total bacteria, respectively) for 1 min and 72 °C for 40 s, and melting curve analysis at 95 °C for 15 s, followed by 1 min at 55 °C and finally at 95 °C for 1 s. All reactions were carried out in a CFX Duet Real-Time PCR System (BioRad).

RNA extraction, sequencing

For RNA extraction, the microbial cultures were sampled during the exponential phase of acid degradation, after the second substrate addition, to ensure sufficient biomass and active acid degradation. Sampling occurred on day 125 for acetate-fed cultures (CA, StA, ShA) and on day 338 for propionate-fed cultures (CP, StP, ShP). Total RNA was extracted using a chloroform/phenol-based method, followed by rRNA depletion using riboPOOL™ (as outlined in the RNA extraction and depletion protocol by Perman/Weng [51]). To sample any flocs formed during cultivation, bottles were gently inverted to allow floc sedimentation. For acetate-fed cultures, a single 50 mL sample was taken from each bottle and transferred to N_2-flushed Falcon tubes that were kept on ice. For propionate-fed cultures, triplicate 50 mL samples were collected from each bottle and similarly transferred to N_2-flushed Falcon tubes on ice. All tubes were centrifuged at 5000*g* and 4 °C for 10 min, the supernatant was discarded, and the cell pellets were pooled in 1 mL chilled TRIzol (Thermo Fisher Scientific, MA, USA) and 0.2 mL chloroform. For acetate-fed cultures, pooling was carried out on a biological replicate level, yielding one sample per motion type (CA, StA, ShA). For propionate-fed cultures, technical replicates were pooled, producing one sample per biological replicate (CP1–3, StP, ShP1–3). Two of the stirred propionate cultures did not degrade propionate (StP2, StP3) and failed to yield sufficient RNA for analysis. Resultingly, two technical replicates were extracted from the stirred propionate culture that did degrade the acid, herby referred to as StP1 and StP12. RNA extraction was performed using the Quick-RNA Fecal/Soil Microbe Microprep Kit (Zymo Research, CA, USA) with an additional Dnase I treatment step. Extracted RNA samples were stored at − 80 °C. Ribosomal rRNA was depleted using pan-prokaryote riboPOOL probes with streptavidin-coated Dynabeads (MyOne Streptavidin C1, Invitrogen #65001). Depleted RNA was purified using ethanol precipitation and stored at − 80 °C until submission for sequencing. RNA concentration and quality was assessed using a 2100 Bioanalyzer System with RNA 6000 Nano Kit (Agilent Technologies Inc., CA, USA). The rRNA-depleted RNA was sequenced using paired-end sequencing (2 × 150 bp) on an Illumina NovaSeq X Plus (Eurofins, Germany), using one lane of a 10B flow cell. Sequencing

was conducted at the SNP&SEQ platform (SciLifeLab, Uppsala, Sweden).

RNA analysis

Raw sequences were trimmed off adapters using Cutadapt (v 4.0) [43] and quality filtered using Trimmomatic (v 0.39-2) [42]. In silico-removal of rRNA was carried out using SortMeRNA (v 2.1b) [52]. Quality controlled and trimmed reads were then quantified through a reference-based approach using Salmon (v 1.9.0) [53]. Metagenome-assembled genomes (MAGs) from a previous study investigating the same enrichment culture were used for read mapping [13], and complemented with a single MAG affiliated to the genera *Alkaliphilus* extracted from the high ammonia CSTRs from which the present enrichment culture originates [12]. Quantification results were outputted as raw counts. Differential gene expression analysis was conducted in R using DESeq2 (v 1.36.0) [54] and results were visualised using the packages pheatmap (v 1.0.12) [55] and ggplot2 (v 3.5.0) [56]. For the main differential gene expression analysis investigating the effects of motion, only propionate fed samples were used. Genes with low expression (less than 2 samples with a gene count of at least 10) were sorted out prior to analysis. *P* values were adjusted (p-adj) using the Benjamin–Hochberg method [57]. Genes were assigned as differentially expressed if they had an absolute value of log twofold change (log2FC) > 1.5 and an adjusted p value of < 0.05. For the principal component analysis (PCA), genes with low expression were filtered out as described above and transformed using regularised-logarithm transformation (rlog) of the Deseq2 package.

GapMind [58] was used to identify likely biosynthetic pathways for all amino acids, the associated coding sequences (candidate genes) to each pathway, and the completeness of each pathway for each respective MAG. All reported candidate genes were included in the gene sets used for subsequent pathway enrichment analysis and heatmap visualisation. When multiple candidates were associated with a single gene, the aggregated count was displayed in the heatmaps. Pathway enrichment was tested assuming a hypergeometric distribution with the p value calculated as the probability of observing at least n pathway-related genes among the differentially expressed genes and was tested for up- and down-regulated genes separately. This was done using the R-basic stat function phyper (q−1, m, n, k, lower.tail = FALSE):

q = number of differentially expressed genes in pathway list.

m = number of genes in pathway list.

n = number of background genes not in pathway list.

k = number of differentially expressed genes.

where the background gene set was defined as all genes that passed the initial filtering for low expression (at least two samples with counts > 10). The p value was adjusted for multiple testing according to the Benjamin–Hochberg procedure [57].

Results and discussion

Degradation of acetate and propionate

The acetate-fed cultures had similar degradation rates regardless of the type of motion but stirring extended the lag phase in StA cultures with 7–30 days as compared to cultures grown in static and shaken conditions (CP, ShP, Fig. 1, Table 1, Supplementary Data SE1 and SE2). In accordance with previous studies of the enrichment culture [19], the lag phase was considerably shorter for the second degradation (following the re-addition of 50 mM acetate, Table 1). This difference is likely due to cells and essential enzymes already being present at the point of re-addition. The slightly faster degradation observed in stirred cultures during the second degradation is likely explained by the shorter starvation period between the consumption of the initially supplemented acetate and its re-addition (Fig. 1).

In the propionate batch assays (CP, ShP, StP) the impact by motion on the lag phase was more pronounced. Strikingly, stirring had a negative impact on propionate degradation, as it only began in one (StP1) of the three replicates. The disruptive effect of stirring was further evident from the prolonged lag phase of over 50 days in StP1, compared cultures grown under static conditions (CP). Conversely, shaking motion (ShP) reduced the lag phase by approximately 40 days compared to the static condition in two of the replicates. Interestingly, once propionate degradation commenced, the degradation rates remained relatively similar across all conditions (Table 1). However, propionate degradation remained significantly slower than acetate degradation, consistent with previous studies on the enrichment culture when cultivated in a medium containing yeast extract (Supplementary Data SE2) [13, 19]. Furthermore, similar to SAO, the propionate degrading cultures all had shorter lag phases after substrate spiking compared to the first degradation (Table 1).

Contrary to the biphasic utilisation of propionate previously observed in enrichment cultures grown in yeast extract-supplemented medium [13], the present study revealed simultaneous degradation of acetate and propionate during the initial phase. This simultaneous degradation may be linked to the longer lag phase observed in the present study, likely due to the lack of crucial nutrients typically provided by the yeast extract. During this extended lag phase, the minimal degradation of propionate could allow the

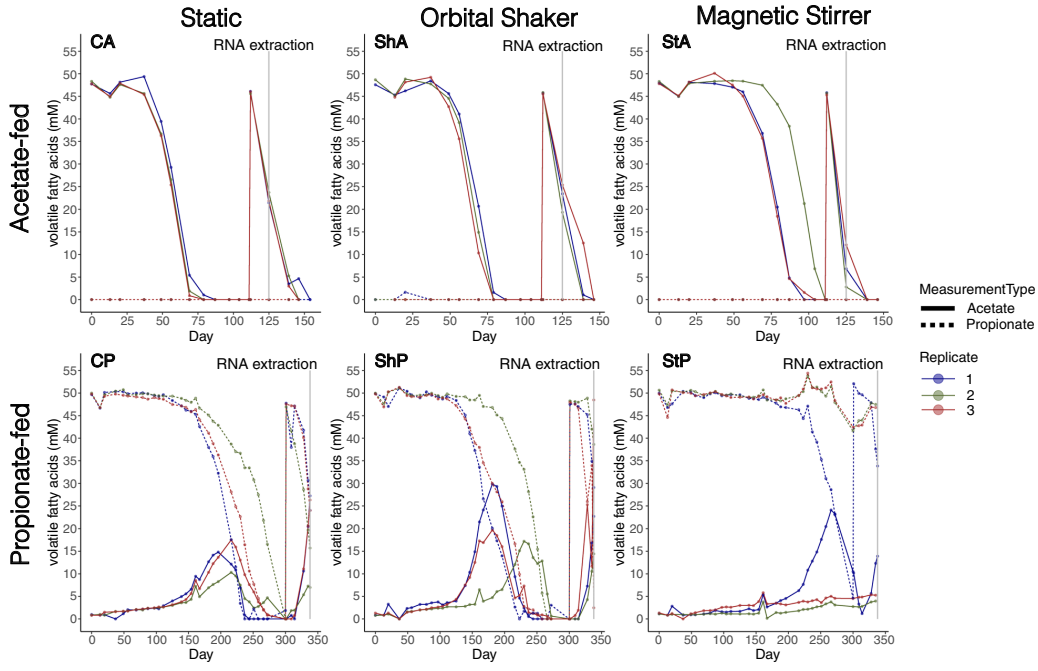

Fig. 1 Degradation dynamics of acetate-fed (top) and propionate-fed (bottom) cultures subjected to different types of agitative motion: no motion (C, left), orbital shaking (Sh, middle), and magnetic stirring (St, right). Solid lines show the acetate concentration, while dashed lines show the propionate concentration (mM) and replicates are shown in different colours. For acetate-fed cultures, additional acetate (up to 50 mM) was added on day 111 and RNA extraction was performed on day 125. In the propionate-fed cultures, propionate was added on day 300 and RNA was extracted on day 338. Note the differing scales on the *x*-axes for acetate-fed and propionate-fed cultures

Table 1 Cultivation metrices of acetate-fed (CA, ShA, StA) and propionate-fed (CP, ShP, StP) cultures subjected to different types of agitative motion: no motion (C), orbital shaking (Sh), and magnetic stirring (St)

Sample	First degradation					After substrate spiking	
	Substrate (50 mM)	Motion	Lag phase (days)	Acid deg. rate (mM/day)	Acetate accum. (mM)[a]	Lag phase (days)	Substrate conc. at RNA extraction (mM)
CA	Acetate	Static	49	1.70–1.77	–	0	21–24 (acetate)
ShA		Shaking	49	1.72–1.94	–	0	19–25 (acetate)
StA		Stirring	56–79	1.73–1.86	–	0	3–12 (acetate)
CP	Propionate	Static	181	0.40–0.70	19	0–13	16–24 (propionate)
ShP		Shaking	139–188	0.48–0.76	33	27–34	2–39 (propionate)
StP1[b]		Stirring	237	0.62	26	34	34 (propionate)

[a] Maximum acetate level during propionate degradation

[b] Only one of the triplicate propionate-fed cultures started to degrade propionate during stirring

SAOB community to acclimate cultivation conditions, priming them for acetate degradation. As a result, once propionate degradation enters the logarithmic phase, the SAOB are already prepared to efficiently convert the acetate produced. Interestingly, despite the extended lag phase, the degradation rates were ultimately comparable between cultures with and without yeast extract

supplementation once degradation had commenced (Supplementary Data SE2).

CFD modelling and floc formation observation

The CFD modelling showed that the stirring motion generated high shear rates, which intensified with vertical depth as proximity to the magnetic stirrer increased, reaching a maximum of ~ 20 s^{-1} (Fig. 2). Contrastingly, the shaking motion resulted in relatively lower shear rates (maximum ~ 5 s^{-1}) and showed minimal variation with vertical depth. Consequently, the hydrodynamic forces acting on solid particles were comparatively greater for magnetic stirring than for orbital shaking.

Regarding the concentration of particles, mapping the volume fraction against the shear rate revealed that the highest solid particle concentrations occurred in areas with steep shear rate gradients, particularly near the bottom and along the walls (Fig. 3). During the shaking motion, a considerably higher volume fraction was observed at the bottom plane, likely due to the relatively weak but higher gradient shear rates that were generated by shaking, which were insufficient to counteract the negative buoyancy of the particles. The stirring motion gave rise to minor differences in particle distribution, mostly confined to the bottom of the liquid located close to the wall.

The results from the CFD modelling indicate that cells in the different setups were subjected to varying shear stress and fluid motion, which likely significantly impacted their ability to form and sustain cellular aggregates. For cell aggregation to occur, cells must be in close proximity to each other or to a surface, as this enables adhesive forces and the development of a shared extracellular matrix [21, 59]. In addition to motions influencing the initial cell aggregation, shear rates can also affect the size of the flocs. This is because higher shear rates impose an upper limit on floc size, leading to the formation of smaller flocs [60]. The present study demonstrated that stirring clearly prevented the formation of visible flocs due to its disruptive effect on aggregation.

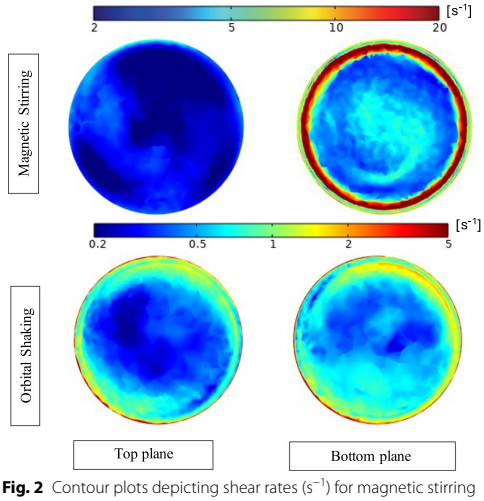

Fig. 2 Contour plots depicting shear rates (s^{-1}) for magnetic stirring (top plane: **a** bottom plane: **b** and orbital shaking (top plane: **c** bottom plane: **d**). Logarithmic scale has been used for both colour legends to highlight the variation in shear rates

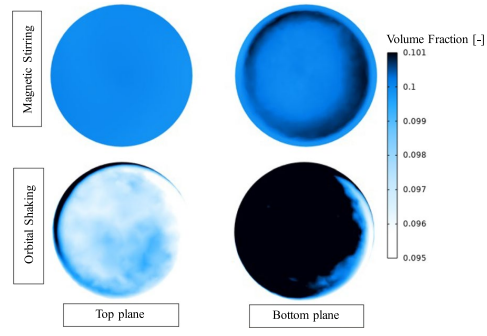

Fig. 3 Contour plots corresponding to volume fraction of solid particles, unitless, with an initial value of solid particles 0.1 (1% of total volume) with homogenous distribution for both motions with magnetic stirring to the top and orbital shaking at the bottom. The deviation greater than 0.1 indicates regions with higher concentration of solid particles

Under shaking conditions, the enhanced volume fraction of particles (cells) likely increased the likelihood of initial cell–cell contact, while lower shear rates than in the stirring favoured the establishment of stable cell–cell adhesion. In line with these hypotheses, visual observations of the cultures revealed that shaking conditions resulted in the largest flocs (Supplementary note 1, Supplementary Fig. S1). This could be attributed to increased particle collision than under static conditions, facilitating the establishment of cell–cell adhesion. The observation aligns with previous studies which have demonstrated that moderate shear forces is necessary for the formation of a specific type of compact cellular aggregates, known as granules [61], and that turbulence promotes cellular aggregation and biofilm formation [62]. In addition, a study of a co-culture of syntrophic butyrate oxidising bacteria and a hydrogenotrophic partner showed that physical disruption through shaking or ultrasound treatment did not affect the tendency of aggregation [63].

For microscopic inspection, all samples were collected from the top phase of the culture assays

to prevent any disturbance of the formed flocs and biofilms, favouring the sampling of platonic over aggregated cells. Nevertheless, aggregates were still observed in the shaking motion samples and, surprisingly, in one of the stirred replicates that was unable to degrade propionate (StP3, Supplementary Fig. S2). The presence of aggregates in the shaking motion samples, but not in the static control samples, aligns with the enhanced volume fraction of particles and the fluidic dynamics predicted by the CDF model under shaking motion. The presence of microscopic flocs in one of the stirred cultures implies that even under the high shear conditions, initial cell–cell adhesion and the formation of microscopic flocs consisting of a few cells is possible. However, although syntrophic relationships had been established by the second substrate addition in StA and StP1, the impact of shear stress under stirring conditions remained significant throughout the experimental period. Even after interactions were formed, microbial communities had to continuously withstand mechanical forces, potentially affecting their structural integrity, metabolic activity, and ability to establish new interspecies connections. Methanogenic autofluorescence was observed in all samples except StP2, which is one of the stirred replicates that was unable to degrade propionate.

Based on these results, it can be hypothesised that stirring and high shear stress impair propionate degradation more than acetate degradation due to the SPOB's greater reliance on flocculation and proximity to the methanogenic partner compared to the SAOB. One potential explanation is that the SPOB may require closer proximity to the methanogenic partner for transferring reducing equivalents, such as through H_2-mediated or direct electron transfer. If hydrogen serves as the primary carrier of reducing equivalents for the SPOB, the close spatial arrangement of the hydrogen producer and consumer within flocs or aggregates creates localised microenvironments, wherein hydrogen partial pressures are lower than the surrounding medium [64]. Stirring disrupts this arrangement, increasing the distance between consumer and producer, and thus elevates the hydrogen partial pressure that the producer is exposed to. It is possible that the SPOB is more sensitive to this elevated partial pressure than the SAOB. Another possibility is that SPOB are dependent on flocculation for protection to the high ammonia levels. A deeper understanding of how syntrophic organisms are affected by and protect themselves from high ammonia levels is needed to determine whether this is indeed the case.

For all stirred samples, it could be hypothesized that the higher shear stress enhanced fluid motion and reduced the boundary layer around microbial cells, improving mass transfer efficiency and allowing substrates to reach cells more rapidly. However, the negative impact of stirring on the acid degradation capacity of the communities, particularly the SPO community, suggests that any potential benefits from enhanced mass transfer were outweighed by the disruption of essential cell-to-cell interactions.

Microbial compositions and dynamics

Approximately 87% of the total reads mapped to amplicon sequence variants taxonomically resolved to the species level. NMDS ordination plots on relative abundance showed a distinct separation between samples fed with acetate and those fed with propionate. However, no clear clustering was observed based on mode of motion (Supplementary Fig. S3 A). Instead, the degree of substrate degradation emerged as the primary determining factor (Supplementary Fig. S3B, C).

The microbial compositions and dynamics were similar across all acetate-fed cultures (Fig. 4, Supplementary Fig. S4). During the lag phase, known SAOB of the genera *Syntrophaceticus* (46–95%) and *Tepidanaerobacter* (13–29%) dominated. Once acetate oxidation had started, the relative abundance of *Syntrophaceticus* increased to > 90% for most of the replicates and remained relatively stable until the second addition of acetate. Members of this genus are frequently highlighted as the main SAOB in AD operating at high ammonia conditions [65, 66]. In the present study, an unclassified species belonging to the genera *Alkaliphilus* increased in relative abundance (from 0–3% to 11–49%) during this second acetate degradation, while acetate was still present in high levels. The activity of *Acetomicrobium* and *Alkaliphilus* in this study is particularly noteworthy, as these genera are frequently detected in biogas processes with high acetate levels, in association with syntrophic bacteria and hydrogenotrophic methanogens [67–69]. They have also been observed during hydrogen injection in power-to-gas applications [70], although their precise role in these systems remains unclear.

During propionate degradation in CP, ShP, and StP1, the microbial community was initially predominated by the genus *Tepidanaerobacter*, comprising over 50% relative abundance in most samples (Fig. 4, Supplementary Fig. S5). In addition, low to intermediate relative abundances of SAOB of the genera *Syntrophaceticus,* the SPOB candidate *'Ca.* Syntrophopropionicum' [12, 13, 19], *Acetomicrobium,* and an uncultured bacterial group belonging to the Family *Tepidimicrobiaceae* (referred to as Mt11) were observed. Once propionate oxidation was initiated, the relative abundance of *'Ca.* Syntrophopropionicum' increased to 46–77%. As acetate levels raised, so did the relative abundance

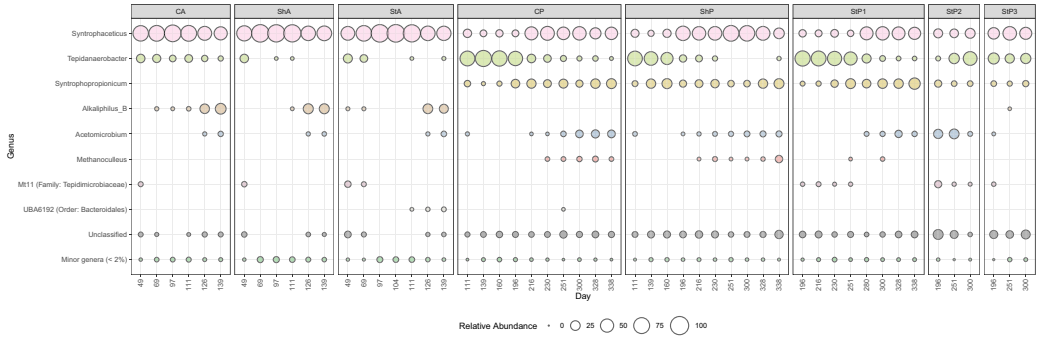

Fig. 4 Bubble plot showing the relative abundance of microbial genera over time in acetate-fed (CA, ShA, StA) and propionate-fed (CP, ShP, StP1–3) cultures. All cultures, except stirred propionate-fed, show the relative abundance of merged counts across replicates. Stirred propionate-fed cultures (StP1–3) display individual replicate data instead. This distinction was made, because stirred propionate cultures exhibited substantial differences in ability to degrade propionate. For a detailed view of replicate-specific data for each condition, see Supplementary Figs. S4 and S5. Bubble size represents relative genus abundance, with genera with less than 2% relative abundance grouped as "Minor genera (< 2%)"

of *Syntrophaceticus. Acetomicrobium* remained at low but persistent relative abundance throughout the degradation in the propionate-fed cultures, with an increasing trend toward the end of the experiment in some samples (CP1–3, ShP1, StP1). Following the second addition of propionate on day 300, the microbial community structures remained relatively stable, except for a few samples which showed a further increase in the relative abundance of *'Ca*. Syntrophopropionicum', reaching higher abundances than those observed during the first degradation. The stirred samples that failed to degrade propionate (ShP2 and ShP3) exhibited microbial compositions similar to the lag-phase of the other cultures, with no observed increase in the relative abundance of the SPOB nor the SAOB as the experiment progressed.

qPCR analyses targeting the order *Methanomicrobiales* (including the genus *Methanoculleus*) revealed an abundance ranging from 5.52–8.50 $\log_{10}$ gene copies/ng DNA, while the total bacteria gene abundance was 8.68–12.27 $\log_{10}$ gene copies/ng DNA in the acetate- and propionate-fed cultures (Supplementary Fig. S6, Supplementary Data SE3). This indicates that the total bacterial community was consistently more abundant than the hydrogenotrophic methanogens (i.e., *Methanomicrobiales)* across all conditions. However, qPCR data showed relatively consistent presence of methanogens in all samples over the course of the study. Furthermore, while qPCR data showed similar abundance of *Methanomicrobiales* in both acetate- and propionate-fed cultures, this was not reflected in the 16S rRNA sequencing data (Fig. 4), where *Methanoculleus* was not detected in acetate-fed cultures.

RNA extraction, sequencing, and differential expression analysis

Approximately 53% of raw metatranscriptomic reads were classified as rRNA and subsequently removed in-silico. Of the total mRNA reads, 71% mapped to the reference MAGs, with the majority mapping to the SAOB *S. schinkii* (34%), followed by the hydrogenotrophic methanogen *'Ca*. Methanoculleus ammoniitolerans' (32%), the SPOB *'Ca.* S. ammoniitolerans' (24%), and members of the genera *Alkaliphilus* (3%) or *Acetomicrobium* (2%) (Supplementary Fig. S7). PCA analysis of the transformed and normalised count data showed a distinct clustering based on substrate type for all samples. However, the PCA using only propionate samples showed a distinct clustering according to the mode of motion (Supplementary Fig. S8).

In the acetate fed samples, the SAOB *S. schinkii* exhibited the highest transcriptional activity, followed by the methanogen and *Alkaliphilus.* In propionate-fed samples, the methanogen and the SPOB displayed the highest activity, while *Alkaliphilus* was low in activity. The activity of SAOB was considerably lower in the propionate-fed samples compared to the acetate-fed, with moderate expression observed only in the stirred samples (StP) and one of the static control samples (Supplementary Fig. S7).

Based on the transcriptional activity and 16S rRNA gene-based microbial abundance, the MAGs for the syntrophic partners (SAOB, SPOB, methanogen) and *Acetomicrobium* were included in the differential expression analysis. As *Alkaliphilus* had low activity in the propionate-fed samples, this MAG was excluded in this analysis. All differential expression comparisons were made relative to the static control samples unless otherwise stated.

For instance, the phrase "downregulated in stirred samples" indicates that the expression levels were lower in stirred samples compared to the static control. The term "motion" is used to collectively refer to the samples subjected to either stirring or orbital shaking. It is important to note that for stirred propionate-fed samples, RNA was extracted from two technical replicates of the same bottle (StP1), as the other two bottles lacked sufficient biomass for RNA extraction.

In the differential gene expression analysis, a total of 1396 differentially expressed genes ($|\log2fc| > 1.5$ and p-adj < 0.05) were identified, mostly originating from the methanogenic MAG (Supplementary Fig. S9). For the other species, most differentially expressed genes were downregulated under both modes of motion. A Venn-diagram revealed a substantial overlap in differentially expressed genes between the two modes of motion for the methanogen and the SPOB, demonstrating that these changes occurred under both conditions (Supplementary Fig. S10). In contrast, the SAOB and the *Acetomicrobium* sp. showed less overlap, suggesting that the two motions induced regulation of a more distinct sets of genes in these species.

The following section discusses the differentially expressed genes related to core metabolic pathways, energy conservation, and microbial interactions and their surrounding genomic region. Emphasis has been placed on annotated genes, where surrounding genes in the genome exhibit a similar log-fold change. The data sheet containing the expression data and differential expression results, primarily used for analysis, can be found in Supplementary Data SE4.

Main metabolic pathways and energy conservation

Consistent with previous studies of the enrichment culture [13], the transcriptomic data in the present study demonstrated that the SPOB *'Ca.* S. ammoniitolerans' expressed genes for all steps of propionate oxidation through the methylmalonyl-CoA pathway. The SAOB *S. schinkii* expressed genes for the Wood–Ljungdahl pathway, used in the reverse direction during syntrophic acetate oxidation [71], whereas the methanogen *'Ca.* Methanoculleus ammoniitolerans' expressed genes for hydrogenotrophic methanogenesis. These core metabolic genes were highly expressed by the species across all investigated conditions (Supplementary Data SE4).

For the SPOB, the shear forces induced by stirring caused a significant downregulation of an oxalate–formate antiporter (OxlT) located next to genes encoding a CoA-transferase (Fig. 5). In anaerobic bacteria, these enzymes have been shown to import oxalate (a divalent anion) by exchanging formate and, through a series of steps, convert the imported oxalate to formate, which is then exchanged for a new oxalate molecule, thereby closing the cycle. For each cycle, one intracellular proton is consumed, creating a proton gradient [72, 73] that could be used for ATP production (Fig. 5). This antiporter has previously been suggested to facilitate formate export in a syntrophic butyrate oxidising bacteria [74] or contribute to ATP production in syntrophic alkane-degrading bacteria [75]. In addition, prior research has linked increased expression of the oxalate–formate antiporter to faster propionate oxidation in thermophilic, ammonia-tolerant SPOB [14]. In combination with the higher expression of the oxalate–formate antiporter in aggregated states (static/shaking) in the present study, these findings suggest that this oxalate–formate cycling activity is dependent on cellular proximity and possibly requires interactions with other members of the syntrophic community. This activity could serve as a potential indicator of a well-performing SPOB community, and future culture studies of the SPOB may shed some light on this. Another question to address is the source of the oxalate in the culture medium, as no gene expression linked to oxalate production or transport was found in any of the other species in the culture.

For the SAOB, the gene expression of the reductive Wood–Ljungdahl pathway and energy conserving systems were relatively unaffected by the motions, which correlated with the observation of the relatively similar acetate degradation profiles of the batch assays. Rather, the most pronounced effects were observed for the methanogen, where both motions evoked upregulation of most of the genes involved in the hydrogenotrophic methanogenesis and a formate transporter. Furthermore, based on the genomic localisation of differentially expressed genes it appears that stirring induced the methanogen to increase the expression of genes involved in the so-called Wolfe cycle, a key energy conserving strategy in hydrogenotrophic methanogenesis (Fig. 5). The cycle plays a crucial role in regenerating reduced cofactors needed for hydrogenotrophic methanogenesis by coupling the exergonic reduction of heterodisulfide (CoM–S–S–CoB) to the endergonic reduction of ferredoxin, using H_2. Alternatively, ferredoxin can be reduced through the energy-converting hydrogenases (Eha, Ech). During shaking, the energy-converting hydrogenase Eha was downregulated, with significant decreases observed in subunits *ehaB* and *ehaD.* Genes encoding the enzyme formylmethanofuran dehydrogenase (Fwd), which catalyse the first step of hydrogenotrophic methanogenesis, wherein reduced ferredoxin is consumed, were distributed at multiple different genomic regions (Supplementary Fig. S11). These fwd genes were located at distinct genomic loci, next to genes associated with either the

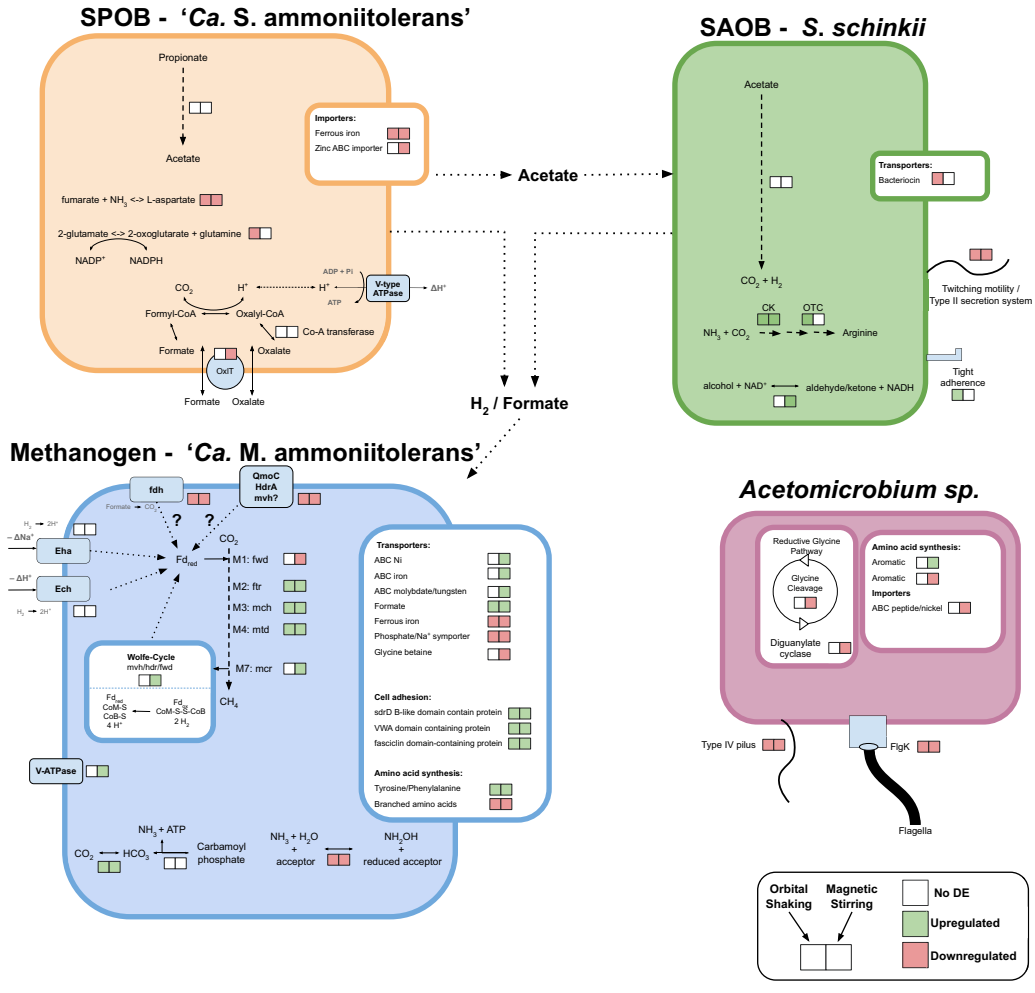

Fig. 5 Graphical overview of the highlighted differentially expressed genes in stirred or orbital shaken samples relative to the static control samples. The red and green squares represent differentially downregulated and upregulated genes, respectively. White squares indicate that no differential change in expression was observed

Wolfe cycle, the energy-converting hydrogenases, or, intriguingly, next to a formate dehydrogenase. The formate dehydrogenase was downregulated under both motions, and the Fwd-gene downregulated in response to stirring. This co-localisation could suggest that the formate dehydrogenase is involved in ferredoxin reduction. However, formate has a redox potential similar to H_2, and like hydrogen cannot reduce ferredoxin directly. To our knowledge, no such route of ferredoxin reduction via formate has been previously described. The Fwd encoding genes located next to the energy converting hydrogenase Eha were not differentially expressed. Furthermore, the methanogen upregulated a V/A-type ATPase during stirring, used to convert proton/sodium gradients to ATP, which can be related to the strive to maintain cellular activity during these harsh conditions.

In addition, both motions induced the methanogen to downregulate a quinone-modifying oxidoreductase, subunit QmoC. This enzyme is found in sulfate-reducing bacteria, where it is thought to play a role in the electron transfer from menaquinone to the terminal electron acceptor sulfate [76]. However, while QmoC is membrane-bound, our analysis indicated the differentially expressed QmoC to be cytoplasmic. The operon also contained a downregulated heterodisulfide reductase subunit (Hdr-A) and multiple hypothetical genes with similarities to iron–sulfur proteins, indicating involvement in electron transfer. A similar protein complex has been suggested to be involved in ferredoxin reduction through a QmoC/HdrA/Mvh-hydrogenase complex [77]. However, in the methanogen of this study, the operon lacked genes encoding the Mvh-hydrogenase, although genes for this enzyme were expressed and located elsewhere in the genome.

The transcriptomic activities of the *Acetomicrobium* sp. in propionate and acetate cultures and the *Alkaliphilus* sp. in acetate cultures were notable findings, considering the absence of any other sources for growth apart from the acids in the present study. These species expressed some genes of the Wood–Ljungdahl pathway but lacked key genes for the complete pathway. However, both species expressed genes related to the glycine synthase reductase pathway [78], suggesting its use for either acetate consumption or production. The *Alkaliphilus* MAG was not included in the differentially expressed gene analysis, as the expression by this MAG was negligible in propionate samples. A description on general expression and discussion on genomic potential for the *Alkaliphilus* MAG can be found in Supplementary note 2. Under stirred conditions, the *Acetomicrobium* sp. downregulated a glycine dehydrogenase and a dihydrolipoyl dehydrogenase, both components of the glycine cleavage system. They located within an operon that also contained a downregulated diguanylate cyclase, an enzyme regulating the ubiquitous second messenger cyclic di-GMP, which is an important regulator of bacterial behaviour, modulating processes such as biofilm formation and motility [79]. The reduced expression of diguanylate cyclase during stirring, when cells were more dispersed, suggests a possible link between glycine cleavage system activity and the flocculation state.

Microbial interactions, motility, and biofilm formation

We expected that the motions, particularly stirring, would influence the expression for genes associated with motility, biofilm formation, and cell–cell interactions. However, in the SPOB no characterised genes linked to these functions were found to be differentially expressed. Nevertheless, the congregation of cells induced by orbital shaking caused the SAOB to upregulate an operon encoding tight adherence proteins (tadB, tadC) and pilus assembly proteins (CpaE, CpaF, CpaB). Expression of this operon was almost absent in static and stirred cultures. Some of these genes (tadB, tadC, CpaF) are known to be associated with the capability of colonisation of the mucus layer surrounding phytoplankton by oceanic bacteria [80], thus indicating a potential role in floc-formation of the SAOB during shaking. Shaking motion also caused the SAOB to downregulate an operon encoding ABC transporters involved in lipoprotein transport and the efflux of antimicrobial peptides. One of the genes in this operon showed BlastP similarity to bacteriocins, which are antimicrobial peptides that inhibit similar or closely related species, thereby offering a competitive advantage to the producer in the competition for resources and ecological niches [81]. Since cultures subjected to shaking motion formed the largest flocs, the downregulation of this bacteriocin system could represent an adaption to the close proximity to partner species on which they depend for metabolic activity.

Moreover, both motions caused the SAOB and the *Acetomicrobium* sp. to downregulate type IV pilus containing operons, including twitching motility proteins. Twitching motility allows bacteria to move over surfaces, and it is plausible that this mode of motility was only beneficial in the absence of shear stress and fluidic movement, as was the case for the static cultures. This is supported by the observation of surface-attached biofilms and biomass aggregation at the bottom of the culture bottles in static cultures, while both stirring and shaking seemed to prevent such formations. Furthermore, contact with surfaces has been shown to enhance the expression of type IV pilus in bacteria of the genus *Pseudomonas* [82, 83]. Therefore, it is possible that contact with the bottom of the bottle during static conditions contributed to the higher expression of type IV pilus in SAOB and *Acetomicrobium* sp. In addition to type IV pilus genes, the *Acetomicrobium* sp. downregulated a Flagellar hook-associated protein (FlgK) in response to both motions. The hook-associated protein plays a crucial role in connecting the flagellar hook to the flagellar filaments [84], suggesting increased motility under the static control conditions.

For the methanogen, both types of motions invoked upregulation of an operon containing numerous hypothetical proteins with BlastP similarity to "von Willebrand A (VWA) domain-containing protein". While VWA domain-containing proteins are well-studied in eukaryotes, and are associated with cell adhesion and extracellular matrix proteins, less is known about their roles in prokaryotes [85]. The operon also included genes involved in methanogenesis (*mer* and *mtd*) of which

mtd was upregulated. In addition, the operon contained genes encoding a Tubulin-like protein (CetZ), which in *Haloferax volcanii* regulates cell shape, contributed to the rod-shaped morphology needed for normal swimming motility [86]. However, considering that *Methanoculleus* species are irregular cocci this protein likely has a different role in this species. Furthermore, both motions evoked upregulation of unannotated genes, with BlastP similarities to proteins containing domains that indicate an involvement in adhesion and cell–surface interactions, namely: fasciclin-domain which is involved in ancient cell adhesion in plants and animals [87], PKD-domain found surface layer proteins of archaea [88], and SdrD B-like-domain which is important for cell adhesion [89].

Transport, ammonia tolerance, amino acid, and other noteworthy gene expression changes

It is noteworthy that both the SPOB and the methanogen downregulated ferrous iron transport proteins under both types of motions. Ferrous iron is the predominant form of iron in anaerobic environments, and the downregulation of the transport systems may suggest that iron is a limited resource in the static control conditions, where mass transfer is determined by diffusion rates. In a separate experiment, the influence of iron level was tested under static conditions (data not shown). The addition of extra iron (ferric or ferrous 250 μM) seemed to have a negative effect on the syntrophic acid degradation, suggesting that iron deficiency is unlikely to be a major constraint in the current study. However, considering the interaction between iron and sulphide [90], it is possible that the iron addition inadvertently caused deficiency in bioavailable sulphur. Other differentially expressed transport proteins included downregulation of zinc transport under stirring by SPOB, whereas the methanogen upregulated ABC transport of nickel, iron, and molybdate/tungsten under stirred conditions and downregulated a phosphate/Na^+ symporter under both motions. The *Acetomicrobium* sp. exhibited differential expression in genes for the transport of aromatic amino acids, with one operon downregulated during shaking motion and another upregulated under stirring motion. This suggests an adaption strategy to cope with the more challenging conditions associated with stirring. An ABC importer for peptide/nickel was also downregulated in stirred samples for the *Acetomicrobium* sp. (Fig. 5). In the methanogen, changes in amino acids metabolism included downregulation of genes involved in the synthesis of branched-chain amino acids (valine, isoleucine, leucine) under both motions. Conversely, several genes encoding phenylacetate-CoA ligase family protein, which are involved in phenylalanine and tyrosine metabolism, were upregulated under both motions.

Cultures were grown in high ammonia conditions (0.3 M) and many enzymes involved in ammonia-related reactions or osmotic stress showed differential expression. Notably, many of these enzymes exhibited similar expression patterns for both modes of motion. These systems could assimilate ammonia, thereby reducing intracellular ammonia levels, or to synthesise compatible solutes that help the cells manage ammonia stress. Furthermore, cellular aggregation could be employed by certain microbes to mitigate osmotic stress caused by the high ammonia [91]. If so, the disruption of aggregates through agitative motion, especially stirring, could undermine this strategy. This could explain the observed changes in expression between static and mixed cultures. For SPOB, both motions induced downregulation of aspartate ammonia lyase, converting ammonia and fumarate into L-aspartate. As fumarate is an intermediary of the methylmalonyl CoA pathway, the observed expression changes may reflect a shift in the SPOB's metabolism toward catabolic processes in response to motion. This enzyme has also been shown to be upregulated in iron starved conditions in various bacterial species [92–95]. Moreover, the shaking motion evoked a downregulation of a NADPH dependent glutamate synthase in the SPOB, an enzyme that in conjunction with glutamine synthase is an important pathway of ammonia assimilation [96]. However, genes encoding glutamine synthase were located at other genomic locations and not differentially expressed. Glutamate is also an important counter-ion to potassium, a ion-pair which accumulates as a short-term response to osmotic shock [97]. However, given the long-term exposure to elevated ammonia levels, this function of glutamate is less probable for the species. Both motions caused the SAOB to upregulate a carbamate kinase, an enzyme that utilises ammonia and CO_2 to produce carbamoyl phosphate. The operon also included an ornithine carbamoyltransferase, involved in arginine synthesis, which was upregulated in stirred cultures. In the methanogen, two operons with a potential role in ammonia assimilation were differentially expressed. The first operon included a carbonic anhydrase which converts carbon dioxide into carbonate, upregulated under both motions (Fig. 5). Surrounding genes encoded a carbamoyl-phosphate synthase, which combines bicarbonate and ammonia to form carbamoyl phosphate, an intermediary in pyrimidine synthesis and the urea cycle. The cluster also contained genes encoding a transport system for the compatible solute glycine betaine, which could indicate that the operon is involved in ammonia tolerance. The transport system was, however, downregulated in response to stirring, directly contrasting the carbonic anhydrase. The second operon was downregulated under both motions and contained a hydroxylamine reductase,

which catalysed the reversible oxidation of ammonia to hydroxylamine (NH_2OH), transferring electrons to an electron acceptor.

Finally, although certain differentially expressed genes were interesting, they did not fit into any of the previous categories. For the SAOB, the shear forces by stirring induced upregulation of two genes encoding a zinc dependent alcohol dehydrogenase, one of which was among the most highly expressed for the species. Alcohol dehydrogenases catalyse the reversible conversion of aldehydes/ketones to their corresponding alcohol while simultaneously oxidising NADH. In *S. schinki*, the enzyme has been proposed to partake in ethanol degradation in conjunction with acetaldehyde dehydrogenase, converting ethanol to acetyl-CoA, reducing NAD^- in the process [71]. This gene has been shown to be expressed by *Zhaonella formicivorans* in co-culture with a methylotrophic methanogen, utilizing the fourth mode of syntrophy, where methanol serves as an electron carrier [98]. However, this is unlikely to be the function of the alcohol dehydrogenase gene in *S. schinki*, as this species lacks several key genes for the methanol-producing pathway and was not associated with a methylotrophic methanogen in the enrichment culture. The high upregulation of this alcohol dehydrogenase containing operon is a notable finding, although its function and high expression remains enigmatic.

Differences in gene expression between acetate- and propionate-fed cultures and potential coordinated cross-feeding of amino acids

The microbial composition varied between acetate- and propionate-fed cultures, with the primary distinction being the presence of the SPOB in the propionate-fed cultures and the *Alkaliphilus* sp. in the acetate-fed cultures. To investigate how both substrate type and microbial composition influenced gene expression in the SAOB, methanogen, and *Acetomicrobium* sp., a differential gene expression analysis was conducted (Supplementary Data SE5). This analysis compared the transcriptomes of all acetate-fed (three in total) with all propionate-fed cultures (nine in total). Changes in gene expression are reported relative to the propionate-fed cultures, with upregulation indicating higher expression in acetate-fed than in propionate-fed cultures.

Both the SAOB and methanogen downregulated several formate dehydrogenases and formate transporters in the acetate-fed cultures. Given that formate and hydrogen are considered as the primary carriers of reducing equivalents in syntrophic cultures, an upregulation of hydrogenases would typically be expected if the flux of reducing equivalents is to be maintained. However, no such upregulation was observed for the methanogen. Furthermore, the SAOB, contrary to expectations, downregulated hydrogenases [NiFe] 4e (ech) and [NiFe] 3B. These finding indicates that electron transfer in the acetate-fed cultures is more extensively routed through alternative pathways, such as direct electron transfer, or that the overall flux was reduced. For core metabolic pathways, gene expression remained largely unchanged, except for the upregulation of methenyltetrahydromethanopterin cyclohydrolase by the methanogen (step M3, Fig. 5).

Regarding pilus and flagellar systems, the SAOB downregulated most genes associated with the pilus system (pilABC), while genes involved in tight adherence and twitching motility were upregulated in the acetate culture. The methanogen downregulated the archaeal type IV pilus assembly protein (pilA), which is shown to be important for surface adherence [99]. These adaptions may contribute to the more pronounced surface attached biofilm growth observed in acetate-fed cultures (Supplementary Fig. S1).

Interspecies amino acid exchange is a particularly relevant aspect of the present study, as the metagenomic analyses indicated that all syntrophic microorganisms are auxotrophic (Supplementary Data, SE6 and SE7) and that they are cultivated under amino acid-limited conditions, aside from cysteine. The necessity of cross-feeding in the enrichment culture is further supported by the requirement of yeast extract by the SAOB *S. schinkii* when grown in pure-culture [30]. Experimental validation of auxotrophy in *'Ca.* M. ammoniitolerans' and *'Ca.* S. ammoniitolerans' awaits their isolation but SPOB such as *P. thermopropionicum* and several *Methanoculleus* species require the presence of yeast extract in mono-cultivation [100–102]. Still, our findings demonstrate that the propionate oxidiser is not essential for providing amino acids in acetate-degrading community, as these cultures managed to grow without yeast extract, even in the absence of the propionate oxidiser. Even though, no enrichment of amino-acid-related genes was observed for the methanogen, the SAOB had enrichment of upregulated genes involved in the synthesis of the branched-chain amino acids leucine and isoleucine in the acetate-fed cultures. The SPOB expressed the necessary genes for the leucine and isoleucine synthesis as observed in the propionate-fed cultures (Supplementary Fig. S12), indicating that the exchange of leucine/isoleucine from the SPOB to the SAOB is possible. However, these expression changes may not solely link to microbial interactions, as they could also result from the differences in acetate or propionate concentrations. For example, *Escherichia coli* can synthesise isoleucine by converting propionate to 2-ketobutyrate through an alternate pathway under anaerobic conditions in the presence of propionate [103].

In acetate-fed cultures, the SAOB exhibited enrichment of downregulated genes involved in threonine synthesis. Both the SPOB, the SAOB, and the *Alkaliphilus* sp. have the capability to produce threonine, complicating the ability to draw conclusions as to why the SAOB is downregulating its synthesis. Potential explanations include threonine provision by the *Alkaliphilus* sp. in acetate-fed cultures or overproduction and provision of threonine by the SAOB in propionate-fed conditions. Furthermore, the *Acetomicrobium* sp. showed enrichment of upregulated genes for tryptophan synthesis in acetate-fed conditions. This species had a complete set of genes for the synthesis of the tryptophan, unlike both the *Alkaliphilus* sp. and the SPOB, which lacked a complete set of genes. Taken together, the upregulation could indicate that *Acetomicrobium* sp. is providing the *Alkaliphilus* sp. with tryptophan in acetate-fed cultures. Tryptophan is a relatively costly amino acid to produce [104] and these amino acids have been shown to promote stronger auxotrophic interactions than the exchange of amino acids that are cheaper to produce [105]. Tryptophan has previously been suggested to play a role in coordinated cross-feeding between the SPOB *Pelotomaculum schinkii* and *Methanospirillum hungatei* [106]. However, given the complex and interconnected nature of interaction within these syntrophic communities further research is needed to confirm these findings.

Conclusion

This study provides critical insights into how different mixing strategies affect syntrophic acid-degrading cultures, which play a key role in AD processes. Stirring substantially hindered initiation of syntrophic propionate oxidation while having minimal effect on syntrophic acetate oxidation. CFD modelling showed that stirring generated high shear rates and resulted in an even particle (cell) distribution, while shaking induced lower shear rates with more pronounced spatial gradients, causing cells to concentrate near the bottom. As a result, shaking reduced the lag phase and promoted the formation of larger microbial aggregates in the syntrophic propionate oxidizing community. This suggests that the movement, characterized by low shear stress, facilitated the initial connection and enhanced cell-to-cell interactions between SPOB and the methanogen.

Although motion had a limited impact on microbial community composition and the acid degradation rate, it triggered several key transcriptional changes in the syntrophic community (SAOB, SPOB, and methanogen), and the two species expressing the glycine synthase reductase pathway. Notably, stirring led to downregulation of an oxalate–formate antiporter in the SPOB. The higher expression of this system in the biofilm/aggregate forming cultures suggests a reliance on proximity for this activity, which may be linked to ATP production. Another notable effect was the upregulation of genes associated with hydrogenotrophic methanogenesis, particularly under stirred conditions, where the connection between the first and the last step in the hydrogenotrophic methanogenesis to regenerate ferredoxin appeared to have a prominent role. This has been suggested as an important strategy for methanogens for energy conservation. In addition, shaking caused the upregulation of tight adherence and pilus assembly genes in the SAOB, likely promoting cell aggregation. Conversely, both motions caused downregulation of motility-related genes in the SAOB and a *Acetomicrobium* sp., suggesting that motility was primarily beneficial under static conditions. Furthermore, pathway enrichment revealed potential cross-feeding of the branched amino acids leucine and isoleucine in propionate-fed cultures.

In particular, this study demonstrated that mixing and high shear stress disrupt the initial cell-to-cell connections between syntrophic propionate-oxidising bacteria and hydrogenotrophic methanogens, thereby negatively affecting the propionate degradation. These findings highlight the need to carefully control mixing strategies in anaerobic digesters, especially during periods of rising propionate levels when these communities need to establish themselves. Excessive shear stress may hinder the initiation of key syntrophic processes, particularly propionate oxidation, potentially leading to higher VFA accumulation and process instability. Conversely, moderate agitation that promotes microbial aggregation without excessive disruption could enhance syntrophic efficiency and biogas yield. These results have deepened the understanding of how hydrodynamic forces affect syntrophic interactions, which is crucial for optimizing anaerobic reactor design to maximize performance and stability, particularly under high-ammonia and high-VFA conditions. Furthermore, this knowledge could be leveraged in designing systems specifically aimed at producing propionate and other VFAs as end-products by adjusting mixing conditions to minimize syntrophic propionate degradation.

Supplementary Information

The online version contains supplementary material available at https://doi.org/10.1186/s13068-025-02644-3.

Supplementary Material 1.

Supplementary Material 2.

Supplementary Material 3.

Author contributions
NW: Experimental design, Laboratory work, Analysis, Data visualisation, writing (original draft, reviewing and editing) MW: Experimental design, Supervision, Writing (original draft, reviewing, and editing), Project administration, Funding acquisition HNN: All analysis and visualisation of computational fluid dynamics modelling, Writing (original draft sections on CFD modelling, reviewing and editing) All authors reviewed and approved the manuscript.

Funding
Open access funding provided by Swedish University of Agricultural Sciences. Research reported in this publication was supported by the HR2020 ERC—Grant European Research Council (Grant Number 948138), the Swedish Research Council (VR, Grant Number 2019-03846) and the Novo Nordisk Foundation (grant number NNF23OC0081830).

Availability of data and materials
All data generated or analysed during this study is included in this published article and its supplementary information files. The sequencing data generated and analysed in this study is available in the NCBI BioProject (PRJNA1187519). The 16S rRNA gene sequencing data have the SRA accession numbers SRR31396638-SRR31396766, and the metatranscriptomic sequencing data have the accession numbers SRR31439851-SRR31439861.

Declarations

Ethics approval and consent to participate
Not applicable.

Consent for publication
Not applicable.

Competing interests
The authors declare no competing interests.

Author details
[1]Department of Molecular Sciences, Swedish University of Agricultural Sciences, Uppsala, Sweden. [2]Department of Management and Engineering, Linköping University, 581 83 Linköping, Sweden.

Received: 12 December 2024 Accepted: 31 March 2025
Published online: 19 April 2025

References

1. Anukam A, Mohammadi A, Naqvi M, Granström K. A review of the chemistry of anaerobic digestion: methods of accelerating and optimizing process efficiency. Processes. 2019;7:504.
2. Giduthuri AT, Ahring BK. Current status and prospects of valorizing organic waste via arrested anaerobic digestion: production and separation of volatile fatty acids. Fermentation. 2023;9:13.
3. Scarlat N, Dallemand J-F, Fahl F. Biogas: developments and perspectives in Europe. Renew Energy. 2018;129:457–72.
4. O'Connor J, Mickan BS, Rinklebe J, Song H, Siddique KHM, Wang H, et al. Environmental implications, potential value, and future of food-waste anaerobic digestate management: a review. J Environ Manage. 2022;318: 115519.
5. EurObserv'ER. 21st annual overview barometer. 2022. https://www.eurobserv-er.org/21st-annual-overview-barometer/. Accessed 10 July 2023.
6. De Vrieze J, Saunders AM, He Y, Fang J, Nielsen PH, Verstraete W, et al. Ammonia and temperature determine potential clustering in the anaerobic digestion microbiome. Water Res. 2015;75:312–23.
7. Fischer MA, Ulbricht A, Neulinger SC, Refai S, Waßmann K, Künzel S, et al. Immediate effects of ammonia shock on transcription and composition of a biogas reactor microbiome. Front Microbiol. 2019;10:2064.
8. Wang Z, Wang S, Hu Y, Du B, Meng J, Wu G, et al. Distinguishing responses of acetoclastic and hydrogenotrophic methanogens to ammonia stress in mesophilic mixed cultures. Water Res. 2022;224: 119029.
9. Westerholm M, Müller B, Isaksson S, Schnürer A. Trace element and temperature effects on microbial communities and links to biogas digester performance at high ammonia levels. Biotechnol Biofuels. 2015;8:154.
10. Rajagopal R, Massé DI, Singh G. A critical review on inhibition of anaerobic digestion process by excess ammonia. Bioresour Technol. 2013;143:632–41.
11. Westerholm M, Liu T, Schnürer A. Comparative study of industrial-scale high-solid biogas production from food waste: process operation and microbiology. Bioresour Technol. 2020;304: 122981.
12. Singh A, Schnürer A, Westerholm M. Enrichment and description of novel bacteria performing syntrophic propionate oxidation at high ammonia level. Environ Microbiol. 2021;23:1620–37.
13. Weng N, Singh A, Ohlsson JA, Dolfing J, Westerholm M. Catabolism and interactions of syntrophic propionate- and acetate oxidizing microorganisms under mesophilic, high-ammonia conditions. Front Microbiol. 2024;15:1389257.
14. Singh A, Schnürer A, Dolfing J, Westerholm M. Syntrophic entanglements for propionate and acetate oxidation under thermophilic and high-ammonia conditions. ISME J. 2023;17:1966–78.
15. Boone DR, Johnson RL, Liu Y. Diffusion of the interspecies electron carriers H2 and formate in methanogenic ecosystems and its implications in the measurement of Km for H2 or formate uptake. Appl Environ Microbiol. 1989;55:1735–41.
16. McInerney MJ, Bryant MP, Pfennig N. Anaerobic bacterium that degrades fatty acids in syntrophic association with methanogens. Arch Microbiol. 1979;122:129–35.
17. de Bok FAM, Plugge CM, Stams AJM. Interspecies electron transfer in methanogenic propionate degrading consortia. Water Res. 2004;38:1368–75.
18. Doloman A, Besteman MS, Sanders MG, Sousa DZ. Methanogenic partner influences cell aggregation and signalling of *Syntrophobacterium fumaroxidans*. Appl Microbiol Biotechnol. 2024;108:127.
19. Pinela E, Schnürer A, Neubeck A, Moestedt J, Westerholm M. Impact of additives on syntrophic propionate and acetate enrichments under high-ammonia conditions. Appl Microbiol Biotechnol. 2024;108:433.
20. Ishii S, Kosaka T, Hori K, Hotta Y, Watanabe K. Coaggregation facilitates interspecies hydrogen transfer between *Pelotomaculum thermopropionicum* and *Methanothermobacter thermautotrophicus*. Appl Environ Microbiol. 2005;71:7838–45.
21. Doloman A, Sousa DZ. Mechanisms of microbial co-aggregation in mixed anaerobic cultures. Appl Microbiol Biotechnol. 2024;108:407.
22. Jefferson KK. What drives bacteria to produce a biofilm? FEMS Microbiol Lett. 2004;236:163–73.
23. Katharios-Lanwermeyer S, Xi C, Jakubovics NS, Rickard AH. Mini-review: microbial coaggregation: ubiquity and implications for biofilm development. Biofouling. 2014;30:1235–51.
24. Cai Y-M. Non-surface attached bacterial aggregates: a ubiquitous third lifestyle. Front Microbiol. 2020;11: 557035.
25. Whitmore TN, Lloyd D, Jones G, Williams TN. Hydrogen-dependent control of the continuous anaerobic digestion process. Appl Microbiol Biotechnol. 1987;26:383–8.
26. McMahon KD, Stroot PG, Mackie RI, Raskin L. Anaerobic codigestion of municipal solid waste and biosolids under various mixing conditions—II: microbial population dynamics. Water Res. 2001;35:1817–27.
27. Singh B, Szamosi Z, Siménfalvi Z. Impact of mixing intensity and duration on biogas production in an anaerobic digester: a review. Crit Rev Biotechnol. 2020;40:508–21.
28. Perman E, Karlsson A, Westerholm M, Isaksson S, Schnürer A. High-solid digestion—a comparison of completely stirred and plug-flow reactor systems. Waste Manage. 2024;189:265–75.
29. Campanaro S, Treu L, Rodriguez-R LM, Kovalovszki A, Ziels RM, Maus I, et al. New insights from the biogas microbiome by comprehensive genome-resolved metagenomics of nearly 1600 species originating from multiple anaerobic digesters. Biotechnol Biofuels. 2020;13:25.

30. Westerholm M, Roos S, Schnürer A. *Syntrophaceticus schinkii* gen. nov., sp. nov., an anaerobic, syntrophic acetate-oxidizing bacterium isolated from a mesophilic anaerobic filter. FEMS Microbiol Lett. 2010;309:100–4.
31. Westerholm M, Hansson M, Schnürer A. Improved biogas production from whole stillage by co-digestion with cattle manure. Bioresour Technol. 2012;114:314–9.
32. COMSOL Multiphysics® v. 6.2. www.comsol.com. COMSOL AB, Stockholm, Sweden.
33. Nienow AW, Rielly CD, Brosnan K, Bargh N, Lee K, Coopman K, et al. The physical characterisation of a microscale parallel bioreactor platform with an industrial CHO cell line expressing an IgG4. Biochem Eng J. 2013;76:25–36.
34. Kaiser SC, Löffelholz C, Werner S, Eibl D. CFD for Characterizing Standard and Single-use Stirred Cell Culture Bioreactors. In: Minin IV, Minin OV, editors. Computational fluid dynamics. Rijeka: IntechOpen; 2011. https://doi.org/10.5772/23496.
35. Sucosky P, Osorio DF, Brown JB, Neitzel GP. Fluid mechanics of a spinner-flask bioreactor. Biotechnol Bioeng. 2004;85:34–46.
36. Nagata S. Mixing: principles and applications. New York: Wiley; 1975.
37. Kubitschek HE. Increase in cell mass during the division cycle of *Escherichia coli* B/rA. J Bacteriol. 1986;168:613–8.
38. Celik IB, Ghia U, Roache PJ, Freitas CJ. Procedure for estimation and reporting of uncertainty due to discretization in CFD applications. ASME J Fluids Eng. 2008;130.
39. Hugerth LW, Wefer HA, Lundin S, Jakobsson HE, Lindberg M, Rodin S, et al. DegePrime, a program for degenerate primer design for broad-taxonomic-range PCR in microbial ecology studies. Appl Environ Microbiol. 2014;80:5116–23.
40. Herlemann DP, Labrenz M, Jürgens K, Bertilsson S, Waniek JJ, Andersson AF. Transitions in bacterial communities along the 2000 km salinity gradient of the Baltic Sea. ISME J. 2011;5:1571–9.
41. Müller B, Sun L, Westerholm M, Schnürer A. Bacterial community composition and *fhs* profiles of low- and high-ammonia biogas digesters reveal novel syntrophic acetate-oxidising bacteria. Biotechnol Biofuels. 2016;9:48.
42. Bolger AM, Lohse M, Usadel B. Trimmomatic: a flexible trimmer for Illumina sequence data. Bioinformatics. 2014;30:2114–20.
43. Martin M. Cutadapt removes adapter sequences from high-throughput sequencing reads. EMBnet J. 2011;17:10–2.
44. Callahan BJ, McMurdie PJ, Rosen MJ, Han AW, Johnson AJA, Holmes SP. DADA2: High-resolution sample inference from Illumina amplicon data. Nat Methods. 2016;13:581–3.
45. Alishum A. DADA2 formatted 16S rRNA gene sequences for both bacteria & archaea, Zenodo; 2021. https://zenodo.org/records/4735821. Accessed 9 May 2024.
46. Parks DH, Chuvochina M, Waite DW, Rinke C, Skarshewski A, Chaumeil P-A, et al. A standardized bacterial taxonomy based on genome phylogeny substantially revises the tree of life. Nat Biotechnol. 2018;36:996–1004.
47. McMurdie PJ, Holmes S. phyloseq: an R package for reproducible interactive analysis and graphics of microbiome census data. PLoS ONE. 2013;8: e61217.
48. Merkel AY, Tarnovetskii IY, Podosokorskaya OA, Toshchakov SV. Analysis of 16S rRNA primer systems for profiling of thermophilic microbial communities. Microbiology. 2019;88:671–80.
49. Yu Y, Lee C, Kim J, Hwang S. Group-specific primer and probe sets to detect methanogenic communities using quantitative real-time polymerase chain reaction. Biotechnol Bioeng. 2005;89:670–9.
50. Maeda H, Fujimoto C, Haruki Y, Maeda T, Kokeguchi S, Petelin M, et al. Quantitative real-time PCR using TaqMan and SYBR Green for Actinobacillus actinomycetemcomitans, Porphyromonas gingivalis, Prevotella intermedia, tetQ gene and total bacteria. FEMS Immunol Med Microbiol. 2003;39:81–6.
51. Weng N, Perman E. RNA extraction & depletion. Protocols.io. 2024. https://www.protocols.io/view/rna-extraction-amp-depletion-dt2d6qa6. Accessed 11 Dec 2024.
52. Kopylova E, Noé L, Touzet H. SortMeRNA: fast and accurate filtering of ribosomal RNAs in metatranscriptomic data. Bioinformatics. 2012;28:3211–7.
53. Patro R, Duggal G, Love MI, Irizarry RA, Kingsford C. Salmon provides fast and bias-aware quantification of transcript expression. Nat Methods. 2017;14:417–9.
54. Love MI, Huber W, Anders S. Moderated estimation of fold change and dispersion for RNA-seq data with DESeq2. Genome Biol. 2014;15:550.
55. Kolde R. pheatmap: Pretty Heatmaps. 2019. https://CRAN.R-project.org/package=pheatmap. Accessed 18 Jan 2023.
56. Wickham H. ggplot2: elegant graphics for data analysis. Springer, New York. 2016. https://ggplot2.tidyverse.org. Accessed 18 Jan 2023.
57. Benjamini Y, Hochberg Y. Controlling the false discovery rate: a practical and powerful approach to multiple testing. J Roy Stat Soc B Met. 1995;57:289–300.
58. Price MN, Deutschbauer AM, Arkin AP. GapMind: automated annotation of amino acid biosynthesis. mSystems. 2020. https://doi.org/10.1128/msystems.00291-20.
59. Sauer K, Stoodley P, Goeres DM, Hall-Stoodley L, Burmølle M, Stewart PS, et al. The biofilm life cycle: expanding the conceptual model of biofilm formation. Nat Rev Microbiol. 2022;20:608–20.
60. Jarvis P, Jefferson B, Gregory J, Parsons SA. A review of floc strength and breakage. Water Res. 2005;39:3121–37.
61. Liu Y, Tay J-H. The essential role of hydrodynamic shear force in the formation of biofilm and granular sludge. Water Res. 2002;36:1653–65.
62. Tsagkari E, Connelly S, Liu Z, McBride A, Sloan WT. The role of shear dynamics in biofilm formation. NPJ Biofilms Microbiomes. 2022;8:1–10.
63. Cong S, Xu Y, Lu Y. Growth coordination between butyrate-oxidizing syntrophs and hydrogenotrophic methanogens. Front Microbiol. 2021;12: 742531.
64. Conrad R, Phelps TJ, Zeikus JG. Gas metabolism evidence in support of the juxtaposition of hydrogen-producing and methanogenic bacteria in sewage sludge and lake sediments. Appl Environ Microbiol. 1985;50:595–601.
65. Westerholm M, Dolfing J, Schnürer A. Growth characteristics and thermodynamics of syntrophic acetate oxidizers. Environ Sci Technol. 2019;53:5512–20.
66. Li C, Hao L, Lü F, Duan H, Zhang H, He P. Syntrophic acetate-oxidizing microbial consortia enriched from full-scale mesophilic food waste anaerobic digesters showing high biodiversity and functional redundancy. mSystems. 2022;7:e00339-e422.
67. Dyksma S, Jansen L, Gallert C. Syntrophic acetate oxidation replaces acetoclastic methanogenesis during thermophilic digestion of biowaste. Microbiome. 2020;8:105.
68. Kovács E, Wirth R, Maróti G, Bagi Z, Nagy K, Minárovits J, et al. Augmented biogas production from protein-rich substrates and associated metagenomic changes. Bioresour Technol. 2015;178:254–61.
69. Li C, He P, Hao L, Lü F, Shao L, Zhang H. Diverse acetate-oxidizing syntrophs contributing to biogas production from food waste in full-scale anaerobic digesters in China. Renew Energy. 2022;193:240–50.
70. Kamravamanesh D, Rinta Kanto JM, Ali-Loytty H, Myllärinen A, Saalasti M, Rintala J, et al. *Ex-situ* biological hydrogen methanation in trickle bed reactors: integration into biogas production facilities. Chem Eng Sci. 2023;269: 118498.
71. Manzoor S, Bongcam-Rudloff E, Schnürer A, Müller B. Genome-guided analysis and whole transcriptome profiling of the mesophilic syntrophic acetate oxidising bacterium *Syntrophaceticus schinkii*. PLoS ONE. 2016;11: e0166520.
72. Anantharam V, Allison MJ, Maloney PC. Oxalate:formate exchange. The basis for energy coupling in Oxalobacter. J Biol Chem. 1989;264:7244–50.
73. Kuhner CH, Hartman PA, Allison MJ. Generation of a proton motive force by the anaerobic oxalate-degrading bacterium *Oxalobacter formigenes*. Appl Environ Microbiol. 1996;62:2494–500.
74. Hao L, Michaelsen TY, Singleton CM, Dottorini G, Kirkegaard RH, Albertsen M, et al. Novel syntrophic bacteria in full-scale anaerobic digesters revealed by genome-centric metatranscriptomics. ISME J. 2020;14:906–18.
75. Qin Q-S, Feng D-S, Liu P-F, He Q, Li X, Liu A-M, et al. Metagenomic characterization of *Candidatus* Smithella cisternae Strain M82_1, a syntrophic alkane-degrading bacteria, enriched from the shengli oil field. Microbes Environ. 2017;32:234–43.

76. Ramos AR, Keller KL, Wall JD, Pereira IAC. The membrane QmoABC complex interacts directly with the dissimilatory adenosine 5′-phosphosulfate reductase in sulfate reducing bacteria. Front Microbiol. 2012;3:137.
77. Buessecker S, Chadwick GL, Quan ME, Hedlund BP, Dodsworth JA, Dekas AE. Mcr-dependent methanogenesis in *Archaeoglobaceae* enriched from a terrestrial hot spring. ISME J. 2023;17:1649–59.
78. Song Y, Lee JS, Shin J, Lee GM, Jin S, Kang S, et al. Functional cooperation of the glycine synthase-reductase and Wood-Ljungdahl pathways for autotrophic growth of *Clostridium drakei*. Proc Natl Acad Sci USA. 2020;117:7516–23.
79. Chua SL, Hultqvist LD, Yuan M, Rybtke M, Nielsen TE, Givskov M, et al. In vitro and in vivo generation and characterization of *Pseudomonas aeruginosa* biofilm-dispersed cells via c-di-GMP manipulation. Nat Protoc. 2015;10:1165–80.
80. Isaac A, Francis B, Amann RI, Amin SA. Tight adherence (Tad) pilus genes indicate putative niche differentiation in phytoplankton bloom associated *Rhodobacterales*. Front Microbiol. 2021;12: 718297.
81. Sugrue I, Ross RP, Hill C. Bacteriocin diversity, function, discovery and application as antimicrobials. Nat Rev Microbiol. 2024;22:556–71.
82. Cowles KN, Gitai Z. Surface association and the MreB cytoskeleton regulate pilus production, localization, and function in *Pseudomonas aeruginosa*. Mol Microbiol. 2010;76:1411–26.
83. Laventie B-J, Sangermani M, Estermann F, Manfredi P, Planes R, Hug I, et al. A surface-induced asymmetric program promotes tissue colonization by *Pseudomonas aeruginosa*. Cell Host Microbe. 2019;25:140-152.e6.
84. Imada K. Bacterial flagellar axial structure and its construction. Biophys Rev. 2018;10:559–70.
85. Whittaker CA, Hynes RO. Distribution and evolution of von willebrand/integrin a domains: widely dispersed domains with roles in cell adhesion and elsewhere. Mol Biol Cell. 2002;13:3369–87.
86. Duggin IG, Aylett CHS, Walsh JC, Michie KA, Wang Q, Turnbull L, et al. CetZ tubulin-like proteins control archaeal cell shape. Nature. 2015;519:362–5.
87. Huber O, Sumper M. Algal-CAMs: isoforms of a cell adhesion molecule in embryos of the alga Volvox with homology to *Drosophila* fasciclin I. EMBO J. 1994;13:4212–22.
88. Jing H, Takagi J, Liu J, Lindgren S, Zhang R, Joachimiak A, et al. Archaeal surface layer proteins contain β propeller, PKD, and β helix domains and are related to metazoan cell surface proteins. Structure. 2002;10:1453–64.
89. McCrea KW, Hartford O, Davis S, Eidhin DN, Lina G, Speziale P, et al. The serine-aspartate repeat (Sdr) protein family in *Staphylococcus epidermidis*. Microbiology. 2000;146(Pt 7):1535–46.
90. Shakeri Yekta S, Ziels RM, Björn A, Skyllberg U, Ejlertsson J, Karlsson A, et al. Importance of sulfide interaction with iron as regulator of the microbial community in biogas reactors and its effect on methanogenesis, volatile fatty acids turnover, and syntrophic long-chain fatty acids degradation. J Biosci Bioeng. 2017;123:597–605.
91. Flemming H-C, van Hullebusch ED, Neu TR, Nielsen PH, Seviour T, Stoodley P, et al. The biofilm matrix: multitasking in a shared space. Nat Rev Microbiol. 2023;21:70–86.
92. Wang Z, Li L, Liu P, Wang C, Lu Q, Liu L, et al. Role of aspartate ammonia-lyase in *Pasteurella multocida*. BMC Microbiol. 2020;20:369.
93. Holmes K, Mulholland F, Pearson BM, Pin C, McNicholl-Kennedy J, Ketley JM, et al. *Campylobacter jejuni* gene expression in response to iron limitation and the role of Fur. Microbiology. 2005;151:243–57.
94. Dumpala PR, Peterson BC, Lawrence ML, Karsi A. Identification of differentially abundant proteins of *Edwardsiella ictaluri* during iron restriction. PLoS ONE. 2015;10: e0132504.
95. Deslandes V, Nash JH, Harel J, Coulton JW, Jacques M. Transcriptional profiling of *Actinobacillus pleuropneumoniae* under iron-restricted conditions. BMC Genomics. 2007;8:72.
96. Canfield DE, Kristensen E, Thamdrup B. The nitrogen cycle. In: Canfield DE, Kristensen E, Thamdrup B, editors. Aquatic geomicrobiology. New York: Academic Press; 2005. p. 205–67.
97. Sleator RD, Hill C. Bacterial osmoadaptation: the role of osmolytes in bacterial stress and virulence. FEMS Microbiol Rev. 2002;26:49–71.
98. Huang Y, Igarashi K, Liu L, Mayumi D, Ujiie T, Fu L, et al. Methanol transfer supports metabolic syntrophy between bacteria and archaea. Nature. 2025;1–6.
99. Esquivel RN, Xu R, Pohlschroder M. Novel archaeal adhesion pilins with a conserved N terminus. J Bacteriol. 2013;195:3808.
100. Kato S, Kosaka T, Watanabe K. Substrate-dependent transcriptomic shifts in *Pelotomaculum thermopropionicum* grown in syntrophic co-culture with *Methanothermobacter thermautotrophicus*. Microb Biotechnol. 2009;2:575–84.
101. Dianou D, Miyaki T, Asakawa S, Morii H, Nagaoka K, Oyaizu H, et al. *Methanoculleus chikugoensis* sp. nov., a novel methanogenic archaeon isolated from paddy field soil in Japan, and DNA-DNA hybridization among methanoculleus species. Int J Syst Evol Microbiol. 2001;51:1663–9.
102. Romesser JA, Wolfe RS, Mayer F, Spiess E, Walther-Mauruschat A. Methanogenium, a new genus of marine methanogenic bacteria, and characterization of *Methanogenium cariaci* sp. nov. and *Methanogenium marisnigri* sp. nov. Arch Microbiol. 1979;121:147–53.
103. Cotton CA, Bernhardsgrütter I, He H, Burgener S, Schulz L, Paczia N, et al. Underground isoleucine biosynthesis pathways in *E. coli*. Elife. 2020;9: e54207.
104. Akashi H, Gojobori T. Metabolic efficiency and amino acid composition in the proteomes of *Escherichia coli* and *Bacillus subtilis*. Proc Natl Acad Sci USA. 2002;99:3695–700.
105. Mee MT, Collins JJ, Church GM, Wang HH. Syntrophic exchange in synthetic microbial communities. Proc Natl Acad Sci USA. 2014;111:E2149–56.
106. Hidalgo-Ahumada CAP, Nobu MK, Narihiro T, Tamaki H, Liu W-T, Kamagata Y, et al. Novel energy conservation strategies and behaviour of *Pelotomaculum schinkii* driving syntrophic propionate catabolism. Environ Microbiol. 2018;20:4503–11.

Publisher's Note

Acta Universitatis Agriculturae Sueciae

Doctoral Thesis No. 2025:42

Anaerobic digestion of protein-rich substrates often leads to high ammonia concentrations that destabilise the process by inhibiting microbial activity. This thesis investigated ammonia-tolerant syntrophic communities involved in propionate and acetate oxidation, crucial for volatile fatty acid conversion under these inhibitory conditions. Using highly enriched cultures, molecular and cultivation-based methods, thermodynamic calculations, and novel visualisation tools, the study revealed key metabolic pathways, a novel methanogen, and adaptive responses such as microbial aggregation and mechanisms for coping with ammonia and salt stress.

Nils Weng received his graduate education at the Department of Molecular Sciences, SLU, Uppsala. He received his M.Sc. Eng. in Engineering Biology at Linköping University, Sweden.

Acta Universitatis Agriculturae Sueciae presents doctoral theses from the Swedish University of Agricultural Sciences (SLU).
SLU generates knowledge for the sustainable use of biological natural resources. Research, education, extension, as well as environmental monitoring and assessment are used to achieve this goal.

ISSN 1652-6880
ISBN (print version) 978-91-8046-477-2
ISBN (electronic version) 978-91-8046-527-4